

The Role of Mammalian *Brinps* in Neurobiology and Neural Development

Susan Ruth Berkowicz, BSc

Department of Biochemistry and Molecular Biology
Monash University

September 2015

Table of Contents

The Role of Mammalian <i>Brinps</i> in Neurobiology and Neural Development	1
I. Abstract.....	11
II. Declaration of Authenticity.....	13
III. Dedications	14
IV. Acknowledgements.....	15
V. Abbreviations	16
Chapter 1: General Introduction	19
1.1 Chapter 1 Overview.....	20
1.2 Neurodevelopmental disorders	20
1.2.1 Autism spectrum disorder (ASD)	21
1.2.2 Attention deficit hyperactivity disorder (ADHD)	22
1.2.3 Intellectual disability (ID)	23
1.2.4 Schizophrenia.....	23
1.3 Mice as a model to study neurodevelopment and neurodevelopmental disorders.....	24
1.4 Mammalian cortical development	26
1.4.1 Neurogenesis and neuronal migration in the mammalian neocortex	26
1.4.2 Neurogenesis and neuronal migration in the developing hippocampus	34
1.5 The role of MACPF proteins in neurodevelopment	37
1.5.1 The MACPF superfamily.....	37
1.5.2 Neurodevelopmental MACPFs	39
1.5.3 An overview of Astrotactin and BRINPs.....	42
1.5.4 Astrotactins and BRINPs are linked genes	43
1.6 Astrotactins	45
1.6.1 Localization of Astrotactins	45
1.6.2 The role of Astrotactin1 and Astrotactin2 in cortical development.....	46
1.6.3 Astrotactins and neurodevelopmental disorders (NDDs).	50
1.7 <i>Brinps</i>	52
1.7.1 Localization of <i>Brinps</i>	52
1.7.2 <i>Brinps</i> are induced upon differentiation	54
1.7.3 A role for <i>Brinps</i> in regulating cell cycle progression or neuroplasticity?	54
1.7.4 BRINP1 and neurodevelopmental disorders (NDDs).....	55
1.7.5 BRINP2 / BRINP3 and neurodevelopmental disorders (NDDs).....	55
1.7.6 Non-NDD pathologies associated with BRINPs.....	56
1.7.7 Brinp Summary	59

1.8	Hypothesis	61
1.8.1	<i>Brinps facilitate migration of post-mitotic neurons.</i>	61
1.9	Thesis aims	62
1.9.1	<i>To investigate the role of Brinp1, Brinp2 and Brinp3 on neuroanatomy and behavior.</i>	62
1.9.2	<i>To determine the relationship between the three Brinp genes and their molecular role in the mammalian nervous system.</i>	62
Chapter 2: Materials and methods.....		63
2.1	Antibody list	64
2.2	Oligonucleotide primer list.....	65
2.2.1	<i>List of mouse genotypes (C57BL/6 background)</i>	67
2.4	Buffers and solutions.....	68
2.4.1	<i>Plasmids</i>	70
2.4.2	<i>Cell lines</i>	70
2.5	Methods	71
2.5.1	<i>Animal husbandry and ethics</i>	71
2.5.2	<i>Gene targeting</i>	71
2.5.3	<i>Mouse breeding.</i>	72
2.5.4	<i>Extraction and purification of spleen DNA</i>	73
2.5.5	<i>Brinp1 southern blotting</i>	74
2.5.6	<i>Genotyping</i>	74
2.5.7	<i>RNA isolation</i>	75
2.5.8	<i>cDNA synthesis</i>	76
2.5.9	<i>Quantitative real-time PCR ($\Delta\Delta C_q$ method)</i>	78
2.5.10	<i>Cell culture</i>	79
2.5.11	<i>Differentiation of NT2 cells</i>	79
2.5.12	<i>Transfection of COS-1 cells</i>	80
2.5.13	<i>Immunofluorescence</i>	80
2.5.14	<i>Preparation of cell lysates</i>	80
2.5.15	<i>Preparation of mouse brain lysates</i>	81
2.5.16	<i>Immuno-blotting</i>	81
2.5.17	<i>Histopathology</i>	82
2.5.18	<i>Immunohistochemistry</i>	82
2.5.19	<i>Reproductive phenotyping</i>	84
2.5.20	<i>Dietary experiment: Supplementation of diet with sunflower seeds</i>	85
2.5.21	<i>Behavioral testing</i>	85
2.5.21.1	<i>Animals</i>	85
2.5.21.2	<i>Visual placing test</i>	86

2.5.21.3 Acoustic startle and pre-pulse inhibition (PPI).....	86
2.5.21.4 Elevated plus maze.	86
2.5.21.5 Y-maze.	86
2.5.21.6 Rotarod.....	87
2.5.21.8 Three chamber social interaction test.....	87
2.5.21.9 Locomotor cell.....	88
2.5.21.12 Morris water maze.....	89
2.5.21.13 Self-directed digging and grooming behaviors.	89
2.5.21.14 Wire hang test.....	89
2.5.21.15 Novel object recognition test (NORT).....	89
2.5.21.16 Nesting.....	91
2.5.21.18 Statistical analysis.....	92
Chapter 3: The generation and characterization of <i>Brinp1</i> , <i>Brinp2</i> and <i>Brinp3</i> knockout mice.....	93
3.1 Chapter 3 Overview.....	94
3.2 Targeting strategy to generate <i>Brinp</i> knockout mice.....	94
3.3 Breeding strategy to generate <i>Brinp</i> knockout mice.....	95
3.4 Southern blotting.	96
3.5 Genotyping.....	96
3.6 Validation of <i>Brinp</i> knockout lines.....	106
3.6.1 RT PCR validation.....	106
3.6.2 Western blot validation.....	106
3.7 Analysis of survival of <i>Brinp1</i> , <i>Brinp2</i> and <i>Brinp3</i> knockout mice.....	109
3.8 Postnatal weight of <i>Brinp</i> knockout mice.....	112
3.9 Histopathology of <i>Brinp</i> knockout mice.....	115
3.9.1 Macroscopic observations.....	115
3.9.2 Microscopic observations.....	115
3.9.3 Brain pathology.....	115
3.9.4 Tissue inflammation in <i>Brinp1</i> knockout mice.....	118
3.9.5 Analysis of <i>Brinp1</i> knockout late stage embryos.....	120
3.10 Behavioral screen of <i>Brinp</i> knockout mice.....	122
3.10.1 Visual placing test.....	122
3.10.2 Olfactory test.....	122
3.10.3 Startle response and pre-pulse inhibition (PPI).....	122
3.10.4 Rotarod.....	126
3.10.5 Elevated plus maze.....	126
3.10.6 Y-maze.....	131
3.10.7 Sociability.....	136

3.10.8	<i>Brinp1, Brinp2 and Brinp3 KO behavioral summary</i>	141
3.11	Chapter 3: Discussion	142
3.11.1	<i>Brinp1, Brinp2 and Brinp3 KO are viable, show a reduction in body weight, with no gross anatomical abnormalities</i>	142
3.11.2	<i>Brinp1, Brinp2 and Brinp3 KO mice show no impairment in sensory gating</i>	143
3.11.3	<i>Brinp1, Brinp2 and Brinp3 KO mice motor co-ordination is not impaired</i>	144
3.11.4	<i>Brinp1 KO mice showed a marked reduction in sociability.</i>	145
3.11.5	<i>Hyper-exploratory behavior exhibited by Brinp1 and Brinp3 KO mice</i>	146
3.11.6	<i>Brinp1 KO mice may have impaired spatial memory, or an altered response to novelty.</i> ...	147
3.11.7	<i>Implications for the reported phenotypes of Brinp1, Brinp2 and Brinp3 knockout mice</i>	148
	Chapter 4: Characterization of <i>Brinp2/3</i> double and <i>Brinp1/2/3</i> triple knockout mice	151
4.1	Chapter 4 Overview.....	152
4.1.1	<i>Rationale for the generation of Brinp2/3 KO mice</i>	152
4.2	Generating <i>Brinp2/3</i> and <i>Brinp1/2/3</i> KO mice	154
4.2.1	<i>Breeding of Brinp2/3 triple KO mice.</i>	154
4.2.2	<i>Breeding of Brinp1/2/3 triple KO mice.</i>	154
4.2.3	<i>Validation of Brinp2/3 and Brinp1/2/3 KO mice</i>	157
4.3	Phenotyping of <i>Brinp2/3</i> KO mice	158
4.3.1	<i>Postnatal weights of Brinp2/3 KO mice.</i>	158
4.3.2	<i>Histopathological analysis of Brinp2/3 KO mice</i>	158
4.3.3	<i>Brinp2/3 behavioral testing</i>	161
4.3.4	<i>Brinp2/3 KO behavioral summary and conclusions</i>	168
4.4	Phenotyping of <i>Brinp1/2/3</i> KO mice	169
4.4.1	<i>Rationale for generating Brinp1/2/3 KO mice</i>	169
4.4.2	<i>Brinp1/2/3 KO mice exhibit low viability and poor reproductive success.</i>	169
4.4.3	<i>Histopathological analysis of Brinp1/2/3 Triple knockout mice</i>	172
4.4.4	<i>Brain pathology of Brinp1/2/3 KO mice</i>	173
4.4.5	<i>Microscopic observations of Brinp1/2/3 KO mice - signs of inflammation</i>	173
4.4.6	<i>Brinp1/2/3 KO summary</i>	174
4.5	Expression profile of <i>Brinps</i> and <i>Astrotactins</i> in the mouse brain.	175
4.5.1	<i>A comparison of WT Brinp and Astn expression in the adult mouse brain.</i>	175
4.5.2	<i>Alterations in expression of neuronal-MACPFs in the Brinp1 KO mouse brain</i>	183
4.6	Chapter 4: Discussion	185
4.6.1	<i>Brinp2/3 KO mice do not exhibit an enhanced phenotype of Brinp2 or Brinp3 KO mice</i>	185
4.6.2	<i>Brinp1/2/3 KO mice have poor viability, decreased body weight, with no gross anatomical abnormalities</i>	186
4.6.3	<i>Brinps and Astrotactins are co-expressed in neuron-specific regions</i>	187

Chapter 5: In-depth characterization of <i>Brinp1</i> KO mice	191
5.1 Chapter 5 Overview.....	192
5.2 The study of <i>Brinp1</i> KO mice reveals an ASD-like phenotype and hyperactivity, underpinned by changes in cortical lamination	193
5.2.1 Author names and affiliations	193
5.2.2 Corresponding authors	193
5.2.3 Conflict of interest.....	193
5.3 Acknowledgements.....	193
5.4 Abstract	194
5.5 Background	194
5.6 Materials and methods	196
5.7 Results	196
5.7.1 Generation of <i>Brinp1</i> knockout mice	196
5.7.2 <i>Brinp1</i> KO mice exhibit decreased postnatal survival and a reduced body weight.....	198
5.7.3 <i>Brinp1</i> KO mice have fewer layer IV neurons	201
5.7.4 Behavioral alterations of <i>Brinp1</i> KO mice	212
5.7.5 <i>Brinp1</i> KO mice exhibit reduced sociability and altered vocalizations	212
5.7.6 <i>Brinp1</i> KO mice are hyperactive and exhibit changes in exploratory behavior.....	215
5.7.7 Methylphenidate does not decrease hyperactivity of <i>Brinp1</i> KO mice.....	215
5.7.8 <i>Brinp1</i> KO mice have impaired short-term memory	216
5.7.9 <i>Brinp1</i> knockout mice exhibit normal sensory gating	216
5.7.10 Increased expression of <i>Astn1</i> and <i>Astn2</i> in the developing brain of <i>Brinp1</i> KO mice.	219
5.8 Chapter 5: Discussion	221
5.8.1 <i>Brinp1</i> KO mice model core social communication symptoms ASD	221
5.8.2 <i>Brinp1</i> KO mice are hyperactive, with short-term memory impairment.....	222
5.8.3 <i>Brinp1</i> KO mice exhibit changes in cortical lamination.....	222
5.9 Conclusions	225
Chapter 6: General Discussion.....	233
6.1 Discussion Overview.....	234
6.1.1 Given that <i>Brinps</i> are almost exclusively expressed in the nervous system of mammals, does their absence result in changes to behavior?.....	234
6.1.2 <i>Brinp1</i> , <i>Brinp2</i> and <i>Brinp3</i> KO mice in context of neurodevelopmental disorders.....	236
6.1.3 Evaluating the hypothesis: <i>Brinps</i> facilitate migration of post-mitotic neurons.....	240
6.1.4 Future directions	241
Chapter 7: Appendix.....	245
7.1 Anti-BRINP1 antibody generation	247

7.2	Supplementation of <i>Brinp1</i> het breeder diet with sunflower seeds	251
7.3	Bibliography	253

Figures

Figure 1-1	– Sagittal section of an adult mouse brain	25
Figure 1-2	- Origins of projection neurons and interneurons in the murine nervous system	28
Figure 1-3	- Laminar formation of projection neurons in the developing neocortex.....	30
Figure 1-4	– Neocortical Interneurons.....	33
Figure 1-5	– Embryonic development of the hippocampus	36
Figure 1-6	– MACPF protein membrane assembly and pore formation.....	38
Figure 1-7	– Phylogeny of the vertebrate MACPF family	41
Figure 1-8	– Protein motifs of neuronal-MACPFs: Astrotactins and BRINPs	43
Figure 1-9	– The <i>ASTN</i> / <i>BRINP</i> loci are conserved between humans and mice.....	44
Figure 1-10	– <i>Astn1</i> facilitates migration of granule neurons migrating along glial fibers	47
Figure 2-1	–Novel object recognition test	90
Figure 2-2	– Nest scoring system	91
Figure 3-1	– Targeting strategy of the <i>Brinp1</i> locus.....	97
Figure 3-2	– Southern blotting of <i>Brinp1</i> targeted, <i>Brinp1</i> FLPe, <i>Brinp1</i> KO, <i>Brinp1</i> het and WT DNA	98
Figure 3-3	– Targeting strategy of the <i>Brinp2</i> locus.....	99
Figure 3-4	– Southern blotting of <i>Brinp2</i> targeted, <i>Brinp2</i> FLPe, <i>Brinp2</i> KO, <i>Brinp2</i> het and WT DNA	100
Figure 3-5	– Targeting strategy of <i>Brinp3</i> locus	101
Figure 3-6	– Southern blotting of <i>Brinp3</i> targeted, <i>Brinp3</i> FLPe, <i>Brinp3</i> KO, <i>Brinp3</i> het and WT DNA	102
Figure 3-7	– Genotyping of <i>Brinp1</i> targeted, <i>Brinp1</i> KO and <i>Brinp1</i> FLPe mice	103
Figure 3-8	– Genotyping of <i>Brinp2</i> targeted, <i>Brinp2</i> KO and <i>Brinp2</i> FLPe mice	104
Figure 3-9	– Genotyping of <i>Brinp3</i> targeted, <i>Brinp3</i> KO and <i>Brinp3</i> FLPe mice	105
Figure 3-10	– Validation of <i>Brinp</i> knockout lines by reverse-transcriptase PCR and immuno-blotting.....	107
Figure 3-11	– Sequence alignments of <i>Brinp1</i> ^{tm1.1/Pib} , <i>Brinp2</i> ^{tm1.1/Pib} and <i>Brinp3</i> ^{tm1.1/Pib} alleles	108
Figure 3-12	– Analysis of offspring for from <i>Brinp1</i> , <i>Brinp2</i> and <i>Brinp3</i> heterozygous breeders	110
Figure 3-13	– <i>Brinp1</i> , <i>Brinp2</i> and <i>Brinp3</i> KO mice weighing	114
Figure 3-14	– Brain sections of <i>Brinp1</i> , <i>Brinp2</i> and <i>Brinp3</i> knockout mice.....	116
Figure 3-15	– Tissue inflammation in <i>Brinp1</i> KO mice	119
Figure 3-16	– Body length and brain histopathology of late embryonic (E18.5) <i>Brinp1</i> KO embryos	121
Figure 3-17	– Visual placing test	123
Figure 3-18	– Olfaction test	124
Figure 3-19	– Acoustic startle and pre-pulse inhibition.....	125
Figure 3-20	– Rotarod	127
Figure 3-21	– Elated plus maze (EPM)	129
Figure 3-22	– Y-maze: <i>Brinp1</i> KO (cohort 1 and cohort 2).....	132

Figure 3-23 – Y-maze: <i>Brinp2</i> and <i>Brinp3</i> KO mice	134
Figure 3-24 – Three chamber social interaction test: <i>Brinp1</i> cohort 1 and 2	138
Figure 3-25 – Three chamber social interaction test: <i>Brinp2</i> and <i>Brinp3</i> KO	140
Figure 4-1 – Genotyping of mice carrying the <i>Brinp2</i> ^{tm1.1Pib} and <i>Brinp3</i> ^{tm1.1Pib} alleles to generate <i>Brinp2/3</i> double KO mice	155
Figure 4-2 – Genotyping of mice carrying the <i>Brinp1</i> ^{tm1.1Pib} , <i>Brinp2</i> ^{tm1.1Pib} and <i>Brinp3</i> ^{tm1.1Pib} alleles to generate <i>Brinp1/2/3</i> triple KO mice.....	156
Figure 4-3 – Validation of knockout lines by RT-PCR, including <i>Brinp2/3</i> KO and <i>Brinp1/2/3</i> KO mice	157
Figure 4-4 – <i>Brinp2/3</i> : weights	159
Figure 4-5 Brain histopathology of <i>Brinp2/3</i> KO mice	160
Figure 4-6 – <i>Brinp2/3</i> : Visual placing test, PPI, Rotarod and Y-maze	162
Figure 4-7 – <i>Brinp2/3</i> : Elevated plus maze	164
Figure 4-8 – <i>Brinp2/3</i> : Locomotor cell	165
Figure 4-9 – <i>Brinp2/3</i> : Three chamber social interaction test	166
Figure 4-10 – <i>Brinp1/2/3</i> : weights.....	171
Figure 4-11 Brain histopathology of <i>Brinp1/2/3</i> KO mice	173
Figure 4-12 – Tissue inflammation in <i>Brinp1/2/3</i> KO mice.....	174
Figure 4-13 – A comparison of <i>Brinp1</i> , <i>Brinp2</i> and <i>Brinp3</i> , <i>Astn1</i> and <i>Astn2</i> mRNA distribution in the adult (P56) mouse brain in coronal and sagittal view	176
Figure 4-14 – A comparison of <i>Brinp1</i> , <i>Brinp2</i> , <i>Brinp3</i> , <i>Astn1</i> and <i>Astn2</i> mRNA distribution in the adult (P56) mouse olfactory bulb.....	177
Figure 4-15 – A comparison of <i>Brinp1</i> , <i>Brinp2</i> , <i>Brinp3</i> , <i>Astn1</i> and <i>Astn2</i> mRNA distribution in the adult (P56) mouse neocortex and hippocampus	178
Figure 4-16 – A comparison of <i>Brinp1</i> , <i>Brinp2</i> , <i>Brinp3</i> , <i>Astn1</i> and <i>Astn2</i> mRNA distribution in the adult C57BL/6 cerebellum at 8 weeks	179
Figure 4-17 – Combinations of neuronal-MACPF co-expression in the adult mouse brain	182
Figure 4-18 – Up-regulation of <i>Astn1</i> and <i>Astn2</i> mRNA in the embryonic brain and adult hippocampus of <i>Brinp1</i> KO mice	184
Figure 5-1 – <i>Brinp1</i> targeting.....	197
Figure 5-2 – Reduced litter survival and postnatal growth of <i>Brinp1</i> KO mice.....	200
Figure 5-3 – Neuronal distribution in the adult <i>Brinp1</i> KO neocortex and hippocampus	204
Figure 5-4 – Interneuron distribution in the adult <i>Brinp1</i> KO neocortex and hippocampus.....	205
Figure 5-5 Astrocyte distribution in the adult <i>Brinp1</i> KO neocortex and hippocampus	207
Figure 5-6 – E18.5 <i>Brinp1</i> KO mice show impaired neuronal positioning of neocortical cells generated at days E14.5 and E16.5	208
Figure 5-7 – Normal proliferation and apoptosis in the neocortex and hippocampus of <i>Brinp1</i> KO E18.5 embryos.....	210
Figure 5-8 – Altered social interaction and vocalization of <i>Brinp1</i> KO mice.....	214
Figure 5-9 – <i>Brinp1</i> KO mice exhibit hyperactivity, altered exploratory behavior and impaired short-term memory	217
Figure 5-10 – Up-regulation of <i>Astn1</i> and <i>Astn2</i> mRNA in the embryonic brain and adult hippocampus of <i>Brinp1</i> KO mice	220

Supplementary Figure 5.11 – Brain dimensions of adult <i>Brinp1</i> knockout mice.....	226
Supplementary Figure 5-12 – Distribution of BrdU positive cells in the cortex of E18.5 <i>Brinp1</i> KO embryos	227
Supplementary Figure 5-13 – <i>Brinp1</i> KO mice: nesting observations, cage observations, and wire hang test	228
Supplementary Figure 5-14 – <i>Brinp1</i> KO mice: locomotor cell - light / dark	229
Supplementary Figure 5.15 – <i>Brinp1</i> KO mice: Novel object recognition test	230
Supplementary Figure 5-16 – The effect of MPH on <i>Brinp1</i> KO mice locomotor activity	231
Figure 6-1 – Summary of neuronal-MACPF gene association with neurodevelopmental disorders, knockout mouse phenotypes, and cellular processes	239
Appendix Figure 6-2 – BRINP1 antibody validation	249
Appendix Figure 6-3 – BRINP1 is induced upon differentiation with retinoic acid	250
Appendix Figure 6-4 – The effect of dietary supplementation with sunflower seeds on the reproductive success of <i>Brinp1</i> heterozygous breeders.	252

Tables

Table 1-1 - MACPF subclasses. Adapted from table by (Rosado et al., 2008)	40
Table 1-2 - Associations of Astrotactins with neurological disorders.....	51
Table 1-3 - Associations of <i>BRINPs</i> with neurological disorders.....	57
Table 2-4 - Primary antibodies used for immunohistochemistry and immuno-blotting	64
Table 2-5 –Secondary antibodies used for immunohistochemistry and immuno-blotting.....	64
Table 2-6 - Oligonucleotide primer list	65
Table 2-7 - Nomenclature for <i>Brinp</i> transgenic mice genotypes.....	67
Table 2-8 - Genotyping PCR annealing temperatures	75
Table 3-9 - Nomenclature designation for <i>Brinp</i> mutant mice	95
Table 3-1 – Reproductive Phenotyping	111
Table 3-2 - <i>Brinp1</i> , <i>Brinp2</i> and <i>Brinp3</i> KO mice show normal macroscopic size for internal organs.....	117
Table 3-3 - <i>Brinp1</i> , <i>Brinp2</i> and <i>Brinp3</i> KO behavioral testing summary	141
Table 4-4 - Nomenclature for <i>Brinp</i> double and triple KO mice	153
Table 4-5 - Macroscopic measurements of <i>Brinp2/3</i> KO mice	160
Table 4-6 - Behavioral analysis summary, comparing the <i>Brinp2/3</i> KO phenotype with single <i>Brinp</i> KO phenotypes.....	168
Table 4-7 - Macroscopic measurements <i>Brinp1/2/3</i> KO mice.....	172
Table 4-8 - Neuronal-MACPF expression summary	180
Table 5-1 - Reproductive Phenotyping #	198
Table 6-2 – Phenotype of <i>Brinp1</i> KO mice compared to examples of established ASD mouse models.....	235

I. Abstract

Background: Bone morphogenetic protein / retinoic acid inducible neural-specific proteins, *Brinp1*, *Brinp2* and *Brinp3* are almost exclusively in the mammalian nervous system from mid-embryonic development through to adulthood. *Brinps* are highly conserved in vertebrates, indicating an important function. *Brinps* share homology via a MACPF domain with neuronal migration proteins, Astrotactin1 and Astrotactin2. *BRINPs* and Astrotactins are found at two conserved loci, with a high number of neural genes. The loci have been implicated in several neurodevelopmental disorders.

Approach: To investigate the function of *Brinps* in the developing and adult mammalian brain, *Brinp1*, *Brinp2* or *Brinp3* conditional knockout (KO) mice were generated via by Cre-recombinase mediated removal of the 3rd exon of *Brinp1*, *Brinp2* or *Brinp3*. Histopathological analysis was performed on each of the three KO lines. Cohorts of *Brinp1*, *Brinp2* and *Brinp3* KO mice were then tested by behavioral screening, which examined multiple aspects of behavior: motor co-ordination, sensory processing, anxiety response, sociability and memory. To investigate whether the absence of multiple *Brinps* would result in an enhanced phenotype, a double KO mouse line (*Brinp2/3*) and a triple KO line were generated (*Brinp1/2/3*). These lines were characterized in a similar manner to the single KO lines. Further phenotypic analysis was undertaken for the *Brinp1* KO mice, with additional behavioral testing and immuno-staining of cell populations in the adult and embryonic (E18.5) *Brinp1* KO mouse brains.

Results: Adult *Brinp1* knockout adult mice exhibited a marked reduction in sociability and altered ultrasonic vocalizations. *Brinp1* KO mice also demonstrated impaired short-term memory, hyperactivity and hyper-exploratory behavior in a novel environment. Methylphenidate (Ritalin), a drug commonly used to treat ADHD in humans, did not reduce hyperactivity in the *Brinp1* KO mice. *Brinp3* KO mice also showed hyper-exploratory behavior, whilst *Brinp2* KO mice showed no impairments in behavior. The absence of both *Brinp2* and *Brinp3* in the double reproduced the *Brinp3* KO mice behavioral phenotype.

Brinp1 KO mice were found to have a reduced density of pyramidal neurons in layer IV of the somatosensory neocortex. Altered layer IV formation was detected in the E18.5 neocortex by

labelling E14.5-born cells with 5-bromo-2'-deoxyuridine (BrdU). An increased density of parvalbumin-expressing interneurons was identified in both the neocortex and hippocampus. An increase in *Astrotactin1* and *Astrotactin2* mRNA was detected in the embryonic and postnatal brains of *Brinp1* KO mice.

Conclusions: The altered behavior of *Brinp1* KO mice resemble features of a subset of human neurological disorders, namely autism spectrum disorder (ASD) and the hyperactivity aspect of attention deficit hyperactivity disorder (ADHD). *Brinp1* influences neuronal distribution within the cortex, indicating a role for *Brinp1* in cell migration.

II. Declaration of Authenticity

I declare that this thesis contains no material which has been accepted for the award of any other degree or diploma in any university or other institution and affirm that, to the best of my knowledge, this thesis contains no material previously published or written by another person, except where due reference is made in the text.



Susan Ruth Berkowicz

Copyright Notice

Under the Copyright Act 1968, this thesis must be used only under the normal conditions of scholarly fair dealing. In particular, no results or conclusions should be extracted from it, nor should be copied or closely paraphrased in whole or in part without the written consent of the author. Proper written acknowledgement should be made for any assistance obtained from this thesis.

III. Dedications

I dedicate this thesis to my grandparents Dr. Joachim Memel and Henny Memel who encouraged me to work hard, and to think methodically and critically.

IV. Acknowledgements

A big thank you to my supervisors Professor Phil Bird and Professor James Whisstock for providing me with the opportunity to pursue my interests in neurobiology and conduct my own scientific research, as well as providing guidance throughout this study.

I would also like to thank Dr. Jeanette Rientjes, Dr. Arianna Nenci and Dr. Jose Gonzalez (Monash Gene Targeting Facility) for contract production of the *Brinp1*^{tm1/Pib}, *Brinp2*^{tm1/Pib}, and *Brinp3*^{tm1/Pib} mice.

Many thanks to Travis Featherby and Brett Purcell from Neuro Research Services (The Florey Institute of Neuroscience and Mental Health) for contracted behavioral testing services. Thank you also to the Australian Phenomics Network for their histopathology service. This study would not have been possible without their efforts.

Many thanks also to Zhengdong Qu of the Heng lab (Australian Regenerative Medicine Institute) for his time and skill in training me on histology and dissection techniques, and to Dr. Julian Heng for provision of resources.

I am also very grateful to Dr. Emma Burrows (Florey Institute of Neuroscience), Dr. Matilda Haas, and Dr. Dion Kaiserman (Monash University) for reviewing my work and providing feedback. Thank you to Dr. Natalie Borg, Aminah Giousoh (Monash University) and the Western Australia Institute of Medical Research Antibody Facility, for BRINP1 antibody generation. Thank you to Dr. Lee Wong and Dr. Jane Lin (Monash University) for training and use of their Roche qPCR machine. Thank you to staff at Monash Micro Imaging for training and assistance on the confocal microscopes.

A huge thank you to fellow Bird lab members for being fantastic people to work with, and for the training and assistance they have provided. Lastly, a big thank you to my wonderful husband, Iain Chesworth, for his moral support, IT support, thesis proof-reading, and gifting me a new laptop that has made writing this thesis possible.

V. Abbreviations

ADHD	<u>A</u> ttention <u>d</u> eficit <u>h</u> yperactivity <u>d</u> isorder
AF	<u>A</u> lexa <u>F</u> luor [®]
ANOVA	<u>A</u> nalysis of <u>v</u> ariance
ASD	<u>A</u> utism <u>s</u> pectrum <u>d</u> isorder
ASTN	<u>A</u> stro <u>t</u> actin
BRINP	<u>B</u> MP and <u>r</u> etinoic acid <u>i</u> nduced <u>n</u> euro-specific <u>p</u> rotein
BMP	<u>B</u> one <u>m</u> orphogenetic <u>p</u> rotein
BrdU	<u>B</u> romo <u>d</u> eoxy <u>u</u> ridine
CA	<u>C</u> ornu <u>A</u> mmonis
CGE	<u>C</u> entral <u>g</u> anglionic <u>e</u> minence
CNV	<u>C</u> opy <u>n</u> umber <u>v</u> ariation
CP	<u>C</u> ortical <u>P</u> late
CR	<u>C</u> al <u>r</u> etinin
Cux1	<u>C</u> ut-like homeobox <u>1</u>
DAPI	4',6- <u>d</u> iamidino-2- <u>p</u> henyl <u>i</u> ndole
DG	<u>D</u> entate <u>g</u> yrus
DSM-5	<u>D</u> iagnostic and <u>s</u> tatistical <u>m</u> anual of mental disorders, 5 th edition
EPM	<u>E</u> levated <u>p</u> lus <u>m</u> aze
GAPDH	<u>G</u> lyc <u>e</u> ralde <u>h</u> ide-3- <u>p</u> hosphate <u>d</u> e <u>h</u> ydrogenase
GFAP	<u>G</u> lial <u>f</u> ibrillary <u>a</u> cidic <u>p</u> rotein
Gr	<u>G</u> ranule layer
FOXP2	<u>F</u> orkhead box protein <u>P</u> 2
HPF	<u>H</u> ippocampal <u>F</u> ormation
HRP	<u>H</u> orse <u>r</u> adish <u>p</u> eroxidase
ID	<u>I</u> ntellectual <u>D</u> isability
IZ	<u>I</u> ntermediate <u>z</u> one

KO	<u>K</u> nock <u>o</u> ut
LGE	<u>L</u> ateral <u>g</u> anglionic <u>e</u> minence
MACPF	<u>M</u> embrane <u>a</u> ttack <u>c</u> omplex / <u>P</u> er <u>f</u> orin
MGE	<u>M</u> edial <u>g</u> anglionic <u>e</u> minence
Mi	<u>M</u> itral layer
ML	<u>M</u> olecular <u>L</u> ayer
MPH	<u>M</u> ethyl <u>p</u> henidate
MWM	<u>M</u> orris <u>w</u> ater <u>m</u> aze
MZ	<u>M</u> arginal <u>z</u> one
Neo ^r	<u>N</u> eomycin <u>r</u> esistant cassette
NeuN	<u>N</u> euronal <u>n</u> uclear antigen
NPY	<u>N</u> europeptide <u>Y</u>
NORT	<u>N</u> ovel <u>o</u> bject <u>r</u> ecognition <u>t</u> est
OB	<u>O</u> lfactory <u>b</u> ulb
PAPPA	<u>P</u> regnancy-associated <u>p</u> lasma <u>p</u> rotein <u>A</u>
pHH3	<u>p</u> hospho- <u>h</u> istone <u>H</u> 3
PL	<u>P</u> urkinje <u>l</u> ayer
PPI	<u>P</u> re- <u>p</u> ulse <u>i</u> nhibition
PV	<u>P</u> ar <u>y</u> albumin
RA	<u>R</u> etinoic <u>A</u> cid
SNP	<u>S</u> ingle <u>n</u> ucleotide <u>p</u> olymorphism
SST	<u>S</u> omatostatin
SP	<u>S</u> ubplate
SVZ	<u>S</u> ub <u>v</u> entricular <u>z</u> one
VZ	<u>V</u> entricular <u>z</u> one

Chapter 1: General Introduction

1.1 Chapter 1 Overview

Chapter one introduces the core purpose of this study: to increase understanding of the genetic and molecular basis of neurodevelopmental disorders (NDDs). The need for correct diagnosis and treatment of NDDs is high due the significant psychological, emotional, physical, and economic consequences for individuals, and in turn their families and society in general. Despite real progress in some aspects, current treatments do not work well for many patients. There is a great need to further understand the complex underlying biology to improve patient outcomes. The use of rodent animal models has provided an important platform to investigate the molecular mechanisms involved in normal and abnormal mammalian brain development. This is discussed within this introductory chapter, along with background of current knowledge on cortical development in the murine neocortex and hippocampus.

In the second half of this introduction, the focus changes to the specific proteins under investigation: the Membrane Attack Complex/Perforin (MACPF) superfamily, with an emphasis on those MACPF proteins highly expressed in the mammalian brains; *Brinps* and Astrotactins. Background is provided of the body of literature on *Brinp1*, *Brinp2*, *Brinp3*, Astrotactin1 and Astrotactin2, and current evidence for their role within the mammalian brain. The chapter ends with the hypothesis for the role of *Brinps* in mammalian development.

1.2 Neurodevelopmental disorders

Neurodevelopmental disorders (NDDs) are a group of psychiatric disorders that are usually first diagnosed in infancy, childhood, or adolescence, resulting from impairments in growth or connectivity of the developing brain, arising from a multitude of genetic and environmental factors (Bellani et al., 2013; Devlin & Scherer, 2012; First & APA, 2013; Mitchell, 2011). NDDs encompass widely varying degrees of impairment in brain function. These include movement disorders, communication / speech disorders, learning disorders and emotional regulation disorders. In many cases, more than one facet of brain function is affected. For example, lissencephaly is a rare, brain malformation characterized by the absence of normal convolutions (folds) in the cerebral cortex and an abnormally small head (microcephaly). Symptoms of this disorder may include failure to thrive, muscle spasms, seizures, intellectual disability and severe psychomotor retardation (Verloes et al., 2007).

The four NDDs listed below are some of the most prevalent, and are of greatest relevance to this study. These disorders have a distinct set of criteria for diagnosis. Whilst diagnosed separately, it is widely recognized that co-morbidity between disorders exists, in which an individual often presents with two or more separate NDD diagnoses. For example, autism spectrum disorder also frequently occurs with at least one other NDD, such as attention deficit hyperactivity disorder (ADHD), anxiety disorder, and intellectual disability (Rybakowski et al., 2014; Tureck et al., 2014).

1.2.1 Autism spectrum disorder (ASD)

ASD affects an estimated 0.6% of children (Folstein & Rosen-Sheidley, 2001; Fombonne, 2005), with similar prevalence in adults (Brugha et al., 2011). ASD is diagnosed, according to the Diagnostic and Statistical Manual of Mental Disorders (DSM-5), by the presentation of atypical social behavior, persistent deficits in social communication and social interaction, accompanied by restricted, repetitive patterns of behavior, interests, or activities (First & APA, 2013). ASD patients commonly have moderate to severe impairments in expressive language (McGonigle-Chalmers et al., 2013; Tek et al., 2014). The autism spectrum is variable, with symptoms ranging from mild to severe, sometimes with poor clinical outcomes and quality of life (Reszka et al., 2014; van Heijst & Geurts, 2015). Rett syndrome and Fragile X syndrome (FXS) each present with autistic traits, but are classified as separate traits based on a known genetic cause and distinct behavioral patterns (Brown et al., 1986; Olsson & Rett, 1985).

Although no major anatomical pathologies have been observed in brains of ASD cases (Amaral et al., 2008), several molecular and neuroimaging studies have linked certain brain regions to ASD. Neuroimaging studies have highlighted changes in cortical regions of autistic brains in the neocortex, hippocampus and cerebellum (Carper & Courchesne, 2005; Stoner et al., 2014; Wegiel et al., 2010). In addition, a variety of studies have pointed to various molecular mechanisms that might be altered in the autistic brain (Voineagu et al., 2011). Genes involved in cell adhesion, neuronal migration, and synaptic function, have all been found to be deregulated in people with ASD (Alarcon et al., 2008; Garber, 2007; Gilman et al., 2011). Changes in the balance of excitatory and inhibitory neurotransmitters glutamate and γ -aminobutyric acid (GABA) have also been described in the brains of ASD patients (Rubenstein

& Merzenich, 2003; Thatcher et al., 2009) which may arise from changes in cortical networks (Rubenstein & Merzenich, 2003).

There is currently no clinically proven drug treatment that directly improves the core deficits of ASD (Hampson et al., 2012). The drugs Arbaclofen (a GABA (B) agonist), and antagonists for the metabotropic glutamate receptor (mGluR5), are being developed for the treatment of Fragile X syndrome (Gurkan & Hagerman, 2012). Drugs such as Risperidone are used to treat irritability associated with autism, but on a limited basis due to serious side effects (Dinnissen et al., 2015).

1.2.2 Attention deficit hyperactivity disorder (ADHD)

ADHD affects approximately 4% of children (Castellanos and Tannock 2002), and is diagnosed, according to the DSM-5, by symptoms of inattention, hyperactivity, and impulsivity that are inconsistent with a child's developmental level. Symptoms present before seven years of age, and extend for at least six months (First & APA). ADHD behaviors make sustaining focus on a task challenging, and negatively impact social and academic and/or occupational activities (Arnold et al., 2015; Wehmeier et al., 2010).

Whilst the precise molecular mechanisms that lead to ADHD are unclear, historically, neurobiological research on ADHD has focused on dopaminergic pathways (Sharma & Couture, 2014). The neurotransmitter dopamine is thought to play a major role in ADHD pathology due to the pharmacological effects of drugs such as methylphenidate (MPH) and amphetamine; which act on dopamine synaptic transmission, to improve ADHD symptoms (Gustafsson et al., 2008; Kordon et al., 2011; Sharma & Couture, 2014). Not all ADHD patients respond to MPH or amphetamine (Contini et al., 2013; Krause et al., 2005) and other monoamine neurotransmitters are thought to be involved in the disorder. For example, atomoxetine, a re-uptake inhibitor of the neurotransmitter norepinephrine, is also effective for some ADHD patients (Sharma & Couture, 2014).

More recently, research focus has moved to trying to understand the molecular mechanisms that underlie cellular and anatomical changes reported in the brains of ADHD patients (Purper-Ouakil et al., 2011). There have been reports of brain abnormalities in ADHD subjects, such as reduced total brain volume (Cortese & Castellanos, 2012; Makris et al., 2007; Valera et al., 2007) and alterations in neural networks (Konrad & Eickhoff, 2010; Rubia et al., 2010).

1.2.3 Intellectual disability (ID)

ID diagnosis is based on impairments in intellectual functions, e.g. reasoning, problem solving, planning, abstract thinking, judgment, academic learning, and learning from experience. Such deficits result in failure to meet developmental and sociocultural standards for personal independence and social responsibility (First & APA, 2013). Whilst some ID patients present with extreme autistic traits, the two are distinct NDDs with only modest genetic correlation (Hoekstra et al., 2009). The neuropathology of ID is broad, with the dysregulation of many genes, involved in a wide number of neurodevelopmental pathways associated with the disorder (Gecz, 2004).

1.2.4 Schizophrenia

Schizophrenia occurs in approximately 0.7% of the adult population (Saha et al., 2005). Schizophrenia is diagnosed by the presentation of positive, negative and cognitive symptoms. Positive symptoms, include delusions, hallucinations, and disorganized speech and behavior. Negative symptoms may present as social withdrawal, anhedonia and flattened mood. Cognitive deficits may include impairments in working memory, attentional deficits and poor executive function. For diagnosis, symptoms must have been present for six months and include at least one month of active symptoms. Schizophrenia typically begins in late adolescence or early adulthood (First & APA, 2013; Mueser & McGurk, 2004).

The neurobiology of schizophrenia is complex, with a plethora of reported neuro-anatomical changes (Tandon et al., 2008). Some consistent pathologies include reduced cortical thickness, and enlargement of 3rd ventricular spaces (Cannon et al., 2015; Johnstone et al., 1976; Zugman et al., 2013). Such anatomical changes are present at the point of onset of the disease (Lawrie & Abukmeil, 1998; Pantelis et al., 2003). The neurotransmitter dopamine is widely accepted to be central to schizophrenia pathology. Dopamine agonists exacerbate schizophrenia symptoms whilst dopamine receptor 2 antagonists alleviate them (Kapur, 2004; Kapur et al., 2005; Lieberman et al., 1987). Whilst the effect of dopaminergic pathways on schizophrenia has been the most extensively studied, other neurotransmitter pathways are also central to schizophrenia pathology. For example, drugs that act on glutamate transmission can also exasperate and alleviate symptoms (Keshavan et al., 2008; Tandon et al., 2008). GABA-ergic pathways are also effected in schizophrenia (Taylor & Tso, 2014).

Dopamine-2 antagonists, such as Risperidone and Clozapine, are widely used to alleviate several of the positive symptoms of schizophrenia. (Creese et al., 1976; Kapur et al., 2005). Such anti-psychotic drugs vary greatly in their efficacy between individuals, and often have serious side effects (Gaertner et al., 1989; Lieberman et al., 2005; Tandon et al., 2008; van Strien et al., 2015). Additionally, dopamine antagonists are ineffective at treating cognitive symptoms (Kasper & Resinger, 2003). A greater understanding of the underlying neurobiology schizophrenia is required to allow for targeted treatment of individuals (Ahmed & Bhat, 2014).

1.3 Mice as a model to study neurodevelopment and neurodevelopmental disorders

Mice are routinely used in laboratories to study mammalian neural development due to striking similarities to humans in physiology, anatomy and genetics. Despite the human brain being 3×10^3 the mass of the mouse brain, and possessing far greater complexity, the majority of brain regions show conservation between mice and humans (Koch & Reid, 2012). At a genetic level, the mouse and human genomes share over 90% similarity, with gene expression profiles highly similar between mice and humans (Lockhart & Barlow, 2001; Strand et al., 2007; Su et al., 2004; Xing et al., 2007).

Whilst many disease related genes have been identified by Genome Wide Association Studies (GWAS), the understanding of the molecular function of these genes within the brain is key to developing potential target therapies. Transgenic rodents (most commonly mice and rats) have been used as model organisms to directly manipulate a target gene to study the underlying molecular process, and so have been used to study genes associated with neurodevelopmental disorders (Moy et al., 2006; Robertson & Feng, 2011; Russell et al., 2005). The use of gene targeting via DNA recombination in rodent embryonic stem (ES) cells allows for the generation of knockout mice to directly target specific genes. Knockout lines can then be characterized using established behavioral, physiological and histological assays, to understand the underlying molecular processes (Leo & Gainetdinov, 2013; Silverman et al., 2010; Tarantino & Bucan, 2000). In studies to date, rodents have provided great insight into mammalian brain development.

In the next section, I will detail some of the processes involved in mouse brain cortical development, and how perturbation to these processes can lead to neurodevelopmental disorders. Whilst the developmental steps that occur relate to both mice and humans, the developmental time points cited are specific to the mouse brain development. Figure 1-1 is provided as a reference of regions of the adult mouse brain mentioned throughout the introductory chapter.

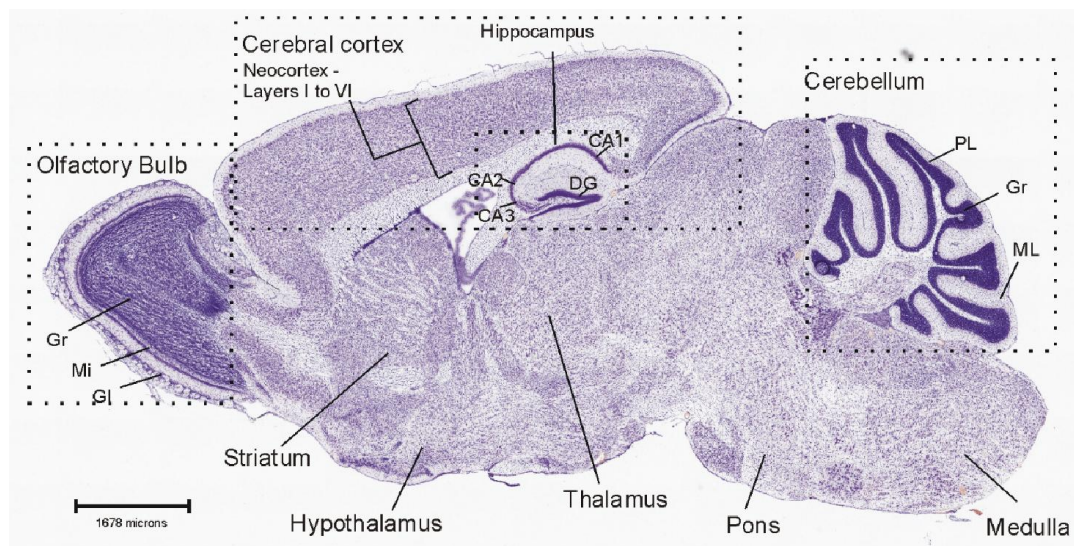


Figure 1-1 – Sagittal section of an adult mouse brain

A Nissl stain (purple) shows distribution of neurons in the adult (p56) mouse brain. Brain regions mentioned in the introductory chapter are framed and labelled.

CA = cornu ammonis area, DG = dentate gyrus, Gl = glomerular layer Gr = granule layer, Mi = mitral layer, PCL= Purkinje cell layer, ML = molecular layer. Source: Allen Mouse Brain Atlas: <http://mouse.brain-map.org/>.

1.4 Mammalian cortical development

The mammalian cerebral and the cerebellar cortices are comprised of densely populated and highly organized layers of neurons and glial cells. The neuronal types can be divided into two broad categories – excitatory glutamatergic projection neurons, and inhibitory GABA (γ -aminobutyric acid)-containing interneurons that together form networks of excitation and inhibition. Within the cerebral cortex (comprising the neocortex and hippocampus), glutamatergic projection neurons project their axons long distances both within the cortex, and to distant brain regions (Molyneaux et al., 2007). GABAergic interneurons are local circuit cells responsible for inhibitory transmission in the neocortex and hippocampus (Sultan et al., 2013).

During embryonic development, the cerebral and cerebellar cortices form from different regions of the neural tube, and develop different neuronal cell types, with cells originating in highly proliferative areas known as germinal zones, and undergoing directed migration to reach their destined layer within the cortex (Tan et al., 1998). As demonstrated in Figure 1-2A, projection neurons of the cerebral cortex originate from the ventricular zone, a dorsal lining of the lateral ventricles. Interneurons originate from more ventral germinal zones, where they migrate long distances into the developing cortex (Wonders & Anderson, 2006).

1.4.1 Neurogenesis and neuronal migration in the mammalian neocortex

During neocortical development, radial glial (RG) cells are generated from a layer of neuroepithelial (NE) cells in a proliferative region known as the ventricular zone (VZ) (Caviness, 1982; Wood et al., 1992). The NE cells divide asymmetrically to produce more NE cells, plus RG cells. These RG cells are themselves precursors that divide asymmetrically to generate neural precursor cells, and self-renew for more RG cells (Kriegstein & Gotz, 2003; Noctor et al., 2001; Noctor et al., 2002). The neural precursor cells go on to divide into excitatory post-mitotic neurons (Sild & Ruthazer, 2011; Tamamaki et al., 2001).

A layer of cells forms above the VZ known as the marginal zone (MZ) which contains the processes of radial glia. During cortical development, the radial glia have their cell bodies still embedded in the VZ and form the scaffolding for neuronal migration. (Rakic, 1972). Once a neuron is post-mitotic, it begins to migrate away from the VZ along the processes of the radial glial cell from which it was generated (Noctor et al., 2002; Stitt et al., 1991, Kriegstein & Gotz,

2003). The radial glial fibers run parallel to each other throughout the developing cortex, acting as scaffolding for each migrating neuron in order for it to reach the correct location within the cortex (Rakic, 1971, 1972). Radial migration of projection neurons has been characterized by distinct migratory phases in which neurons change shape and direction of movement as they migrate along glial networks towards the cortex (Kriegstein & Noctor, 2004). Figure 1-2B shows the composition of the neocortex during the later stages of murine embryonic development (E16), including the migration of projection neurons along glial fibers (Govek et al., 2011).

Radial migration has been shown to guide around 80% of migrating neurons, with tangential migration of inhibitory GABA-ergic interneurons occurring within the intermediate zone and the marginal zone (Metin et al., 2006; O'Rourke et al., 1992). There is some evidence to suggest these interneurons may use in-growing axons tracts to guide tangential migration, although this remains speculative (Andrews et al., 2006; McManus et al., 2004). An additional type of neuronal migration is followed by a subset of neurons that remain mitotically active along a rostral trajectory that continues in both the VZ and SVZ, forming the rostral migratory stream. These neurons migrate in the direction of the olfactory bulb (Alvarez-Buylla, 1997; Curtis et al., 2009).

1.4.1.1 Laminar organization projection (pyramidal) neurons in the neocortex

The organization of the developing lamination of projection neurons in the murine neocortex is depicted in Figure 1-3. The first set of neurons generated in the ventricular zone migrate to form the pre-plate (Valverde et al., 1995). With continued neuronal migration, the pre-plate develops into the cortical plate, splitting into the MZ above, cortical plate in the middle, and a subplate below (Wood et al., 1992). Axons from subplate and cortical plate neurons project into the intermediate zone (IZ); a region between the VZ and the marginal zone (McConnell et al., 1989, 1994). The IZ also contains axons from subcortical structures such as the thalamus (McConnell et al., 1989).

Projection neurons migrating through the subplate await the arrival of axon projections from other areas of the cortex, and then continue to migrate into the cortical plate (Del Rio et al., 2000). Neurons that fail to make appropriate synaptic connections undergo apoptosis (Clarke, 1992; Martin, 2001).

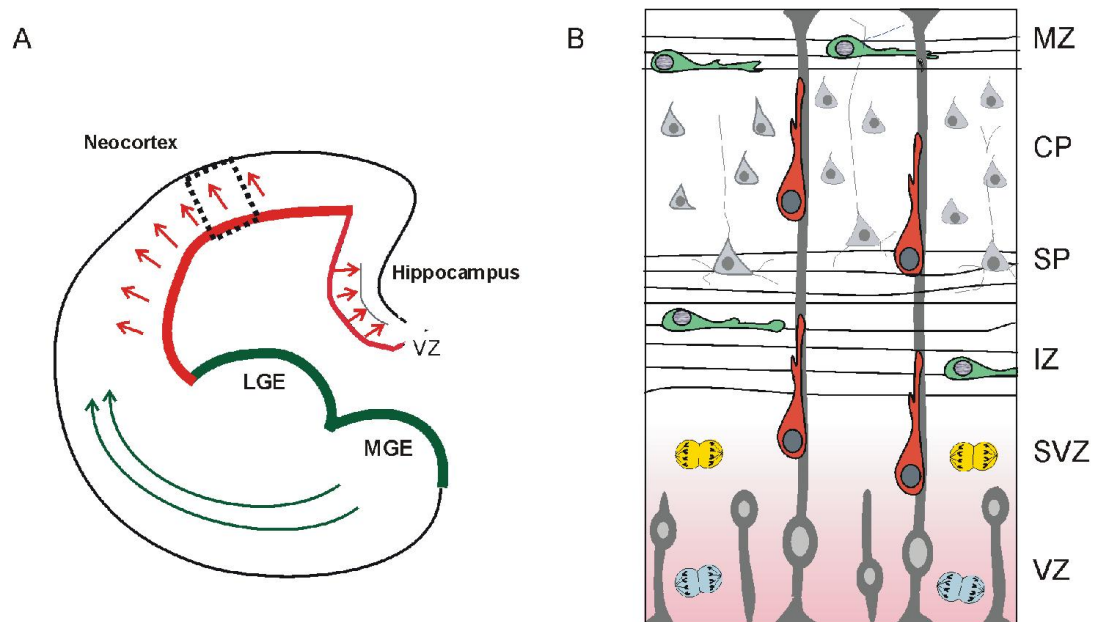


Figure 1-2 - Origins of projection neurons and interneurons in the murine nervous system

- A) The murine cerebral cortex is formed from neurons arising from multiple germinal zones. The graphic depicts a coronal hemi-section of the developing mouse brain. Germinal zones are shown as bold green and red lines. Cortical projection neurons (red) arise in the dorsally located ventricular zone, and migrate radially. Interneurons (green) move tangentially from their distant ventral sources: the medial ganglionic eminence (MGE), central ganglionic eminence (CGE – not shown), and lateral ganglionic eminence (LGE). The dotted rectangle frames a cross section of neocortex that is depicted in Figure B.
- B) A cross section of the developing mouse neocortex. The neocortex develops in an organized fashion, with trajectories and positioning dependent on cell type. During the later stages of embryonic development (depicted here at embryonic day 16) the neocortex is organized into the ventricular zone (VZ), sub-ventricular zone (SVZ), an intermediate zone (IZ), a sub-plate (SP), cortical plate (CP), and marginal zone (MZ) as the most superficial region.

The VZ contains large populations of proliferating progenitor cells (light blue) that become either neurons or glial cells. These include a network of radial glial cells (dark blue) that project through into the CP to the MZ. Projection neurons (orange) generated in the VZ, migrate along a radial network of glial fibers, into the developing CP. The majority of interneurons (green) (approximately 80%), migrate tangentially through the IZ and MZ. A further set of subset of neurons that remain mitotically active (yellow) follow the rostral migratory stream trajectory through the SVZ. Adapted from figure by Govek et al (Govek et al., 2011).

The subplate layer acts to provide important cues that aid the process by which cortical axons grow towards, select, and invade their subcortical targets (Caviness, 1982; Del Rio et al., 2000; McConnell et al., 1994; Wood et al., 1992). During later stages of neurogenesis, a second region of mitotically active cells develops; known as the subventricular zone (SV) (Brazel et al., 2003; Luskin, 1993). The cortical plate develops as six layers, forming in an inside-out manner where the most internal layer (layer 6) forms first and the most superficial (layer 2) forms last, and the MZ becomes layer 1 (Luskin & Shatz, 1985; Rakic, 1974). The subplate persists into the adult brain; forming part of the deepest cortical layer (layer VIb) (Chun & Shatz, 1989; Molyneaux et al., 2007). Different classes of projection neurons are born within different temporal waves, to generate the laminar structure of the neocortex (Molyneaux et al., 2007). The embryonic birthdate of projection neurons determines their position within the neocortex. In mice, corticothalamic deep layer neurons are generated first, forming layer VI at E12.5. Layer IV neurons are born at E14.5, and upper layer (II-III) neurons are generated last at E16.5 onwards. In the adult cerebral cortex, the intermediate zone becomes the subcortical white matter, and neuronal layers are molecularly distinct and can be identified through the expression of layer specific genes (Molyneaux et al., 2007). The original VZ exists as a single cell layer along the ventricle wall. Despite the cessation of neurogenesis in ventricular zone in the mammalian adult, the SVZ still retains stem cells in the adult brain capable of differentiating into neurons (Bayer, 1983; Ming & Song, 2011).

Aberrations in one or more of the neurodevelopmental processes driving projection neuron layer formation, i.e. proliferation, migration or cell survival, can result in abnormal lamination of the neocortex. Proliferation defects include loss of tightly regulated events by cell cycle machinery, such as at the G1-S phase transition. Such a defect is evident in cyclin D1-deficient mice, where reduced cell proliferation results in thinner layers within the cortex (Geng et al., 2001). Conversely, in cyclin-dependent kinase inhibitor 1B (p27kip) KO mice, progenitors keep proliferating past the point when they would normally cease mitosis, producing extra cells that abnormally spill out into other layers. Deletion of both cyclin D1 and p27kip restores normal proliferation and cortical lamination (Geng et al., 2001). Migration defects of projection neurons are associated with behavioral deficits in mouse models of NDDs (Valiente & Marin, 2010).

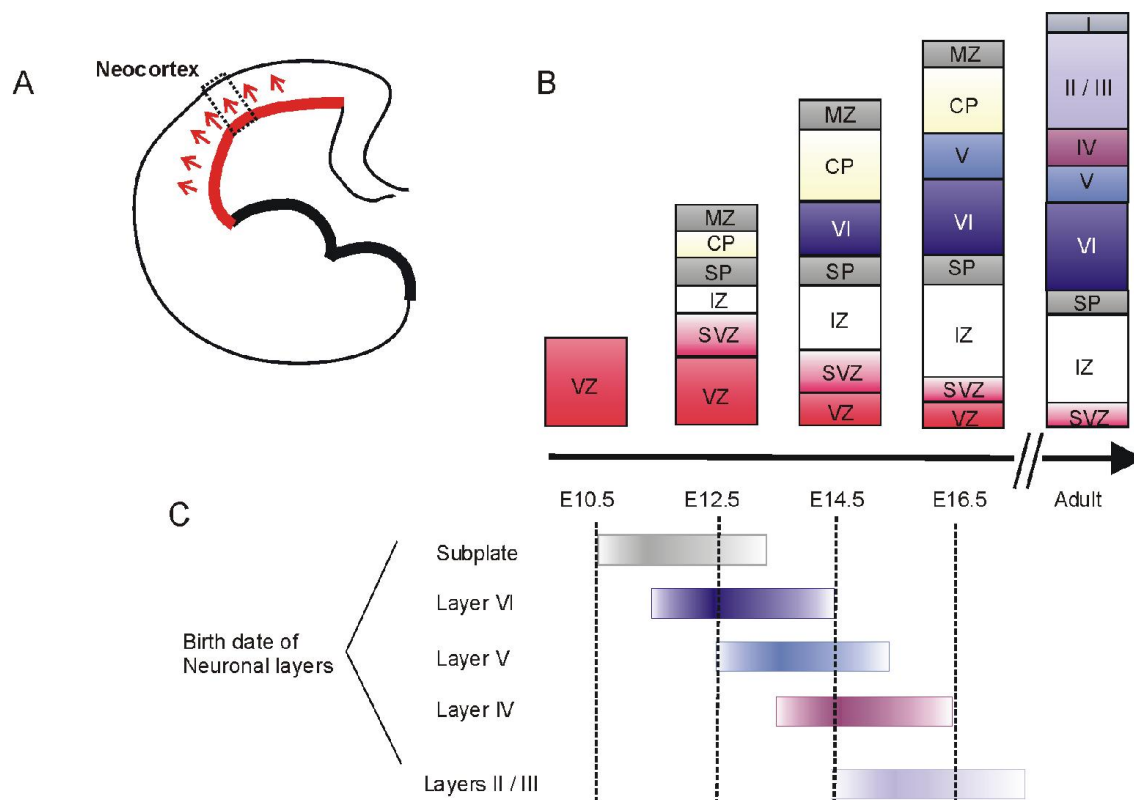


Figure 1-3 - Laminar formation of projection neurons in the developing neocortex

- A) Representation of the developing mouse neocortex (coronal). The germinal zone of neocortical projection neurons is highlighted in red. The dotted rectangle frames a column section depicted at different developmental stages in figure B.
- B) Schematic showing column sections of the developing neocortex at multiple developmental time points. Progenitor cells in the ventricular zone (VZ) and subventricular zone (SVZ) divide and post-mitotic neurons migrate, to form distinct layers of projection neurons in the neocortex. Earliest born neurons form the preplate, which later splits to become the superficially located marginal zone (MZ), and the more deeply located subplate (SP). An intermediate zone (IZ) forms between the subplate and the SVZ. The cortical plate (CP) begins to form between the MZ and subplate and gives rise to the multi-layered neocortex. Cortical layers are formed in an 'inside-out' manner, such that later born neurons arriving in the cortical plate radially migrate past earlier born neurons.
- C) Birthdate of projection neuron subtypes in the VZ /SVZ. The colored bars represent the embryonic birthdates of projection neurons that will go on to form sequential layers within the neocortex. Corticothalamic deep layer neurons are generated first at E12.5-E13.5, forming layer VI-V. Layer IV neurons are born at E14.5, and upper layer (II-III) neurons are generated last at E16.5 onwards.

CH = cortical hem; E = embryonic day; Ncx = neocortex; IZ = intermediate zone; LGE = lateral ganglionic eminence; MGE = medial ganglionic eminence; WM = white matter. Adapted from figure by Molyneaux et al (Molyneaux et al., 2007).

Commonly cited examples of NDD mouse models with altered cortical lamination as a result of changes in neuronal migration include the Reeler mouse (Reelin)(Caviness, 1982; Folsom & Fatemi, 2013), *Lis1* mutants (Paylor et al., 1999) and *ApoER2/Vldlr* (Hack et al., 2007). In humans, many instances of lamination defects of projection neurons have been reported in patients with neurodevelopmental disorders, including autism, lissencephaly, epilepsy and intellectual disability (Fatemi, 2001; Hu et al., 2014; Penagarikano et al., 2011; Pilz et al., 1998; Wegiel et al., 2010).

1.4.1.2 Origins and migration of inhibitory interneurons in the neocortex

Interneurons are close network inhibitory neurons that form chemical and electrical connections with neocortical projection neurons, as well as other interneurons. Whilst projection neurons are relatively uniform, interneuron subtypes can be defined by their differing morphological, physiological and neurochemical properties, that dictate their functional role within the neocortex (Markram et al., 2004; Petilla Interneuron Nomenclature et al., 2008; Wonders & Anderson, 2006). The distribution of subtypes in the adult murine neocortex is illustrated in Figure 1-4A.

In the mouse brain, approximately 40% of neocortical interneurons exhibit fast-spiking electrophysiological profiles, and these exhibit distinct morphologies, described as basket or chandelier cells. These cells express the cytoplasmic calcium binding protein parvalbumin (PV) (Markram et al., 2004; Taniguchi et al., 2013). A second subgroup (around 30% of neocortical interneurons) express the neuropeptide somatostatin (SST) or neuropeptide Y (NPY) and are morphologically heterogeneous. They typically exhibit non-fast spiking physiological characteristics (Ma et al., 2006; McGarry et al., 2010; Wonders & Anderson, 2006). The remaining ~30% of neocortical interneurons express calretinin (CR), and possesses the 5-hydroxytryptamine (serotonin) receptor 3A (5-HT3AR). They may exhibit either bipolar or double-bouquet morphologies and they display rapidly adapting firing patterns (Armstrong et al., 2012; Lee et al., 2010; Luth et al., 1993).

Interneurons are produced in the developing ventral telencephalon and migrate tangentially over long distances, to reach their destination in the cortex (Anderson et al., 2002; Anderson et al., 2001; Rakic, 1978). Tangential migration occurs through the marginal zone (MZ) or the intermediate zone (Cooper, 2014; Corbin et al., 2001; Marin & Rubenstein, 2001). This

tangential migration is illustrated in Figure 1-2. Upon entering the cortex, interneurons shift from tangential to a radial migration along the glial scaffold to invade cortical layers and integrate into the cortical circuit (Ang et al., 2003; Elias et al., 2010).

As with projection neurons, interneuron populations also exhibit a temporal distribution and are organized in an inside out pattern, where earlier born interneurons occupy deeper cortical laminae than their more superficial cohorts (Anderson et al., 2002; Faux et al., 2012). Most interneurons are born between embryonic days 11 and 18 (E11-E18) in mice (Butt et al., 2005; Miyoshi et al., 2007; Xu et al., 2004). The medial ganglionic eminence (MGE) is the germinal zone for most (~70%) of cortical interneurons, which produces a heterogeneous group of interneurons expressing either PV or SST (Wichterle et al., 1999; Wichterle et al., 2001; Xu et al., 2004). There is a temporal gradient of interneurons from this region, where a high proportion of SST+ cells are born at early developmental stages, and are almost absent in E15.5, while PV+ cells are generated at a consistent rate throughout MGE-derived interneuron production. Interneurons generated from a second germinal zone, the central ganglionic eminence (CGE), such as CR+ interneurons, are produced at later developmental time points (E12.5–E18.5, with a peak ~E16.5)(Butt et al., 2005; Miyoshi et al., 2010; Nery et al., 2002).

Figure 1-4B illustrates the directional migration of interneuron subtypes from the MGE and CGE. An interesting observation is that projection neurons and interneurons born at the same embryonic time point often reside in the same cortical layers, suggesting a level of coordination between interneurons and projection neurons during neurogenesis (Lodato et al., 2011; Marin & Rubenstein, 2001; Parnavelas, 2000; Tamamaki et al., 1997; Valcanis & Tan, 2003).

Correct proliferation, migration and positioning of interneurons is also required for normal brain development. In humans, interneuron perturbations can result in neurological disorders such as ASD, schizophrenia and epilepsy (Gandal et al., 2012; Lawrence et al., 2010; Powell, 2013; Schmidt & Mirnics, 2012).

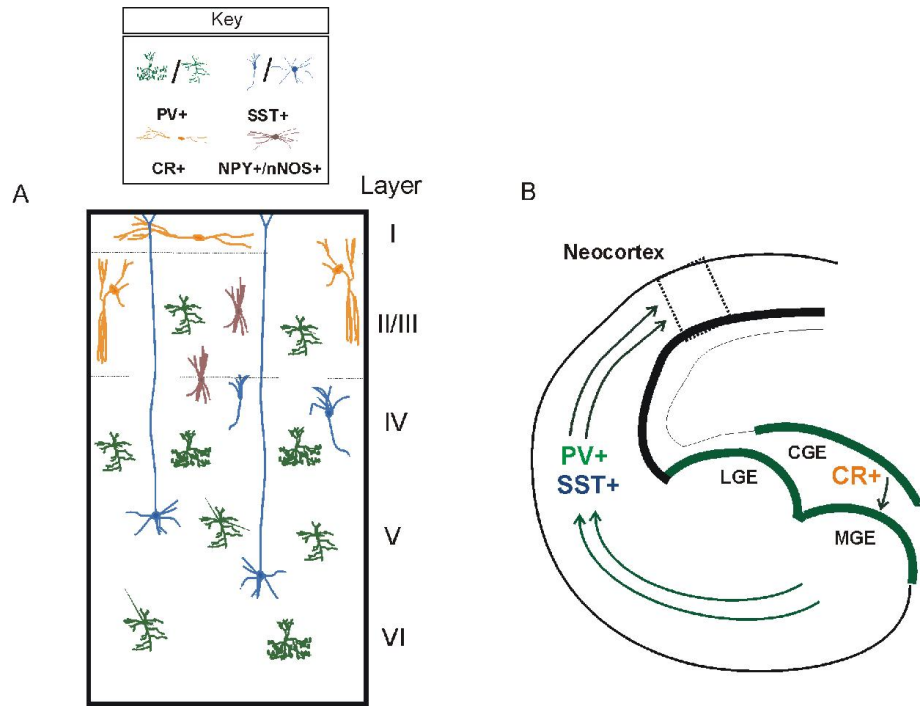


Figure 1-4 – Neocortical Interneurons

- A) A cross section of the adult murine neocortex, showing distribution of interneuron subtypes. CR+ interneurons are positioned in the superficial layers of the neocortex, whereas PV+ and SST+ interneurons are distributed throughout the cortical layers II to IV. PV+ interneurons exhibit their highest density in layer IV of the murine neocortex. CR = calretinin, NPY=neuropeptide Y, PV = parvalbumin, SST = somatostatin. Adapted from figure by Guo and Anton (Guo & Anton, 2014).
- B) A representation of the developing murine brain, showing the ganglionic eminence (GE) (green); the interneuron germinal region within the ventral telencephalon. The GE is subdivided into proliferation regions, known as the medial ganglionic eminence (MGE), central ganglionic eminence (CGE) and lateral ganglionic eminence (LGE). In general, early born interneurons are generated in the MGE, with subtypes expressing parvalbumin (PV) or somatostatin (SST). Later born interneurons are generated in the CGE, including those expressing calretinin (CR). Interneurons from the LGE follow a rostral migratory stream to the olfactory bulb (Guo & Anton, 2014; Metin et al., 2006).

1.4.2 Neurogenesis and neuronal migration in the developing hippocampus

The hippocampus is a temporal medial region of the brain, important for encoding of short term and long term memory, as well as spatial navigation (Khalaf-Nazzal & Francis, 2013). It is comprised of three major fields – the Cornu Ammonis 1 (CA1), Cornu Ammonis 3 (CA3) and the Dentate Gyrus (DG). The connecting region between the CA1 and CA3 is known as the Cornu Ammonis 2 (CA2).

Hippocampal development in mice begins from mid-gestation (E10) and the hippocampus forms from the medial regions of the telencephalon (Figure 1-5). Hippocampal neurogenesis occurs from E10 until well beyond birth. The CA is comprised predominately projection (pyramidal) neurons that show a wide range of characteristics depending on their radial and septo-temporal distributions in each field. In general, projection neurons of the CA1, CA2 and CA3 are generated in a relatively large area of epithelium within the ventricular zone (VZ). DG cells are generated in the dentate neuroepithelium, a narrow region of the VZ and migrate tangentially along glial fibers through the sub-pial area to form the granule cell layer of the dentate gyrus at P1-P2 (Nakahira & Yuasa, 2005). The DG develops later than the CA fields and DG granule cell neurogenesis continues at a high rate for the first month of life in mice, after which time the output is gradually reduced (Danglot et al., 2006).

Post-mitotic CA projection (pyramidal) neurons migrate along radial glial fibers to their specified laminar position. In the developing hippocampus, radial glia have their somata located in the ventricular zone and extend projections to the pial surface (Kriegstein & Noctor, 2004). Neurons migrate from the VZ, through the intermediate zone (IZ) to their laminar position, where they undergo morphological differentiation into mature neurons and form synaptic connections. The glial fibers disappear once migration is complete at postnatal day 9 (P9) (Altman & Bayer, 1990).

Migrating hippocampal neurons passing through the intermediate zone of the hippocampus pause or sojourn for a period of time before continuing to migrate (Altman & Bayer, 1990). The pause is distinctly longer for hippocampal neurons, of 2-4 days, compared with one day for neocortical neurons. This may be because interneurons take longer to migrate from the ventral telencephalon to the hippocampus, compared to interneuron migration into the neocortex (Khalaf-Nazzal & Francis, 2013; Marin et al., 2010). As with the neocortex, the

Cornu Ammonis (CA) forms in an inside-out manner. Earliest born pyramidal neurons (represented as white circles) at E11.5 form the outer boundary of the CA3 field. Subsequent waves of newly-born neurons radially migrate past this layer to more superficial layers. A proportion of later CA3 pyramidal cells first migrate tangentially in the sub-pial stream (Tol & Grove, 2001).

Hippocampal interneurons originate in the medial and the caudal ganglionic eminences (MGE and CGE, respectively) (Nery et al., 2002; Pleasure et al., 2000; Wichterle et al., 2001). A peak of CA interneurons are generated at E12–13, and DG interneurons at E13–14 (Soriano et al., 1986, 1989). As within the neocortex, interneurons migrate tangentially from the MGE and CGE through the intermediate zone (IZ) and marginal zone (MZ) of the cortex to the developing hippocampus (Marin & Rubenstein, 2001).

Mouse models of lissencephaly show lamination defects within the hippocampus. These include DCX, LIS1, Reelin and Tuba1A mutants (Reiner et al., 1993; des Portes et al., 1998; Gleeson et al., 1998; Hong et al., 2000; Keays et al., 2007). Lis1 and Tuba1A mutant mice exhibit malformation of CA1 and CA3 regions, with fragmented pyramidal cell layers. Reeler mutants are the most severely affected with severe hippocampal disorganization affecting all fields (Lambert de Rouvroit and Goffinet, 1998; Fleck et al., 2000; Keays et al., 2007).

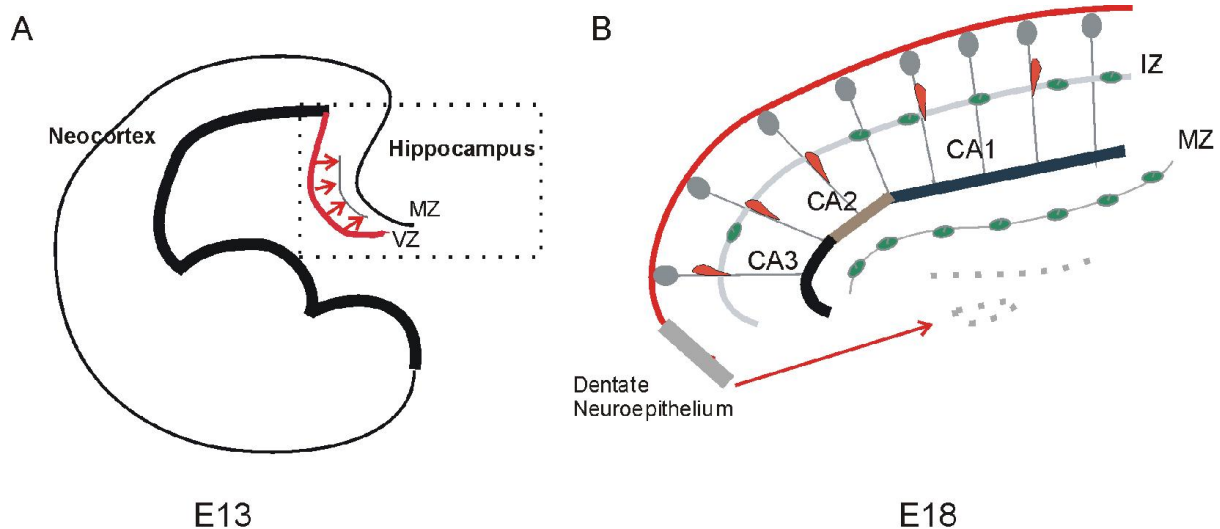


Figure 1-5 – Embryonic development of the hippocampus

- A) Coronal representation of the developing mouse neocortex. The germinal origin of hippocampal pyramidal neurons is highlighted in red. Initiation of the hippocampal formation begins from the temporal medial telencephalon at E13. Arrows show direction of neuronal migration of pyramidal neurons.
- B) Diagram showing glial guided migration of pyramidal neurons in the developing hippocampus represented at E17-18. Radial glia (grey) extend from the VZ to the MZ, providing a migration surface for transiting pyramidal neurons (orange). Interneurons (green) are generated from the ventral telencephalon and migrate in two tangential streams through the IZ and MZ. The dentate gyrus begins to form from the dentate neuroepithelium. Arrow represents the direction of DG neuronal migration.

MZ = Marginal zone, VZ = Ventricular zone, IZ = Intermediate zone, CA1, CA2, CA3 = Cornu ammonis regions 1, 2 and 3. Adapted from figure by Khalaf-Nazzal and Francis (2013) (Khalaf-Nazzal & Francis, 2013).

1.5 The role of MACPF proteins in neurodevelopment

The following section of this general introduction focuses on the specific group of proteins under investigation: Membrane Attack Complex/Perforin (MACPF) superfamily proteins, and the role of a subset of these proteins (Astrotactins and *Brinps*) in the development, distribution and function of the mammalian brain.

1.5.1 The MACPF superfamily

The MACPF superfamily comprises proteins containing a Membrane Attack Complex/Perforin domain. The domain is named after well characterized immune proteins; the Membrane Attack Complex (MAC) of the complement system and a cytotoxic, membrane binding protein called Perforin.

The Membrane Attack Complex (MAC) is formed from the terminal components of the complement system and acts to target pathogenic gram-negative bacteria. As illustrated in Figure 1-6A, there is a step-by-step succession of complement protein assembly; C5b, C6, C7, C8 α , C8 β associate at the cell membrane of gram-negative bacteria. The recruitment of poly-C9 creates a doughnut-shaped structure associated with the cell membrane. A conformational change in the C9 protein, via the MACPF domain, results in the puncturing of the target cell membrane to form a pore (Steckel et al., 1983; Tschopp et al., 1986). The formation of multiple pores is claimed to result in osmotic lysis of the bacterial cell (Bhakdi & Tranum-Jensen, 1978).

Perforin, is a lytic mammalian MACPF protein released by cytotoxic T lymphocytes (CTLs) and natural killer cells in order to kill virally infected and transformed host cells, by forming pores and permitting the delivery of the protease Granzyme B (Voskoboinik et al., 2010). Like C9, Perforin has been shown to associate at the target cell membrane and oligomerize, via the MACPF domain, into a circular complex. The Perforin oligomer forms without cofactors and inserts into the membrane, resulting in pore formation (Figure 1-6B). The end result is lysis of the target cell (Voskoboinik et al., 2006). As demonstrated with the examples of C9 and Perforin, some MACPF proteins are pore-formers and are cytotoxic, whereas complement members C6, C7, C8 α and C8 β bind to the membrane, but do not insert into the membrane, form pores or lyse the target cell. C8 α has been observed to penetrate the target cell

membrane, without pore formation (Muller-Eberhard, 1986). Such examples highlight roles for the MACPF domain in membrane association and insertion, in addition to the classical pore formation role.

It is important to note that MACPF pore-forming proteins follow different cellular trafficking pathways to integral membrane proteins, such as ion channels, that are inserted directly into the host cell membrane during protein synthesis (Deutsch et al., 2012; Schwarzer et al., 2013). Pore-forming proteins are synthesized by the host cell, then exit the cell via the constitutive or regulated secretory pathways as soluble molecules (Berke, 1995; Kinoshita et al., 1981; Voskoboinik et al., 2006). Both Perforin oligomers and the MAC assemble as multi-protein unit on the surface of the hydrophobic target cell membrane, followed by a conformational change in the MACPF domain to puncture a hole in the membrane (Kondos et al., 2010; Muller-Eberhard, 1986). Thus, trafficking via the secretory pathway and exocytosis from the host cell are believed to be integral to MACPF protein function in the mammalian system.

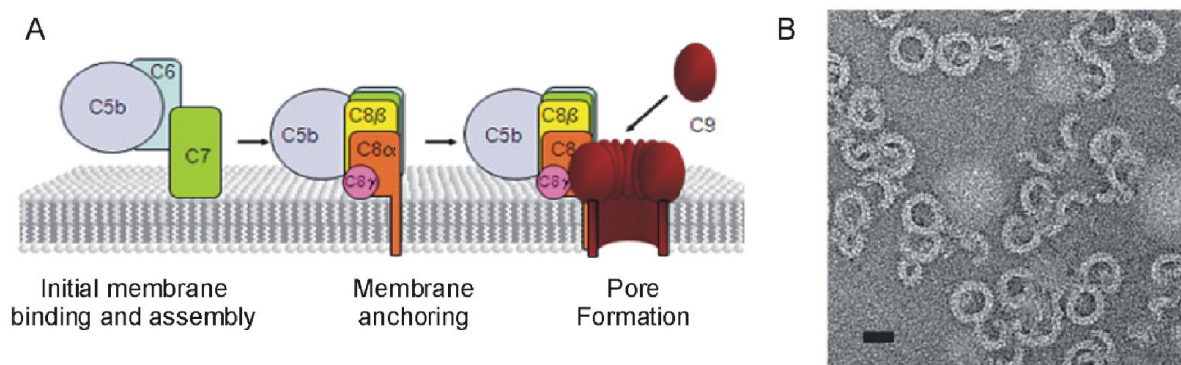


Figure 1-6 – MACPF protein membrane assembly and pore formation

- A) A schematic showing Complement Membrane Attack Complex (MAC) assembly. MAC proteins C5b, C6, C7, C8 α and C8 β assemble at the membrane of a target bacterial cell. Poly-C9 is recruited, forming a ring structure on the membrane. A conformational change in the C9 oligomer results in insertion of poly-C9 into the cell membrane, via the MACPF domain, forming a pore. Figure produced by Kondos et al (Kondos et al., 2010).
- B) A negative stain electron microscopy image of Perforin pores on a lipid bilayer. Scale bar: 20 nm. Image by Lopez et al (Lopez et al., 2013).

1.5.2 Neurodevelopmental MACPFs

Proteins containing the MACPF are found in most kingdoms of life; plants, animals, protozoa, fungi and bacteria, several of which act as pore forming toxins (PFTs) (Rosado et al., 2008). Once believed to act solely in an immunological role, some MACPF proteins are now known to be expressed in cell types not involved in immune defense (Ponting, 1999). Such examples include Apexrin, a protein with unknown function found in sea urchins (Haag et al., 1999), and Torso-like, a protein expressed during embryonic patterning in *Drosophila* (Martin et al., 1994). Table 1-1 summarizes the MACPF subclasses and their currently understood roles.

Two groups of MACPF proteins are expressed in the vertebrate brain during neural development: three *Brinps* and two Astrotactins. In 1999, Ponting et al. identified the MACPF domain in Astrotactins and *Brinp1* (Ponting, 1999). In this publication, Astrotactin2 is annotated as KIAA0634, and *Brinp1* as IB3089A. *Brinp2* and *Brinp3* were subsequently reported by Kawano et al to also have a MACPF domain motif (Kawano et al., 2004).

In vertebrate phylogeny, there exist two clades of MACPF proteins: a complement / Perforin clade and neuronal MACPF clade (Figure 1-7). The earliest split divides the mammalian MACPFs into two (well statistically supported) clades, a BRINP/ASTN clade and a Perforin/C6-9 clade (D'Angelo, 2014). Since the *ASTN* and *BRINP* MACPF domains are more similar to each other than any other vertebrate MACPF domain, it is reasonable to suggest that *ASTNs* and *BRINPs* also shared a common ancestor.

In both Astrotactins and BRINPs, the function of the MACPF domain is unknown: indeed it is not known whether these proteins oligomerize. It is also unclear why a domain that has long been associated with cytotoxic proteins is found in proteins associated with development. There is currently no published evidence that these neuronal-MACPFs are cytotoxic pore-formers. There is however evidence that Astrotactin1 is able to associate with the membrane of another cell (Edmondson et al., 1988). In this instance, Astrotactin1 is demonstrated to form part of the cohesive junction between a migrating granule neuron and a radial glial cell, as discussed in the next section. This role for Astrotactin1 appears to be different from the cytotoxic function of Perforin or C9, and is likely more akin to the membrane association role of complement C5-C8.

Table 1-1 - MACPF subclasses. Adapted from table by (Rosado et al., 2008)

Kingdom	MACPF subclasses	Protein Name	Demonstrated lytic activity?	Description of expression pattern and function (Role)
Animal-Vertebrates	Membrane Attack Complex	C6, C7, C8 α , C8 β , C9	Yes (as assembly)	Vertebrate membrane attack complex (MAC). Lysis of bacterial cells.(Bhakdi & Tranum-Jensen, 1986)
	Perforin-like	Perforin,	Yes	Immune response of natural killer and cytotoxic T lymphocytes, to lyse targeted cells (Voskoboinik et al., 2006).
		MPEG	No	Macrophage Proliferation-specific Gene-1, in differentiated macrophages. (D'Angelo et al., 2012; Spillsbury et al., 1995).
	Astrotactin	Astrotactin1	No	Required for neuronal migration along glial fibers (Zheng et al., 1996).
		Astrotactin2		Facilitates trafficking of <i>Astn1</i> during neuronal migration (Wilson et al., 2010).
	BRINP	BRINP1, BRINP2, BRINP3	No	Neuron-enriched proteins, role is under investigation (Kawano et al., 2004).
	EPCS50	EPCS50	No	Expressed in the trophoblast upon embryo implantation (Hemberger et al., 2000).
Animal Invertebrates	- Tsl1 (Drosophila melanogaster)	Torso-like protein (Tsl)	No	Hypothesized to activate the receptor, Torso, via the protein Trunk (Stevens et al., 1990).
	- Apexrin (sea urchin, amphioxus)	Apexrin	No	Located in secretory vesicles in sea-urchin eggs (Haag et al., 1999). Up-regulation upon bacterial infection in amphioxus (Huang et al., 2007).
	- Sea anemone toxins	PsTX-60A / B, AvTX-60A	Yes	Hemolytic toxin released from sea anemone nemocysts, to kill prey (Oshiro et al., 2004).
Plant	Plant protein	CAD1	No	Involved in plant immune response (Morita-Yamamuro et al., 2005).
Fungi	Fungal protein	SpoC1-C1C	No	Expressed during maturation of the conidia (Stephens et al., 1999).
Bacteria	Plu-MACPF	Plu-MACPF	No	From the bacteria <i>Photobacterium luminescens</i> (Rosado et al., 2007).
	Chlamydia proteins	-	No	Hypothetical protein: <i>C. trachomatis</i> , <i>C. pneumonia</i> , & <i>C. muridum</i> (Ponting, 1999).
Cyano-bacteria	Cyanobacteria protein	-	No	Hypothetical protein of <i>Trichodesmium erythraeum</i> (cyanobacteria).
Plasmodium falciparum	Malaria parasite proteins	SPECT2 and MAOP	No	Required for parasite invasion into the human liver (Ishino et al., 2004) and the mosquito host (Kadota et al., 2004).

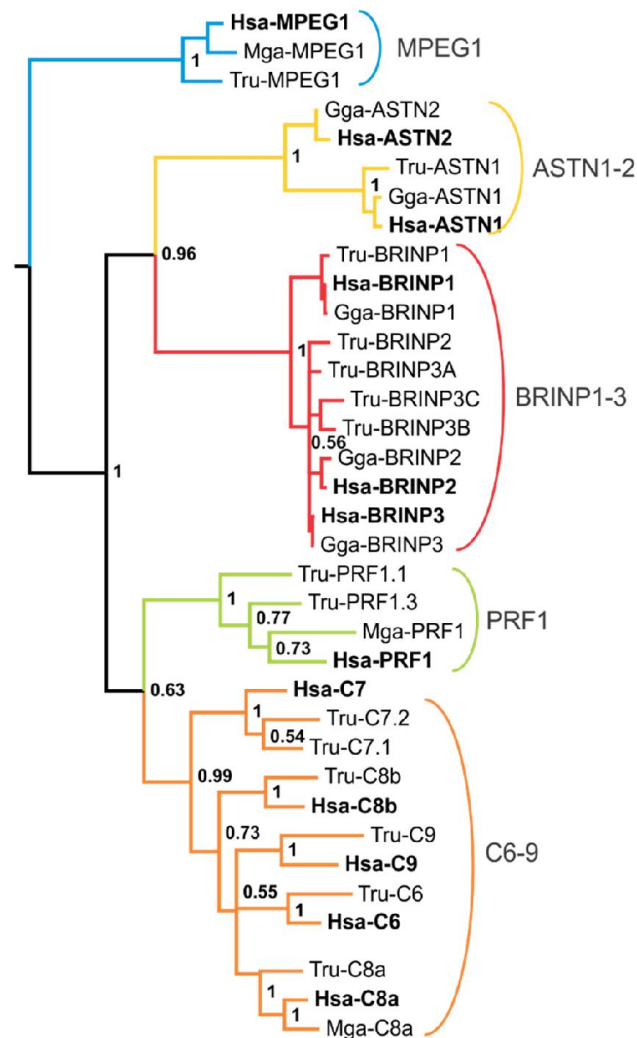


Figure 1-7 – Phylogeny of the vertebrate MACPF family

Bayesian inference tree with posterior probabilities shown at the nodes, using Refseq protein sequences from human (Hsa), chicken or turkey (Gga or Mga) and fugu (Tru) for each of the MACPF proteins found in the human genome. The tree compares protein sequence within the MACPF domain region for each homologue. Note: BRINP3 has 3 paralogues (A-C) in fish.

This figure was produced for thesis publication by M. D'Angelo (D'angelo, 2014), and included here with permission from the author.

1.5.3 An overview of Astrotactin and BRINPs

Astrotactins

Family group: Astrotactin1, Astrotactin2

Synonyms: ASTN1, ASTN2, KIAA1747, KIAA0634, bA67K19.1

Astrotactin1 (ASTN1) and Astrotactin2 (ASTN2) are a family of proteins expressed in the CNS during development (Wilson et al., 2010). As with BRINPs, Astrotactins are also highly conserved in mammalian vertebrate systems. ASTN1 and ASTN2 share 48% sequence identity overall and 58% homology within the MACPF domain (Wilson et al., 2010). In addition to the C-terminal MACPF domain, ASTN1 and ASTN2 also have a signal sequence, a trans-membrane domain, a Fibronectin domain and three Epidermal Growth Factor (EGF) repeats as shown in Figure 1-8.

BRINPs

Family group: BRINP1, BRINP2, BRINP3

Synonyms: DBC1, DBC2, DBC3, DBCCR1, FAM5A, FAM5B, FAM5C, DBCR1L1, DBCR1L2, and IB3089A.

Note: DBC1 is also the name of an unrelated gene: Deleted in Breast Cancer.

BMP and Retinoic Acid Induced Neuro-specific Protein-1 (BRINP1) was first identified as a protein that is induced upon neuronal differentiation with BMP and Retinoic acid in embryonic rat neurons (Kawano et al., 2004). A subsequent genome search identified two further family members, BRINP2 and BRINP3. Comparative analysis shows 75% homology between BRINP2 and BRINP3, and homology of 50% for both to BRINP1. BRINPs are highly conserved in vertebrates – including human, mouse, chicken, and zebra fish – indicating an important function. All three BRINPs contain a MACPF domain at the N-terminus, spanning approximately one third of the entire protein (Figure 1-8). Other than a signal peptide and the MACPF domain, the rest of the protein remains uncharacterized, although a C-terminus coiled-coiled domain has been suggested but not confirmed (Kawano et al., 2004). A cysteine rich region exists within the uncharacterized c-terminal region, which may be important for protein-protein interaction. Seven potential glycosylation sites have been identified, suggesting that BRINPs are trafficked through the secretory pathway.

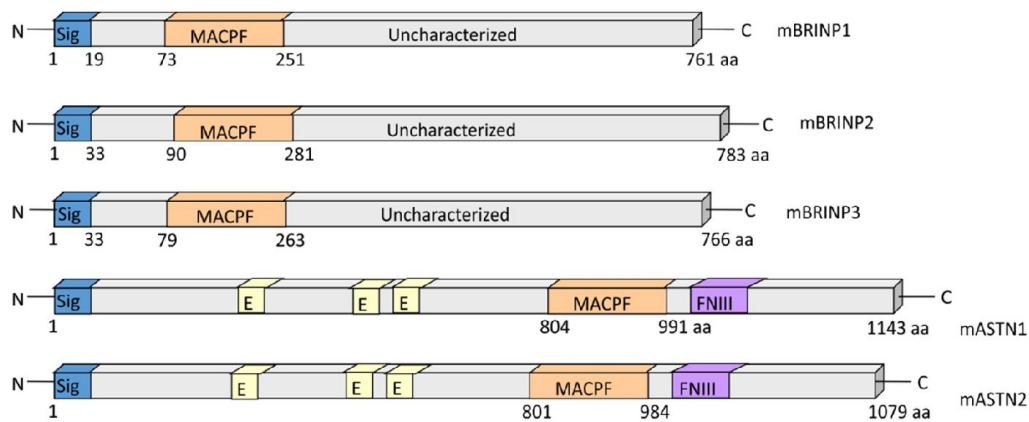


Figure 1-8 – Protein motifs of neuronal-MACPFs: Astrotactins and BRINPs

BRINP1, BRINP2 and BRINP3 have a common N-terminal MACPF domain and signal sequence (sig). The unique C-terminus consists of unique amino acid sequence.

ASTN1 and ASTN2 have a C-terminal MACPF domain and Fibronectin III domain (FNIII), three N-terminal EGF domains (E) and a signal sequence (sig).

Note: A putative transmembrane domain, suggested by Wilson et al, 2010, has been excluded from the figure due to bioinformatic analysis strongly suggesting that no transmembrane domain exists in this region (unpublished data, Whisstock and Bird labs).

1.5.4 Astrotactins and *BRINPs* are linked genes

BRINPs and Astrotactin genes are found at two conserved loci in vertebrates. *ASTN1* and *BRINP2* are adjacent on the long arm of chromosome 1 in humans and mice (Fink et al., 1997). *BRINP3* is located 11.8 million base pairs from *BRINP2* on chromosome 1. At a separate locus, *ASTN2* and *BRINP1* are flanking genes in humans on the long arm of chromosome 9, and chromosome 4 in mice (Figure 1-9).

Other genes also conserved at both loci are the *PAPPA* and Tenascin family proteins. *PAPPA1* and *PAPPA2* are members of a metalloprotease family. *PAPPA* cleaves insulin-like growth factor binding partner-4 (IGF-BP4) and so acts as a growth promoter, allowing for the activation of IGF (Phang et al., 2010). Tenascins are expressed during neural development, and are extracellular matrix proteins, facilitating neuronal migration (Porcionatto, 2006).

The human *BRINP1* locus at 9q33.1 contains a high number of brain specific genes (Jeffrey D. Falk, 1995) and patients with interstitial deletions including the region have been reported to show postnatal growth delay and broad neurological dysfunctions (Chien et al., 2010; Kulharya et al., 2008).

The *BRINP*/Astrotactin loci are of particular interest as copy number variations (CNVs) of individual genes have been reported in neurological disorders. Some examples include the *ASTN2/BRINP1* locus on chromosome 9 in humans, which is associated with autism (Glessner et al., 2009) ADHD (Lionel et al., 2011; Rommelse et al., 2010) and schizophrenia (Vrijenhoek et al., 2008). The *ASTN1/BRINP2* locus at 1q25 has also been associated with ADHD, microencephaly and mental retardation (Hu et al., 2013; Romanos et al., 2008).

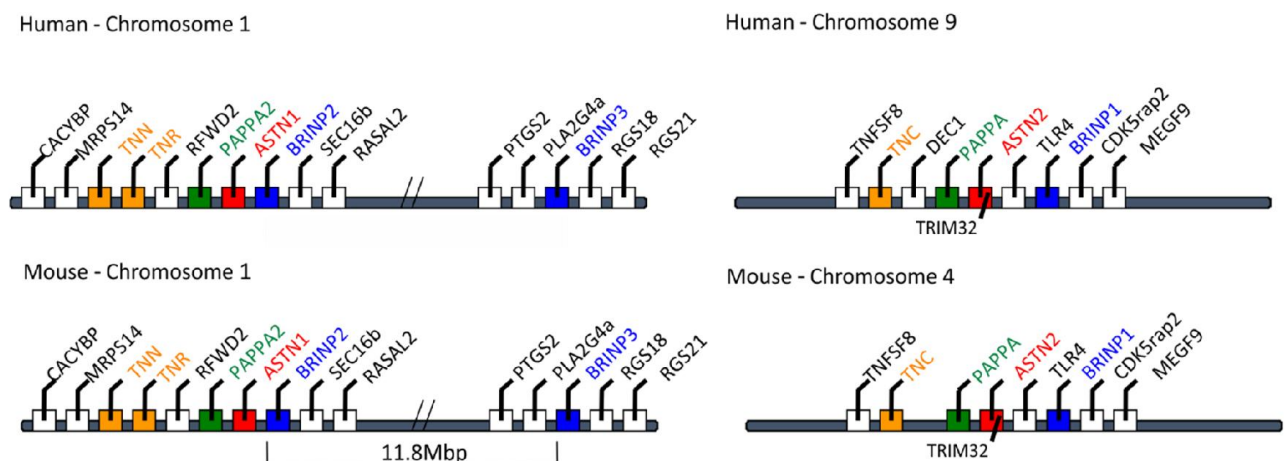


Figure 1-9 – The *ASTN* / *BRINP* loci are conserved between humans and mice

BRINP1 and *ASTN2* are adjacent genes at locus 9q33.1 in humans. *BRINP2* and *ASTN1* are adjacent genes found at human chromosome locus 1q25.2. *BRINP3* is located on the same chromosome as *BRINP2*, 11.8M bp apart.

1.6 Astrotactins

This section details current knowledge on Astrotactin1 (*Astn1*) and Astrotactin2 (*Astn2*), including cellular localization, the molecular role of these two genes in the developing and adult brain, and their association with neurodevelopmental disorders.

1.6.1 Localization of Astrotactins

1.6.1.1 Astrotactins are highly expressed in differentiated neurons

Astrotactins are almost exclusively expressed in neuronal cell populations. In the CNS, *Astn1* and *Astn2* are expressed in differentiated neurons of both the neocortex and cerebellar cortex (Wilson et al., 2010; Zheng et al., 1996). During cortical development, *Astn1* and *Astn2* are highly expressed in the pyramidal cells of the neocortex and hippocampus, and in granule neurons of the cerebellum. *Astn2* expression is absent from glial cells (Wilson et al., 2010).

1.6.1.2 Astrotactin expression during development

Wilson et al., (2010) detail the expression of Astrotactin2 (*Astn2*) in the developing mouse brain. *Astn2* expression occurs from embryonic day 12 (E12.5) in the cerebellum and cerebral cortex. *Astn2* expression in the cerebellum is high from birth until adulthood, peaking around postnatal day 10. This notable peak in expression in the juvenile brain for *Astn2* matches with a number of important developmental processes, including postnatal neurogenesis of the cerebellum, hippocampus and olfactory bulb (Altman, 1969; Bayer, 1980, 1983). In the case of cerebellum neurogenesis, Astrotactin2 has been shown to be expressed in granule neurons present in the external germinal zone (EGL), and in a punctate pattern near the surface of migrating granule neurons (Wilson et al., 2010). The peak period of cerebral granule cell proliferation and neuronal migration occurs around postnatal day 8 (P8), and both processes are complete by P15, at which time the external germinal layer (EGL disappears) (Govek et al., 2011). The expression pattern of *Astn2* in the cerebellum fits with the developmental timing for these processes. *Astn1* is shown to be broadly expressed in most brain regions at P6 (Wilson et al., 2010).

1.6.1.3 Astrotactin expression in the adult mouse brain

Wilson et al., 2010, generated *in-situ* hybridization data of expression of *Astn2* in the adult mouse brain. *Astn2* is most highly expressed in the cerebellum, within the granule cell and Purkinje cell layers. In the olfactory bulb, *Astn2* is also shown to be highly expressed in the

glomerular layer, the mitral cell layer, the granule cell layer and the anterior olfactory nuclei. *Astn2* shows only very low levels of expression in the neocortex and subcortical regions. Whilst *Astn2* is expressed in the P10 hippocampus, expression is diminished in the adult mouse hippocampus (Wilson et al., 2010). The distribution of *Astn1* mRNA in the adult mouse brain has not been published.

1.6.2 The role of Astrotactin1 and Astrotactin2 in cortical development

1.6.2.1 Astrotactin1 (*Astn1*) facilitates glial guided neuronal migration

Of the five neuronal-MACPF proteins, *Astn1* and its role in cortical development has been the most extensively studied and characterized by the work of Edmondson, Fishell and Hatten. *Astn1* was discovered as a protein that facilitates neuronal migration during cortical development; acting as an adhesion molecule for newly generated neurons (Edmondson et al., 1988; Fishell & Hatten, 1991). *Astn1* was shown to play a role in neuronal migration using an anti-Astrotactin1 polyclonal antibody that partially blocked neuronal migration *in vitro*. During cerebellar development, granule neurons bind to Bergmann glial cells and migrate along their processes *in vivo* and *in vitro*. When Astrotactin1 was blocked with an anti-Astrotactin1 antibody, granule neurons showed weaker binding and a slower migration rate. (Edmondson et al., 1988; Fishell & Hatten, 1991). The weaker binding of neurons to the glial fiber changes the neuron migration profile, as is depicted in Figure 1-10.

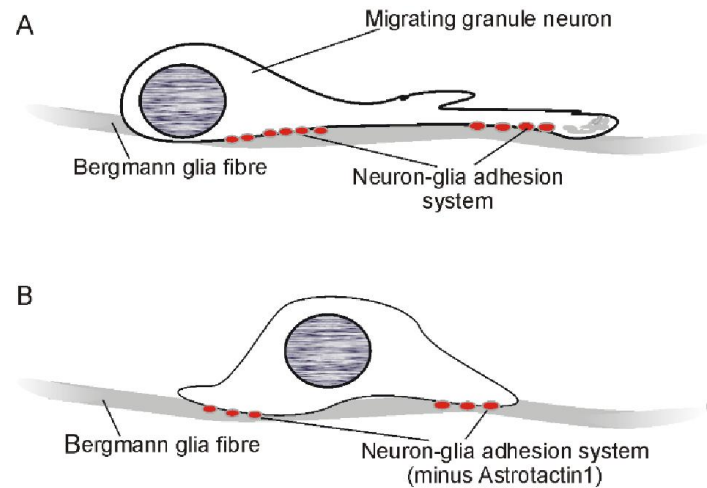


Figure 1-10 – *Astn1* facilitates migration of granule neurons migrating along glial fibers

- A) Cerebellar granule neurons form a distinctive migration profile as they move along Bergmann glial fibers. Neuron extends a leading process in the direction of travel, and the nucleus is translocated to the posterior end of the cell. Adhesion junctions form between the neuronal cell membrane and the glial cell membrane, facilitated by the adhesion molecule Astrotactin1 (Hatten, 2002).
- B) Granule neurons, in the presence of an anti-Astrotactin1 antibody, show weaker binding to the glial fiber, altering the migration profile, resulting in a slower rate of migration.

1.6.2.2 The Astrotactin1 knockout mouse phenotype

The *Astn1* knockout mouse displayed a phenotype that corresponded with *in vitro* studies showing impaired granule cell neuronal migration when Astrotactin1 is blocked (Adams et al., 2002). Granule neurons isolated from *Astn1* KO mice showed impaired migration along Bergmann glia fibers in a similar manner to addition of a blocking antibody (Adams et al., 2002). The fact that migration was able to occur in the *Astn1* KO mouse cerebellum, but at a slower rate, demonstrates that other adhesion molecules can facilitate migration in the absence of *Astn1*, and may partially compensate for the absence of *Astn1*. Other adhesion molecules are known to facilitate neuronal migration, including integrin $\beta 1$, and tenascin C, although *Astn1* is unique in facilitating neuron-glia binding (Chiquet-Ehrismann & Tucker, 2011; Hatten, 1993; Husmann et al., 1992).

Adams et al. explored the effect of disrupted migration in *Astn1* KO mice during cerebellar development. Migration of granule neurons from the external granule layer (EGL) to the internal granule layer (IGL) was impacted by weaker neuronal binding. Fewer neurons were reported to arrive at the IGL destination, resulting in decreased IGL thickness in the juvenile (P6, P15) and adult *Astn1* KO mouse brain. In the adult KO mice, there was a 10% decrease in IGL thickness. An abnormal Purkinje cell morphology was also observed, where dendrites extended across territories normally occupied by neighboring cells. The aberrant alignment of Purkinje cells was attributed to the failure of innervation of the parallel fibers of granule cells due to impaired migration. TUNEL labelling showed a mean increase of apoptotic cells in the IGL. This implies that reduced migration rates result in fewer granule cells reaching their correct IGL location, thus failing to form their correct connections, and resulting in their programmed cell death. Failure of granule cells to reach their correct location was supported by the observation of ectopic clumps of granule cells in the molecular layer in *Astn1* KO mice (Adams et al., 2002).

The functional consequences of aberrant granule migration within the cerebellum of *Astn1* KO mice were also examined by Adams et al, 2010. Behavior was analyzed by the Rotarod treadmill test, measuring the mouse's ability to balance on a rotating rod. *Astn1* KO mice were reported to have impaired motor coordination, with greater difficulty to make the correct postural adjustments to remain on the treadmill.

Interestingly, the authors chose to focus primarily on the cerebellar cortex, without studying or reporting on any defects observed in the cerebral cortex, despite *in-situ* hybridization results showing abundant *Astn1* transcripts in the cerebral cortex. An explanation may be that the cerebellum provides a good model for *in vivo* migration due to the vast number of granule cells which can be purified, and an observable phenotype of impaired motor co-ordination suggested the cerebellum as the focus of the study. Investigation of the cerebellum alone does leave open the possibility of perturbations within other brain regions, such as the neocortex or hippocampus, and changes in behavior unrelated to motor co-ordination.

1.6.2.3 The role of Astrotactin2 in cortical development.

In 2010, Wilson et al published experimental results that demonstrate *Astn2* regulates trafficking of *Astn1* during glial guided neuronal migration (Wilson et al., 2010). Localization experiments showed both *Astn1*-mCherry and *Astn2*-mCherry co-localizing with an endosomal marker (Clathrin-Venus) at the leading edge of a migrating granule neuron. A second co-localization experiment showed *Astn1*-mCherry and *Astn2*-mCherry co-localize with an endosomal marker GFP-Endo (RhoB) in HEK293T cells. *Astn1* and *Astn2* were reported to be trafficked to the cell membrane of migrating neurons. The group showed that both *Astn1* and *Astn2* are membrane bound by detecting the protein in membrane fractions of the purified cells.

Wilson et al also provided evidence that *Astn1* interacts with *Astn2*. Interaction did not depend on any individually conserved domains, an unexpected finding considering the likely importance of MACPF domains. Experimental data suggesting that *Astn2* regulates *Astn1* expression in migrating neurons was provided via live cell imaging of *Astn1*-Venus and *Astn2*-mCherry in migrating granule neurons. When *Astn1*-Venus was co-expressed with *Astn2*-mCherry there was a reported reduction in cell surface localization of *Astn1* (Wilson et al., 2010). The co-localization experiments add weight to the evidence that Astrotactins are found in the endosome, however the mCherry tag used in such experiments may affect the localization. Following the native protein by indirect immunofluorescence would give definitive evidence of the localization of the ASTN2 protein. An *Astn2* KO mouse has yet to be generated and characterized. A study of an *Astn2* KO mouse is needed to determine whether *Astn2* is required for neuronal migration.

1.6.3 Astrotactins and neurodevelopmental disorders (NDDs).

ASTN2 has emerged as an important candidate risk gene for NDDs, including autism and ADHD. Copy Number Variations (CNVs) of *ASTN2* have been identified in patients with attention deficit hyperactivity disorder and autism (Glessner et al., 2009; Lesch et al., 2008; Lionel et al., 2011; Lionel et al., 2014), as well as intellectual disability (Bernardini et al., 2010; Kashevarova et al., 2014). Table 1-2 details reports of association of *ASTN1* and *ASTN2* with NDD. In a recent large cohort study by Lionel et al, consisting of genetic testing of 64,114 NDD patients and 25,871 controls, 46 NDD subjects were identified to have part or all of the 3' end of the *ASTN2* gene deleted (Lionel et al., 2014). Several of the deletions at the 3' end of *ASTN2* also encompassed *TRIM32*, a small two-exon gene nested within an intron of *ASTN2*, transcribed from the opposite strand to *ASTN2*. The diagnoses of individuals with *ASTN2/TRIM32* deletions included ASD, ADHD and speech delay. Significant correlation between the deletion of 3' end *ASTN2* and NDD presentation was found for male NDD subjects. Twelve copy number gains of *ASTN2* were also reported in NDD patients.

The emergence of *ASTN2* as a candidate risk gene for neurodevelopmental disorders fits with evidence that alterations to several other neuronal migration genes can result in neurodevelopmental disorders (Valiente & Marin, 2010). Examples included *CNTNAP2* and *Reelin* genes, where SNPs and CNVs have been associated with increased susceptibility to autism (Alarcon et al., 2008; Folsom & Fatemi, 2013). A deletion at the *ASTN2* locus has been reported in two patients with schizophrenia (Vrijenhoek et al., 2008), suggesting that the deletion of *ASTN2* can give rise to multiple psychiatric disorders. Reports of CNVs for *ASTN1* are rarer, with two losses and one gain detected in NDD patients, affecting regions including *ASTN1/BRINP2* plus other flanking genes (Lionel et al., 2014). *ASTN1* has also been linked to alcohol dependence in a GWAS study (Hill et al., 2012).

Table 1-2 - Associations of Astrotactins with neurological disorders

Astrotactin	Neurological disorder	Study type and findings
Astrotactin1	Intellectual Disability (ID)	Screen of Russian children with ID for CNVs. Identified one patient (Case 12) with a 6.14 Mb multi-gene duplication at 1q25.1–q25.2, including <i>ASTN1/BRINP2</i> (Kashevarova et al., 2014)
	Unspecified NDD	Large scale screen of 64,114 NDD subjects for CNVs at the 1q25.2 locus. Identified two patients with a deletion in a region spanning <i>ASTN1/BRINP2</i> , and one patient with a duplication (Lionel et al., 2014).
	Alcohol dependence	GWAS identifying four alcohol dependent families with SNPs in <i>ASTN1</i> (Hill et al., 2012).
Astrotactin2	ASD, ADHD, ID	Large scale screen of 64,114 NDD subjects for CNVs at the 9q33.1 locus. Identified 46 patients with deletions within <i>ASTN2</i> , and 12 patients with <i>ASTN2</i> duplications (Lionel et al., 2014).
	ASD and ADHD	Screen of ADHD and ASD patients for CNVs at the 9q33.1 locus. Identified two ADHD patients with a deletions in <i>ASTN2</i> . Also identified three ASD patients with deletions in <i>ASTN2</i> and one <i>ASTN2</i> duplication (Lionel et al., 2011)
	ASD	Whole-genome CNV study on a cohort of 859 ASD subjects. Identified <i>ASTN2</i> CNV enrichment relative to controls (Glessner et al., 2009).
	ADHD	GWAS showed pedigree linkage of <i>ASTN2</i> mutations and ADHD (Lesch et al., 2008)
	ID	Screen of 70 ID patients for CNVs. Identified one patient with an <i>ASTN2</i> deletion (Bernardini et al., 2010)
	Tourette Syndrome (TS)	Screen of 460 TS subjects for CNVs. Identified one deletion and one duplication in <i>Astn2</i> (Fernandez et al., 2012)
	Schizophrenia, epilepsy	Whole genome screening of 54 patients with deficit schizophrenia for CNVs. Identified one patient with an <i>ASTN2</i> deletion (Vrijenhoek et al., 2008).
	Alzheimer's disease	GWAS showed linkage of <i>ASTN2</i> with reductions in hippocampal volume, possibly associated with cognitive decline (Bis et al., 2012)
	Alzheimer's disease	GWAS of 791 AD patients and 782 control subjects. Identified age of onset association with <i>ASTN2</i> polymorphisms (Wang et al., 2014)

1.7 *Brinps*

This section details current knowledge on *Brinp1*, *Brinp2* and *Brinp3*, including cellular localization in the developing brain, proposed molecular function and association of *BRINPs* with neurodevelopmental disorders.

1.7.1 Localization of *Brinps*

1.7.1.1 *Brinps* are highly expressed in differentiated neurons

The cellular and global expression of *Brinps* is described by Kawano et al, 2004. *Brinps* are shown to be almost exclusively expressed in neuronal cells in the central and peripheral nervous system (Kawano et al., 2004). All three *Brinps* appear in differentiated neurons in the cerebral and cerebellar cortices during development. *Brinps* are expressed in the pyramidal layers of the hippocampus, a region densely populated with neurons. *Brinps* are also expressed in granule neurons in the cerebellum. *Brinp* mRNA is almost completely absent from non-neuronal cells. The three *Brinps* do not appear in white matter, where glial cells are dominant. *Brinp* expression is also absent from Schwann cells (Kawano et al., 2004).

1.7.1.2 *Brinp* expression during development

Kawano et al explore the cellular localization of *Brinps*, and the expression patterns of *Brinp1*, *Brinp2* and *Brinp3* in the developing mouse and rat brain. *Brinp1* is the most widely expressed of the three *Brinps* throughout development, with *Brinp2* and *Brinp3* expression observed in the some of the same cortical areas as *Brinp1* (Kawano et al., 2004).

Reverse transcriptase PCR analysis of tissue from developing rodent brains shows *Brinp1* to be detectable in the mouse brain as early as embryonic day nine (E9), with *Brinp2* and *Brinp3* detectable from embryonic day eleven (E11). *In situ* hybridization data by Kawano et al showed an increase in expression levels of *Brinps* postnatally, peaking at postnatal day 14 (P14), with expression of all three *Brinps* continuing into adulthood in certain brain regions. The notable peak in expression in the juvenile brain coincides with a number of important developmental processes including postnatal neurogenesis of the cerebellum, hippocampus and olfactory bulb (Altman, 1969; Bayer, 1980, 1983). In the case of cerebellum neurogenesis, the peak period of cerebral granule cell proliferation and neuronal migration occurs around postnatal day 8 (P8), and both processes are complete by P15, at which time the EGL disappears (Govek et al., 2011). The expression patterns of *Brinp1*, *Brinp2* and *Brinp3* appear

to show overlap with the developmental timing for these processes. The expression of *Brinps* post-development i.e. in the adult mouse brain, indicates that *Brinps* may also have an additional role unrelated to the promotion of cell proliferation or neuronal migration.

1.7.1.3 *Brinp* expression in the adult mouse brain

In situ hybridization data on sagittal adult mouse brain sections by Kawano, et al. shows high *Brinp1* expression in the cerebral cortex, cerebellum, hippocampus, and the olfactory bulb. Expression of *Brinp1* is also evident in subcortical regions, such as the thalamus. *Brinp2* and *Brinp3* are also expressed in the adult mouse brain, but are more region-specific. All *Brinp* genes are expressed in the cortex, with highest expression in layers II-IV (Kawano et al., 2004). In the hippocampus *Brinp1* and *Brinp2* are highly expressed. *Brinp3* expression levels are much lower in this region. *Brinps* also show different distribution in the cerebellum. *Brinp1* is expressed in the external granule cell and Purkinje cell layers, whereas *Brinp2* and *Brinp3* are expressed exclusively in the Purkinje cell layer. In the olfactory bulb, *Brinp2* and *Brinp3* are almost exclusively in the granule cell layer. *Brinp1* is also highly expressed in the glomerular layer, the mitral cell layer and the anterior olfactory nuclei as well as the granule cell layer. In subcortical regions, *Brinp1* is most highly expressed in the striatum. Only *Brinp3* is not expressed in the thalamus. *Brinp1* and *Brinp3* are expressed in the hypothalamus. *Brinp1* is expressed in the brain stem (pons and medulla), *Brinp2* and *Brinp3* are not. *Brinp1* and *Brinp3* are highly expressed in the amygdala complex.

1.7.1.4 *Brinp* expression in the peripheral nervous system

Brinp1 was first identified in the Superior Cervical Ganglia of the rat peripheral nervous system. RT-PCR analysis by Kawano et al showed *Brinp1* and *Brinp2* to be highly expressed in this cell type at early postnatal stages, peaking between postnatal day 2 and day 5. Weak expression of *Brinp1*, *Brinp2* and *Brinp3* is shown in the spinal cord by Northern blot analysis.

1.7.1.5 Subcellular localization of BRINPs

There have been no published studies that show the localization of BRINP1, BRINP2 or BRINP3 by directly labelling endogenous protein. The literature currently has conflicting data on BRINP localization. All three BRINPs are reported to be located in the cytoplasm of transfected carboxyl-terminal-EGFP-tagged BRINP PC12 cells (Kawano et al., 2004). In NIH3T3 (non-neuronal) cells transfected with carboxyl-terminal-EGFP-tagged BRINP, localization is

reported in the intra-nuclear space and endoplasmic reticulum (Kawano et al., 2004). It is possible that the addition of C-terminal tag may affect the localization. Anti-BRINP antibodies are required to detect endogenous-BRINP subcellular localization.

BRINP1 has also been reported to be localized at the post synaptic density of neurons in proteomic studies (Dahlhaus et al., 2011; Laumonnier et al., 2007). This is currently unverified by immunofluorescence studies.

1.7.2 *Brinps* are induced upon differentiation

Kawano et al and Terashima et al. have described this family of proteins based on their induction upon differentiation from progenitor cell types into post-mitotic neurons in a number of primary and secondary cell lines (Kawano et al., 2004; Terashima et al., 2010). *Brinp1* was initially discovered in an experiment where a combination of BMP and retinoic acid induced transcription of *Brinp1* mRNA in E17 Superior cervical ganglion (SCG) neurons. This observation resulted in the naming of the protein BMP and RA Induced Neural specific Protein 1. Despite the two other genes (*Brinp2* and *Brinp3*) sharing this name, it is important to note that they are not induced by BMP/RA in this cell type. In fact, despite the BRINP name suggesting BMP and retinoic acid induction of all three genes, levels of *Brinp2* mRNA decrease upon differentiation in SCG neurons. Therefore the synergistic effect of BMP/RA combined should be attributed to *Brinp1* alone. *Brinp2* mRNA is seen even in undifferentiated neurons, implying that the gene is already switched on before differentiation, therefore acting at a different time point to the other two *Brinps*. *Brinp3* shows a pattern of low levels / absence in secondary cell lines. *Brinp3* is induced in a similar pattern to *Brinp1* in primary lines, possibly indicating it acts at the same time point as *Brinp1* at lower levels. Whether *Brinps* themselves play a role in the differentiation process or the genes are turned on in order to facilitate a molecular role for the post-mitotic neuron is unknown.

1.7.3 A role for *Brinps* in regulating cell cycle progression or neuroplasticity?

Brinp1 has been suggested to have a role in cell cycle suppression. Overexpression of *Brinp1*, *Brinp2* and *Brinp3* in non-neuronal cell lines was shown to result in a decrease in G1 to S-phase transition (Kawano et al., 2004; Terashima et al., 2010; Toshiyuki & Ichiro, 2004). Whilst these experiments suggest a role for *Brinps* in cell cycle regulation, the overexpression of non-endogenous protein may itself be the cause of cell cycle arrest. Greater proof is

needed to determine whether *Brinps* control cell proliferation, e.g. evidence of increased proliferation after gene deletion.

Brinp1 and *Brinp3* have also been found to be upregulated in song learning in birds, suggesting a role for *Brinps* in neuroplasticity (Lovell et al., 2008; Wood et al., 2008).

1.7.4 *BRINP1* and neurodevelopmental disorders (NDDs)

Genome wide association studies have provided some evidence that changes to the *BRINP1* gene can result in other neurological disease. Genome wide screens have identified associations between *BRINP1* and Alzheimer's (Heinzen et al., 2010), Parkinson's disease (Do et al., 2011; Edwards et al., 2010), and multiple sclerosis (International Multiple Sclerosis Genetics et al., 2007). *BRINP1* has also been implicated as a biomarker for schizophrenia (Vawter et al., 2011). One ClinVar case (GRCh38/hg38 9q33.1-33.2) does report a patient where a copy number deletion resulted in developmental delay (no further details of the patient diagnosis are provided).

As mentioned previously, *BRINP1* and *ASTN2* are found at the same gene locus on chromosome 9 in humans. The close proximity of these two genes mean that in several instances of CNVs, more than one gene at the screened loci may be disrupted. Lionel et al, report a subset of NDD patients with changes to the 9q33.1 locus covering not only *ASTN2*, but also sections of DNA containing the *BRINP1* gene (Lionel et al., 2014). Table 1-3 details reports of association of *BRINPs* with NDD.

1.7.5 *BRINP2* / *BRINP3* and neurodevelopmental disorders (NDDs)

Neither *BRINP2* nor *BRINP3* genes have been reported to be altered in patients with neurodevelopmental disorder, however *BRINP2/ASTN1* locus 1q25.2 has been associated with ADHD (Romanos et al., 2008), microcephaly and intellectual disability (Hu et al., 2013). Two CNVs (one deletion and one duplication) were reported in patients with NDD that span both *ASTN1/BRINP2* gene loci, making it impossible to discern whether alteration to one or both of these genes is responsible for the neuropathology (Lionel et al., 2014). The close proximity of *ASTN1* means that either gene could be causing the underlying genetic etiology in these patients.

Mutations in *BRINP2* have been linked to substance abuse and reward dependence in two studies (Drgon et al., 2011; Verweij et al., 2010), which may suggest a role for *BRINP2* in dopaminergic reward systems and addiction.

No *BRINP3* association with NDD has been reported, however changes in *BRINP3* levels have been reported to correlate with changes in norepinephrine (a neurotransmitter and stress hormone) during exercise (Károly et al., 2012).

1.7.6 Non-NDD pathologies associated with *BRINPs*

This section discusses reports of *BRINPs* in non-neurological human disease. Such findings may indicate more general roles for *BRINPs* and, together with studies using animal models, provide insight into a functional role of *BRINP1* gain or loss.

1.7.6.1 *BRINPs* and cancer

Intriguingly, despite the very low level of expression in non-neuronal tissue (Kawano et al., 2004), all three *BRINPs* have been implicated in several different forms of cancer. In particular *BRINP1* has been described as a putative tumor suppressor, where loss of *BRINP1* expression has been detected in bladder cancer samples (Habuchi et al., 1998), and reduced *BRINP1* expression has been associated with poor bladder cancer prognosis (Shim et al., 2013). Loss of heterozygosity and hyper-methylation of the *BRINP1* (*DBCCR1*) gene has been reported in oral squamous cell carcinoma tumors (Gao et al., 2004). *BRINP1* loss has also been reported in astrocytic tumors (Beetz et al., 2005). It is unclear whether the loss of *BRINP1* directly contributes to cancer, or whether reduced expression of *BRINP1* in cancer tissue, reported by Habuchi et al, 1998 and Shim et al, 2013, is the result of overall dysregulation of gene expression at the *BRINP1* locus.

Alterations to the *BRINP2* (*FAM5b*) gene were detected in oral squamous cell carcinoma (Cha et al., 2011). *BRINP3* has been reported to be overexpressed in pituitary adenomas by a study comparing 10 gonadotropinomas with nine normal pituitaries by cDNA array. Overexpression of *BRINP3* in gonadotrope cell pituitary adenomas was demonstrated to result in an increase in proliferation, migration and invasion (Shorts-Cary et al., 2007).

Table 1-3 - Associations of *BRINPs* with neurological disorders

BRINP	Neurological disorder	Study type
<i>BRINP1</i>	Unspecified NDD	Large scale screen of 64,114 NDD subjects for CNVs at the 9q33.1 locus. Duplication of region including both <i>ASTN2</i> and <i>BRINP1</i> in reported in seven NDD patients (Lionel et al., 2014).
	Schizophrenia	<i>BRINP1 (DBC1)</i> reported as one of four genes that discriminates with first episode Schizophrenia by GWAS. No supporting data included or referenced (Vawter et al., 2011).
	Parkinson's disease (PD)	GWAS of 3,426 PD cases and 29,624 controls). <i>BRINP1 (DBC1)</i> SNP within top 50 associations (Do et al., 2011).
	Parkinson's disease	GWAS of 604 cases and 619 controls. <i>BRINP1 (DBC1)</i> SNPs shows strong association to Parkinson's disease (Edwards et al., 2010).
	Late onset Alzheimer's disease	Genome-wide scan of Alzheimer's disease in a set of 331 cases and 368 controls, including assessments of CNVs. Intergenic SNPs within <i>BRINP1 (DBC1)</i> reported within top 20 associations with late-onset dementia (Heinzen et al., 2010).
	Multiple Sclerosis	Analysis of SNPs from 2322 case subjects, and 5418 control subjects. <i>BRINP1 (DBC1)</i> SNPs within highest 17 statistical associations (International Multiple Sclerosis Genetics et al., 2007).
<i>BRINP2</i>	Intellectual Disability (ID)	Screen of Russian children with ID for CNVs. Identified one patient (Case 12) with a large (6.14 Mb) multi-gene duplication at 1q25.1–q25.2, including <i>ASTN1/BRINP2</i> (Kashevarova et al., 2014).
	Unspecified NDD	Large scale screen of 64,114 NDD subjects for CNVs at the 1q25.2 locus. Identified two patients with a deletion, and one patient with a duplication of <i>ASTN1/BRINP2</i> (Lionel et al., 2014).
	Drug addiction	GWAS of 1620 individuals with substance dependence identifies SNPs within <i>ASTN1/BRINP2 (FAM5B)</i> region associated with drug addiction (Drgon et al., 2011).
	Reward dependence	A GWAS of Cloninger's Temperament scales on 5117 individuals. <i>BRINP2 (FAM5B)</i> SNPs within top five strongest associations for reward dependent personality (Verweij et al., 2010).
<i>BRINP3</i>	No reported associations between <i>BRINP3 (FAM5C)</i> and neurological disease.	

1.7.6.2 *BRINPs* and heart disease

BRINP2 has been linked to coronary heart disease (Angelakopoulou et al., 2012). Polymorphisms were identified within *BRINP3 (FAM5C)* that were in a region that showed moderate linkage in a GWAS for myocardial infarction and a separate scan for coronary artery disease. In this study the presence of a T>A SNP at the 3' end of the *BRINP3* coding region is shown to result correlate with a reduction in *BRINP3* expression in human aorta tissue (Connelly et al., 2008).

1.7.6.3 *BRINP3* and aggressive periodontitis

BRINP3 (FAM5C) was identified as a candidate gene for aggressive periodontitis. No significant changes in the coding region were found for either of the two markers, but variations in the intronic regions were identified. *BRINP3 (FAM5C)* mRNA levels were reported to be elevated in diseased tissue (Carvalho et al., 2010).

1.7.7 *Brinp* Summary

The current body of evidence gives some suggestion as to the role of *Brinps* in neurodevelopment, whilst the mechanism is largely unknown. The high expression in the mammalian brain during development, and high level of conservation in vertebrates suggests important functions for each of the three *Brinps*.

Clues to *Brinp* function may come from their closest related protein family; Astrotactins, with which *Brinps* share a common MACPF domain, and proteins of these families are expressed in similar brain regions. Some notable overlaps in expression patterns can be observed between the MACPF proteins that may provide clues to the function of *Brinps* within the mammalian brain. It is certainly interesting how closely *Brinp1* matches the expression pattern for *Astn2* in several regions of the adult mouse brain. This may be co-incidental, but could also suggest a common function, or that these two genes at the same locus are coordinately regulated. The partially overlapping expression of *Brinp2* and *Brinp3* also suggest possible interaction between *Brinp2* and *Brinp3*, or between *Brinp1* and the other two *Brinps*. The timing of *Brinp* expression may also offer a clue to their molecular role. For example, the peak in expression of these MACPF proteins may highlight a critical role for *Brinps* in processes occurring at this developmental stage. This has been shown to be the case with *Astn2*, which

is most highly expressed at around P14 in the cerebellum, coinciding with peak granule neuron migration in the cerebellum (Wilson et al., 2010).

Given the high expression of neuronal-MACPFs in multiple brain regions, predictions can be made on the effect of deletion of these genes on brain development and behavior in knockout mouse models. The abundance of expression in critical brain regions suggests that absence of any of the *Brinps* could be embryonic lethal if the protein is required in brain development or to regulate basic autonomic functions such as breathing or heart rate. The hippocampus plays an important role in memory encoding and spatial memory (O'Keefe & Dostrovsky, 1971; Scoville & Milner, 1957). The high expression of these genes in the hippocampus means that deletion of any of the *Brinp* or *Astrotactin* genes could impair performance on a working memory or spatial orientation task. The cerebellum has a key function in fine motor control (Fine et al., 2002). Deletion of *Astn1* has been shown to result in impaired motor co-ordination in mice (Adams et al., 2002). A similar motor co-ordination phenotype may therefore exist for mice lacking one or more *Brinps*. The olfactory bulb is the brain region important for processing olfactory information (Mori et al., 2006). High expression of *Brinp1*, *Brinp2*, *Astn1* and *Astn2* could indicate that a knockout mouse lacking any of these genes would have an impaired sense of smell. Olfaction is also important in recognition and identification of other mice, so sociability may be affected (Feierstein, 2012). The amygdaloid complex has been demonstrated to be important in emotional regulation and fear (Kalin et al., 2004; Prather et al., 2001). The high expression of *Brinp* genes in the amygdala suggests that these genes may be involved in emotional regulation. Knockout mice lacking one or more *Brinps* may show changes in emotional responses such as anxiety, fear, or sociability.

BRINPs currently show limited association with NDDs, and have been linked to cancer and heart disease, despite low levels of expression in non-neuronal tissue. Investigating the absence of *Brinps* from the mammalian system will likely contribute to a greater understanding of the role of *Brinps* in the mammalian brain.

1.8 Hypothesis

1.8.1 *Brinps* facilitate migration of post-mitotic neurons.

Brinps and Astrotactins are expressed in overlapping temporal and spatial patterns in the rodent brain, and the two sets of genes are found at common chromosome loci in rodents and humans. Furthermore, Astrotactins and *Brinps* share homology via the MACPF domain. From these observations, we predict a common mechanism for the five neuronal-MACPF proteins. Astrotactin1 has been demonstrated to facilitate adhesion of the migrating neuron on glial fibers (Edmondson et al., 1988). We hypothesize that one or more *Brinps* also function in this role during neural development.

If *Brinps* and Astrotactins are able to associate at the cell membrane, it is possible that this would occur as part of a complex, reminiscent of the assembly of Membrane Attack Complex members C6, C7, C8 α and C8 β . If *Brinps* do form a complex, we would predict that the interdependence of the three genes would mean that knocking out any of the three *Brinp* genes would result in the same neurological phenotypes. If *Brinps*, like Astrotactins, are involved in the neuronal migration, we predict that *Brinp* KO mice will have a similar phenotypic result to the *Astn1* KO mice, namely changes in neuronal positioning, which would result in changes in cellular architecture of the brain. This may be either in the cerebellum (as reported for *Astn1* KO mice) or in another brain region where *Brinps* are highly expressed. This, in turn, is predicted to result in behavioral malfunction which may be impaired motor co-ordination if the cerebellum is affected, or other behavioral changes that may allude to a potential association between *Brinps* and human NDDs.

1.9 Thesis aims

1.9.1 To investigate the role of *Brinp1*, *Brinp2* and *Brinp3* on neuroanatomy and behavior.

Questions to be addressed:

- Given that *Brinps* are almost exclusively expressed in the nervous system of mammals, does their absence result in changes to behavior?
- If so, do any changes in behavior correlate with anatomical changes in specific brain regions where the genes are expressed?

1.9.2 To determine the relationship between the three *Brinp* genes and their molecular role in the mammalian nervous system.

Question to be addressed:

- Do neuronal-MACPF genes compensate when one gene is deleted?

Chapter 2: Materials and methods

2.1 Antibody list

Table 2-4 - Primary antibodies used for immunohistochemistry and immuno-blotting

Antigen	Host	Working dilution	Supplier	Cat. #	Mono/ Poly
CUX1	Rabbit	1:100	Santa Cruz	CDP(M-222)	Polyclonal
GFAP	Rabbit	1:200	Dako	Z0334	Polyclonal
Parvalbumin	Mouse	1:200	Sigma	P3088	Monoclonal
NeuN	Mouse	1:100	Millipore	MAB377	Monoclonal
Calbindin	Mouse	1:500	Abcam	CB-955	Monoclonal
Calretinin	Rabbit	1:200	Swant	6B3	Monoclonal
Somatostatin	Rabbit	1:200	Millipore	AB5494	Polyclonal
BRINP1	Rat	1:200	Custom made	Rat 2	Polyclonal
βIII-Tubulin	Rabbit	1:500	Covance	MMS-435P	Monoclonal
BrdU	Mouse	1:100	BD	347580	Monoclonal
β-Actin (I-19)	Rabbit	1:1000	Santa Cruz	Sc-1616-R	Polyclonal
Caspase 3	Rabbit	1:1000	R&D systems	AF835	Polyclonal
Ki67	Rabbit	1:1000	Leica	NCL-Ki67p	Monoclonal
pHH3	Rabbit	1:400	Millipore	06-570	Polyclonal
FOXP2	Rabbit	1:500	Abcam	Ab16046	Polyclonal

Table 2-5 –Secondary antibodies used for immunohistochemistry and immuno-blotting

Conjugate	Species	Working dilution	Supplier	Cat. #
HRP	Rat	1:5000	Rockland	612-703-002
HRP	Mouse	1:5000	Millipore	AP326P
AF 488	Mouse	1:800	Molecular probes	A11029
AF 586	Mouse	1:800	Molecular probes	A11031
AF 488	Rat	1:800	Molecular probes	A21208
AF 586	Rat	1:800	Molecular probes	A11077
AF 488	Rabbit	1:800	Molecular probes	A11008
AF 586	Rabbit	1:800	Molecular probes	A10042

2.2 Oligonucleotide primer list

Table 2-6 - Oligonucleotide primer list

Primer	Gene	Sequence	Direction	PCR type
PB154	<i>Neo'</i>	ATATTGCTGAAGAGCTTGGCGGC	Sense	Genotyping
PB1412	<i>Brinp1 / Brinp3</i>	AAAAGCGCCTCCCCTACCCG	Sense	Genotyping
PB1413	<i>Brinp1</i>	GCTTCACGTTATCATTGCCATC	Sense	Genotyping
PB1414	<i>Brinp1</i>	TGTTAACCTCTTCCAAGCCC	Antisense	Genotyping
PB1415	<i>Brinp2</i>	TATCGTTCTATTTCCCTGCATC	Sense	Genotyping
PB1416	<i>Brinp2</i>	AGACCAGTCCCCACCGCC	Antisense	Genotyping
PB1417	<i>Brinp3</i>	TACTCTGGGAGGTAGGAGAC	Sense	Genotyping
PB1418	<i>Brinp3</i>	GTCCTTCATGCTCATTCAATCC	Antisense	Genotyping
PB1457	<i>Brinp1</i>	CTATGGCTGTGTTCTCACC	Antisense	Genotyping
PB1458	<i>Brinp2</i>	CTCTGTGAGGCAGGGCAACTG	Sense	Genotyping
PB1459	<i>Brinp2</i>	CTCCACAGTGCCCTTCCCACG	Antisense	Genotyping
PB1461	<i>Brinp3</i>	CTGTAGAGTAGGTCGTCGTCCCA	Antisense	Genotyping
PB1473	<i>Brinp1</i>	CCAGGGACCACAGTAATTCTC	Sense	Genotyping
PB1497	<i>Brinp3</i>	GAATTGGGAAGATATCTTGGGAATG	Sense	Genotyping
PB1556	<i>Brinp1</i>	CTGGGACAGACCAACATGTCTC	Sense	RT-PCR
PB1562	<i>Brinp1</i>	GCTCTCCGTGCTTTGCAGAAGG	Antisense	RT-PCR
PB1557	<i>Brinp2</i>	GGACTGGCTGCTCACAGACCG	Sense	RT-PCR
PB1558	<i>Brinp2</i>	GTGCTCTCTGTCAATGAAG	Antisense	RT-PCR
PB1559	<i>Brinp3</i>	CCCCTTCGACTGGCTCCTCTC	Sense	RT-PCR
PB1560	<i>Brinp3</i>	CCTGTCCGTGTTTCTGTACC	Antisense	RT-PCR
PB584	<i>GAPDH</i>	GACCCCTTCATTGACCTCAAC	Sense	RT-PCR
PB585	<i>GAPDH</i>	GATGACCTTGCCACAGCCTT	Antisense	RT-PCR
PB1614	<i>Brinp1</i>	TATGCGAGCTGGACGCAGG	Sense	qPCR
PB1615	<i>Brinp1</i>	TGCTGCCGGCCTTTTCCTC	Antisense	qPCR
PB1616	<i>Brinp2</i>	TCCGCCTGCCCAAGGAGAGA	Sense	qPCR
PB1617	<i>Brinp2</i>	CCAAGGCACATGGGATGGG	Antisense	qPCR
PB1610	<i>Brinp3</i>	AGGTCCTCTGGCTGCAGTA	Sense	qPCR
PB1611	<i>Brinp3</i>	GCAGATAAACTCGCCCTCAG	Antisense	qPCR
PB1698	<i>Astn1</i>	AGGATCCTGTCCACAAGCAC	Sense	qPCR

PB1699	<i>Astn1</i>	CCCCGAGGGTATAGGTGAAT	Antisense	qPCR
PB1700	<i>Astn2</i>	CGTGACTGCTCAAGGAACAA	Sense	qPCR
PB1701	<i>Astn2</i>	AAGCCATCAGAGCAGTCGAT	Antisense	qPCR
PB1651	<i>B-Actin</i>	CAGGTCATCACTATTGGCAACGAG	Sense	qPCR
PB1652	<i>B-Actin</i>	CCACAGGATTCCATACCCAAGAAG	Antisense	qPCR
PB1653	<i>GAPDH</i>	TGTGTCCGTCGTGGATCTGA	Sense	qPCR
PB1654	<i>GAPDH</i>	TTGCTGTTGAAGTCGCAGGAG	Antisense	qPCR

2.2.1 List of mouse genotypes (C57BL/6 background)

Table 2-7 - Nomenclature for *Brinp* transgenic mice genotypes

Abbreviated designation	Allele designation	Allele Accession ID
WT	<i>Brinp</i> ^{+/+}	
<i>Brinp1</i> targeted	<i>Brinp1</i> ^{tm1Pib/tm1Pib}	MGI:5604540
<i>Brinp2</i> targeted	<i>Brinp2</i> ^{tm1Pib/tm1Pib}	MGI:5604614
<i>Brinp3</i> targeted	<i>Brinp3</i> ^{tm1Pib/tm1Pib}	MGI:5604619
<i>Brinp1</i> knockout (KO)	<i>Brinp1</i> ^{tm1.1Pib/tm1.1Pib}	MGI:5604542
<i>Brinp1</i> heterozygous (het)	<i>Brinp1</i> ^{tm1.1Pib/+}	
<i>Brinp2</i> knockout (KO)	<i>Brinp2</i> ^{tm1.1Pib/tm1.1Pib}	MGI:5604615
<i>Brinp2</i> heterozygous (het)	<i>Brinp2</i> ^{tm1.1Pib/+}	
<i>Brinp3</i> knockout (KO)	<i>Brinp3</i> ^{tm1.1Pib/tm1.1Pib}	MGI:5604620
<i>Brinp3</i> heterozygous (het)	<i>Brinp3</i> ^{tm1.1Pib/+}	
<i>Brinp2/3</i> knockout (KO)	<i>Brinp2</i> ^{tm1.1Pib/tm1.1Pib}	MGI:5604615
	<i>Brinp3</i> ^{tm1.1Pib/tm1.1Pib}	MGI:5604620
<i>Brinp1/2/3</i> knockout (KO)	<i>Brinp1</i> ^{tm1.1Pib/tm1.1Pib}	MGI:5604542
	<i>Brinp2</i> ^{tm1.1Pib/tm1.1Pib}	MGI:5604615
	<i>Brinp3</i> ^{tm1.1Pib/tm1.1Pib}	MGI:5604620
<i>Brinp1</i> ^{FLPe}	<i>Brinp1</i> ^{tm1.2Pib/tm1.2Pib}	MGI:5604543
<i>Brinp2</i> ^{FLPe}	<i>Brinp2</i> ^{tm1.2Pib/tm1.2Pib}	MGI:5604617
<i>Brinp3</i> ^{FLPe}	<i>Brinp3</i> ^{tm1.2Pib/tm1.2Pib}	MGI:5604621
<i>Brinp2/3</i> knockout (KO)	<i>Brinp2/3</i> ^{tm1.1Pib/tm1.1Pib}	MGI:5604615, MGI:5604620
<i>Brinp1/2/3</i> knockout (KO)	<i>Brinp1/2/3</i> ^{tm1.1Pib/tm1.1Pib}	MGI:5604542, MGI:5604615, MGI:5604620

2.4 Buffers and solutions

Acrylamide, 30% (w/v) stock

30% (w/v) acrylamide, 0.8% (w/v) N,N'-methylene-bis-acrylamide.

Antibody diluent

PBS with 0.02% (w/v) NaN_3 .

Blocking solution

5% (w/v) skim milk powder in TBS, 0.02% (w/v), NaN_3 in TBS.

DEAE-dextran/ chloroquine

400 $\mu\text{g}/\text{ml}$ diethylaminoethyl-dextran, 100 μM chloroquine, filter sterilised and stored at 4°C.

DEPC treated water

Milli-Q water was treated with 0.1% (v/v) diethyl pyrocarbonate (DEPC) for 1 hr with stirring. DEPC was then inactivated by autoclaving for 30 min.

Dithiothreitol (DTT) stock

1 M DTT in 10 mM sodium acetate, pH 5.2.

DMEM (Dulbecco's modified Eagle's medium), complete

DMEM supplemented with 10% (v/v) heat inactivated foetal calf serum (FCS), 2 mM L-glutamine, 50 U/ ml penicillin and 50 $\mu\text{g}/\text{ml}$ streptomycin.

DNA loading buffer

0.1% (w/v) bromophenol blue, 0.1% (w/v) xylene cyanol, 50% (v/v) glycerol.

DNA wash buffer

70 % (w/v) ethanol + 30 % (w/v) (15 mM NaCl, 10 mM Tris pH8.0, 2 mM EDTA).

Frank's tail buffer

0.2% (w/v) SDS, 0.2 M NaCl, 0.1 M Tris pH 8.0, 5 mM EDTA.

Laemmli sample buffer (LSB)

62.5 mM Tris, pH 6.8, 2% (w/v) SDS, 10% (v/v) glycerol, 0.1% (w/v) bromophenol blue, dithiothreitol (DTT) was added to 100 mM immediately before use.

Lysis buffer

150 mM NaCl, 10 mM EDTA, 10 mM Tris pH 7.5, 0.4% SDS, 20 µl/ml 10 mg/ml Proteinase K.

Mowiol reagent

6 g glycerol, 2.4 g Mowiol 4.88 (Sigma-Aldrich, cat. # 81381), 100 mM Tris-HCl, pH8.5, 0.02% NaN₃.

Phosphate-buffered saline (PBS)

136 mM NaCl, 2.6 mM KCl, 10 mM Na₂HPO₄, 1.76 mM KH₂PO₄, pH 7.4.

SDS-PAGE running buffer

25 mM Tris, 192 mM glycine, 0.01% (w/v) SDS.

SDS-PAGE running gel

375 mM Tris, pH 8.8, 0.1% (w/v) SDS, acrylamide added from 30% stock to the required concentration.

SDS-PAGE stacking gel

4% (w/v) acrylamide from 30% stock, 125 mM Tris, pH 6.8, 0.1% (w/v) SDS.

Stripping buffer

62.5 mM Tris-HCl, 2% (w/v) SDS, 100 mM 2-mercaptoethanol, pH 6.8.

Taq DNA polymerase buffer (10 x)

20 mM MgCl₂, 50 mM KCl, 0.1% (v/v) Triton X-100, 10 mM Tris, pH 8.8.

Transfer buffer

25 mM Tris, 192 mM glycine, 20% (v/v) methanol.

Tris borate EDTA buffer (TBE)

9 mM Tris, 9 mM borate, 2 mM EDTA, pH 8.0.

Tris-buffered saline (TBS)

20 mM Tris, pH 7.4, 150 mM NaCl.

Tris-buffered saline Tween (TTBS)

20 mM Tris, pH 7.4, 150 mM NaCl, 0.1% Tween.

2.4.1 Plasmids

- **pSVTf**

Mammalian expression vector used for expressing a target sequence in COS-1 cells.

- **pCIG2-ires-GFP**

Mammalian expression vector with an ires GFP nuclear fluorescent marker; and amp resistance. Contains a CMV promoter. Provided by Dr. Julian Heng.

2.4.2 Cell lines

- **Cos-1**

Origin: African Green Monkey. Reference: (Gluzman, 1981).

- **NT2**

Origin: Human, malignant pluripotent embryonal carcinoma. Reference: (Cheung et al., 1999).

Synonyms: NTera2, NTERA2/D1

- **SH-SY5Y**

Origin: Human, neuroblastoma

2.5 Methods

2.5.1 Animal husbandry and ethics

Breeding of *Brinp* knockout lines was approved under animal ethics committee application SOBS/B/2008/30BC. All experiments carried out on mice were approved by Monash Animal Ethics Committee under applications MARP/2011/106 (histology) and MARP/2013/031 (behavioral testing). Mice were monitored daily by animal house staff for body condition and euthanized if they showed signs of pain or distress.

Mice were kept in individually ventilated Thoren cages, with a maximum of five adult mice per box (mixed genotype littermates). Mice were fed on a diet of an abundant supply of Barastoc rodent feed (Ridley AgriProducts), and constant access to water. Mice were maintained on a 12 hr light/dark cycle (light 7am-7pm) and with a controlled room temperature of 18-24°C. Cages and bedding were changed weekly.

Breeders were typically set up at 6-8 weeks of age, with one male and one female per box. The male remained in the box throughout gestation, parturition and nursing. The diet of breeders was supplemented weekly with 3 g of sunflower seeds. Sunflower seeds were also provided to weaned mice for one week post weaning. See Appendix Figure 6-4 for further details. At postnatal day 10 (P10), mice were assigned an ID by toe tattoo and tail snips taken for genotyping. Mice were weaned at day 21 (P21). Breeders were kept together for up to 6 months, producing multiple litters. The colonies were maintained with a minimum of two breeders per line, and sibling matings were avoided.

2.5.2 Gene targeting

Brinp1^{tm1Pib}, *Brinp2^{tm1Pib}* and *Brinp3^{tm1Pib}* targeted mice were each generated on a Bruce-4 C57BL/6 background by the Gene Recombineering Facility, Australian Regenerative Medicine Institute. Mice carrying a single copy of the targeted allele within their germline were provided. Table 2-7 details the full name designations and abbreviated names of the mouse line used for this study.

The targetted deletion of exon 3 of *Brinp1*, *Brinp2* or *Brinp3* KO mice was designed to remove the start of the MACPF domain, via Cre-mediated recombination of LoxP sites. The deleted sequence of DNA was devised to result in a frame shift, and introduce a stop codon near the

beginning of exon 4. This was designed to result in a truncated, non-functional version of the protein (BRINP1, BRINP2 or BRINP3), lacking both the MACPF domain and unique C-terminal sequence. See Figure 3-1, Figure 3-3, and Figure 3-5 for full details.

2.5.3 Mouse breeding.

2.5.3.1 Breeding *Brinp* conditional knockout mice

Mice with the targeted allele for *Brinp1*^{tm1Pib} (originating from ES cell clone 5C8B), *Brinp2*^{tm1Pib} (originating from ES cell clone 1C4H) or *Brinp3*^{tm1Pib} (originating from ES cell clone 10G) were bred to homozygosity (*Brinp1*^{tm1Pib/tm1Pib}, *Brinp2*^{tm1Pib/tm1Pib} or *Brinp3*^{tm1Pib/tm1Pib}).

Global knockout mice were then created by crossing *Brinp1* targeted, *Brinp2* targeted or *Brinp3* targeted mice to C57BL/6 Cre-deleter transgenic mice (Tg(CMV-Cre)1Cgn to remove exon 3 and the neomycin cassette from the targeted alleles. This produced animals heterozygous for the *Brinp1*^{tm1.1Pib}, *Brinp2*^{tm1.1Pib} or *Brinp3*^{tm1.1Pib} mutation.

These heterozygous mice were inter-crossed to generate *Brinp1*^{tm1.1Pib/tm1.1Pib} (*Brinp1* KO), *Brinp2*^{tm1.1Pib/tm1.1Pib} (*Brinp2* KO) or *Brinp3*^{tm1.1Pib/tm1.1Pib} (*Brinp3* KO) mice. Lines were maintained with heterozygous breeders, to also produce WT (*Brinp*^{+/+}) and heterozygous (*Brinp1*^{tm1.1Pib/+}, *Brinp2*^{tm1.1Pib/+} or *Brinp3*^{tm1.1Pib/+}) littermates.

In parallel, homozygous *Brinp1*, *Brinp2* or *Brinp3* targeted mice were crossed to global C57BL/6 FLPe-deleter transgenic mice to remove the Neo^r cassette, thus creating the *Brinp1*^{tm1.2Pib}, *Brinp2*^{tm1.2Pib} or *Brinp3*^{tm1.2Pib} allele.

Mice heterozygous for the *Brinp1*^{tm1.2Pib}, *Brinp2*^{tm1.2Pib} or *Brinp3*^{tm1.2Pib} mutation were inter-crossed to generate *Brinp1*^{tm1.2Pib/tm1.2Pib} (*Brinp1*^{FLPe}), *Brinp2*^{tm1.2Pib/tm1.2Pib} (*Brinp2*^{FLPe}) or *Brinp3*^{tm1.2Pib/tm1.2Pib} (*Brinp3*^{FLPe}) mice. *Brinp1*^{FLPe} mice were cryo-preserved by the Australian Phenomics Bank and were not used further in this project.

2.5.3.2 Breeding *Brinp2/3* double knockout mice

Brinp2^{tm1.1Pib/+} mice were bred with *Brinp3*^{tm1.1Pib/tm1.1Pib} (*Brinp3* KO) mice. The resultant offspring that were heterozygous for both *Brinp2*^{tm1.1Pib} and *Brinp3*^{tm1.1Pib} were bred. Sibling matings were avoided. Multiple F2 litters were screened for a cross-over event occurring between the *Brinp2*^{tm1.1Pib} allele and the *Brinp3*^{tm1.1Pib} allele, resulting in a chromosome with the mutant version of both genes.

The presence of a *Brinp2*^{tm1.1Pib} *Brinp3*^{tm1.1Pib} chromosome was screened for as a genotyping result showing a mouse homozygous for one floxed gene, and heterozygous for the other – a scenario only possible if a cross-over event has occurred. Mice found to have *Brinp2*^{tm1.1Pib} and *Brinp3*^{tm1.1Pib} on the same chromosome were bred to generate *Brinp2/3* KO mice.

2.5.3.3 Breeding *Brinp1/2/3* triple knockout mice

Female *Brinp2/3* double KO mice were bred with male *Brinp1* KO mice, resulting in mice heterozygous for *Brinp1*^{tm1.1Pib}, *Brinp2*^{tm1.1Pib} and *Brinp3*^{tm1.1Pib} in the F1 generation. These triple heterozygous mice were mated to generate *Brinp1/2/3* KO mice in the F2 generation, along with WT littermates.

2.5.4 Extraction and purification of spleen DNA

Half a mouse spleen was dissociated into a single cell suspension by placing between the frosted ends of two sterile Superfrost Plus slides (VWR), and gently pressing in a circular motion, to release approximately 1x10⁸ cells into a 10cm dish. Cells were washed in PBS, then lysed overnight in 7.5 ml lysis buffer at 37°C. DNA was extracted with equal volume (7.5 ml) Phenol-Tris pH8.0. The tube was rocked gently for 10 min at RT, then centrifuged at 840 *g* for 10 min.

The aqueous phase was collected and DNA extracted twice with an equal volume (7.5 ml) of Phenol-chloroform (25: 24: 1 ratio of phenol: chloroform: isoamyl alcohol), and centrifuged at 840 *g* for 10 min.

The aqueous phase was then collected and DNA extracted twice with an equal volume of CHCl₃ 24:1 isoamyl alcohol, then centrifuged at 840 *g* for 10 min.

The aqueous phase was collected once more, and 2x volume of 100% ethanol was added, tilting the tube gently. The DNA clot that formed was carefully removed with a hooked 9 inch Pasteur pipette. The DNA clot was allowed to air dry on the end of the pipette for 2 hr. The clot was washed twice in 5 ml of DNA wash buffer for 15 min. The clot was then washed twice in 5 ml 100% ethanol. The DNA was allowed to air dry completely. The DNA was dissolved in 2.5 ml 10 mM Tris, 1mM EDTA overnight at 37°C. DNA concentration was measured by BioRad NanoDrop 1000.

2.5.5 *Brinp1* southern blotting

Genomic DNA (spleen) from the following mice was extracted from one mouse per genotype: WT, *Brinp1* targeted, *Brinp1* KO, *Brinp1* het, *Brinp1*^{Fple}, *Brinp2* targeted, *Brinp2* KO, *Brinp2* het, *Brinp2*^{Fple}, *Brinp3* targeted, *Brinp3* KO, *Brinp3* het, and *Brinp3*^{Fple}. The DNA samples were provided to the Monash Gene Targeting Facility, where Southern blotting was carried out under contract.

2.5.6 Genotyping

At postnatal day 10, mice were identified by toe tattooing. Tail tips (approx. 2 mm) were taken and placed in a 1.5 ml tube. Each tail tip was digested overnight at 55°C in 0.1 mg/ml Proteinase K (Astral, cat. # AM0706-100mg), diluted fresh from 20 mg/ml stock in 300 µl Frank's Tail Buffer.

The following day, 300 µl phenol-chloroform (25: 24: 1 ratio of phenol: chloroform: isoamyl alcohol) was added to each tube, vortexed, then collected by centrifugation at 16,100 *g* for 10 min at 4°C. The aqueous phase was transferred to a new tube, and 30 µl of 5 M NaCl added. DNA was precipitated with 660 µl of 100% ethanol, then centrifuged at 16,100 *g* for 20 min at 4°C. The pellet was washed with 150 µl 70% (v/v) ethanol and centrifuged at 16,100 *g* for 10 min at 4°C. The DNA was resuspended in 10 µl Milli-Q water, and dissolved for 30-60 min at 37°C.

2.5.6.1 Genotyping PCR:

Genotyping PCR reactions were performed in a 25.5 µl volume. See Table 2-6 for primers used to identify each of the WT and mutant alleles. The concentration for all primers used was 10 pmol/µl. PCR reactions were set up with the following components: 2.5 µl Taq DNA polymerase buffer, 0.5 µl 10 mM dNTP, 0.5 µl primer 1, 0.5 µl primer 2, 0.5 µl primer 2, 0.5 µl Taq DNA polymerase, 19.5 µl dH2O, 1µl genomic DNA.

Genotyping PCR steps:

95°C 3 min
 95°C 30 sec
 * See Table 2.5 for annealing temperature
 72°C 30 sec
 34 x cycle (steps 2, 3 and 4)
 72°C 2 min
 4°C hold

Table 2-8 - Genotyping PCR annealing temperatures

Annealing Temp.	Allele to be amplified
55°C	<i>Brinp3</i> Targeted – WT band only <i>Brinp1</i> ^{FLPe} <i>Brinp2</i> ^{FLPe} <i>Brinp3</i> ^{FLPe} <i>Brinp1</i> KO <i>Brinp2</i> KO <i>Brinp3</i> KO
60°C	<i>Brinp1</i> Targeted <i>Brinp2</i> Targeted
62°C	<i>Brinp3</i> Targeted – Targeted band only

PCR products (25 µl) were each mixed with 5 µl DNA loading buffer, and the DNA was resolved in a 2% agarose gel, in a TBE-filled electrophoresis tank containing 5µl ethidium bromide. The gel was imaged using a UV imaging station.

2.5.7 RNA isolation

For isolation of cortical and hippocampal tissue, brains were removed and cut in half through the sagittal plain, then placed in 2 ml RNA later (Sigma-Aldrich, cat # R0901-100 ML) at 4°C. After three days of incubation in RNALater, the brains became brittle, allowing for easier dissection. Dissections were performed under a LED illumination microscope (Zeiss Stemi DV4 Stereo Microscope) by placing the left hemisphere's cortex side down and removing any non-cortical forebrain and cerebellar tissue. The left hemisphere was held in place using forceps, taking caution so as not to damage the hippocampus. The meningeal tissue was removed with

a second pair of forceps. The hippocampus was dissected away from the cortex by carefully sliding forceps underneath the hippocampus, and separating the tissue.

Brain tissue was placed in TRI Reagent (Sigma-Aldrich, cat. # T9424) using 1 ml per 50–100 mg of tissue and homogenized in a 5 ml polystyrene FACS tube using a TH tissue homogenizer (OMNI International, Inc.). The suspension was rested at room temperature for 5 min to allow dissociation of nuclear complexes. 200 μ l chloroform was added and the tube was vortexed and allowed to sit for 3 min, then centrifuged at 16,100 *g* for 20 min at 4°C. 600 μ l of the aqueous phase was transferred to a 1.5 ml tube and RNA was recovered by isopropanol precipitation for 10 min at RT. The RNA was collected into a pellet for 20 min at 16,100 *g*, then rinsed with 75% ethanol and re-dissolved in 20 μ l of DEPC RNase-free water for 10 min at 55°C. RNA was stored for short term at -20°C and long term at -80°C.

2.5.8 cDNA synthesis

2.5.8.1 cDNA synthesis for validation of knockout mouse targeting.

The concentration of RNA was measured at A260 nm using a BioRad NanoDrop 1000. RNA samples were first treated with RQ1 RNase-free DNase (1 U/ μ g RNA) (Promega, cat. # M6101) with in a final volume of 10 μ l, at 37°C for 30 min. The reaction was stopped by heating the sample to 65°C for 10 min to inactivate the enzyme. RNA concentration post DNase treatment was measured on a BioRad NanoDrop 1000 (260 nm). 1 μ g of RNA was used for cDNA synthesis reactions.

1 μ g of RNA was reverse transcribed into cDNA using the SSIII First Strand Synthesis kit (Life Technologies, # 18080051). Each RNA sample was prepared as follows, using kit reagents provided: 1 μ l 50 μ M oligo(dT) 20, 1 μ l 10 mM dNTP mix, 1 μ g RNA, DEPC-treated water to a total volume of 10 μ l. The mixture was incubated at 65°C for 5 min, then placed on ice for at least 1 min. The SuperScript III mix was prepared from the following components: 2 μ l 10x RT buffer, 4 μ l 25 mM MgCl₂, 2 μ l 0.1 M DTT, 1 μ l RNaseOUT (40 U/ μ L), 1 μ l SuperScript III RT (200 U/ μ L). A no RT negative control sample was prepared with the same reagents, replacing the RT enzyme with 1 μ l DEPC-treated water.

10 μ l of the cDNA synthesis mix was combined with 10 μ l of the RNA/oligo dT mix. A no RT control was prepared by combining 10 μ l of the RNA/oligo dT mix with 10 μ l of the no RT sample mix. Tubes were incubated at 50°C for 50 min. The reaction was terminated at 85°C

for 5 min, then allowed to cool on ice. 1 µL of RNase H was added to each tube and incubated for 20 min at 37°C. cDNA was stored at -20 °C.

2.5.8.2 cDNA synthesis for qPCR.

MMLV Reverse Transcriptase (Promega, cat. # M3682) was used for cDNA synthesis of RNA samples used for qPCR. 1 µg of RNA was added to 1 µg Oligo dT primer (Promega, cat. # C1101), made up to a total volume of 10 µl in RNase-free water and heated at 70°C for 5 min. The tube was allowed to cool on ice for 5 min. The qPCR reaction was set up with the following reagents: 5 µl Reaction Buffer (5x), 1.25 µl 10 mM dNTPs, 7.75 µl nuclease free water, and 1 µl (200 U/µl) M-MLV RT (H-) Point Mutant. For no-RT samples, 1 µl of water was added in place of the reverse transcriptase. 15 µl of RT master-mix was added to each tube of RNA to a total reaction volume of 25 µl, and incubated at 40°C for 60 min. The RT enzyme was inactivated by heating at 70°C for 15 min.

2.5.8.3 Reverse Transcriptase PCR (RT-PCR)

Brinp1 KO mouse RNA was extracted from the whole brain of a knockout embryo (E18.5). RNA from a WT E18.5 embryo was prepared as a control. *Brinp2* KO and *Brinp3* KO RNA were each prepared from the cerebellum of P28 mice. *Brinp2/3* and *Brinp1/2/3* KO RNA were each prepared from the cerebellum of adult mice. For each KO RNA preparation, WT RNA was also prepared from littermates at the same time. RNA was reverse transcribed into cDNA as described above. For the PCR reaction, RT-PCR primers are listed in Table 2-6.

PCR reactions were set up with the following components: 2.5 µl Taq Reaction Buffer, 0.5 µl 10 mM dNTP, 0.5 µl 5 pmol primer 1, 0.5 µl 10pmol/µl primer 2, 0.5 µl Taq DNA polymerase, 19.5 µl dH₂O, 1µl cDNA. A master mix was prepared for each primer set. RT minus reactions were prepared at the same time. PCR conditions: 95°C 60 sec (95°C 30 sec, 61°C 30 sec, 72°C 30 sec) x 35 cycles, 72°C 120 sec.

PCR products (25 µl) were each mixed with 5 µl DNA loading buffer and the DNA was resolved on a 2% agarose gel (in a TBE-filled tank containing 5µl ethidium bromide). The DNA was excised, and then purified using UltraClean®15 DNA Purification Kit (GeneWorks, cat. # MB-12100-300).

For DNA sequencing, a BigDye Terminator reaction was performed using 5 pmol of the RT-PCR forward primer, along with 0.4 µg of PCR DNA in the BigDye® Terminator system (Applied Biosystems®, cat. # 4337449). Products were precipitated from residual salts and proteins, by adding 50 µl ethanol, 2 µl 125 mM EDTA, and pH 8.0 and 2 µl of 3 M sodium acetate. PCR samples were then washed twice with 70% ethanol and provided to Micromon, Monash University: <https://platforms.monash.edu/micromon/>, for sequencing.

2.5.9 Quantitative real-time PCR ($\Delta\Delta C_q$ method)

Quantitative PCR primers were designed using the Primer3 Real Time PCR program: <http://simgene.com/Primer3>. Primers used are listed in Table 2-6. Primers were designed to meet the following criteria: The PCR product to cross and Intron/Exon boundary, the GC content $\geq 50\%$, and to produce a single PCR product within a range of 80-190 bp (optimal size of 150 bp). Exon boundaries were defined with UCSC Genome Bioinformatics > BLAT. Primer specificity was checked by BLAST against the mouse nucleotide database. Primers were first validated by RT-PCR, checking that a single PCR product of the predicted size was amplified.

qPCR reactions were set up in a 96 well plate format as 10 µl reactions: 5 µl SYBR Green (SYBR® Green JumpStart™ Taq ReadyMix™, Cat # S4438, Sigma- Aldrich), 4.1 µl water, 0.2 µl primer 1, 0.2 µl primer 2, 0.5 µl cDNA. A master mix was prepared for each primer set and all reactions were prepared in duplicates. RT minus reactions were also prepared for each primer set. Reactions were performed on a Roche Light Cycler 96: 95°C 1 min, 95°C 30 sec, 61°C 15 sec, repeated 45 times. 72°C 2 min, Melt 92-94. All reactions were run in duplicate. Duplicate reactions containing a) GAPDH and b) β -actin controls were run alongside all test genes.

Melt curves were viewed to confirm single product amplification of each primer set. The raw data from the Light Cycler 96 (Roche) was loaded into Lin Reg PCR program: <http://www.hartfaalcentrum.nl/index.php?main=files&sub=LinRegPCR> to set baseline values and calculate primer efficiency per group and integrate efficiency values when calculating C_q values.

To calculate relative changes in transcript levels between WT and knockout tissue, the following steps were taken:

1. An average Cq value was calculated per duplicate reaction.
2. ΔCq values were calculated per tissue sample for each gene using the reference genes:
 $\Delta Cq (\text{sample}) = Cq \text{ target gene} - Cq \text{ reference gene}^*.$
3. A calibrator value per target gene was calculated as average ΔCq for all of the WT samples. ΔCq for each WT mouse were averaged to produce a calibrator ΔCq :
 $\text{Calibrator } \Delta Cq = \text{Average (WT sample 1, 2, 3, 4 } \Delta Cq)$
4. The $\Delta \Delta Cq$ was calculated as the difference between each sample ΔCq and the calibrator ΔCq for each gene.
 $\Delta \Delta Cq = \Delta Cq (\text{sample}) - \Delta Cq (\text{calibrator}).$
5. The normalized level of the target gene expression (E) was calculated using the formula: $E = 2^{-\Delta \Delta Cq}$. Note: For a $\Delta \Delta Cq$ of 0, $E = 1$ i.e. no change.
6. Expression values of each target gene for WT and *Brinp1* knockout samples were plotted in GRAPHPAD PRISM 5 (GraphPad).

* Two reference genes were used for independent calculations, to generated two expression (E) data sets: GAPDH and β -Actin.

2.5.10 Cell culture

COS-1, SH-SY5Y and NT2 cells were grown in DMEM cell culture medium, in a 5% CO₂ incubator at 37°C. A class II laminar flow cabinet was used for cell culture operations and sterile disposable plastic ware (Falcon) was used. Cells were grown in 6cm dishes and passaged every 2-3 days.

2.5.11 Differentiation of NT2 cells

NT2 cells were differentiated following the methods described by NT2 Cheung et al (Cheung et al., 1999). In brief, cells were seeded at 1×10^6 cells/mL in a sterile 8.5 cm bacteriological grade Petri-dish. Cells were treated with 5 μ M all-trans RA (Sigma) for up to 3 weeks, until aggregates formed. Floating or loosely attached cell aggregates were then pipetted to a 6cm tissue culture dish coated with a 1 ml layer of BD Matrigel Matrix (BD, cat. #354234). The cell aggregates were incubated at 37°C, 5% CO₂ for two weeks of neurite outgrowth. Media was changed every 2 – 3 days.

2.5.12 Transfection of COS-1 cells

Three to four hours prior to transfection, COS-1 cells were passaged at a density of 0.5×10^6 in a 6cm dish. Cells were incubated at 37°C for 3 to 4 h, allowing them to reach exponential growth phase. The monolayer of cells was washed with PBS and 2.5 ml serum-free DMEM was added, plus 100 μl of dextran/ chloroquine. Plasmid DNA was added (2-3 μg) and cells were incubated at 37°C for 2-3 h. The DMEM medium was then aspirated and replaced with 2 ml 10% DMSO in serum-free DMEM, followed by a 2 min incubation at 37°C . The DMSO-containing medium was then replaced with 4 ml complete DMEM. Cells were analysed by immunofluorescence 48 hr post-transfection.

2.5.13 Immunofluorescence

COS-1 cells were removed from the 6cm dish by the addition of 1ml trypsin-EDTA, then resuspended in DMEM at a dilution of 1×10^5 cells/ ml. Cells were seeded onto a 12 well slide, 50 μl per well, and incubated overnight at 37°C . The following day, media was aspirated and the slide washed with PBS. Cells were fixed and with 3.7% (w/v) formaldehyde in PBS for 20 min. The fixative was removed with three PBS washes. Cells were permeabilized with 0.5% Triton X-100 in PBS for 5 min and then washed three times with PBS.

Primary antibody (anti-BRINP1 rat 2 sera) was added to each well (20 μl) and incubated for 30 min. Slides were then washed three times in PBS. The AF568-conjugated secondary antibody (20 μl) was then added and incubated in the dark for 30 min. Slides were washed with PBS, then coverslip mounted with Mowiol reagent. Bright field and fluorescent images were captured on an epifluorescence microscope (Olympus®), using a MCID digital capture system.

2.5.14 Preparation of cell lysates

Cells were allowed to grow to confluency in a 6cm dish (1×10^6 cells). The dishes were placed on ice, the cell medium was removed and the cells were rinsed once with PBS. 1 ml of, LSB was then added to the dish and the cells were scraped off using a plastic cell scraper, and transferred to an Eppendorf tube. The tubes were immediately placed on ice. The cell lysates were then sonicated for 3 seconds to disrupt cell membranes and fragment genomic DNA. Lysates were prepared for SDS-page mixing 20 μl cell lysates with 2 μl of dithiothreitol (dTT), and boiling at 100°C for 5 min.

2.5.15 Preparation of mouse brain lysates

Whole brain lysates were made from *Brinp1* KO and WT postnatal day 12 mice. Cerebellar brain tissue (0.5cm²) was placed in 2 ml 5x Laemmli sample buffer, in a 10 ml Falcon tube. Lysates were prepared by homogenization, using a TH tissue homogenizer (OMNI International, Inc.). Lysates were immediately placed on ice, then sonicated for 3 sec. For SDS-page, 2 µl of dithiothreitol (dTt) was added to 20 µl of the lysate and boiled at 100°C for 5 min.

2.5.16 Immuno-blotting

Lysate preparations (20 µl), were run alongside 6 µl of ColourPlus™ pre-stained protein ladder (NEB, cat. # P7703) in wells of a 4% stacking gel, above a 10% SDS-polyacrylamide gel. The gel was resolved at 200 V in a Mini-Protean II assembly (Bio-Rad®) filled with running buffer, until the dye front migrated off the bottom of the gel (approximately 50 min). After SDS-page, the gel was transferred to a nitrocellulose membrane at 250 mA for 1 hr in a Mini-Protean II assembly (Bio-Rad®) filled with transfer buffer. Heat generated during the transfer was controlled with an ice block and magnetic stir bar placed in the transfer cell. Following transfer, membranes were blocked with blocking solution for 45 min, then probed with primary antibody overnight at 4°C.

The next day, the membrane was washed 3 x 15 min in TTBS, then incubated with HRP-conjugated secondary antibody rocking at room temperature for 1 hr. The membrane was washed again with 3 x 15 min in TTBS. Immuno-reactive proteins were detected by use of chemiluminescence substrates: Western lightning Plus ECL (Pierce™, cat. #32106). 1ml Enhanced luminol reagent plus was mixed with 1ml oxidised reagent plus and added to the membrane. The membrane was rocked for 1 min to allow coverage with the ECL reagent. The membrane was then placed in a sealed transparent pouch, ensuring no air bubbles, and immediately exposed to X-ray film for 30 sec and 1 min.

For detection of loading control proteins, antibodies were removed from the membrane using stripping buffer at 50°C for 30 min, then washed 6x 10 min in Tris-Saline. The blot was re-probed with primary antibody overnight at 4°C, then washed with TTBS and probed with an HRP-conjugated secondary antibody. Blots were washed and then developed as described above.

2.5.17 Histopathology

Mice were analyzed under contract by the Australian Phenomics Network (APN). (<http://www.australianphenomics.org.au/>). Mice were assessed at age seven to eight weeks. Embryos were assessed at day 18.5 (E18.5).

Two mice per genotype were first observed for body condition, weighed, and assessed for signs of ill health. For histopathological assessment, the following organs were examined for macro-morphological abnormalities: adrenal glands, bladder, brain (forebrain, midbrain and cerebellum), cecum, cervix, clitoral gland, colon, duodenum, epididymis, eyes, gall bladder, Harderian glands, heart, hind leg, ileum, jejunum, kidney, liver, lungs, lymph nodes, mammary tissue, mesenteric lymph node, ovaries, oviducts, pancreas, penis, preputial gland, prostate glands, salivary glands, seminal vesicles, skin, spinal cord, spleen, stomach, testes, thymus, thyroids, trachea, tail, uterus, and vagina. E18.5 were examined in three parts: body, head and placenta.

All tissue was prepared as formalin fixed, paraffin wax embedded sections (10 μ m). Cells and nuclei were identified using Hematoxylin and Eosin (H&E) stain. Myelin fibers were stained with Luxol Fast Blue. Neurons were identified by Nissl labelling.

2.5.18 Immunohistochemistry

2.5.18.1 Immunohistochemistry: adult mouse brains

The brains of adult *Brinp1* KO mice were examined at aged 3-4 months. Mice were anaesthetized by IP injection of 50 mg/kg sodium pentobarbital. Mice were checked for loss of consciousness by toe pinch. Transcardial perfusions were performed by injection of 20 ml of PBS into the left ventricle of the mouse, allowing blood to flush out of the right atrium. For tissue fixation, 4% (w/v) paraformaldehyde (PFA) in PBS (20-30 ml) was then injected at a steady rate into the left ventricle. Brains were removed then incubated for 20 – 24 hr in 4% (w/v) PFA in PBS at 4°C, then cryo-protected with 20% sucrose in PBS for 72 hr. Brains were frozen in Tissue-Tek™ OCT (VWR, cat. # 25608-930), in plastic molds (2.5 x 2.5 cm) using an isopentane bath cooled with liquid nitrogen. Coronal sections were cut at 14 μ m on a cryostat (Leica) and mounted onto Superfrost Plus slides (VWR). Slides were stored at -80°C.

Slides were air-dried in the fume hood for 60 min, then rehydrated with PBS for 5 min at room temperature, then permeabilized twice with PBS-Triton (0.1%) 2 for 5 min. For blocking, 10% Normal Goat Serum (NGS) / PBS - 0.1% Triton was added to the sections for 30 min at RT. Primary antibodies (Table 2-4) were diluted in antibody diluent. The NGS was removed from the slides and sections were incubate in the diluted antibody overnight at 4°C. Slides were then washed three times in PBS-0.1% Triton. Secondary antibodies (Table 2-5) was prepared at 1:800 in PBS and incubated for 2 hr at RT. Slides were washed once in PBS then DAPI was added at 10 µg/mL in PBS for 10 min. Slides were washed three times in PBS, then mounted with Mowiol reagent and cover-slipped.

2.5.18.2 Immunohistochemistry: Bromodeoxyuridine labelling of embryos.

Heterozygous dams at embryonic day 12.5 (E12.5), day 14.5 (E14.5) and day 16.5 (E16.5) were weighed and injected with a single dose (100 mg/kg), of Bromodeoxyuridine solution (BrdU, 10mg/ml in PBS). Pregnant dams were killed at day 18.5 of gestation, and embryos harvested. Embryo brains were drop fixed in 4% (w/v) PFA in PBS for 12 h at 4°C, then cryopreserved in 20% sucrose solution. Tails were taken from each embryo and genotyped. WT and *Brinp1* KO embryo brains were cryopreserved in Tissue-Tek™ OCT (VWR, cat. # 25608-930) in plastic molds (0.5 x 0.5 cm), and sectioned at 14 µm onto Superfrost® Plus slides (VWR, cat. # 48311-703). For immuno-staining of BrdU, slides were incubated in 1:7 HCL: PBS (37% concentrated stock) at 37°C for 1 hr. Slides were then washed with PBS, and permeabilized with PBS-0.1% Triton X-100, then blocked with 10% NGS/PBS-Triton, 30 min. A BrdU antibody (1:100, BD) was applied and slides incubated O/N for at 4°C. Slides were then washed three times in PBS-0.1% Triton, than an anti-mouse AF488 (1:800) secondary antibody incubated for 2 hr at RT. Slides were washed once in PBS then DAPI was added at 1 µg/mL in PBS for 10 min. Slides were washed three times in PBS, then mounted with Mowiol reagent.

2.5.18.3 Immunohistochemistry: Imaging and analysis

Images were captured on a Nikon C1 Confocal microscope using a 20x magnification lens. Tiling was used to generate large images: 5 x 5 tiling for adult brains and 3 x 5 tiles for E18.5 brains. Tiled sections contained the medial hippocampus, the lateral parietal and somatosensory cortex (Bregma region -1.94). A minimum of three representative sections per mouse were imaged. Images were saved as NIS files. For analysis, images were converted to

TIFF files using Image J software. Coronal cortical sections were rotated, using Image J software, to orient the somatosensory cortex, with the pia surface and VZ along the horizontal axis, then cropped to the region of interest. The adult somatosensory neocortex images were cropped to 400 μm x 1000 μm . Embryonic (E18.5) somatosensory cortex images were cropped to a size of 1200 μm x 2200 μm . Cropped images were analyzed using Imaris 7.6.3. and cell counts were performed blind of genotype. The following Imaris 7.6.3 settings were used for cell counts: Analysis type: spots. Estimated spot diameter: 10 μm . Background subtraction: on. Filter type: quality. The quality filter was kept consistent for each dataset.

Cell counts were performed to calculate the total number of immuno-labelled cells. For regional counts, cortical regions were divided into equal bins. Region of interest size was defined as 35 μm x 400 μm per bin for NeuN, Cux1 and BrdU cell counts, and 75 μm x 400 μm for PV cell counts. Subventricular zone (SVZ) cell counts for number of BrdU+ cells were performed on 35 μm x 400 μm regions of interest. Cropped hippocampal images (1200 μm x 2200 μm) were counted using Imaris 7.6.3. For GFAP cell counts, the hippocampus was divided into 13 equal bins (size) and cell counts were performed per bin. To count numbers of E12.5-BrdU+ cells in the dentate gyrus of E18.5 *Brinp1* KO mice, a region of 200 μm x 800 μm was cropped. The total number of cells in this region was counted using Imaris 7.6.3. A minimum of three representative sections per mouse were analyzed. Unpaired Student's *t*-tests were performed for comparisons between WT and knockout per bin. Statistical tests were performed with GRAPHPAD PRISM 5 (GraphPad).

2.5.19 Reproductive phenotyping

The litters obtained from heterozygous matings (*Brinp1*^{tm1.1Pib/+}, *Brinp2*^{tm1.1Pib/+} or *Brinp3*^{tm1.1Pib/+}) were genotyped from tail tips taken at P10. Genotypes were analyzed for Mendelian inheritance ratios by expressing the number of WT, het and KO mice as a percentage of total mice of all genotypes. In addition, any pups that were found dead from the *Brinp1* line were also genotyped to establish numbers of *Brinp1* KO pups dying as neonates.

To assess the reproductive success of mice of breeders from the *Brinp1* line, four WT x WT, four *Brinp1* het x *Brinp1* het, four *Brinp1* KO x *Brinp1* KO, and four *Brinp1* KO (female) x WT (male) breeder pairs were set up and monitored over four months. These mice were housed

under standard home cage conditions, with two breeders per box. The number of pups in each litter were recorded at birth, 48 hr post birth, and at age of weaning (postnatal day 21). Pups that died from birth onwards were visually inspected for appearance, stomach content and signs of neuro-muscular or cranial defects, based on assessments described by (Turgeon & Meloche, 2009).

2.5.20 Dietary experiment: Supplementation of diet with sunflower seeds

Eight breeding pairs of *Brinp1* heterozygous mice were set up. Breeders were of the same generation, and heterozygous littermate breeders were divided between the two groups of four breeding pairs (group 1 and group 2). Group one was fed a standard diet of Barastoc animal feed. The second group were fed the same Barastoc animal feed and an addition to their diet of sunflower seeds (approximately 3 g). Sunflower seeds were given to breeders weekly from when initially set up, and to pups in the first week of being weaned. Litters were monitored for four months.

2.5.21 Behavioral testing

Behavioral testing was carried out under contract by Neuro Research Services (The Florey Institute of Neuroscience and Mental Health), with the exception of the wire hang test and nesting experiment. Mice were tested blind to genotype and in random order. Tests were separated by a minimum of one day. WT and knockout mice were tested in the same testing sessions. Lighting conditions were 30 lux for all behavioural tests. Testing arenas were cleaned with Equinade disinfectant (lavender scent) between trials. In all instances, mice had previously been habituated to the disinfectant whilst housed at the testing facility. Raw data was provided to the candidate for analysis.

2.5.21.1 Animals

For behavioral testing, knockout and WT mice were bred from heterozygous crosses, in cohort sizes of 10-12 mice aged between 8-12 weeks, unless stated otherwise. A 1:1 ratio of males: females were tested. Mice were provided to Neuro Research Services (The Florey Institute of Neuroscience) one week prior to testing and habituated to the testing facility, then habituated to the testing room overnight.

2.5.21.2 Visual placing test

Mice were lifted by the tail to a height of 15 cm and lowered onto a mesh grid within 1 sec, decelerating as the grid approached. The distance of the animal's nose from the grid was measured the moment before the mouse extended its forelimbs towards it.

2.5.21.3 Acoustic startle and pre-pulse inhibition (PPI)

Mice were placed individually inside a Perspex cylinder, closed at both ends. The cylinder was placed upon a platform sensitive to weight displacement, within a sound attenuating box with a background sound level (San Diego Instruments Startle Response System). The background white noise level was set to 70 dB. To measure acoustic startle, a strong 40 ms startle sound (115 dB) was played and startle response was measured by the jumping reflex (<1 sec) as weight displacement on the platform. Pre-Pulse Inhibition was measured as the percentage reduction in startle response when a non-startling 20 ms pre-pulse of a) 4 dB b) 8 dB c) 16 dB, above the 70 dB background sound, was played 100 ms prior to the startle sound.

2.5.21.4 Elevated plus maze.

Mice were placed on an elevated platform (material: Perspex, colour: beige) at a height of 40 cm above the floor. The platform comprised of two open arms and two closed arms (each 4.5 cm wide, 30 cm in length), connected by a central square (6 cm x 6 cm). The two closed arms were protected by a 15 cm high wall. Mice were placed on the center square and video recorded whilst exploring the maze for 5 min. Time and frequency of entry into each arm was recorded. Tracking software: Noldus EthoVision 3.0.

2.5.21.5 Y-maze.

Mice were tested in two trials of a Y-maze (material: Perspex, colour: grey) with each of the three arms having a distinctive visual cue at the end. Dimensions of each arm were 30 cm x 10 cm, with a triangle centre zone of 10 cm equal sides. Mice received a random association between visual cues and arm location. In Trial 1, a partition blocked off the left arm of the maze. The mouse was placed at the end of the home arm, facing away from the center. The time spent in each of the two available arms over 10 min was recorded. Mice were rested for 2 hr. In Trial 2 testing was repeated in a second trial with the partition removed and all three arms made accessible. Each of the two trials lasted 10 min. Tracking software: Noldus EthoVision XT 5.0.

2.5.21.6 Rotarod

On day 1, mice were pre-trained on the Rotarod (Ugo Basil) for two initial trials at a constant speed of 4 rotations per minute (rpm) for 5 min, followed by a third trial accelerating from 4-40 rpm over five min. Testing was carried out the following day (day 2) as 4 x five min 4-40 rpm accelerating trials, with an inter-trial interval of 30 min.

2.5.21.7 Olfaction test

Filter paper (4 cm x 4 cm) was prepared by soaking with 275 µl water, or 275 µl of peanut butter, at three dilutions (1:10; 1:100; 1:1000). Receptacles were prepared from plastic graduated pipettes (3 ml, Copain) with 2 x 5 mm holes cut into the bulb. A single filter paper was placed in each pipette. Mice were allowed 15 min to habituate to the test cage and empty pipettes prior to testing. For each trial, the test mouse was presented with either a peanut butter dilution receptacle or a water control receptacle. Relative levels of sniffing behaviour were measured as time of the nose touching the receptacle over the 3 min trial. The test cage was changed for each mouse tested. Testing took place over three days, with one dilution per day tested.

2.5.21.8 Three chamber social interaction test

Adapted from methods previously described by Silverman et al (Silverman et al., 2010). Mice were placed in a 3-chamber plexiglass box (60 x 40 x 25 cm), with small rectangular openings allowing access to each of the three chambers. Identical wire cages (8.5 cm x 8.5 cm, 10 cm height) were placed in the left and right chamber.

Trial 1 (habituation): The test mouse was placed in the middle chamber and allowed to freely explore the entire testing arena for 10 min.

Trial 2 (social interaction): An unfamiliar C57BL/6 WT sex matched mouse (stranger 1) was placed enclosed in the wire cage in one of the side chambers. The behavior of the test mouse was recorded over 10 min as time directly interacting with the cages (empty vs stranger mouse). Interaction was defined by tracking within 1 cm perimeter of the cage.

Trial 3 (social preference): An unfamiliar C57BL/6 WT sex matched mouse (stranger 2) was placed in the previously empty cage. The mouse from trial 2 remained in the same cage. The

behavior of the test mouse was recorded over 10 min as time directly interacting with the cages (familiar vs stranger mouse).

The mice serving as strangers were habituated to placement under the wire cage for 5 min prior to the test. Mice were tracked using CleverSys Inc. Tracking and TopScan software. The interaction zone was defined by the software as an unmarked perimeter zone of 2 cm around the metal cages. Interaction was defined as nose within the interaction zone. The chambers were cleaned between trials with Equinade disinfectant (lavender scent).

2.5.21.9 Locomotor cell

Mice were habituated to the 27.5 cm² locomotor arena (TRU SCAN Activity Monitoring System, Coulbourn Instruments) for 10 min and then allowed to explore freely for 30 min. Movement of the test mouse was tracked using 16 Infrared (IR) beams on the lower sensor ring to detect floor plane movement and 16 IR beams on an elevated ring to detect vertical plane movement (rearing). Locomotive activity and rearing behavior were recorded by disturbances in the IR beam sensors.

2.5.21.10 Light / dark locomotor cell

The Locomotor Cell was divided into two equally sized zones; a light zone and a dark zone by the addition of an opaque Perspex chamber. An opening allowed access between the light and dark zones. At the start of testing, mice were placed in the dark zone. Mice were allowed to freely explore both zones for 10 min. Time in each zone, and time taken for emergence from the dark zone was recorded.

2.5.21.11 MPH testing of *Brinp1* knockout mice

A cohort of 20 WT / 20 knockout mice, aged 14-20 weeks, were randomly divided into four groups, with equal number of males and females per group:

- i) WT + MPH
- ii) WT + Saline
- iii) KO + MPH
- iv) KO + Saline

Mice were placed in the locomotor cell for a 15 min habitation phase, then mice were injected by acute IP administration. Locomotor activity was recorded for 60 min post injection. Doses of 1.25 mg/kg and 2.5 mg/kg MPH or 0.9% (w/v) saline were trialed. Testing was carried out blind of genotype and drug administration.

2.5.21.12 Morris water maze

The test was performed as described by Vorhees and Williams (Vorhees and Williams, 2006). A 1.9 m diameter pool was filled to a depth of 30 cm with 25°C water. A 15 cm diameter platform was submerged 1 cm below water level and approximately 500 ml of non-toxic white paint added to hide the platform from the animal. The test mouse was placed in a random quadrant (North, South, East or West) and allowed 2 min to find the platform. Once the platform was found, the mouse was allowed to remain there for 30 sec before being removed. If the platform was not found within 2 min, the mice were guided to the platform. Mice received four training trials per day, each with different start points, for six consecutive days. Tracking software: Noldus EthoVision 3.0.

2.5.21.13 Self-directed digging and grooming behaviors.

Mice were placed in a plexiglass test cage (40 x 40 x 35 cm) with clean sawdust covering the base. Self-directed behavior was video recorded for 20 min from first introduction into the novel cage. Videos were scored manually for duration and frequency of grooming, digging and rearing behaviors.

2.5.21.14 Wire hang test

Mice were tested by being placed on the inside of a wire lid of a standard Thoren cage. The cage was waved gently until the mouse gripped the wires. The lid was gently turned upside down, so that the mouse was hanging inside the Thoren cage. The time taken for the mouse to loosen its grip and drop into the cage below is measured. Mice were tested individually and returned to their home cage after testing. The test was carried out as three trials with a minimum of one hr break between trials.

2.5.21.15 Novel object recognition test (NORT)

Protocol reproduced from methods described by Alkam et al (Alkam et al., 2011).

Trial 1 (habituation phase): Mice were placed individually in a plastic chamber (35 cm x 35 cm x 35 cm) and allowed to explore the empty chamber for 10 min. This allowed mice to become familiar with the testing arena prior to testing.

Trial 2 (acquisition phase): Mice were placed individually in the same chamber, this time with two objects (A and B) to explore. The objects were positioned 10 cm from each other and 8

cm from the nearest wall. Mice were allowed to explore the objects for 10 min. The amount of time the mice explore each object was recorded. At the end of the trial, the two objects, but not the mouse, were removed from the chamber.

Trial 3 (retention phase): One of the objects (A) from trial 2 was placed in the chamber, along with a novel object (C). Mice were allowed to explore for 10 min. The amount of time the mice explore each object was recorded. Figure 2-1 shows the arena layout, and size and shape of each object used in trials 2 and 3.

Object recognition was deemed to have occurred if the mice spend more time exploring the novel object, having recognized the object from trial 2 as familiar. This will be represented as a >50% mean. The Recognition Index (RI) was calculated for each mouse, expressed as the ratio $(TC \times 100)/(TA + TC)$, where TA and TC are the time spent in the interaction zone of object A (familiar) and C (novel) respectively during trial 3 (retention phase).

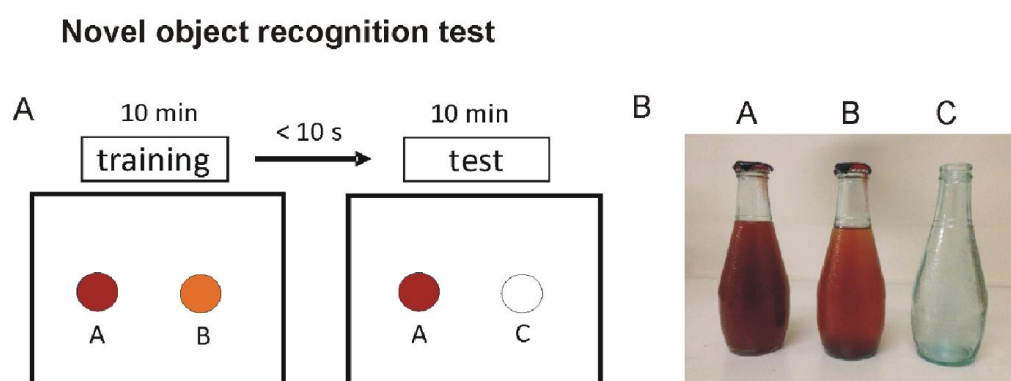


Figure 2-1 –Novel object recognition test

- A) Arena layout for objects in the training and test trials. The same arena (35cm x 35cm x 35cm) was used for the training and test trials, with object B replaced with object C between trials. A = familiar object, C = novel object. Trial durations are listed above.
- B) Objects used in the test trial were glass bottles of identical shape, size and texture, differing only by the color of liquid within the bottle. The colour variation was due to a difference in soft drink content. Object C was clearly distinguishable from A or B due to a difference in transparency of the object. Lids on the liquid-containing bottles were sealed. Letters correspond to the placement of objects within the testing arena.

2.5.21.16 Nesting

Pairs of female, unmated mice aged 10-12 weeks were placed in a clean home cage with bedding and sawdust, three hours before lights out. 8 g of shredded paper was scattered evenly over the base of the cage. Mice were assessed for nest quality at 16 hr (day 1) and 40 hr (day 2). Nesting score system used from Hess et al, (Hess et al., 2008). Examples of nest scoring are shown in Figure 2-2.

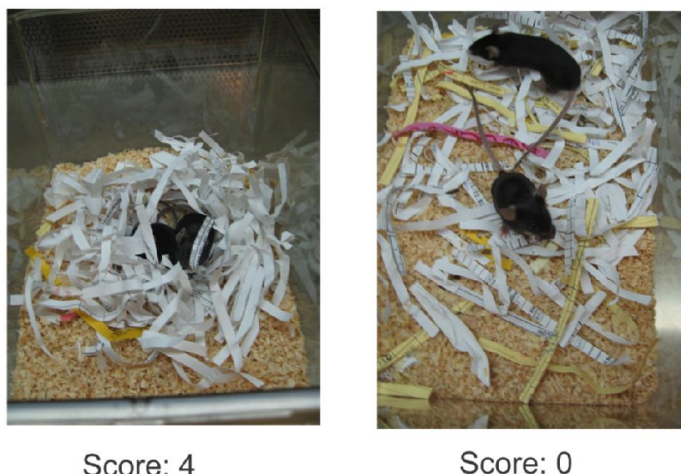


Figure 2-2 – Nest scoring system

Two female mice per box were provided with 8g of shredded paper. Nest construction was assessed 24 and 48hrs later. Pictures show examples of nesting score system for a well-constructed (score: 4) and poorly-constructed nest (score: 0), based on the scoring system by Hess et al., 2008.

2.5.21.17 Ultrasonic vocalization (USV) recording of male mice

Based on methods described by Maggio et al, (Maggio et al., 1983). A cohort of male mice (10 WT, 9 KO) presented with the smell of female urine to induce ultrasonic vocalization in a test setting. Twelve hours prior to testing of males, vaginal smears were taken from an experimentally naïve cohort of female WT littermates of a similar age. After the smear is air-dried, nuclei were visualized by a Diff-Quick stain, and the 3 stages of the estrous cycle are identified by light microscope. Only female mice that are predicted to be in a proestrus or estrous on the day of testing are used. Prior heterosexual experience during adulthood has been shown to enhance the number of male vocalizations to female urine. In order to reduce

variability and ensure that mice will actually make USVs, males were put in a cage with a proestrus or estrous female for 5 min.

For testing, 5 min prior to the urine exposure, male mice were habituated to a cotton tipped applicator. The applicator was then switched for a new applicator dipped in urine from estrous or proestrus female mice. USVs were recorded using Avisoft Recorder and parameters analyzed, as the number of USVs over the 5 min. The mean frequency and amplitude of USVs at the start, center point and end point were also analyzed. Call type criteria were based on those previously defined by Scattoni et al, 2008 (Scattoni et al., 2008).

2.5.21.18 Statistical analysis

For analysis of behavioural and histological data, unpaired Student's t-tests were performed for comparisons between two conditions. This analysis was performed using GRAPHPAD PRISM 5 (GraphPad).

For multivariate comparisons between three or more subjects, one-way ANOVAs were performed, followed by a Tukey HSD post-hoc test, using SPSS Statistics 22 (IBM). For multivariate comparisons between two or more subjects, where repeat measurements were taken, repeat measures two-way ANOVAs were performed, followed by a Tukey HSD post-hoc test, using SPSS Statistics 22 (IBM).

Comparison of reproductive success between genotypes was performed by Chi-square test, using GRAPHPAD PRISM 5 (GraphPad).

Results are represented as the mean \pm standard deviation (SD). Individual data points are shown for clarity wherever possible. Statistical significance was considered at $p < 0.05$.

Chapter 3: The generation and characterization of *Brinp1*, *Brinp2* and *Brinp3* knockout mice

3.1 Chapter 3 Overview

Mice deficient in *Brinp1*, *Brinp2* or *Brinp3* were established to study *Brinp* function *in vivo*. The deletion of exon 3 of *Brinp1*, *Brinp2* or *Brinp3* KO mice was designed to remove the start of the MACPF domain, via Cre-mediated recombination of LoxP sites. The deleted sequence of DNA was devised to result in a frame shift, and introduce a stop codon near the beginning of exon 4. This was designed to result in a truncated, non-functional version of the protein (BRINP1, BRINP2 or BRINP3), lacking both the MACPF domain and unique C-terminal sequence.

The knockout (KO) mice were first validated for correct gene targeting, and the absence of functional transcript or protein. A broad screening approach was then taken to identify a phenotype in these previously uncharacterized lines. Mice were assessed for viability, reproductive success and postnatal growth. Each of the three knockout lines underwent first line phenotyping at 7-8 weeks of age for indicators of a developmental phenotype in any of 25 organs analyzed by histopathological examination. Cohorts of adult *Brinp1*, *Brinp2* and *Brinp3* KO mice were then assessed for a behavioral phenotype, using a set of standard behavioral tests designed to examine a range of sensory and cognitive functions. The overall aim of this broad analysis was to highlight key phenotypes in any of the single knockout lines worthy of closer investigation.

3.2 Targeting strategy to generate *Brinp* knockout mice

Gene targeting was performed under contract by the Monash Gene Targeting Facility. C57BL/6 mice that were heterozygous for the targeted version of *Brinp1*, *Brinp2* or *Brinp3* were provided to the candidate. Table 3-9 summarizes the mutant alleles and abbreviated designations of the *Brinp1*, *Brinp2* or *Brinp3* mutant mice used in this study. The targeted lines were crossed with global Cre-recombinase mice for specific removal of exonic DNA sequence, or global FLPe-recombinase mice for the removal of just the neomycin resistance (Neo^r) selection cassette.

The breeding strategy is described below. See Figure 3-1, Figure 3-3 and Figure 3-5 for construction details of the *Brinp1*^{tm1Pib}, *Brinp2*^{tm1Pib} or *Brinp3*^{tm1Pib} alleles respectively, together with the resultant KO and FLPe alleles.

Abbreviated designation	Full genotype designation	Allele Accession ID
WT	<i>Brinp</i> ^{+/+}	
<i>Brinp1</i> targeted	<i>Brinp1</i> ^{tm1Pib/tm1Pib}	MGI:5604540
<i>Brinp2</i> targeted	<i>Brinp2</i> ^{tm1Pib/tm1Pib}	MGI:5604614
<i>Brinp3</i> targeted	<i>Brinp3</i> ^{tm1Pib/tm1Pib}	MGI:5604619
<i>Brinp1</i> knockout (KO)	<i>Brinp1</i> ^{tm1.1Pib/tm1.1Pib}	MGI:5604542
<i>Brinp1</i> heterozygous (het)	<i>Brinp1</i> ^{tm1.1Pib/+}	
<i>Brinp2</i> knockout (KO)	<i>Brinp2</i> ^{tm1.1Pib/tm1.1Pib}	MGI:5604615
<i>Brinp2</i> heterozygous (het)	<i>Brinp2</i> ^{tm1.1Pib/+}	
<i>Brinp3</i> knockout (KO)	<i>Brinp3</i> ^{tm1.1Pib/tm1.1Pib}	MGI:5604620
<i>Brinp3</i> heterozygous (het)	<i>Brinp3</i> ^{tm1.1Pib/+}	
<i>Brinp1</i> ^{FLPe}	<i>Brinp1</i> ^{tm1.2Pib/tm1.2Pib}	MGI:5604543
<i>Brinp2</i> ^{FLPe}	<i>Brinp2</i> ^{tm1.2Pib/tm1.2Pib}	MGI:5604617
<i>Brinp3</i> ^{FLPe}	<i>Brinp3</i> ^{tm1.2Pib/tm1.2Pib}	MGI:5604621

Table 3-9 - Nomenclature designation for *Brinp* mutant mice

3.3 Breeding strategy to generate *Brinp* knockout mice

Mice lacking *Brinp1*, *Brinp2* or *Brinp3* in all tissues were generated by breeding animals carrying the targeted allele (*Brinp1*^{tm1/Pib}, *Brinp2*^{tm1/Pib} or *Brinp3*^{tm1/Pib}) with animals expressing Cre-recombinase from the two-cell embryonic stage onwards (global Cre-deleter). Progeny exhibiting deletion of the Neo^r cassette and third exon of *Brinp1* (*Brinp1*^{tm1.1/Pib}), *Brinp2* (*Brinp2*^{tm1.1/Pib}), or *Brinp3* (*Brinp3*^{tm1.1/Pib}) were inter-bred to generate homozygous *Brinp1*^{tm1.1Pib/tm1.1Pib} (*Brinp1* KO), *Brinp2*^{tm1.1Pib/tm1.1Pib} (*Brinp2* KO) or *Brinp3*^{tm1.1Pib/tm1.1Pib} (*Brinp3* KO) animals, along with heterozygous and WT littermates. Each of the lines were maintained by heterozygous matings, to produce knockout, heterozygous and WT littermates.

In addition to Cre-deleted lines, targeted mice lacking the neomycin cassette were generated for the purpose of removing the Neo^r gene from all tissues (*Brinp1*^{FLPe}, *Brinp2*^{FLPe} or *Brinp3*^{FLPe}). The *Brinp* coding regions remained unaltered in these mice, whilst still having LoxP elements in introns that allow Cre-mediated deletion. The removal of the Neo^r cassette by FLPe recombinase is important, as its presence is known to have effects on survival and physiology if retained in the targeted locus (Pham et al., 1996; Scacheri et al., 2001). These mice were generated to provide an alternative strategy should any of the *Brinp1* KO, *Brinp2* KO or *Brinp3* KO mice prove to be embryonic lethal. The *Brinp1*^{FLPe}, *Brinp2*^{FLPe} or *Brinp3*^{FLPe} mice could then be crossed with a tissue specific Cre-recombinase line to generate tissue specific knockouts, e.g. a brain specific Cre-recombinase.

Targeted mice were bred with a line expressing a global FLPe recombinase. The progeny from these crosses, that carried the deletion of the Neo^r cassette for *Brinp1* (*Brinp1*^{tm1.1/Pib}), *Brinp2* (*Brinp2*^{tm1.2/Pib}), or *Brinp3* (*Brinp3*^{tm1.2/Pib}), were interbred to generate homozygous *Brinp1*^{FLPe} (*Brinp1*^{tm1.2Pib/tm1.2Pib}), *Brinp2*^{FLPe} (*Brinp2*^{tm1.2Pib/tm1.2Pib}) or *Brinp3*^{FLPe} (*Brinp3*^{tm1.2Pib/tm1.2Pib}) mice.

3.4 Southern blotting.

Southern blotting was carried out under contract by the Monash Gene Targeting Facility (ARMI). Correct targeting was validated using external and internal probes on genomic DNA from WT, targeted, KO, heterozygous and FLPe mice (Figure 3-2, Figure 3-4, and Figure 3-6). All targeted, KO and FLPe mouse DNA showed the predicted product sizes by Southern blotting. The only exception encountered was the presence of an additional DNA fragment from *Brinp1* targeted DNA, detected with an internal probe from the BglII digest. This extra fragment would be due to either partial cleavage of the sample DNA, or an off target integration. Progeny of mice that had been bred with mice expressing Cre-recombinase or FLPe-recombinase were checked by Southern blot for the presence of this fragment. The fragment was absent in all mice tested.

3.5 Genotyping

Mice were genotyped for the WT, Targeted, KO and FLPe alleles of *Brinp1* (Figure 3-7), *Brinp2* (Figure 3-8) and *Brinp3* (Figure 3-9). DNA was extracted from tail tips. PCR products of predicted sizes were seen for all genotyping reactions. To insure that the amplified product matched the correct gene, the product DNA for each genotype was sequenced. All genotyping PCR products showed the correct sequence. All unpredicted PCR products were checked for an unanticipated alteration to the gene in each of the *Brinp* lines. The genotyping results for *Brinp2*^{FLPe} and *Brinp2*^{Floxed} allele both showed a third, larger PCR product that did not match the predicted size of either the WT or *Brinp2* mutant alleles. These DNA species were each sequenced, and found to result from amplification of an unrelated gene resulting from mis-priming. All *Brinp* KO lines were maintained and genotyped throughout this project using heterozygous breeders, to allow for WT controls to be present in each litter.

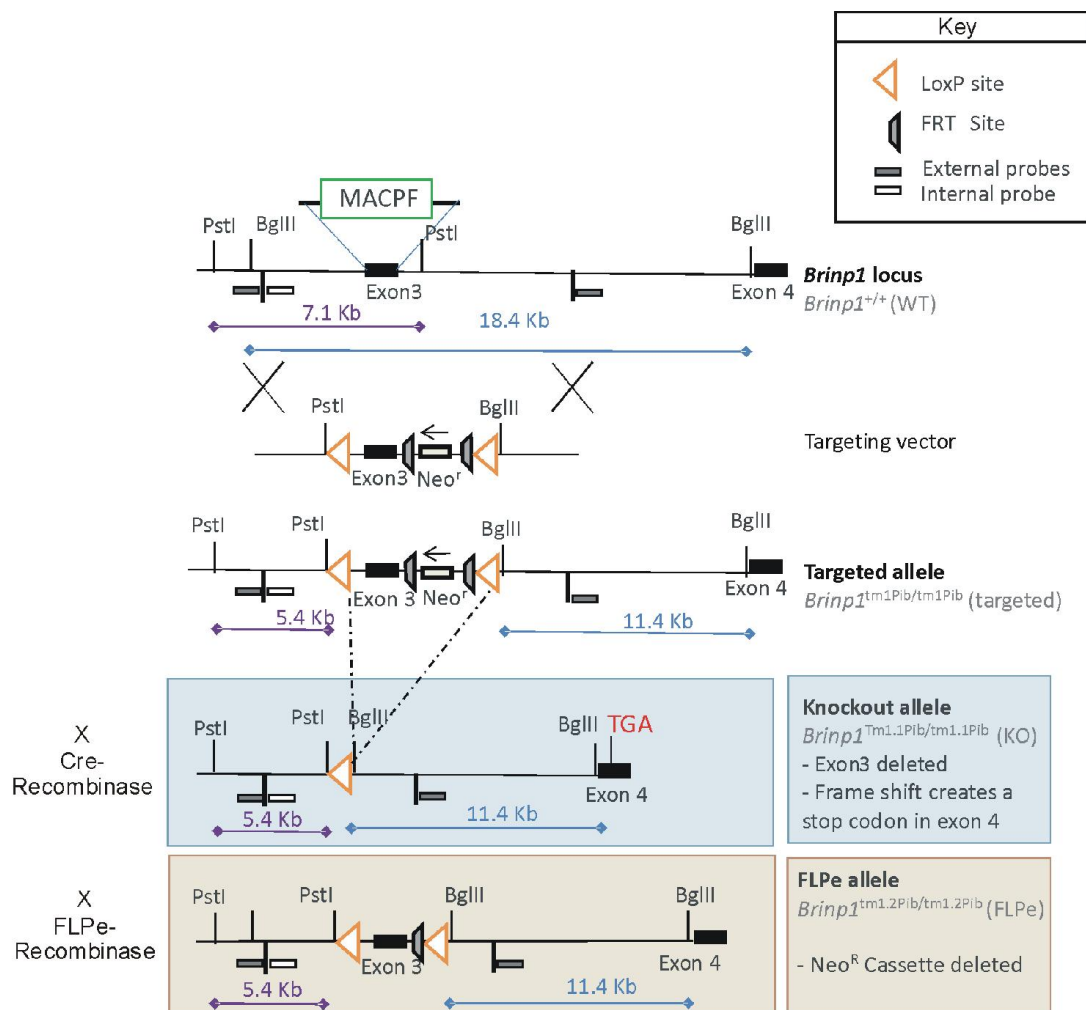


Figure 3-1 – Targeting strategy of the *Brinp1* locus

The 190 bp third exon of *Brinp1* contains the start of the MACPF domain. The *Brinp1* targeting vector was designed with a neomycin resistance (Neo^r) cassette after exon 3, and FRT sites positioned before and after the Neo^r cassette. LoxP sites were placed flanking exon 3 and the Neo^r cassette. The *Brinp1* targeting vector was integrated into the genome of murine ES cells via homologous recombination, to create the *Brinp1* targeted allele. When mice possessing the *Brinp1* targeted allele were crossed with a mouse line expressing Cre-recombinase, the recombination of LoxP sites results in the deletion of exon 3 and the Neo^r cassette. This resulted in a frame shift and introduced a stop codon near the start of exon 4. When crossed with a FLPe recombinase line, the recombination of the FLPe sites resulted in the removal of the Neomycin cassette, with no alteration to the coding sequence.

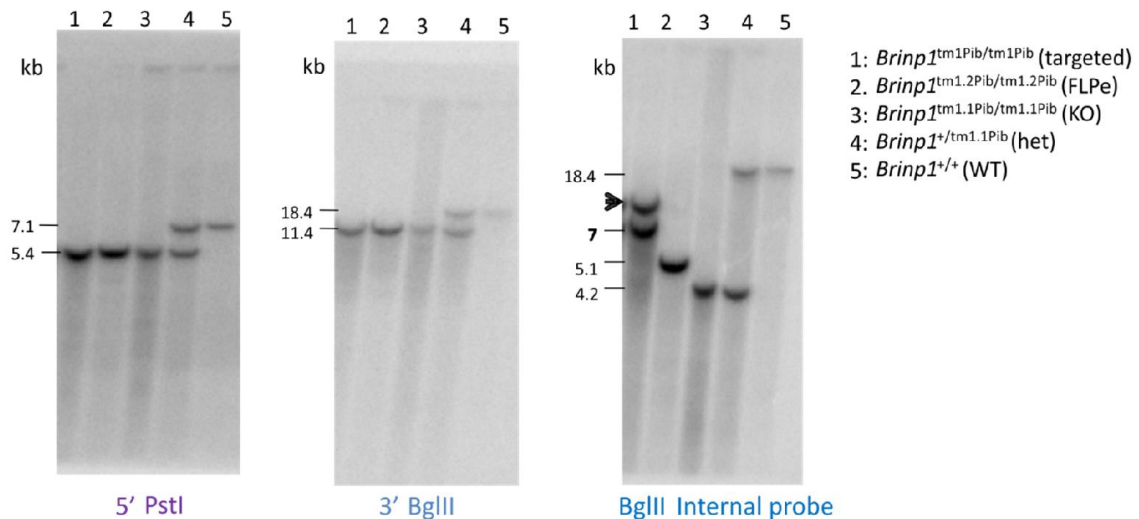


Figure 3-2 – Southern blotting of *Brinp1* targeted, *Brinp1* FLPe, *Brinp1* KO, *Brinp1* het and WT DNA

Genomic DNA isolated from the spleen was cleaved with PstI or BglII and hybridized to 500 bp genomic DNA probes from the 5' region (PstI) or 3' region (BglII) of the targeting construct. For wild-type DNA, species of 7.1 kb (PstI) and 18.4 kb (BglII) were detected. These species were not present in DNA from the *Brinp1* targeted, *Brinp1* FLPe or *Brinp1* KO mice, replaced with shorter species of 5.4kb (PstI) and 11.4 kb (BglII).

An internal BglII probe detected a 4.2Kb band species for the knockout allele, a 5.1 kb band species for the FLPed allele and a 7kb band species for the targeted allele. An arrow indicates a non-predicted species, a likely result of a partial BglII digest. Southern blots were performed under contract by Monash Gene Targeting Facility.

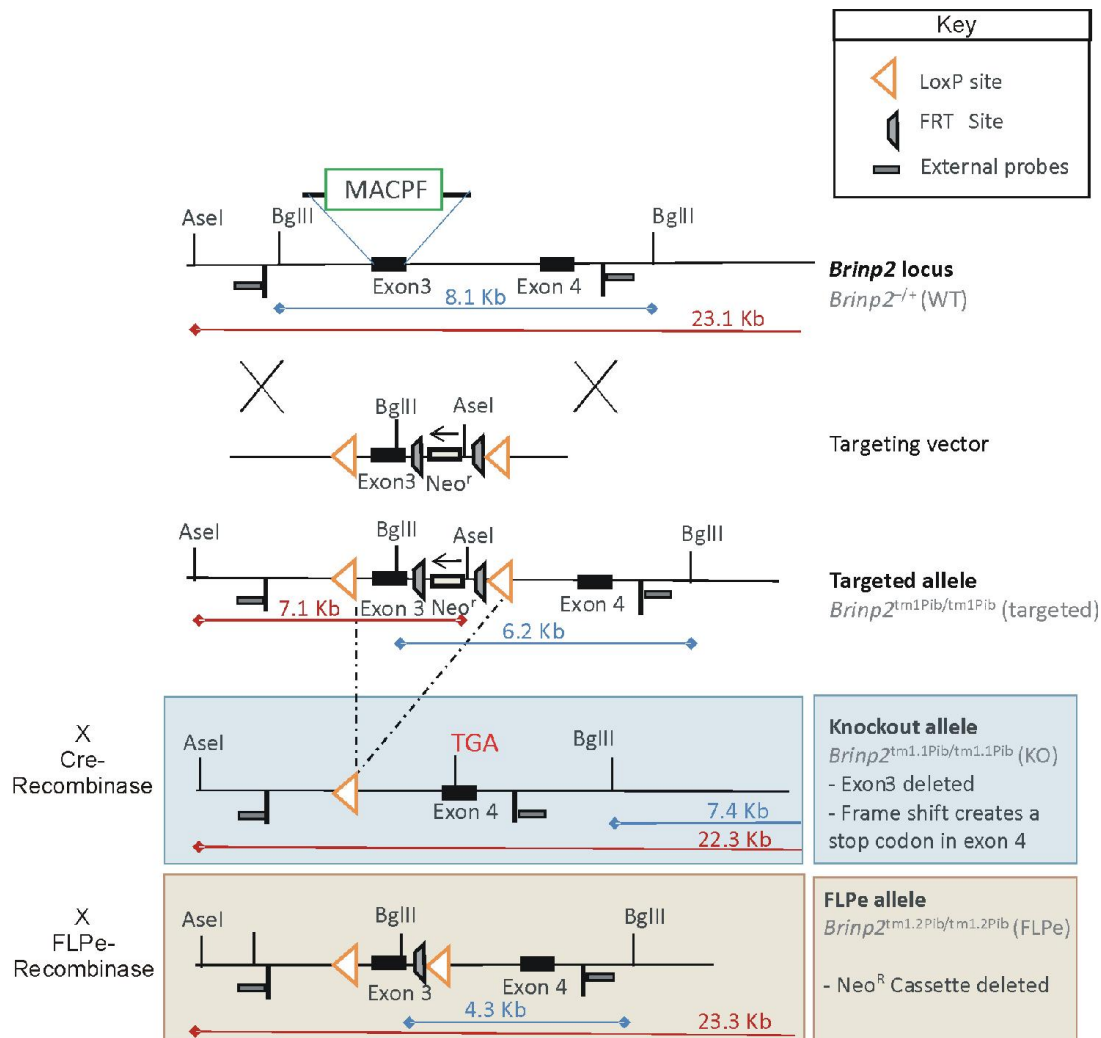


Figure 3-3 – Targeting strategy of the *Brinp2* locus

The 192 bp third exon of *Brinp2* contains the start of the MACPF domain. The *Brinp2* targeting vector was designed with a neomycin resistance (Neo^r) cassette after exon 3, and FRT sites positioned before and after the Neo^r cassette. LoxP sites were placed flanking exon 3 and the Neo^r cassette. The *Brinp2* targeting vector was integrated into the genome of murine ES cells via homologous recombination, to create the *Brinp2* targeted allele. When mice possessing the *Brinp2* targeted allele were crossed with a mouse line expressing Cre-recombinase, the recombination of LoxP sites results in the deletion of exon 3 and the Neo^r cassette. This resulted in a frame shift and introduced a stop codon near the start of exon 4. When crossed with a FLPe recombinase line, the recombination of the FLPe sites resulted in the removal of the Neomycin cassette, with no alteration to the coding sequence.

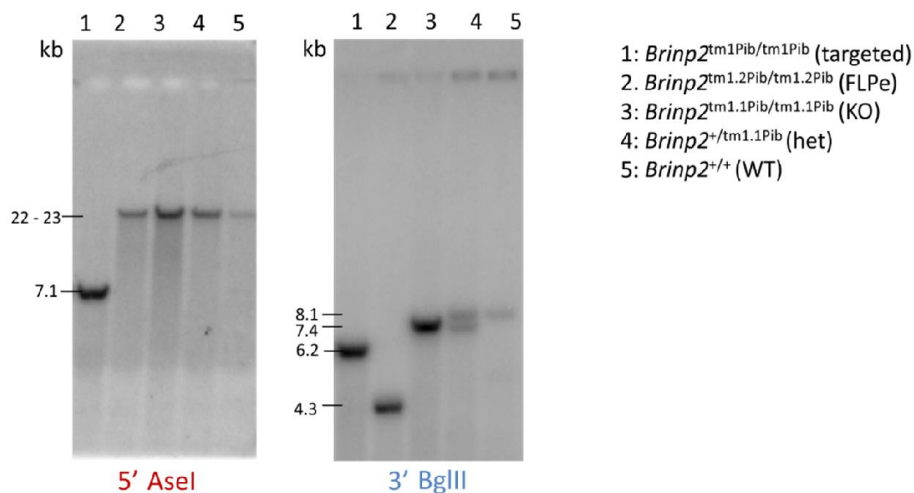


Figure 3-4 – Southern blotting of *Brinp2* targeted, *Brinp2* FLPe, *Brinp2* KO, *Brinp2* het and WT DNA

Genomic DNA isolated from the spleen and digested with *Asel* or *BglII* was probed with 500 bp genomic DNA probes from the 5' region (*Asel*) or 3' region (*BglII*) of the targeting construct. For wild-type DNA, species of 23.1 kb (*Asel*) and 8.1 kb (*BglII*) were detected. These band species sizes were not present in DNA from the *Brinp2* KO, replaced with bands species of 22.3 kb (*Asel*) and 7.4 kb (*BglII*). DNA from *Brinp2* FLPe mice showed the expected bands species of 23.3 kb (*Asel*) and 4.3 kb (*BglII*). DNA from homozygous targeted mice showed expected band species sizes of 7.1 kb (*Asel*) and 6.2 kb (*BglII*). Southern blots were performed under contract by Monash Gene Targeting Facility.

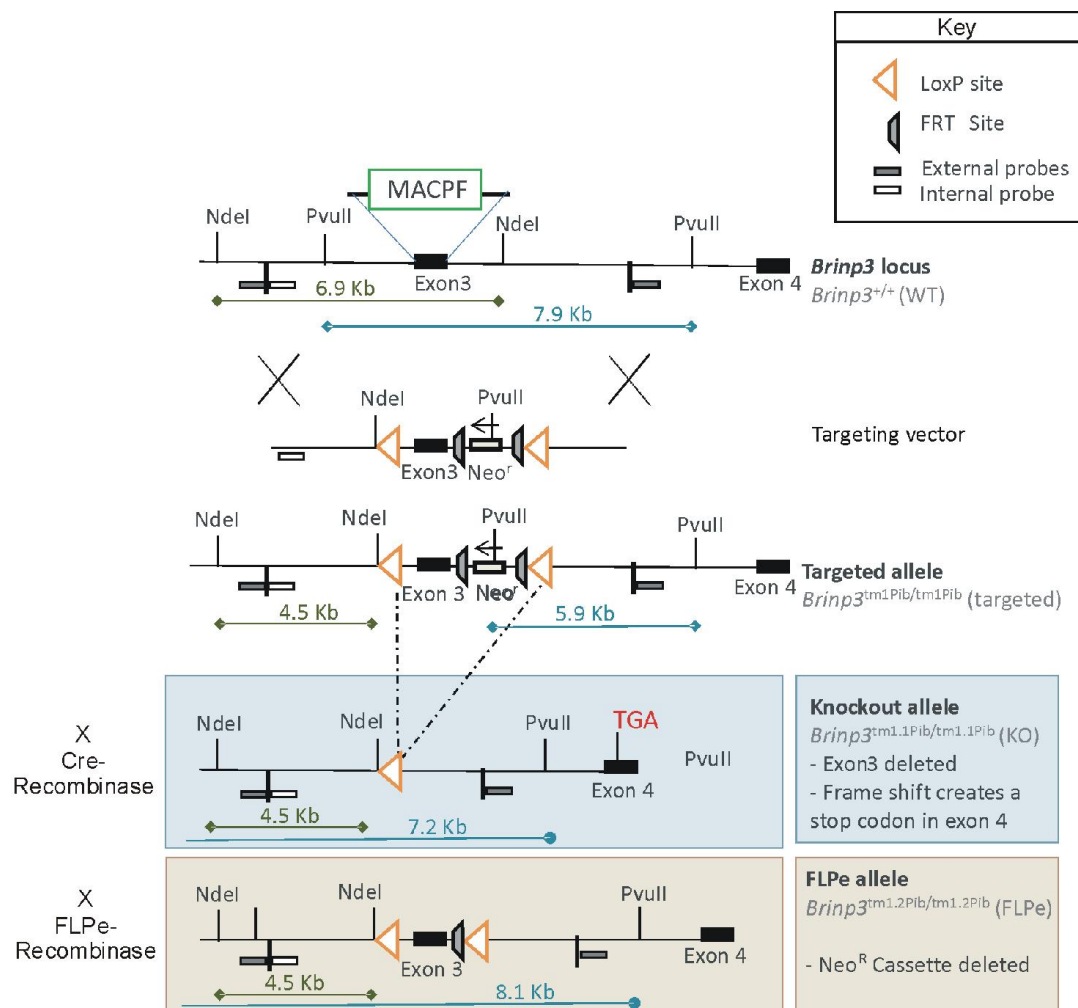


Figure 3-5 – Targeting strategy of *Brinp3* locus

The 289 bp third exon of *Brinp3* contains the start of the MACPF domain. The *Brinp3* targeting vector was designed with a neomycin resistance (Neo^r) cassette after exon 3, and FRT sites positioned before and after the Neo^r cassette. LoxP sites were placed flanking exon 3 and the Neo^r cassette. The *Brinp3* targeting vector was integrated into the genome of murine ES cells via homologous recombination, to create the *Brinp3* targeted allele. When mice possessing the *Brinp3* targeted allele were crossed with a mouse line expressing Cre-recombinase, the recombination of LoxP sites results in the deletion of exon 3 and the Neo^r cassette. This resulted in a frame shift and introduced a stop codon near the start of exon 4. When crossed with a FLPe recombinase line, the recombination of the FLPe sites resulted in the removal of the Neomycin cassette, with no alteration to the coding sequence.

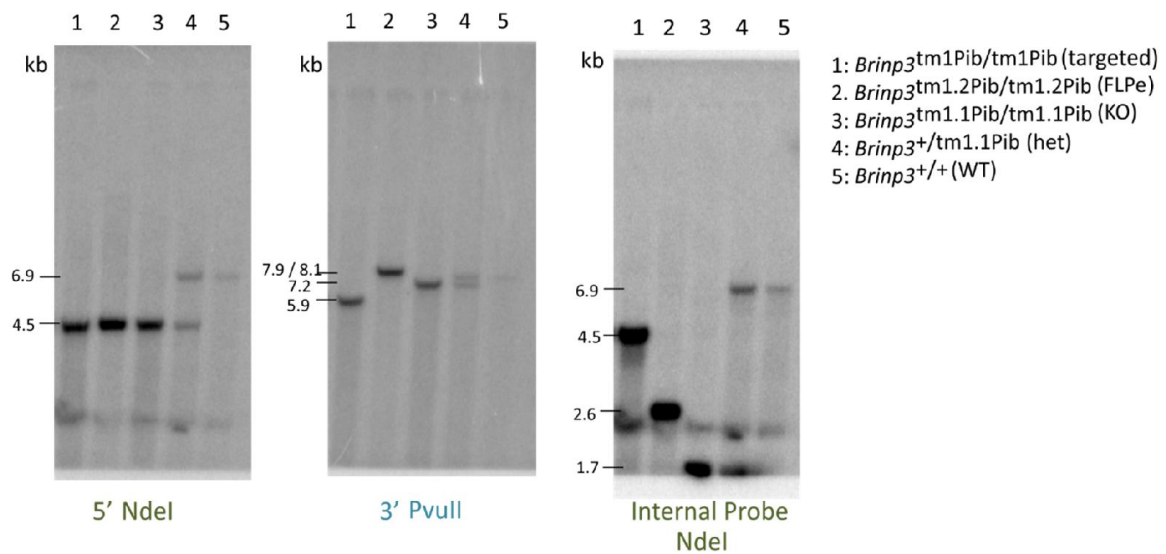
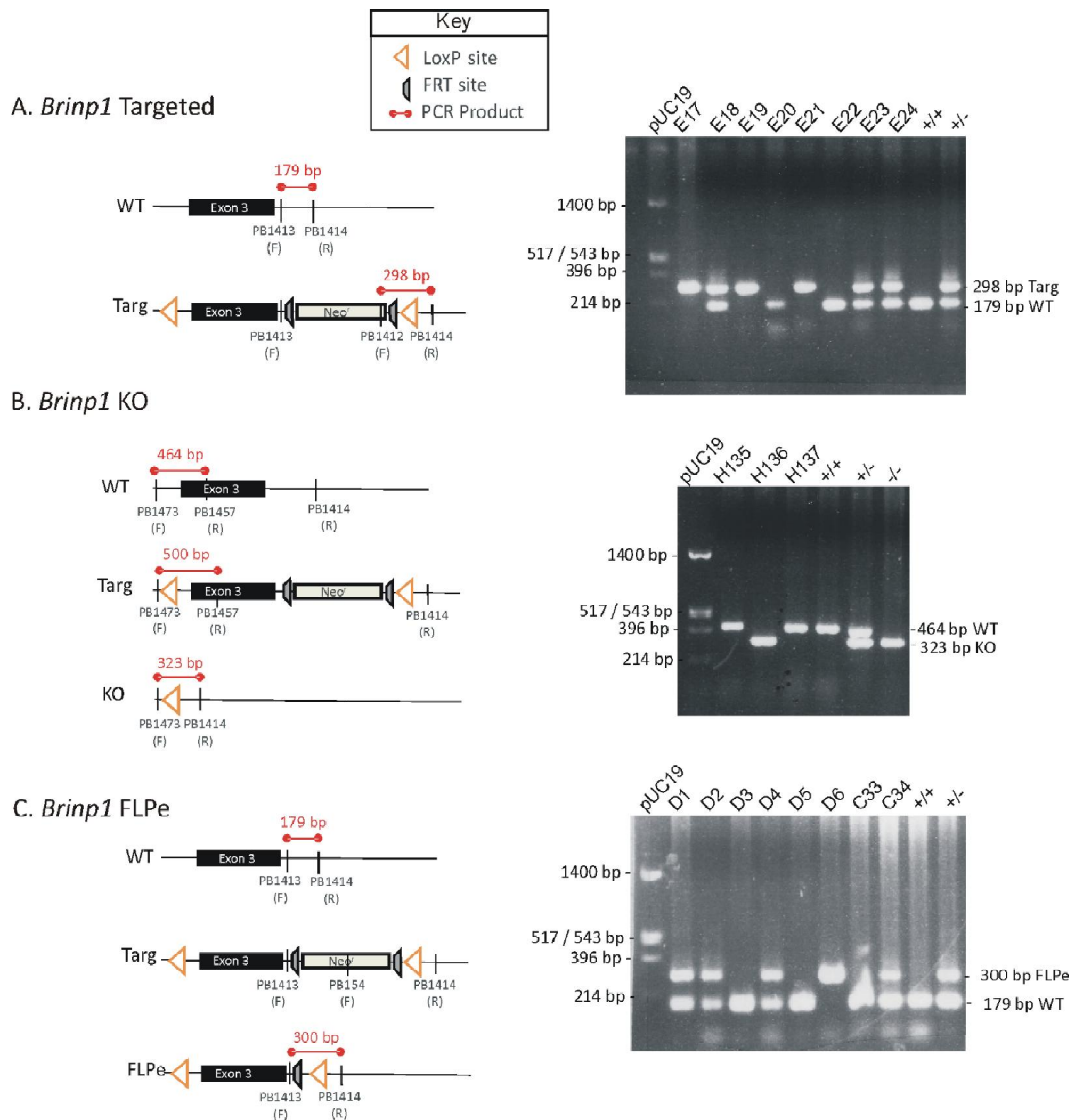


Figure 3-6 – Southern blotting of *Brinp3* targeted, *Brinp3* FLPe, *Brinp3* KO, *Brinp3* het and WT DNA

Genomic DNA isolated from the spleen and digested with NdeI or PvuII was probed with 500 bp genomic DNA probes from the 5' region (NdeI) or 3' region (PvuII) of the targeting construct. For wild-type DNA, species of 6.9 kb (NdeI) and 7.9 kb (PvuII) were detected. These band species sizes were not present in DNA from the *Brinp3* KO, replaced with bands species of 4.5 kb (NdeI) and 7.2 kb (PvuII). DNA from *Brinp3* FLPe mice showed the expected bands species of 4.5 kb (NdeI) and 8.1 kb (PvuII). DNA from homozygous targeted mice showed expected band species sizes of 4.5 kb (NdeI) and 5.9 kb (PvuII). Southern blots were performed under contract by Monash Gene Targeting Facility.



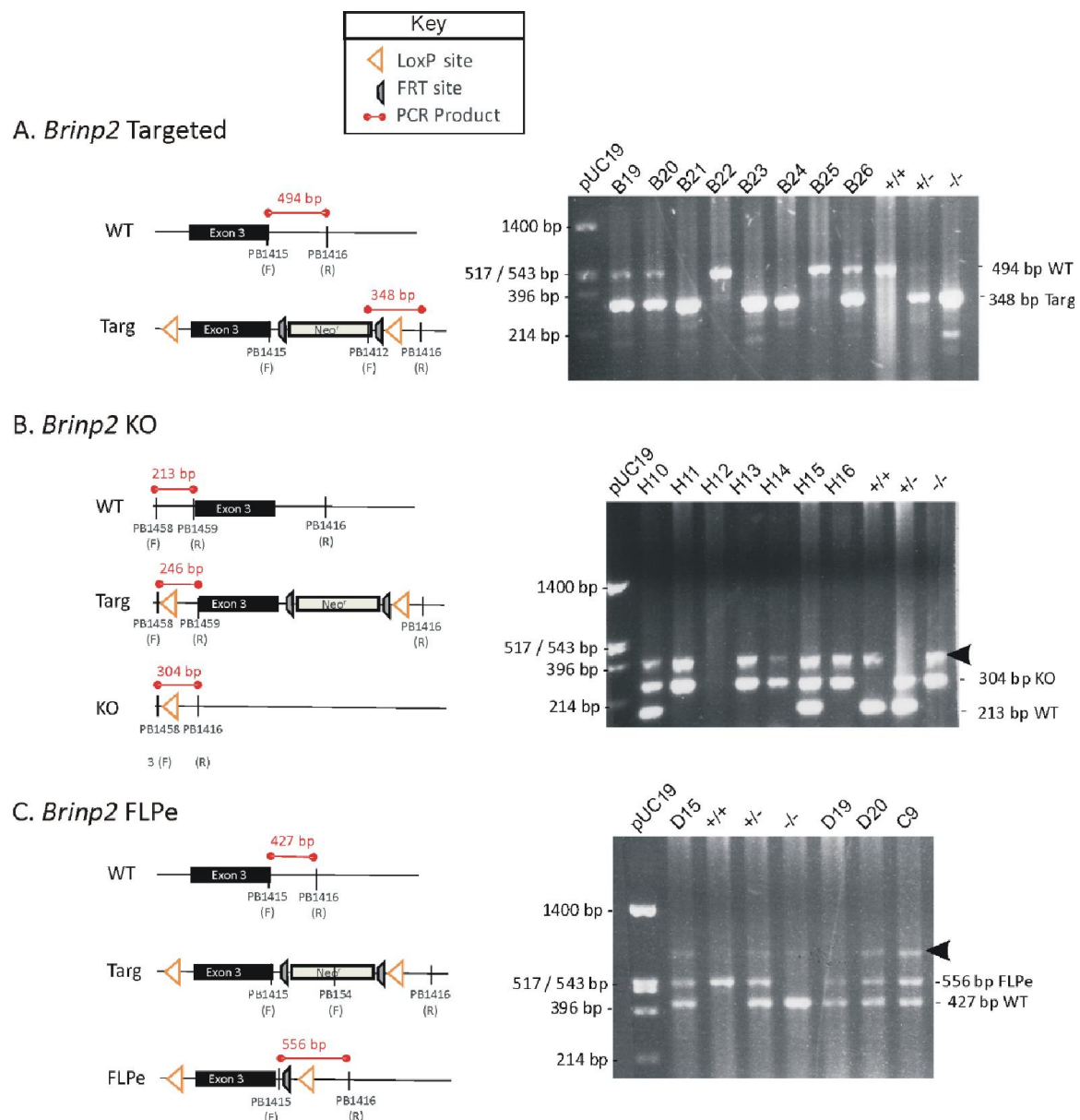


Figure 3-8 – Genotyping of *Brinp2* targeted, *Brinp2* KO and *Brinp2* FLPe mice

- A) The *Brinp2* targeted allele was detected as a 348 bp PCR product. The WT *Brinp2* allele was detected as a 494 bp PCR product.
- B) The *Brinp2* KO allele was detected as a 304 bp PCR product. The WT *Brinp2* allele was detected as a 213 bp PCR product.
- C) The *Brinp2* FLPe allele was detected as a 556 bp PCR product. The WT *Brinp2* allele was detected as a 427 bp PCR product.

Black arrows indicate instances of sequenced unrelated, irrelevant PCR products resulting from mis-priming. Controls: +/+ = WT, +/- = heterozygous mutant, -/- = homozygous mutant.

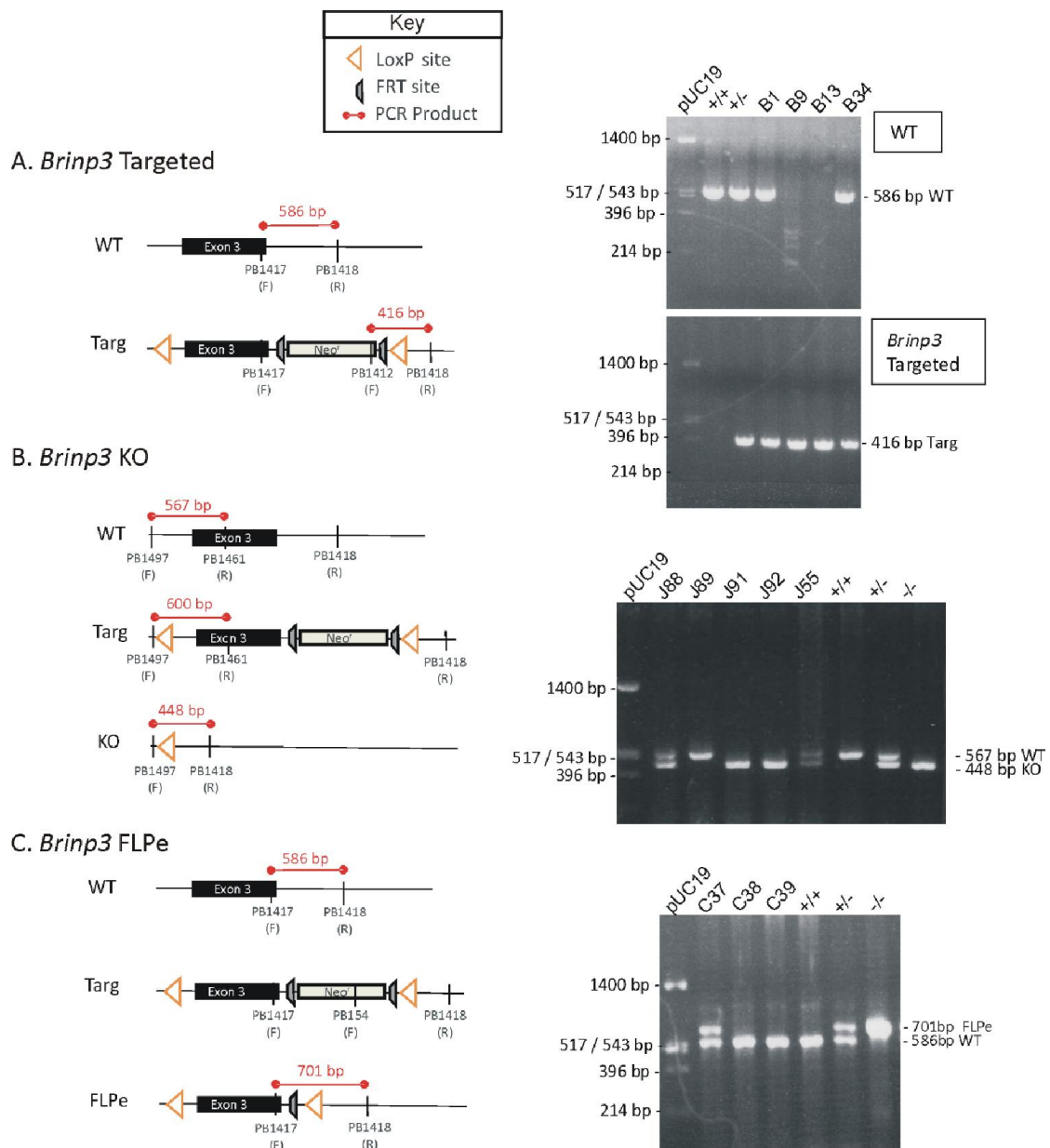


Figure 3-9 – Genotyping of *Brinp3* targeted, *Brinp3* KO and *Brinp3* FLPe mice

- A) The *Brinp3* targeted allele was detected as a 416 bp PCR product. By a separate PCR reaction, the WT *Brinp3* allele was detected as a 586 bp PCR product.
- B) The *Brinp3* KO allele was detected as a 448 bp PCR product. The WT *Brinp3* allele was detected as a 567 bp PCR product.
- C) The *Brinp3* FLPe allele was detected as a 701 bp PCR product. The WT *Brinp3* allele was detected as a 586 bp PCR product.

Controls: +/+ = WT, +/- = heterozygous mutant, -/- = homozygous mutant.

3.6 Validation of *Brinp* knockout lines

3.6.1 RT PCR validation

Total RNA from the brains of Cre-deleted *Brinp* KO lines was assessed for the presence of an mRNA transcript of the targeted gene. Primers were designed to hybridize to sequence spanning the deleted region (exon3). RT-PCR of the Cre-deleted knockout lines showed that mRNA lacking exon 3 is produced in the brain of knockout mice.

RT-PCR of cDNA derived from *Brinp1* KO brain tissue, using primers designed to exon 2 and exon 6, resulted in a single PCR product with a size of 396 bp corresponding to the removal of the 190 bp exon 3 (Figure 3-10A). Sequencing of the knockout allele PCR product showed the expected absence of the third exon and a frame shift in exon 4, as predicted (Figure 3-11A). This shift in the reading frame introduces a stop codon 25 residues downstream, resulting in a severely truncated form of the protein. The predicted 97-residue mutant protein would no longer have any of the MACPF domain or unique C-terminal sequence.

RT-PCR of cDNA derived from *Brinp2* KO brain tissue using primers designed to exon 2 and exon 4 resulted a single PCR product of 247 bp, corresponding to the removal of 192 bp exon 3 (Figure 3-10A). Sequencing of the knockout allele PCR product again showed the expected absence of exon3 and frame shift in exon 4, as predicted (Figure 3-11B). The shift in the reading frame introduces a stop codon 139-residues downstream, resulting in a truncated version of the protein, lacking the MACPF domain and unique C-terminal sequence.

RT-PCR of cDNA derived from *Brinp3* KO brain tissue using primers designed to exon 2 and exon 5. This resulted in a single PCR product of 221 bp corresponded to the removal of the 289 bp exon 3 (Figure 3-10A). Sequencing of the knockout allele PCR product showed the expected absence of exon3 and frame shift in exon 4, as predicted (Figure 3-11C). The shift in the reading frame introduces a stop codon 96-residues downstream. Again, this would produce only a truncated version of the protein, lacking the MACPF domain and unique C-terminal sequence.

3.6.2 Western blot validation

Absence of the BRINP1 protein was confirmed using an anti-BRINP1 antibody to probe lysates by immunoblotting (Figure 3-10B). A full length BRINP1 protein species of approximately 85

kDa was present in lysates of WT mouse brains at postnatal day 12, and absent in *Brinp1* KO mice. *Brinp2* KO and *Brinp3* KO samples were not tested by blotting due to the unavailability of antibodies.

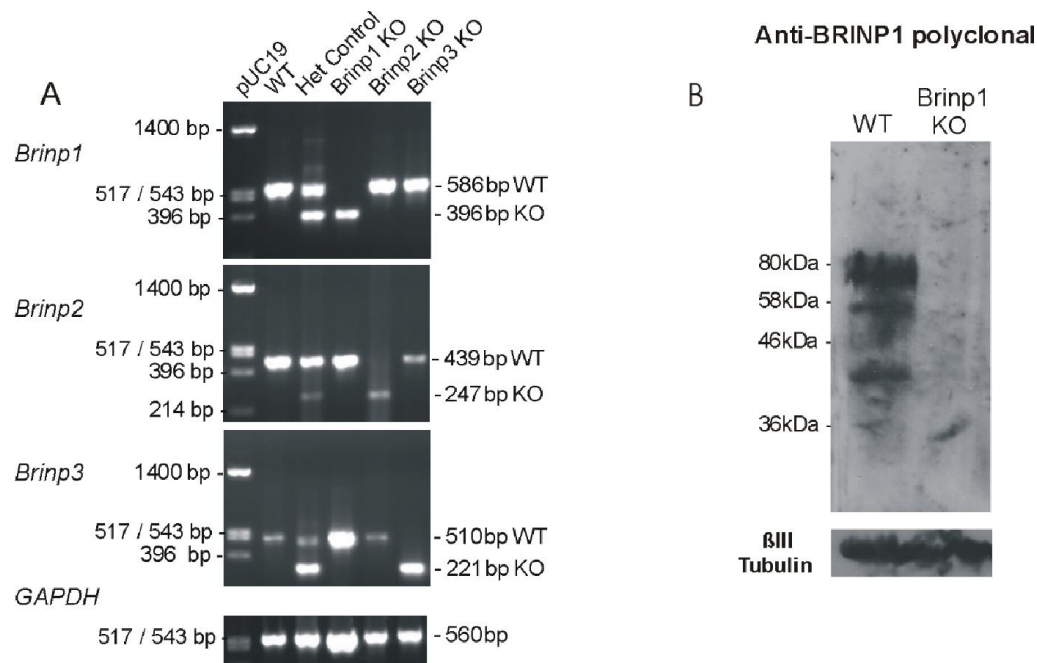


Figure 3-10 – Validation of *Brinp* knockout lines by reverse-transcriptase PCR and immuno-blotting

- A) RT-PCR validation of *Brinp* KO line using cDNA derived from brain tissue mRNA from WT, heterozygous and *Brinp* KO mice. PCR product sizes correspond to the removal of exon3 in the KO allele. Loading control: GAPDH.
- B) By immuno-blotting, full-length 85 kDa BRINP1 protein was present in lysates of WT mouse brains at postnatal day 12, and absent in *Brinp1* KO mice. Loading control: β III Tubulin.

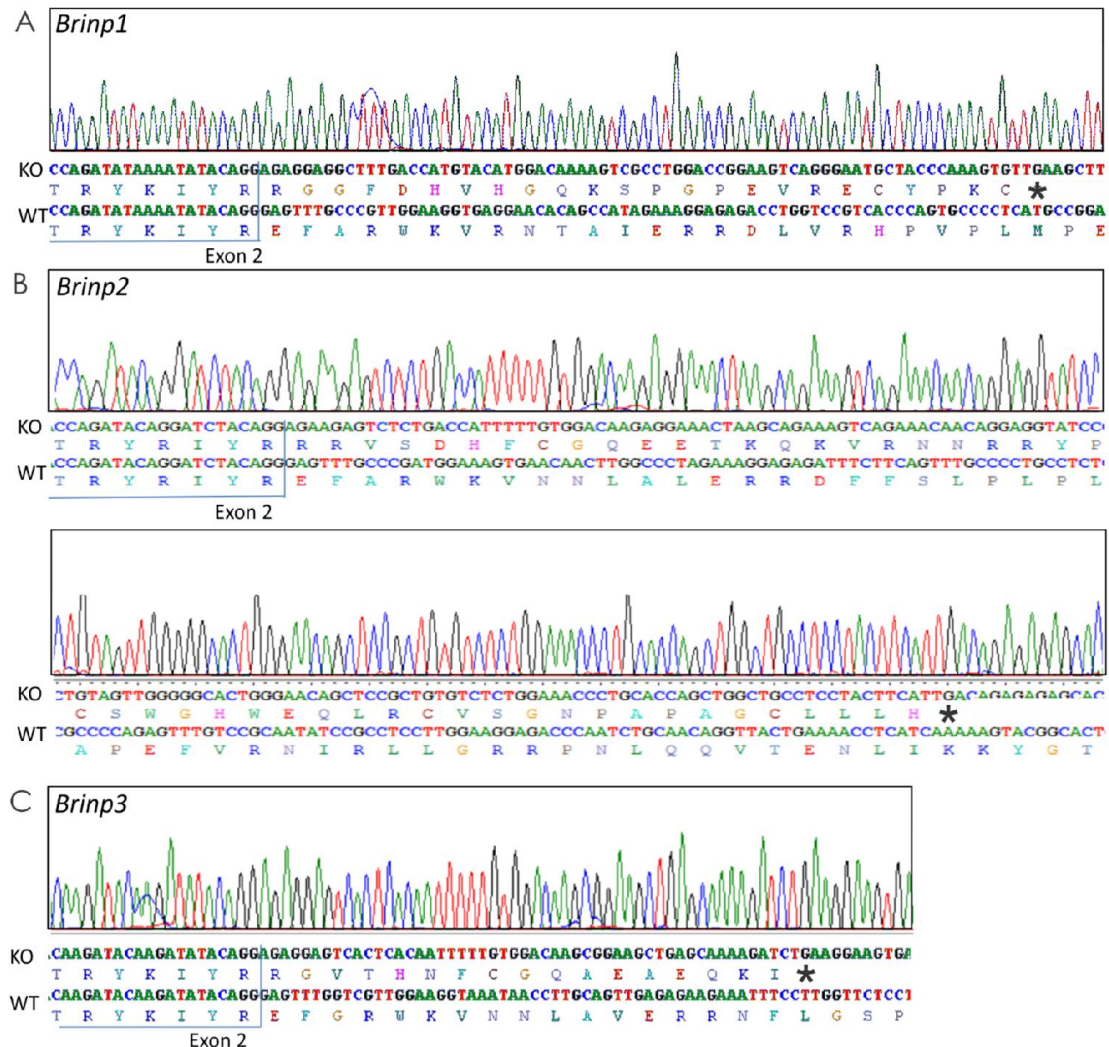


Figure 3-11 – Sequence alignments of *Brinp1*^{tm1.1/Pib}, *Brinp2*^{tm1.1/Pib} and *Brinp3*^{tm1.1/Pib} alleles

The sequence of A) *Brinp1*, B) *Brinp2* and C) *Brinp3* mRNA in knockout tissue. The trace sequences each show the end of exon2 for the respective genes. The deletion break point is shown at the end of exon 2.

In the knockout allele, exon 2 is fused to exon 4. The amino acid sequence of exon 4 shows a missense mutation due to frame shift occurs in exon 4, resulting in a stop codon (*) in the downstream sequence. The unaltered WT-exon3 sequence is shown below the KO sequence.

3.7 Analysis of survival of *Brinp1*, *Brinp2* and *Brinp3* knockout mice

For each of the three *Brinp* lines, litters bred from the heterozygous crosses were monitored for survival. Mice were genotyped at age of weaning (day 21). Genotypes were assessed for Mendelian inheritance (25% of total progeny expected to be KO mice) as an indicator of normal viability.

Brinp2 and *Brinp3* KO mice demonstrated close to Mendelian inheritance for the number of knockouts surviving to age of weaning (*Brinp2*, 19%, *Brinp3* 24%). In contrast, only 12 out of 83 (14%) of the mice weaned from the *Brinp1* line were knockouts (Figure 3-12A).

The number of mice per litter were also notably fewer for the *Brinp1* line bred from heterozygous crosses. An average of three mice per litter survived to age of weaning (P21), less than a typical C57BL/6 litter size of 6-10 pups (Figure 3-12B). The small litter sizes and lower than expected number of *Brinp1* KO mice at weaning age suggested that some of the *Brinp1* KO mice were dying at a prenatal or postnatal stage.

Mice were examined before and after birth to determine the point of death. Pups from heterozygous litters that were found dead at postnatal day 0 to day 2 (P0 – P2) were genotyped. Of those mice dying early (n=43 pups found dead, P0 – P2), 50% were found to be knockouts (26% het and 24% WT), indicating that half of *Brinp1* KO mice from born from heterozygous breeders were dying at, or within, a couple of days after birth.

Homozygous KO breeders were set up to test fertility of KO mating pairs. *Brinp1* KO, *Brinp2* KO and *Brinp3* KO homozygous matings, each resulted in full term gestation. *Brinp2* KO and *Brinp3* KO mice each had viable litters that survived to adulthood. In contrast, the majority of *Brinp1* KO litters from *Brinp1* KO breeders died as neonates.

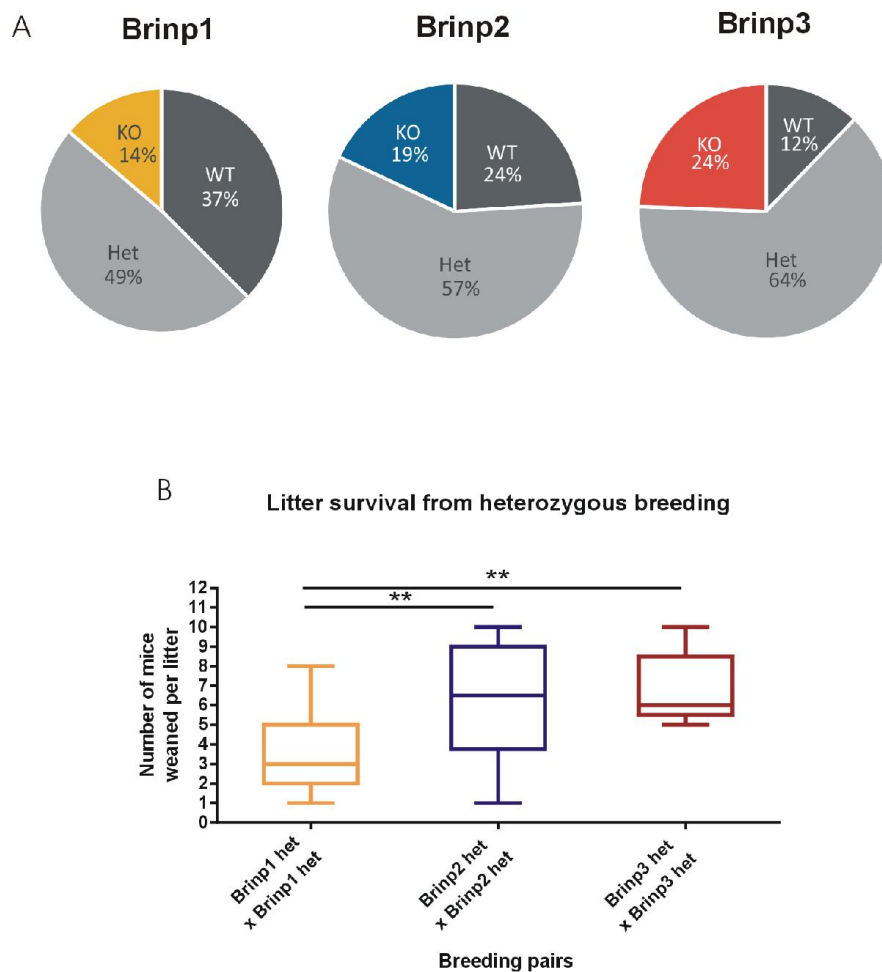


Figure 3-12 – Analysis of offspring for from *Brinp1*, *Brinp2* and *Brinp3* heterozygous breeders

- A) Pie charts showing genotype ratios of mice born from heterozygous crosses, represented as percentage of mice per genotype at age of weaning (P21) (*Brinp1* n=80 mice, *Brinp2* n = 50 mice, *Brinp3* n =41 mice).
- B) Box plots showing number of mice weaned per litter from heterozygous breeders (*Brinp1* n=23 litters, *Brinp2* n = 14 litters, *Brinp3* n = 9). A one-way ANOVA, conducted on number of mice weaned, found significant differences between the breeder genotype: $F(2,43)=9.282$, $p<0.0001$. A Tukey HSD post-hoc test showed significant differences in number of pups weaned between *Brinp1* het and *Brinp2* het breeder ($p=0.003$), as well as between *Brinp1* het and *Brinp3* het breeders ($p=0.003$). No significant difference was found between *Brinp2* het and *Brinp3* het breeders ($p=0.890$). Boxes represent inter-quartile range. The central horizontal line shows the mean. The range is shown by error bars. ** $p = 0.01$.

To investigate the reduced survival of *Brinp1* KO mice, the fecundity of WT x WT, het x het, *Brinp1* KO x *Brinp1* KO and WT x *Brinp1* KO breeding pairs was compared (Table 3-1). Litter numbers at birth were normal for all breeder genotypes, with no delay in first breeding or time between litters. However, post-partum survival of progeny of *Brinp1* KO x *Brinp1* KO breeders was significantly reduced, with an average of only one mouse surviving per litter after 3 days. Litter survival from het x het breeders was also reduced (average of four mice surviving per litter). Specifically, only 19 / 98 (22%) of all pups born to *Brinp1* KO x *Brinp1* KO parents, and 75% born to het x het parents, survived longer than 3 days. This was in contrast to a 91% survival rate of progeny from WT x WT breeders.

Table 3-1 – Reproductive Phenotyping

	Male/Female			
	WT / WT	Het / Het	<i>Brinp1</i> KO / <i>Brinp1</i> KO	WT ♂/ <i>Brinp1</i> KO ♀
Days from mating to first litter	25.8	22.8	25.0	24
Days between litters	26.7	22.1	27.6	27.4
Number of litters	19	22	20	20
Number of pups born (P0)	116	100	98	96
Number of pups weaned (P21)****	105	75	19	50
% survival	91%	75%	22%	52%

Four breeders per genotype (WT/WT, Het/Het, *Brinp1* KO /*Brinp1* KO and WT ♂/*Brinp1* KO ♀) were monitored over four months to investigate reproductive rates and postnatal survival. The survival of mice to age of weaning (P21) was significantly impacted by the presence of *Brinp1*-deleted allele: **** χ^2 (3, n=249) = 63.80, $p < 0.0001$; Chi-square test.

The offspring of *Brinp1* KO x *Brinp1* KO parents were observed post-partum. Although several pups survived birth, most were found dead 12-48 hr later. Little to no milk was present in the stomach of the animals found dead, indicating lack of adequate nutrition as a possible cause of death. Taken together, these results suggest that absence of *Brinp1* is detrimental to survival. The higher pup survival rate when a *Brinp1* KO female was mated with a WT male indicates that *Brinp1* in the pup also contributes to postnatal survival.

3.8 Postnatal weight of *Brinp* knockout mice

Brinp1, *Brinp2* and *Brinp3* KO mice were weighed weekly from three to twelve weeks of age (Figure 3-13). WT littermates from each line were used for comparison. Knockout mice from all three lines showed some degree of reduced body mass, with *Brinp1* KO mice showing the most notable weight difference from infant (week 3) until adulthood (week 12). Adult *Brinp1* KO mice were 10-15% smaller than their WT littermates, with both male and female mice having a reduced body weight at each weighing. *Brinp1* heterozygous mice were weighed to determine whether hemizygous deletion also has an effect on body weight. *Brinp1* het females show a reduced body weight close to that of *Brinp1* null mice, whereas the weight of *Brinp1* heterozygous male mice recovered close to WT. Adult *Brinp1* KO mice body size was assessed to determine whether the reduced mass corresponded with smaller stature; an indicator of impaired growth. Neither male nor female *Brinp1* KO mice showed a statistically significant difference in body length or tail length.

Female *Brinp2* KO mice displayed normal weight throughout the weighing period. Male *Brinp2* KO mice did show reduced body mass from six weeks onwards, weighing 10% less as adults at week 12. Male *Brinp3* KO mice weighed less than their WT littermates in the first few weeks of weighing (3-5 weeks) for both males and females, before their weights recovered to that of their WT littermates.

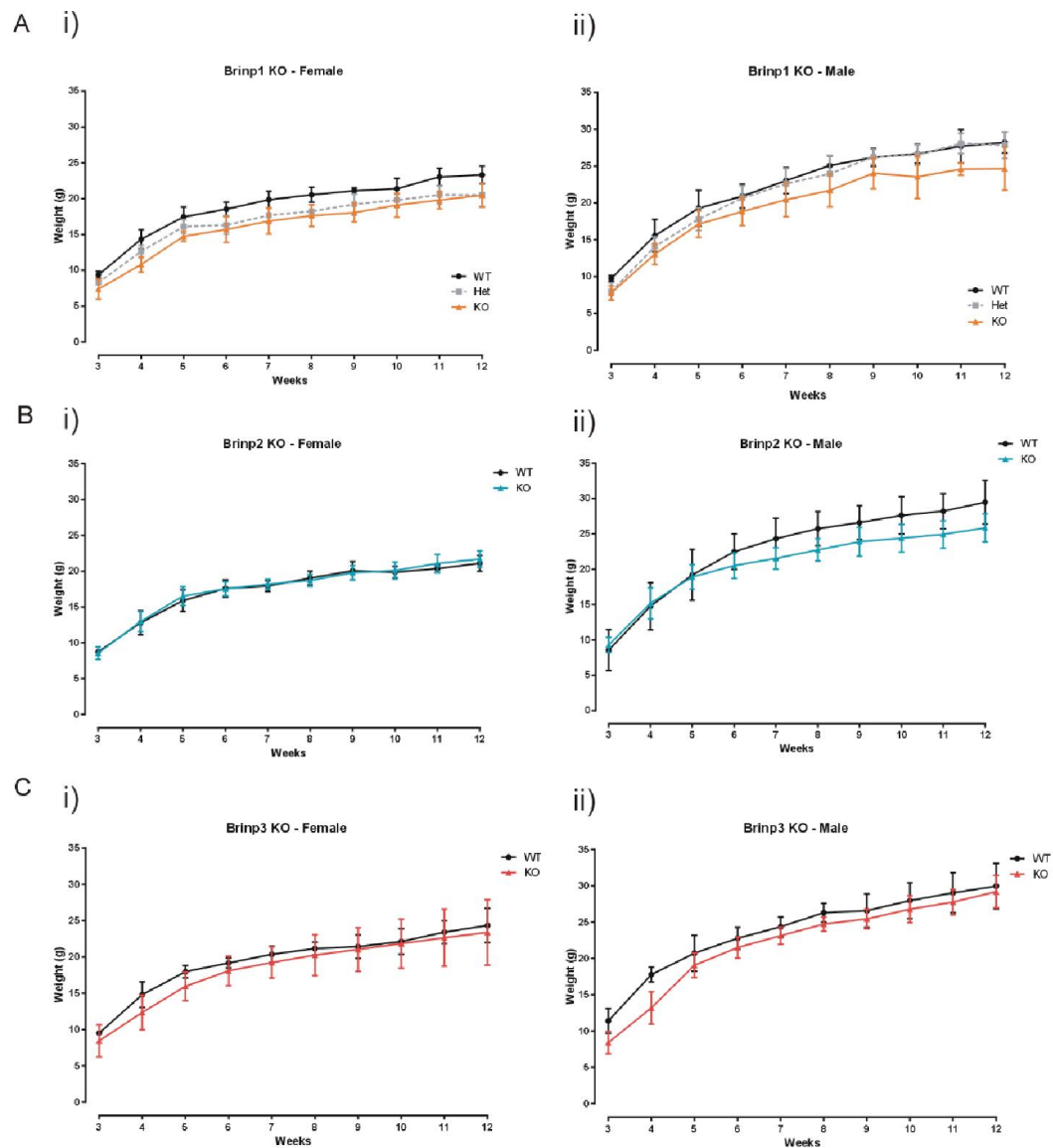


Figure 3-13 – *Brinp1*, *Brinp2* and *Brinp3* KO mice weighing

Male and female A) *Brinp1*, B) *Brinp2* and C) *Brinp3* KO mice were weighed weekly from three to 12 weeks, alongside WT litter mates. Additionally, *Brinp1* het mice were weighed alongside *Brinp1* KO mice.

- A) i) Female *Brinp1* KO mice showed a significant reduction in body weight by repeat measures two-way ANOVA: $F(2,18)=27.580$, $p<0.001$. A Tukey HSD multiple comparison test found female *Brinp1* KO mice to weigh significantly less than WT littermates of the same sex ($p<0.001$). *Brinp1* het female mice were also found to weigh significantly less than WT ($p<0.001$). No significant effect of genotype was found between female *Brinp1* het and KO mice ($p=0.362$).
 ii) Male *Brinp1* KO mice also showed a significant reduction in body weight by repeat measures two-way ANOVA: $F(2,23)=8.312$, $p=0.002$. A Tukey HSD multiple comparison test found a significant difference between male WT and *Brinp1* KO mice ($p=0.002$), and male *Brinp1* het and KO mice ($p=0.013$). No significant effect of genotype was found between male WT and *Brinp1* het mice ($p=0.704$).
- B) i) Female *Brinp2* KO mice showed no significant main effect of genotype on body weight to by repeat measures two-way ANOVA: $F(1,15)=0.155$, $p=0.699$, and no interaction effect of genotype x time: $F(9,135)=0.804$, $p=0.613$.
 ii) Male *Brinp2* KO mice also showed no main effect of genotype on body weight by repeat measures two-way ANOVA: $F(1,13)=2.987$, $p=0.108$, whilst showing a significant interaction of genotype x time: $F(9,117)=5.645$, $p<0.001$.
- C) i) Female *Brinp3* KO mice showed no main effect of genotype on significant on body weight by repeat measures two-way ANOVA: $F(1,12)=0.398$, $p=0.540$, but did show a significant interaction of genotype x time: $F(8,96)=2.115$, $p=0.042$.
 ii) Male *Brinp3* KO mice showed a significant reduction in body weight to their littermates by repeat measures two-way ANOVA: c, and a significant genotype x week interaction $F(9,108)=3.919$, $p<0.001$.

N=7-12 mice per genotype. Results are represented as mean \pm SD.

3.9 Histopathology of *Brinp* knockout mice

A full pathological examination of mice from *Brinp1*, *Brinp2* and *Brinp3* KO lines was carried out at seven to eight weeks of age (APN cases: *Brinp1*: APN12/001, *Brinp2*: APN11-034, *Brinp3*: APN11-039). Two WT and two KO mice per *Brinp* line were assessed for macroscopic observations. This first line phenotyping was intended to identify any changes in overall health and anatomy. Histopathology of *Brinp* KO mice was performed under contract by the Australian Phenomics Network (<http://www.australianphenomics.org.au>).

3.9.1 Macroscopic observations

At the time of necropsy, mice from all three lines were well nourished, well groomed, active/curious. There were no observable dermal lesions and no nasal/ocular discharge. The gastrointestinal tract contained ample ingesta and the thoracic and abdominal viscera showed no macroscopic abnormalities. All 25 organs examined were of normal appearance, with no notable differences in size of vital organs (Table 3-2).

3.9.2 Microscopic observations

Organ pathology was normal for *Brinp1*, *Brinp2* and *Brinp3* KO mice, with no lesions of significance observed in any of the 25 organs examined.

3.9.3 Brain pathology

An emphasis was placed on the analysis of nervous tissue due to the high expression of *Brinps* in the central and peripheral nervous system. Sections of *Brinp1*, *Brinp2* and *Brinp3* KO mice brains showed normal structure for the forebrain, midbrain and cerebellum (Figure 3.14). The brains appeared symmetrical with no ventricular dilation. The cerebellum appeared symmetrical with typical architecture and unremarkable Purkinje cells. There was no evidence of neuronal loss and the myelination appeared normal. Overall, no gross morphological changes were detected within the KO mouse brains at this level of analysis. For a second opinion, the brain sections were further examined by neuropathologist, Professor Catriona McLean, Head Anatomical Pathology, Alfred Health, who agreed with the findings of no significant neuropathology of the brain or spinal cord of *Brinp1*, *Brinp2* and *Brinp3* KO mice brains.

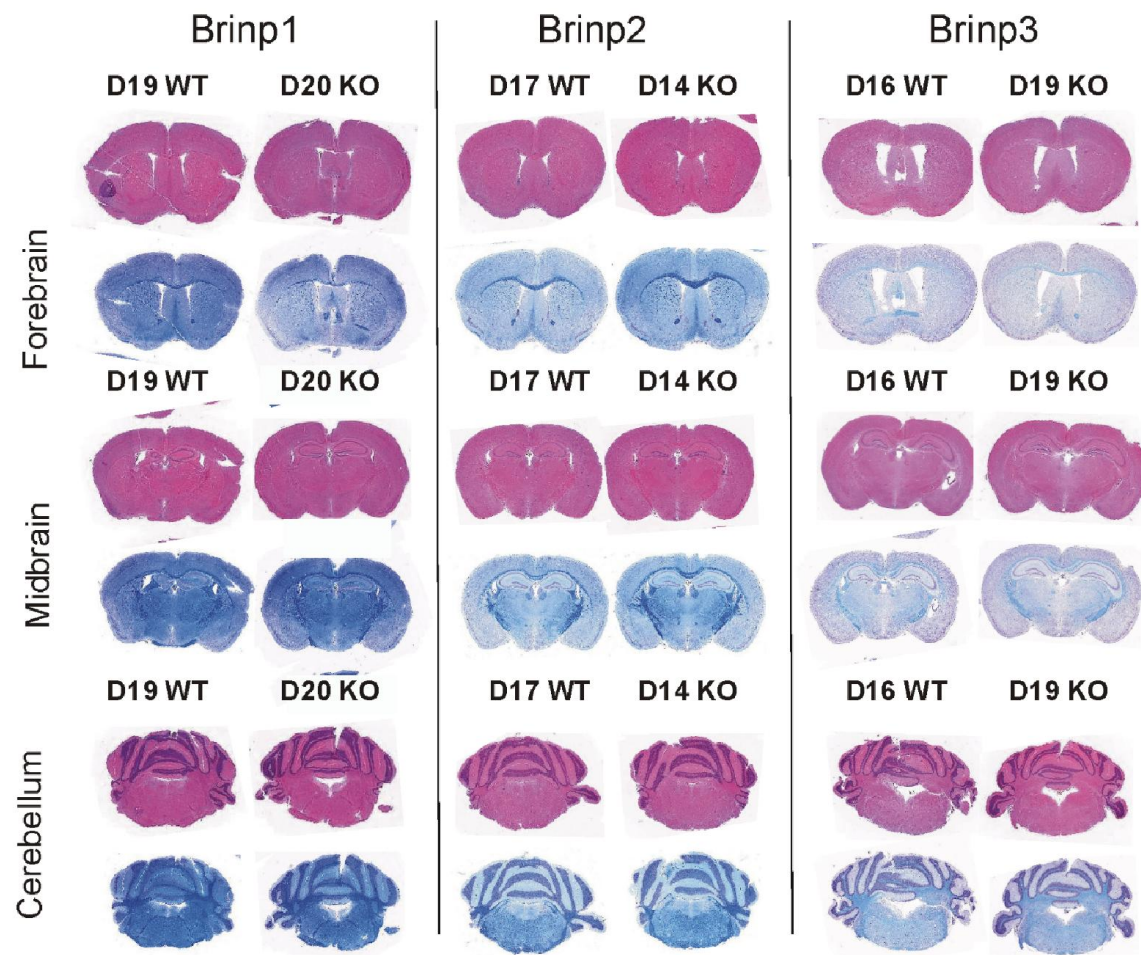


Figure 3-14 – Brain sections of *Brinp1*, *Brinp2* and *Brinp3* knockout mice

Coronal brain sections of *Brinp1*, *Brinp2* and *Brinp3* KO mice, compared to WT littermates. Representative sections are shown of the forebrain, midbrain (including medial hippocampus) and cerebellum of 7-8 week old mice. Brains were stained with Hematoxylin and Eosin (purple), and Luxol Fast Blue. Figure compiled from images provided by the Australian Phenomics Network.

Table 3-2 - *Brinp1*, *Brinp2* and *Brinp3* KO mice show normal macroscopic size for internal organs

Compiled from data provided by the Australian Phenomics Network. *Measurement not taken.

	<i>Brinp1</i>				<i>Brinp2</i>				<i>Brinp3</i>			
Mouse ID	# D19	# D21	# D20	# D22	# D17	# D18	# D14	# D16	# D16	# D19	# D21	# D12
Genotype	WT	WT	KO	KO	WT	WT	KO	KO	WT	WT	KO	KO
Age (days)	49	49	49	49	46	46	65	46	60	60	59	60
Sex	F	F	F	F	M	M	M	M	M	M	F	F
Weight (g)	17.3	18.2	16.7	15.0	23.0	22.7	27.0	23.2	24.0	24.1	18.2	16.1
Spleen (mm)	12x4x2	12x3x2	12x3x2	15x2x2	20x5	12x3x2	15x5x2	15x4x2	13x3x2	15x4x2	12x3x2	14x4x2
Kidney (mm)	10x5x2	10x5x5	10x6x4	10x5x5	12x6	11x5x4	12x6x5	12x6x4	11x5x4	12x6x6	9x5x3	10x5x5
Lungs	Inflated	Inflated	Inflated	Inflated	Inflated	Inflated	Inflated	Inflated	Inflated	Inflated	Inflated	Uninflated
Heart (mm)	9x6x2	10x6x4	10x8x5	8x8x4	8x5x4	8x4x4	10x6x4	10x6x4	7x5x4	10x6x4	7x4x4	-
Brain (mm)	12x9x3	15x10x5	12x9x3	15x10x5	15x10x4	13x9x5	15x10x4	15x11x4	13x9x5	14x9x5	13x9x5	14x10x8
Thymus (mm)	10x8x2	8x8x2	10x8x2	8x8x2	8x6x2	8x6x2	8x8x2	9x7x2	7x7x2	9x8x2	6x6x2	10x10x3
Testes (mm)	n/a	n/a	n/a	n/a	7x5x3	5x5x3	8x5x3	8x4x2	6x4x3	n/a	8x4x3	n/a
Tail length (mm)	80	80	73	75	80	70	80	*	*	*	*	*

3.9.4 Tissue inflammation in *Brinp1* knockout mice

Brinp1 KO mouse D20 (female) showed mild inflammation in submucosal stomach, and moderate perivascular inflammation in lungs. *Brinp1* KO mouse D22 (female) showed a small periadipose inflammatory cluster in a mammary fat pad, with some scattered mast cells were identified (Figure 3-15). Whilst notable, this is a common finding in mouse mammary tissue.

Blood results indicated an elevated percentage of eosinophils in all animals (including WT controls) and low (mild) platelet levels detected in both knockout animals. Bone marrow showed typical myeloid and lymphoid elements.

The detected inflammation was referred to pathologist Professor Rolfe Howlett, R&A Pathology Services, NSW for a supplementary report:

“The inflammation identified in the stomach and lungs of animal D20 and in the mammary fat pad of animal D22 is judged to be of no significance.

The sections and levels examined did not show micro-morphological abnormalities or significant pathology in animals D20 and D22.”

- Professor Rolfe Howlett, R&A Pathology Services, NSW

In conclusion, whilst the inflammation was notable, it was not deemed a significant phenotype because of common occurrence of such inflammation in laboratory mice.

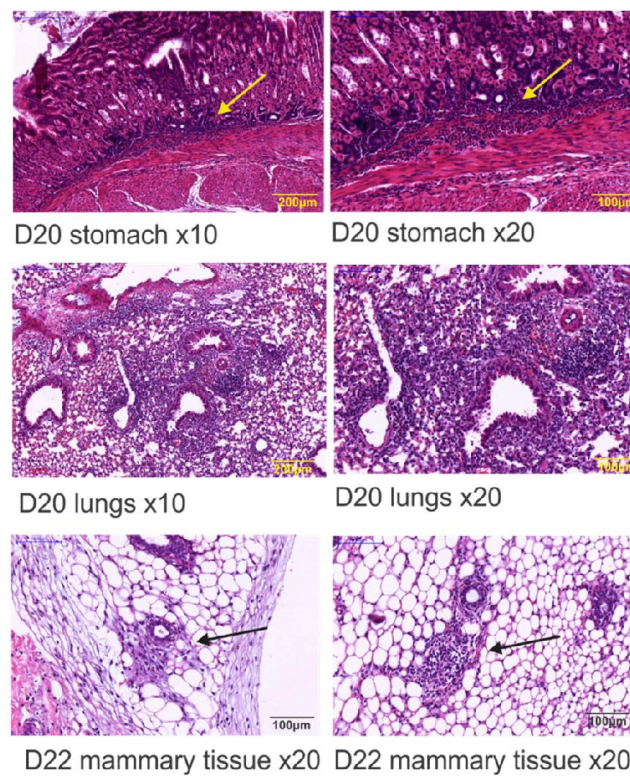


Figure 3-15 – Tissue inflammation in *Brinp1* KO mice

Tissue inflammation in *Brinp1* KO mice, shown by Hematoxylin & Eosin (H&E) staining. Inflammation was observed in the stomach, lungs and mammary tissue, as indicated by arrows. Images courtesy of the Australian Phenomics Network.

3.9.5 Analysis of *Brinp1* knockout late stage embryos

In addition to the whole body analysis at seven weeks of age, *Brinp1* KO mice were also assessed at a late embryonic stage (APN case: APN12/043). Analysis of embryos was carried out solely on the *Brinp1* line to follow up on the lower survival of *Brinp1* KO mice reported in section 3.7, and to determine whether *Brinp1* KO mice show abnormalities in embryonic development.

Embryos were harvested at embryonic day 18.5 from two *Brinp1* heterozygous dams that had been mated with a heterozygous *Brinp1* male. Pregnant female 1 (38.3g) and female 2 (39.7g) showed typical gravid uteruses with eight and nine placental sites respectively. Placentas appeared normal with good coloration and no evidence of placental failure or unviable embryos. WT, heterozygous and *Brinp1* KO embryos were assessed for macroscopic abnormalities. Crown to rump length of all embryos was 20-23mm, within normal range (Figure 3-16A). No visible external lesions were identified in knockout or control embryos. The eyes and ears were closed/fused and pigmented eyes were visible through the skin for all embryos examined.

The head, body and placenta of six *Brinp1* KO, eight *Brinp1* het and three WT embryos were sectioned for microscopic analysis. The *Brinp1* KO and control brains appeared appropriately differentiated for their developmental age with typical migrating neuroblasts identified and layering of the brain with distinct and developing regions. Sections show a well-developed olfactory lobes, neopallial cortex, ventricular zone with surrounding germinal region, cerebellar primordium with an external granule layer, Purkinje plate/cell layer, and developing fissures (Figure 3-16B). No abnormalities or lesions were identified in head, body or placenta of WT or *Brinp1* KO embryos examined. The axial and appendicular skeletons and the progression of the osteogenesis appeared as expected. All organs appeared normal for the developmental stage.

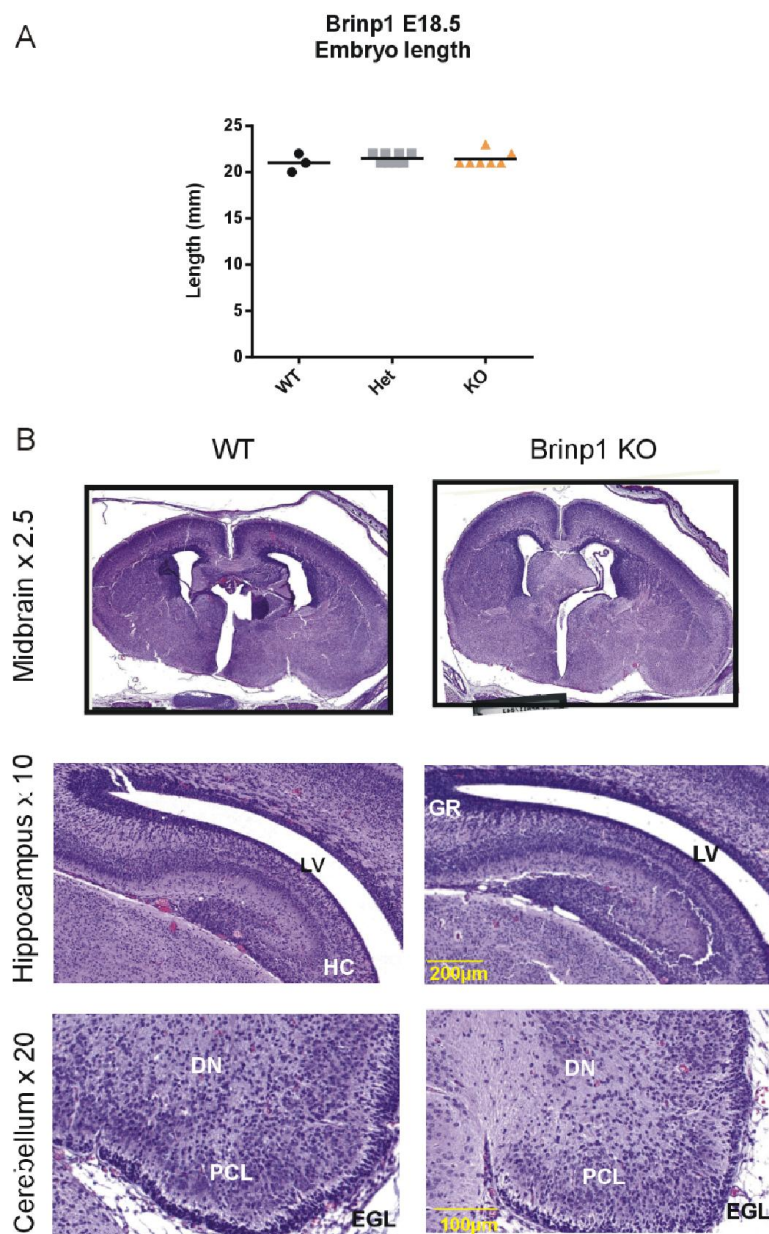


Figure 3-16 – Body length and brain histopathology of late embryonic (E18.5) *Brinp1* KO embryos

- A) No significant differences in embryo crown to rump length between E18.5 *Brinp1* KO, *Brinp1* het and WT embryos were detected by one-way ANOVA: $F(2,15)=0.5478$, $p=0.5893$. Each data point indicates the length of one embryo. The mean is shown as a horizontal line.
- B) Normal brain morphology of *Brinp1* KO embryo brains shown as Nissl labelled coronal midbrain, hippocampus, and cerebellum sections. The representative regions are shown due to high *Brinp1* expression in these areas for WT mice.

Figure compiled from images provided by the Australian Phenomics Network. GR = Granule layer, LV= Lateral ventricle, HC = Hippocampus

3.10 Behavioral screen of *Brinp* knockout mice

Behavioral testing of *Brinp* KO lines was deemed a fundamental area of investigation, given the high expression in the brain and spinal cord for all three *Brinp* genes. A broad behavioral screen of all three single KO lines was designed and carried out, covering different facets of behavior involving the testing of vision, hearing, olfaction, learning and memory, sensory gating, anxiety, motor co-ordination, and sociability. Cohort sizes were 10 to 12 mice per genotype, aged eight to 12 weeks. These well-established tests look at aspects of behavior that are designed to model human sensory, neurodevelopmental or psychiatric disorders. Behavioral tests were carried out under contract by Travis Featherby, Neuro Research Services: (<http://www.melbournebraincentre.edu.au/content/neuro-research-services>).

Data were analyzed and interpreted by the candidate.

3.10.1 Visual placing test

This test is designed to investigate rodent vision. When lowered towards a wire mesh, both WT and KO animals of all three lines extended their forearms at an average of 15 mm from the grid. No significant difference to WT was observed for *Brinp1*, *Brinp2* or *Brinp3* KO mice (Figure 3-17).

3.10.2 Olfactory test

Mice were tested for olfaction sensitivity to three different dilutions of an attractive smell (peanut butter). Both WT and knockout mice of all three lines were unable to distinguish water from peanut butter at a dilution of 10^{-3} . *Brinp1*, *Brinp2* and *Brinp3* KO mice were each able to recognize the peanut butter olfaction at dilutions of 10^{-2} and 10^{-1} , in a similar manner to WT (Figure 3-18).

3.10.3 Startle response and pre-pulse inhibition (PPI)

The primary purpose of this test is to identify animals that model sensory gating deficits commonly seen in patients with schizophrenia. The PPI test is used to measure an animal's ability to inhibit or gate the effect of sensory information. Normally, mice exhibit a decreased startle response to a sudden loud sound when preceded by a quieter sound (a pre-pulse). *Brinp1*, *Brinp2* and *Brinp3* KO were able to inhibit the startle response when primed with pre-pulses of 4, 8 and 16 dB (Figure 3-19).

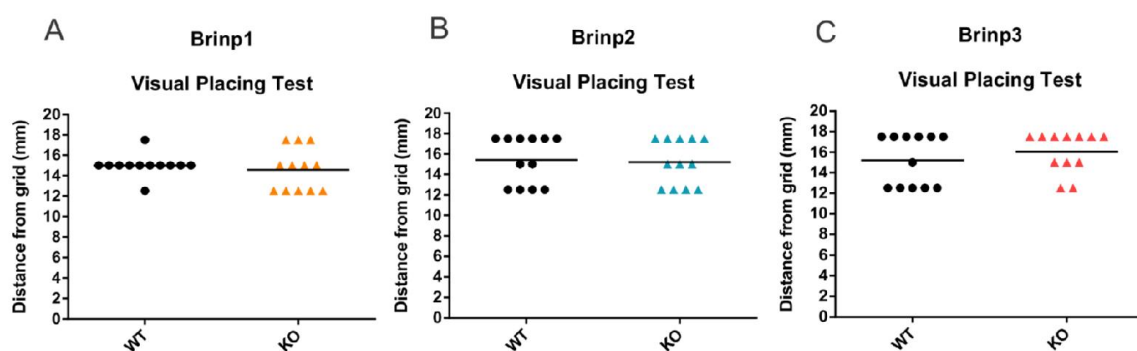


Figure 3-17 – Visual placing test

Normal vision of A) *Brinp1*, B) *Brinp2* and C) *Brinp3* KO mice, measured by the distance with that mice extended their forearms when lowered towards a grid. Data was analyzed by unpaired Student's t-tests, showing no significant difference to WT littermates for each genotype: A) *Brinp1*: $t(22)=0.6159$, $p=0.5443$, B) *Brinp2*, $t(22)=0.2221$, $p=0.8263$, and C) *Brinp3* KO mice $t(22)=0.9069$, $p=0.3743$.

N=12 WT, 12 KO per experiment. Each data point shows the response from one animal. The mean is shown as a horizontal line.

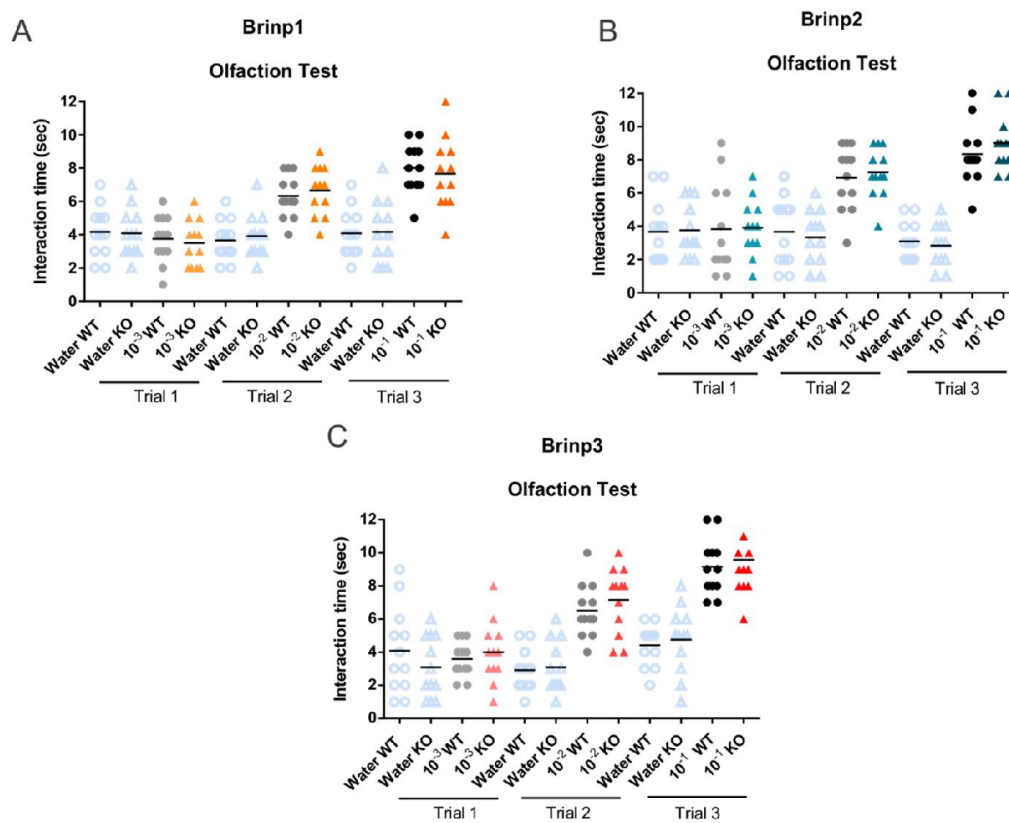


Figure 3-18 – Olfaction test

Brinp1 (A), *Brinp2* (B) and *Brinp3* KO (C) mice each displayed normal olfactory sensitivity by recognizing a peanut butter smell at dilutions of 1×10^{-1} and 1×10^{-2} . The scent was indistinguishable from water for both WT and KO mice at a dilution of 1×10^{-3} . Data was analyzed by repeat measures two-way ANOVA, finding no significant effect of genotype for any of the *Brinp* lines: A) *Brinp1*: $F(1,22)=0.037$, $p=0.849$, B) *Brinp2*: $F(1,22)=0.639$, $p=0.433$. C) *Brinp3*: $F(1,22)=1.948$, $p=0.177$. $N=12$ WT, 12 KO per experiment.

Each data point shows the response from one animal. The mean is shown as a horizontal line.

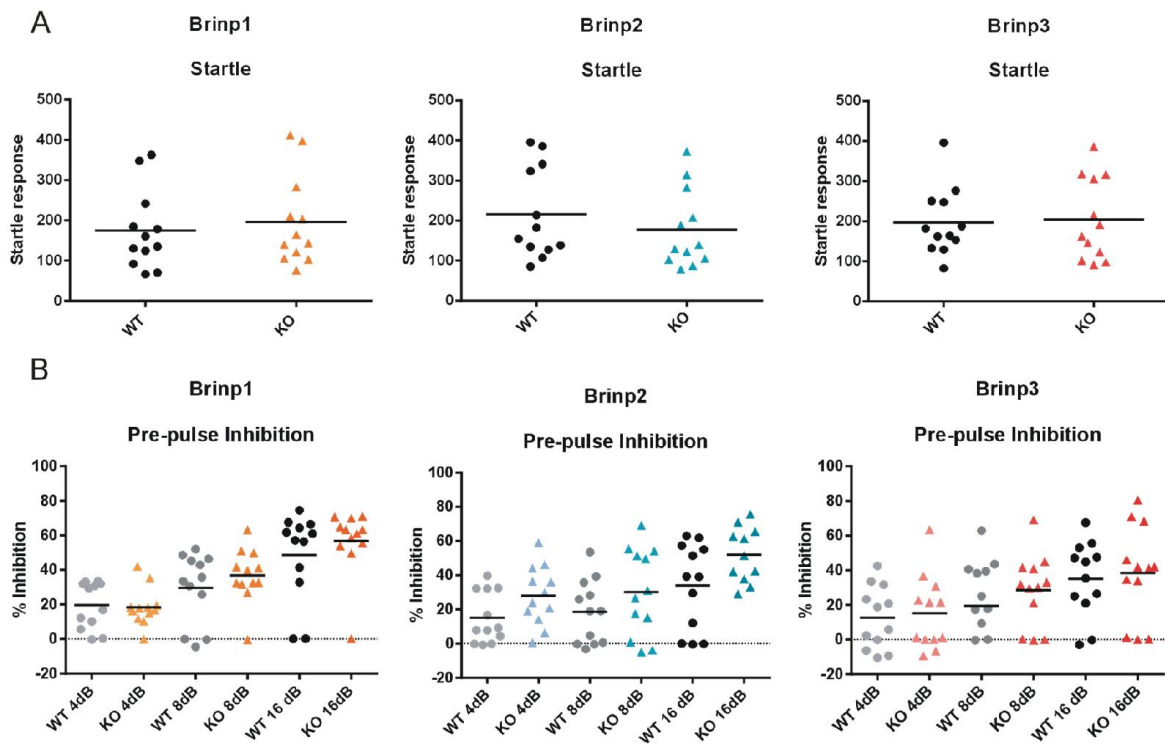


Figure 3-19 – Acoustic startle and pre-pulse inhibition

- A) **Acoustic startle:** Normal startle response for *Brinp1* ($t(22)=0.5077$, $p=0.6167$), *Brinp2* ($t(22)=0.8869$, $p=0.3847$), and *Brinp3* KO mice ($t(22)=0.1930$, $p=0.8487$), unpaired Student's t-test. Startle response was measured as displacement on a platform, and recorded in arbitrary units.
- B) **Pre-pulse inhibition:** *Brinp1*, *Brinp2*, and *Brinp3* KO mice were able to inhibit their startle response when primed with pre-pulse tones at 4, 8 and 16 dB. Data was analyzed by repeat measures two-way ANOVA, and found to show no significant effect of genotype on % inhibition for each of the *Brinp* lines: *Brinp1*: $F(1,22)=0.512$, $p=0.482$, *Brinp2*: $F(1,22)=2.594$, $p=0.122$, and *Brinp3*: $F(1,22)=0.316$, $p=0.579$. Results are represented as percentage inhibition of startle response relative to the unprimed startle response.

N=12 mice per genotype. Each data point indicates the response from one animal. The mean is shown as a horizontal line.

3.10.4 Rotarod

The Rotarod is designed to test the motor co-ordination of rodents on a rotating rod platform, with gradual acceleration from 4 – 40 rpm. The first *Brinp1* KO cohort tested showed a trend of shorter latency to fall on trials 2, 3 and 4, without reaching statistical significance for effect of genotype on latency to fall ($F(1,22)=3.690$, $p=0.068$, repeat measures two-way ANOVA). The same test was repeated for a second *Brinp1* KO cohort. This time *Brinp1* KO performance was equivalent to WT ($F(1,18)=0.197$, $p=0.662$, repeat measures two-way ANOVA).

The training trials (day 1) for *Brinp1* KO cohort 1 and *Brinp1* KO cohort 2 also showed no impairments in performance (Figure 3-20). These results indicate no motor co-ordination deficit for *Brinp1* KO mice.

Brinp2 KO mice showed a statistically significant improvement in Rotarod, with a main effect of genotype on latency to fall, $F(1,22)=7.370$, $p=0.013$, repeat measures two-way ANOVA. *Brinp3* KO mice showed no significant difference to WT for this test.

3.10.5 Elevated plus maze

The elevated plus maze investigates anxiety and fear response by placing mice on a plus-shaped platform at a height of 40 cm above the ground. Mice normally show a species-typical preference for the walled closed arms, and show some hesitation to enter the more exposed open arms. Mice that show a high level of resistance to approach the open arms are interpreted as having an anxiety-like phenotype.

In this test, mice were allowed to freely explore an elevated plus maze for 5 min. *Brinp1* and *Brinp3* KO mice showed a significant reduction in the amount of time spent in a closed arms as compared to their wild type controls. *Brinp2* KO mice showed no significant difference to WT for this test (Figure 3-21A).

The most pronounced phenotype was exhibited by *Brinp3* KO mice, which also spent a significantly greater time on the open arms and center square. *Brinp3* KO mice exhibited greater exploration time at the exposed ends of the open arms, and showed peering down behavior at the edges of the open arms (Figure 3-21B).

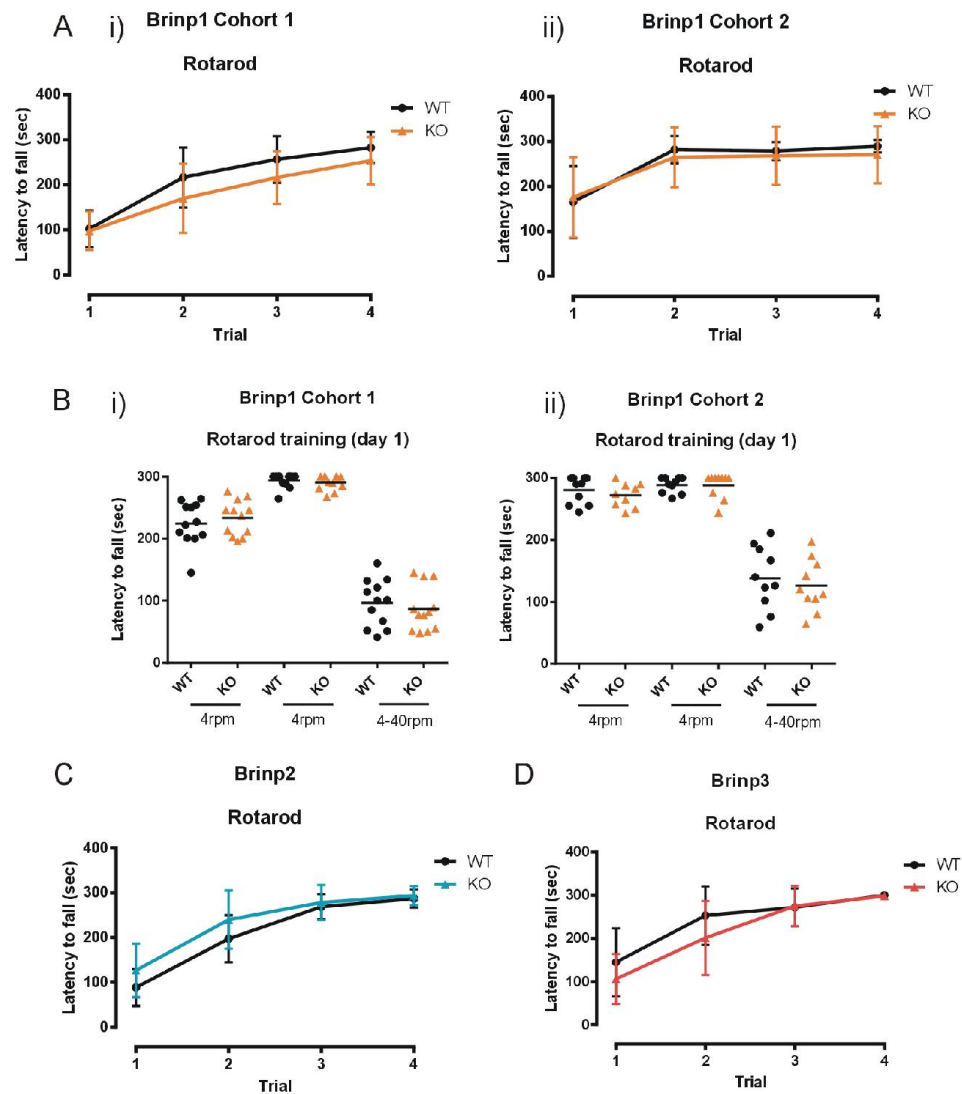


Figure 3-20 – Rotarod

Figure 3-20 – Rotarod

- A) ***Brinp1* KO Rotarod accelerated test** (4-40rpm x 4 trials). No significant motor co-ordination impairment on the Rotarod. Data was analyzed by repeat measures ANOVA showing:
- i) No significant effect of genotype on *Brinp1* cohort 1 latency to fall: $F(1,22)=3.690$, $p=0.0682$ and no significant interaction of genotype x trial: $F(3,66)=0.995$, $p=0.401$, $n=12$ mice per genotype.
 - ii) No significant effect of genotype on *Brinp1* cohort 2 latency to fall: $F(1,18)=0.197$, $p=0.660$, and no significant interaction of genotype x trial: $F(3,54)=0.468$, $p=0.706$, $n=10$ mice per genotype. Results are shown as the mean \pm SD.
- B) ***Brinp1* KO Rotarod training trials** showing no significant differences in first day Rotarod training at 4rpm x 2 trials and one accelerated trial (4-40rpm) for I) *Brinp1* cohort 1 II) *Brinp1* cohort 2, unpaired Student's t-tests. Each data point indicates the response from one animal. The mean is shown as a horizontal line.
- C) ***Brinp2* KO Rotarod accelerated test** (4-40rpm x 4 trials). *Brinp2* KO mice showed a significantly improved performance $F(1,22)=7.370$, $p=0.013$. There was no interaction effect of genotype x trial: $F(3,66)=1.081$, $p=0.363$, repeat measures two-way ANOVA, $n=12$ mice per genotype. Results are shown as the mean \pm SD.
- D) ***Brinp3* KO Rotarod accelerated test** (4-40rpm x 4 trials). No significant difference in *Brinp3* KO latency to fall: $F(1,22)=2.543$, $p=0.125$, and no significant interaction effect between genotype x trial: $F(3,66)=1.661$, $p=0.184$ repeat measures two-way ANOVA, $n=12$ mice per genotype. Results are shown as the mean \pm SD.

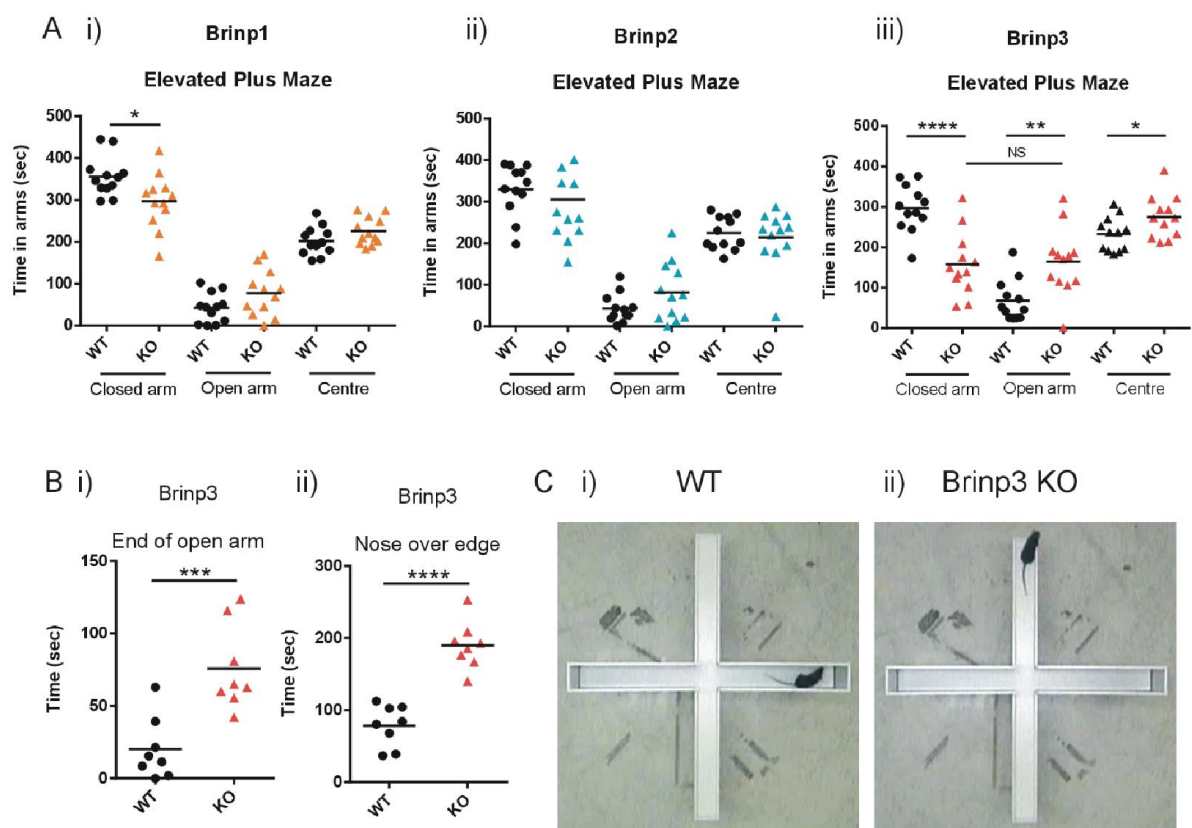


Figure 3-21 – Elevated plus maze (EPM)

Figure 3-21 – Elevated plus maze (EPM)

A) Elevated Plus Maze arm exploration times for *Brinp1* and *Brinp2* and *Brinp3* KO mice.

- i) *Brinp1* KO mice showed a significant decrease in time spent in the EPM_closed arm: $t(22)=2.538$, $p=0.0188$. No significant change in time in the open arm: $t(22)=1.875$, $p=0.0741$, or centre: $t(22)=1.726$, $p=0.0984$, unpaired Student's t-tests.
- ii) No significant changes in arm duration for *Brinp2* KO mice. Time in closed: $t(22)=0.6691$, $p=0.5104$, time in open: $t(22)=1.716$, $p=0.1002$, time centre: $t(22)=0.4416$, $p=0.6631$, unpaired Student's t-tests.
- iii) *Brinp3* KO mice showed a significant decrease in time spent in the EPM closed arm: *Brinp3* closed: $t(22)=4.924$, $p<0.0001$. *Brinp3* KO mice also showed a significant increase in time in the open arm: $t(22)=3.421$, $p=0.0024$, as well as in the centre square: $t(22)=2.174$, $p=0.0407$. In addition, *Brinp3* KO mice did not show the expected preference for the closed arms over the open arm, $t(22)=0.2040$, $p=0.8402$, unpaired Student's t-tests. N=12 mice per genotype.

B) *Brinp3* KO mice spend significantly more time i) at the far end of the open arms $t(14)=4.346$, $p=0.0007$, and ii) peering over the edge of the open arms compared to WT littermates, $t(14)=7.190$, $p<0.0001$, unpaired Student's t-tests. A sample of 8 mice per genotype were assessed.

C) Representative images of i) WT mouse preference for the closed arms of the EPM, and ii) *Brinp3* KO peering down at the end of an open arm.

Each data point indicates the response from one animal. The mean is shown as a horizontal line. NS = not significant. * $p<0.05$, ** $p<0.01$, *** $p<0.001$, **** $p<0.0001$.

3.10.6 Y-maze

The Y-maze investigates short-term spatial memory by first allowing the mouse into the maze to explore only two arms of the maze. After a two hour interval mice are reintroduced, this time with access to all three arms of the Y-maze. If mice show an increase in time in the novel third arm of the maze they are deemed to have remembered the other two arms as familiar (based on a species-typical preference for novelty). *Brinp1* KO mice did not show the expected increase in time spent exploring a novel arm. This result was reproducible with a second cohort, indicating that *Brinp1* KO mice may have impaired spatial memory (Figure 3-22). *Brinp2* and *Brinp3* KO mice were equivalent to WT for this test, indicating normal spatial memory (Figure 3-23).

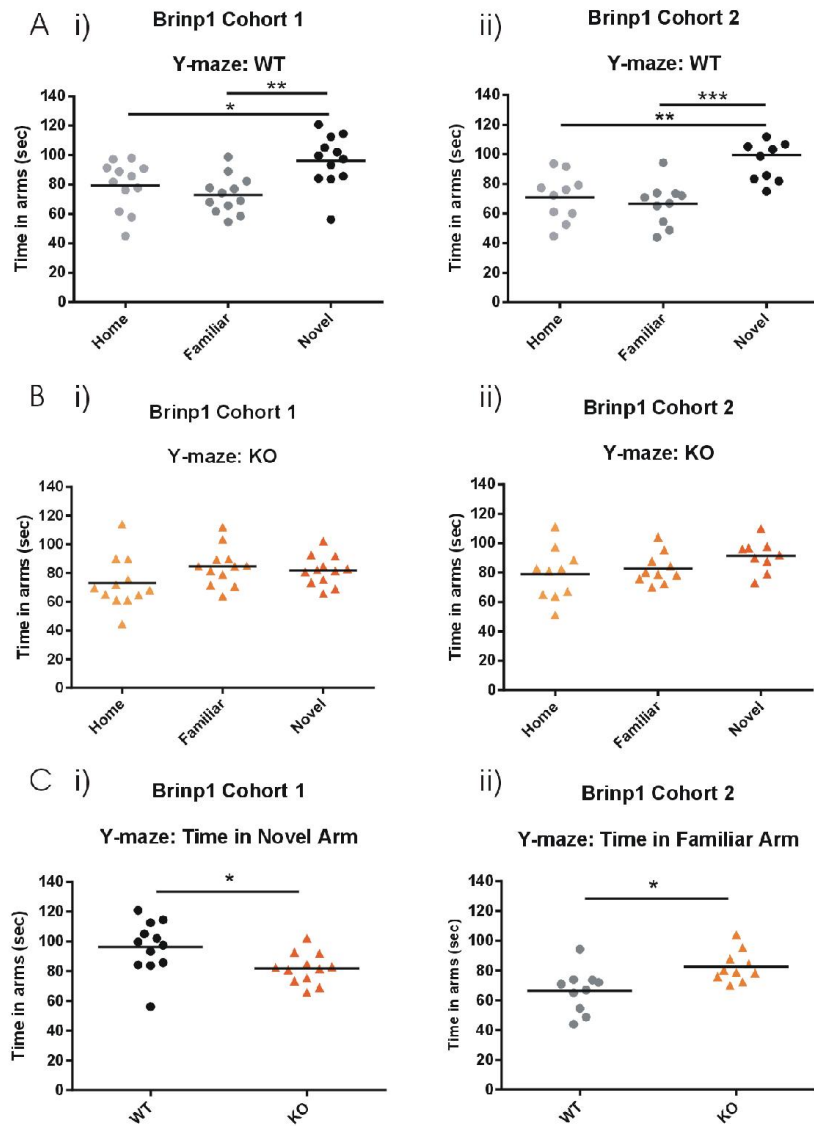


Figure 3-22 – Y-maze: *Brinp1* KO (cohort 1 and cohort 2)

Figure 3-22 – Y-maze: *Brinp1* KO (cohort 1 and cohort 2)

- A) Two cohorts of WT litter mate controls from the *Brinp1* line showed a species-typical increase in time spent in the novel arm of the Y-maze.
- i) *Brinp1* cohort 1 WT: $F(2,33)=6.942$, $p=0.0030$, one-way ANOVA. Tukey HSD multiple comparisons: Home-Familiar: $p=0.596$, Home-Novel: $p=0.034$, Familiar-Novel: $p=0.003$.
ii) *Brinp1* cohort 2 WT: $F(2,27)=11.232$, $p<0.001$, one-way ANOVA. Tukey HSD multiple comparisons: Home-Familiar: $p=0.826$, Home-Novel: $p=0.002$, Familiar-Novel: $p<0.001$.
* $p<0.01$, ** $p<0.01$.
- B) Two cohorts of *Brinp1* KO mice showed no significant difference in time spent investigating the home arm, novel arm and the familiar arm: i) *Brinp1* cohort 1 KO: $F(2,33)=2.190$, $p=0.1279$.
ii) *Brinp1* cohort 2 KO: $F(2,27)=3.087$, $p=0.0620$, one-way ANOVA.
- C) Genotype comparison: i) *Brinp1* KO cohort 1 mice spend significantly less time than WT litter mates investigating the novel arm, $t(22)=2.457$, $p=0.0224$, unpaired Student's t-test. ii) *Brinp1* KO cohort 2 mice spend significantly more time than WT litter mates investigating the familiar arm, $t(18)=2.860$, $p=0.0104$, unpaired Student's t-test.

Cohort 1: $n=12$ mice per genotype, cohort 2: $n=10$ mice per genotype. * $p<0.05$, ** $p<0.01$, *** $p<0.001$ unpaired Student's t-test. Each data point indicates the response from one animal. The mean is shown as a horizontal line.

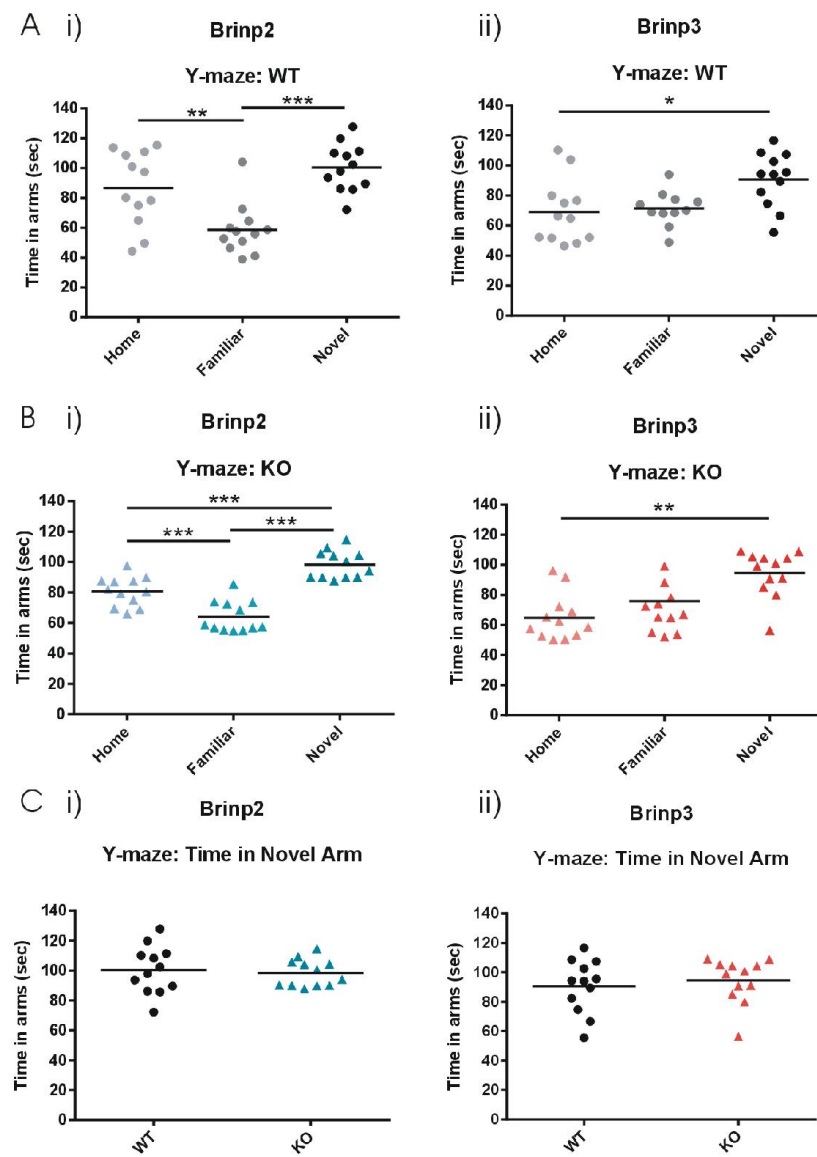


Figure 3-23 – Y-maze: *Brinp2* and *Brinp3* KO mice

Figure 3-23 – Y-maze: *Brinp2* and *Brinp3* KO mice

- A) WT litter mate control mice from the *Brinp2* and *Brinp3* lines show the species-typical increase in time spent in the novel arm of the Y-maze.
- i) *Brinp2* WT: $F(2,33)=13.931$, $p<0.001$, one-way ANOVA. Tukey HSD multiple comparisons: Home-Familiar: $p=0.0040$, Home-Novel: $p=0.219$, Familiar-Novel: $p<0.001$.
ii) *Brinp3* WT: $F(2,33)=3.688$, $p=0.0360$, one-way ANOVA. Tukey HSD multiple comparisons: Home-Familiar: $p=0.6340$, Home-Novel: $p=0.0310$, Familiar-Novel: $p=0.1690$.
- B) Both *Brinp2* KO and *Brinp3* KO mice show an increase time spent investigating the novel arm of the Y-maze.
- i) *Brinp2* KO: $F(2,33)=37.421$, $p<0.0001$, one-way ANOVA. Tukey HSD multiple comparisons: Home-Familiar: $p<0.001$, Home-Novel: $p<0.001$, Familiar-Novel: $p<0.001$.
ii) *Brinp3* KO: $F(2,33)=7.477$, $p=0.002$, one-way ANOVA. Tukey HSD multiple comparisons: Home-Familiar: $p=0.349$, Home-Novel: $p=0.002$, Familiar-Novel: $p=0.054$.
- C) Genotype comparison: *Brinp2* KO and *Brinp3* KO mice showed no significant difference to WT in time spent investigating the novel arm: i) *Brinp2*: $t(22)=0.3900$, $p=0.7003$, ii) *Brinp3*: $t(22)=0.5608$, $p=0.5806$, unpaired Student's t-tests.

* $p<0.05$, ** $p<0.01$, *** $p<0.001$. Each data point indicates the response from one animal. The mean is shown as a horizontal line.

3.10.7 Sociability

The three chamber social interaction test evaluates a subject mouse for interaction time with a sex-matched stranger mouse, versus an empty cage on the opposite chamber. Wild type C57BL/6 mice preferentially interact with the novel mouse when given the choice between a novel mouse and an empty cage. In addition, WT mice show preference for a novel mouse versus a familiar mouse. The three chamber social interaction test is routinely used to investigate sociability in rodents (Silverman et al., 2010).

Brinp1, *Brinp2* and *Brinp3* KO did not show a preference for either the left or the right empty cages in trial 1 of the social interaction test. *Brinp1* KO mice did however show a decrease in time spent interacting with both the left and right empty cages with one of two cohorts tested (Figure 3-24A), indicating a change in object exploration behavior for the second *Brinp1* KO cohort.

A pronounced decrease in sociability was evident when the *Brinp1* KO mice were tested for social interaction with an unfamiliar mouse. Whilst *Brinp1* KO mice showed a preference for the cage with a stranger mouse in contrast to an empty cage, they spent significantly less time interacting with the intruder mouse compared to their wild-type litter mates. This result was reproduced with a repeat of the test using a second cohort (Figure 3-24B). When a second, novel mouse was introduced (*Brinp1* KO cohort only), reduced sociability with the novel mouse was apparent (Figure 3-24C).

Analysis of overall activity of *Brinp1* KO mice in the three chamber social interaction test area revealed that these mice exhibit hyperactivity, whereby the mean velocity of *Brinp1* KO mice cohort 2) was significantly greater than WT in both trial 1 and trial 2 (Figure 3.25D).

Brinp2 and *Brinp3* KO mice showed no preference for the left or right side of the chamber in trial 1 (Figure 3-25A) No significant change in sociability was observed for the *Brinp2* or *Brinp3* KO mice in the three chamber social interaction test in trial 2 (Figure 3-25B). The results for trial 3 are interesting, with *Brinp2* KO mice showing a trend for reduced sociability with the novel mouse ($p=0.079$), without reaching significance (Figure 3-25C).

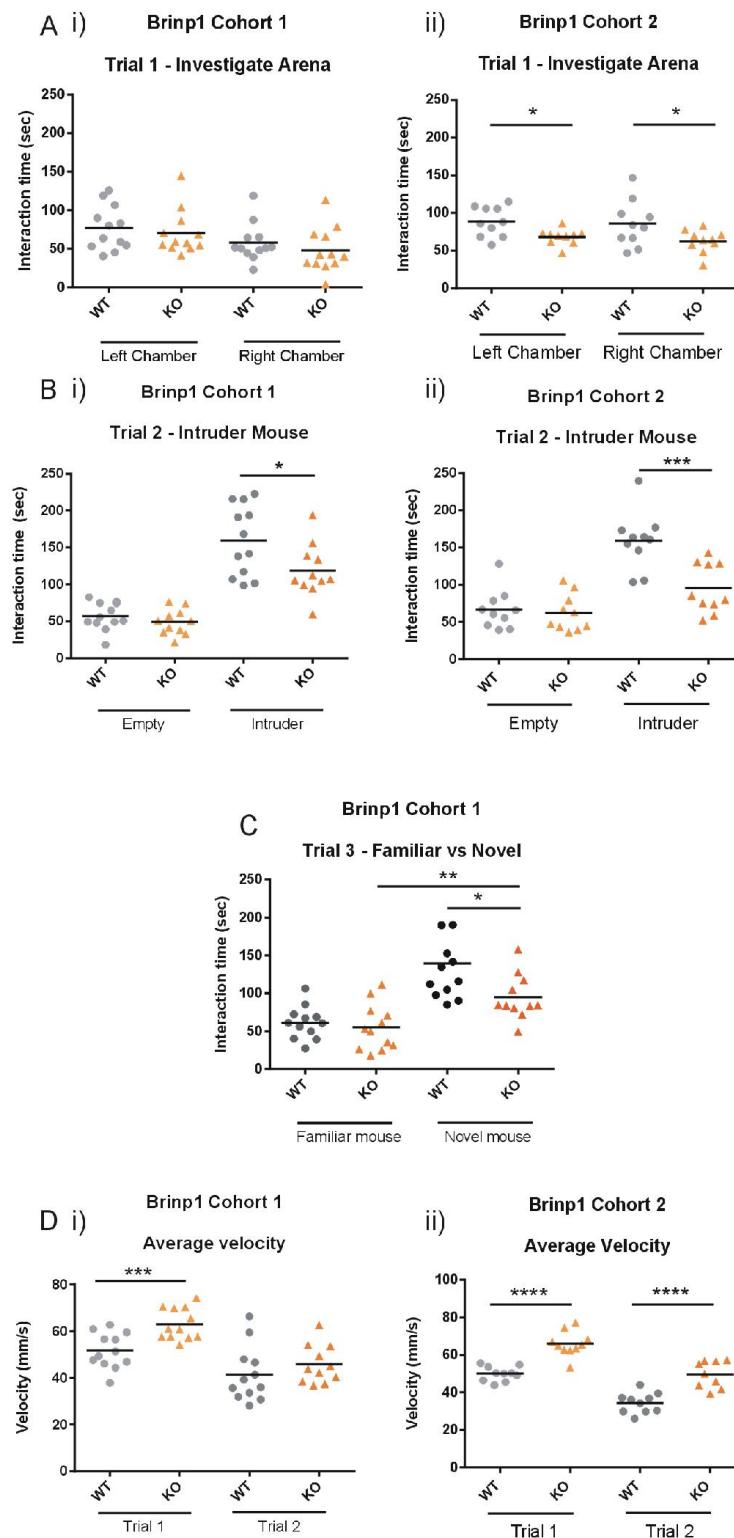


Figure 3-24 – Three chamber social interaction test: *Brinp1* cohort 1 and 2

- A) Trial 1 - Acclimatization of the testing arena for *Brinp1* KO mice. Results show time in the interaction zone (IZ), defined as an area within a 1cm perimeter from the empty cage in either the left or right chamber.
- i) *Brinp1* KO mice (cohort 1) showed no significant difference to WT in time interacting with empty cages in either the left $t(22)=0.5473$, $p=0.5897$, or right chamber $t(22)=0.8873$, $p=0.3845$, unpaired Student's t-tests.
 - ii) *Brinp1* KO mice (cohort 2) spent significantly less time investigating the empty cages during the trial. Cohort 2: $n=10$ mice per genotype, left chamber: $t(18)=2.871$, $p=0.0102$, right chamber $t(18)=2.134$, $p=0.0469$, unpaired Student's t-test. Equivalent times were spent in left and right chamber for both WT and KO mice.
- B) Trial 2 - Social interaction: Results show time in the interaction zone (IZ) of an empty cage compared with the IZ of a cage with a sex-matched stranger mouse. Both cohorts spent significantly less time within the IZ of the cage containing a stranger mouse.
- C) i) Cohort 1: Empty chamber: $t(21)=1.072$, $p=0.2958$, stranger mouse: $t(21)=2.296$, $p=0.0320$.
 ii) Cohort 2: Empty chamber: $t(18)=0.3915$, $p=0.7000$, stranger mouse: $t(18)=3.951$, $p=0.0009$, unpaired Student's t-test. Trial 3 - Social preference: Results show time in the IZ of the mouse used in trial 2 (familiar mouse), compared with the IZ of a cage with a novel mouse. *Brinp1* KO mice (cohort 1) spend less time interacting with a novel mouse. Familiar mouse: $t(22)=0.6050$, $p=0.5514$. Intruder mouse: $t(22)=2.495$, $p=0.0210$, unpaired Student's t-test.
- D) Both cohorts of *Brinp1* KO mice exhibited hyperactivity in the three chamber social interaction test.
- i) *Brinp1* KO mice, cohort 2 showed as an increase in average velocity within the entire area of the testing arena. Cohort 1, Trial 1: $t(18)=6.529$, $p<0.0001$ Cohort 1, Trial 2: $t(17)=5.261$, $p<0.0001$, unpaired Student's t-test.
 - ii) *Brinp1* KO mice, cohort 2 showed as an increase in average velocity within the entire area of the testing arena. Cohort 1, Trial 1: $t(18)=6.529$, $p<0.0001$ Cohort 1, Trial 2: $t(17)=5.261$, $p<0.0001$, unpaired Student's t-tests.
- Cohort 1: $n = 12$ mice per genotype, Cohort 2: $n = 10$ mice per genotype. Each data point indicates the response from one animal. The mean is shown as a horizontal line. * $p<0.05$, *** $p<0.001$, **** $p<0.0001$.

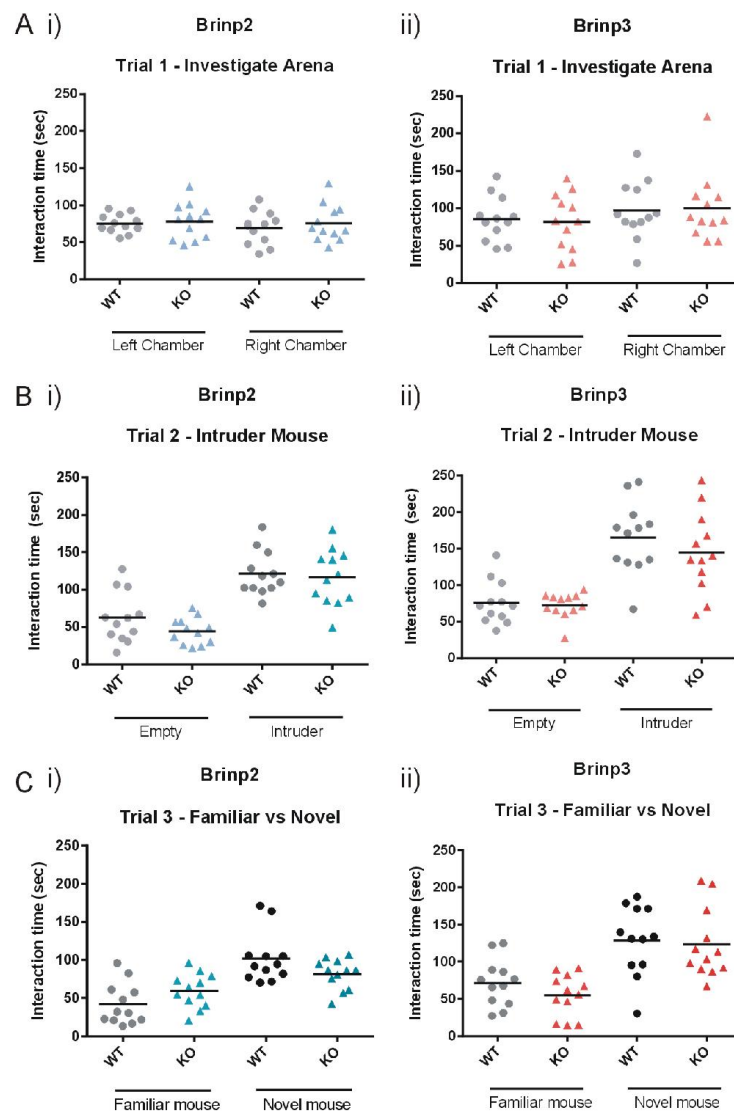


Figure 3-25 – Three chamber social interaction test: *Brinp2* and *Brinp3* KO

- A) Trial 1 - Acclimatization of the testing arena for *Brinp2* KO and *Brinp3* KO mice. Results show time in the interaction zone (IZ) (defined as an area within a 1cm perimeter from the empty cage in either the left or right chamber). *Brinp2* KO mice and *Brinp3* KO mice showed no significant difference to WT controls in time spent in the left or right chambers.
- i) *Brinp2* left chamber: $t(22)=0.3380$, $p=0.7386$, right chamber: $t(22)=0.6541$, $p=0.5198$.
 - ii) *Brinp3* left chamber: $t(22)=0.2978$, $p=0.7686$, right chamber: $t(22)=0.2017$, $p=0.8420$, unpaired student t-test.
- B) Trial 2 - Social interaction: Results show time in the interaction zone (IZ) of an empty cage compared with the IZ of a cage with a sex-matched stranger mouse. No significant differences were observed in time spent interacting with a sex-matched stranger mouse for *Brinp2* or *Brinp3* KO mice.
- i) *Brinp2* empty chamber: $t(22)=1.624$, $p=0.1187$, stranger mouse: $t(22)=0.3598$, $p=0.7224$.
 - ii) *Brinp3* empty cage: $t(22)=0.3466$, $p=0.7322$, stranger mouse: $t(22)=0.9666$, $p=0.3442$, unpaired student t-test.
- C) Trial 3 - Social preference: Results show time in the IZ of the mouse used in trial 2 (familiar mouse), compared with the IZ of a cage with a novel mouse. No significant differences were observed for *Brinp2* or *Brinp3* KO mice for this test.
- i) *Brinp2* familiar mouse: $t(22)=1.748$, $p=0.0944$, novel mouse: $t(22)=1.841$, $p=0.0791$.
 - ii) *Brinp3* familiar mouse: $t(22)=1.340$, $p=0.1940$, novel mouse: $t(22)=0.2755$, $p=0.7855$, unpaired student t-test.

N=12 mice per genotype. Each data point indicates the response from one animal. The mean is shown as a horizontal line.

3.10.8 *Brinp1*, *Brinp2* and *Brinp3* KO behavioral summary

Table 3-3 - *Brinp1*, *Brinp2* and *Brinp3* KO behavioral testing summary

Statistically significant findings are highlighted in red

	Behavioral test	<i>Brinp1</i> KO	<i>Brinp2</i> KO	<i>Brinp3</i> KO
Sensory	Visual placing	No difference	No difference	No difference
	Olfaction test	No difference	No difference	No difference
Sensory processing	Acoustic startle	No difference	No difference	No difference
	Pre-pulse inhibition	No difference	Marginal improvement	No difference
Motor co-ordination	Rotarod	No difference	Improvement	No difference
Learning / memory	Y-maze	Impaired memory	No difference	No difference
Sociability	Social interaction	Decreased sociability	No difference	No difference
	Social preference	Decreased sociability	Marginal difference	Marginal difference
Anxiety / fear	Elevated plus maze	Hyper-exploratory	No difference	Hyper-exploratory

3.11 Chapter 3: Discussion

3.11.1 *Brinp1*, *Brinp2* and *Brinp3* KO are viable, show a reduction in body weight, with no gross anatomical abnormalities

The absence of an embryonic lethal phenotype demonstrates that, individually, *Brinp* genes are not essential for embryogenesis or neurogenesis. Furthermore, the existence of adult *Brinp1* KO, *Brinp2* KO and *Brinp3* KO mice determines that none of the three *Brinp* genes is essential for fundamental survival functions, such as breathing, eating, drinking, sleeping and homeostasis.

There is evidence that the absence of *Brinp1* does impact survival, with only partial postnatal viability of *Brinp1* KO mice from heterozygous matings, and very low survival from homozygous matings. The normal development of *Brinp1* KO embryos, alongside the reported high levels of neonatal death suggests that there are other postnatal survival factors related to *Brinp1* KO phenotype. The factors that result in reduced survival of *Brinp1* KO mice are worthy of further investigation and will be explored in chapter 5.

The compromised viability of the *Brinp1* KO mice is likely to cause artificial selection within the *Brinp1* KO line, with those *Brinp1* KO mice most severely affected dying as neonates. It is therefore the case that the range of any reported phenotype for the *Brinp1* KO mice is limited to those that survive infancy, and therefore the full effect of the absence of *Brinp1* on either histopathology or behaviour on adult mice is not observable. The continued use of WT littermate controls, generated from heterozygous breeders during this study, insures that any selection pressure caused by neonatal death is kept consistent between *Brinp1* KO, heterozygous and WT littermates.

The reduced weight of *Brinp1* KO mice (juvenile to adult), *Brinp2* KO mice (adult only) and *Brinp3* KO mice (juvenile only) demonstrates that *Brinps* do have an impact on mammalian physiology. The reduction in body weight of *Brinp1* KO mice is consistent with variants in the *BRINP1* locus at 9q33.1 in patients with growth delay (Chien et al., 2010; Gamerding et al., 2008). *Brinp1* and *Brinp3* are expressed in the hypothalamus, which controls growth via the hypothalamic-pituitary-adrenal (HPA) axis endocrine system (Kawano et al., 2004; Muller et al., 1967; Scanlon, 1992). It is possible that *Brinps* may effect endocrine production or function, which could, in turn, result in growth impairment. Alternatively, the increase in

overall activity of the *Brinp1* KO mice is likely to cause a change in energy expenditure, which may be causing the reduced body weight by altering fat or muscle composition. Decreased body weight has been observed in several mice that also exhibit hyperactivity, such as the transgenic mice bearing a human mutant thyroid hormone beta 1 receptor (Wong et al., 1997) and *Shank2* KO mice (Schmeisser et al., 2012). The hyperactivity of *Brinp1* KO mice is explored further in chapter 5 of this thesis.

The absence of an identifiable pathological phenotype by H&E or Nissl labelling suggests that *Brinps* do not have a developmental role in organogenesis or neurogenesis. Thus, the role of *Brinps* may be unconnected with neuronal development, e.g. synaptic transmission or neuronal survival. This however, does not fit with the evidence that *Brinp1*, *Brinp2* and *Brinp3* show expression profiles consistent with neurodevelopmental proteins, by gradually increasing until their peak expression around postnatal day 14, and then, in the case of *Brinp2* and *Brinp3*, decreasing to lower levels in adulthood (Hager et al., 1995; Kawano et al., 2004). The lack of gross morphological differences in the brain at this initial level of analysis does not exclude the possibility of a developmental phenotype. Identifying changes in cell distribution or connectivity, requires layer-specific markers. Therefore, immunohistochemical analysis of the neural architecture of the *Brinp* KO mouse brains is required to fully assess the impact of *Brinp* ablation on nervous system development.

3.11.2 *Brinp1*, *Brinp2* and *Brinp3* KO mice show no impairment in sensory gating

Vision, hearing and olfaction were preserved for all *Brinp* KO mice. The lack of an olfaction phenotype was unexpected, given the high expression of *Brinp1*, *Brinp2* and *Brinp3* in the mouse olfactory bulb during development and adulthood (Kawano et al., 2004). There are three scenarios that may explain the absence of a detectable olfactory phenotype: 1) *Brinps* do not have a role in olfactory function, 2) *Brinps* do have a function in olfactory function that was not detectable by the test used, or 3) redundancy within the mammalian system means that compensation by another gene in each set of KO mice is masking a phenotypic effect. The first scenario seems the least likely as it doesn't explain the high expression of *Brinps* in a brain region specialized for olfactory function.

When assessing auditory function in C57BL/6 mice, it is important to note a strain specific effect for these mice, which show age related hearing loss, resulting in deafness at

approximately 30 weeks (Mikaelian et al., 1974; Picciotto & Wickman, 1998). To control for this effect, a narrow age range of 9 – 12 week old mice were tested, with WT littermates of equivalent age. *Brinp1*, *Brinp2* and *Brinp3* KO mice showed no impairment in sensory gating; a common symptom of schizophrenia in humans (Boutros et al., 2009; Sanchez-Morla et al., 2008).

A limitation of the sensory screen performed is the use of a single test for each of the senses tested. For example, the olfaction experiment tested a single olfactory stimulus (peanut butter), therefore changes in olfaction sensitivity to other olfactory stimuli cannot be ruled out. Similarly, the pre-pulse auditory tones do not test the full hearing range. Deficits in hearing ability at other frequencies and amplitudes again cannot be ruled out. Again, the basic nature of the visual placing test would only highlight dramatic vision loss, and more sensitive tests would be required to demonstrate partial vision impairment. Nevertheless, these behavioral screens demonstrated no profound impairments in sensory systems, and rule out profound sensory impairment as an influence on mouse performance in other behavioral tests.

3.11.3 *Brinp1*, *Brinp2* and *Brinp3* KO mice motor co-ordination is not impaired

Rotarod testing indicates that motor-coordination is not impaired in any of the *Brinp* single knockout lines. This contrasts with the motor co-ordination phenotype of the *Astn1* KO mice, which performed poorly on the Rotarod (Adams et al., 2002). The absence of a *Brinp1*, *Brinp2*, or *Brinp3* KO mouse motor co-ordination phenotype goes against the prediction that, like *Astn1*, *Brinps* will have a functional cerebellar defect. The absence of an impaired motor co-ordination phenotype of *Brinp1* KO mice is surprising given the high expression of *Brinp1* in the developing and adult brain in both the Purkinje cell layer and granule layer of the cerebellum. The results imply that either *Brinps* do not function to facilitate granule cell migration in the same manner as *Astn1* in the cerebellum, or their absence is compensated for by another gene, thereby masking the phenotype.

The improved performance of *Brinp2* KO mice on the Rotarod is difficult to explain given that impairments in performance are a more common finding for this test. The result would need to be reproduced before any conclusions can be made. Interestingly, improved Rotarod

performance has reported for several animal models of autism, including the Pten KO mouse, and CNTNAP2 KO mouse (Kwon et al., 2006; Nakatani et al., 2009; Penagarikano et al., 2011).

3.11.4 *Brinp1* KO mice showed a marked reduction in sociability.

Reduced social interaction of the *Brinp1* KO mice was a key behavioral phenotypic finding. *Brinp1* KO mice demonstrated preference for a novel mouse over an empty cage (trial 2) or a familiar mouse (trial 3), but spent significantly less time interacting with a novel mouse compared to WT littermates in each instance. These results indicate that the changes in *Brinp1* KO sociability are not due to novelty preference or impaired social recognition, but rather appears to be an aspect of social withdrawal.

Reductions in social interaction are observed in other mouse models of neurodevelopmental disorders, e.g. MECP2 mutants (Rett syndrome mouse model), Shank 2 KO mice (autism mouse model) and the vasopressin V1a receptor KO mice (Crawley, 2012; Egashira et al., 2007; Moretti et al., 2005; Schmeisser et al., 2012). The reduced social interaction of *Brinp1* KO mice has broader implications for *Brinp1* in connection with neurodevelopmental disorder. Aberrant social behavior or low levels of social interaction are symptoms of several neurodevelopmental disorders, including autism and schizophrenia, as well as anxiety and depression (First & APA, 2013).

It is important to recognize that social behavior is interrelated to communication ability. For mice, this relates to auditory and olfactory communication. Olfactory pheromones are detected by the vomeronasal organ as cues used for social recognition in rodents (Keverne, 2002). Mice also emit ultrasonic vocalizations under several settings, namely juvenile play, pup – dam interactions, female – female interactions, and adult males in response to a mouse (or the scent of a mouse) of the opposite sex (Maggio et al., 1983; Scattoni et al., 2009). Investigation of *Brinp1* KO communication is required to determine whether these mice model social-communication aspects of neurodevelopmental disorders such as autism. For example, investigation of ultrasonic vocalization of *Brinp1* KO mice would determine whether mice show impaired communication, which may be a contributing factor to the reduced sociability phenotype.

The changes in sociability reported for the *Brinp1* KO mice are likely to be key to impaired postnatal survival of knockout litters. Reduced sociability of the *Brinp1* KO breeders may be

impacting on maternal / paternal behavior, which may manifest in reduced attentiveness towards litters. Neonate survival is hindered if mothers fail to provide adequate thermal insulation, nourishment and post-parturition care towards their pups (Turgeon & Meloche, 2009). Further investigation would be to investigate aspects of maternal care that may contribute to survival; for example, are *Brinp1* KO mice able to construct adequate nests, required for providing thermal insulation to offspring? Reduced survival may also be a result of flawed two-way communication between dam and pup, and is another potential area for future investigation.

Brinp1 KO mice were hyperactive in trial 1 and trial 2 of the three chamber social interaction test. This increased activity is worthy of further investigation, and itself may influence sociability. The combination of hyperactivity and decreased sociability is reported in the literature for several other KO mice, including Shank2 KO mice, NLGN3 and CNTNAP2 KO mice, all of which are mouse models for autism (Penagarikano et al., 2011; Schmeisser et al., 2012; XU Jun-Yu1, 2012). Further testing of the *Brinp1* KO mice in a setting that is designed to test overall activity, e.g. the locomotor cell or open field test, is needed to fully document this hyperactivity phenotype.

Overall, *Brinp2* and *Brinp3* KO mice showed no significant difference in sociability. The only notable effect is the decrease in interaction time of *Brinp2* KO with a novel mouse for trials 3, which could indicate subtle effects on sociability.

3.11.5 Hyper-exploratory behavior exhibited by *Brinp1* and *Brinp3* KO mice

The increased exploratory behavior on the Elevated Plus Maze result was particularly interesting for the *Brinp3* KO mice, showing a dramatically reduced aversion to the open arms. Such a result implies that their fear response is diminished, but other factors such as altered perception of a dangerous environment (in this case the open arms of the maze) may also explain the behavior. The repetitive peering down behavior has been previously reported in the dopamine transporter (DAT KO) mouse model for ADHD as an absence of the 'cliff avoidance reaction' (Yamashita et al., 2013), which suggests changes in synaptic dopamine levels may be a contributing factor for this behavior. The hyper-exploratory behavior of *Brinp1* KO mice may be interconnected with the reported hyperactivity, as increased open arm

exploration has been reported for other transgenic mice that exhibit hyperactivity (Keays et al., 2007; Yamashita et al., 2013).

The amygdala is a region of the brain that is heavily involved in emotional processing and fear regulation (Kalin et al., 2004). The fear response and passive avoidance (avoidance of a negative stimuli) is diminished in mice with amygdala lesions (Slotnick, 1973; Swartzwelder, 1981) *Brinp1* and *Brinp3* are both highly expressed in this region (Kawano et al., 2004). The correlation between reduced fear and removal of *Brinp1* or *Brinp3* from the amygdala may explain the behavioral phenotype.

Changes in anxiety levels could also be due to altered endocrine or neurotransmitter production, which could alter levels of stress hormones, e.g. cortisol or glucocorticoids. An additional explanation could be changes in the neurotransmitter norepinephrine, linking this result to a genome variation study in humans reporting changes of *Brinp3* expression in response to changes in norepinephrine levels during exercise (Karoly et al., 2012).

Further investigation of fear response may reveal more about the role *Brinp3* in fear behavior. Suggested future experimental paradigms include fear avoidance, fear conditioning, and avoidance of the edges of an open field arena.

3.11.6 *Brinp1* KO mice may have impaired spatial memory, or an altered response to novelty.

Brinp1 KO mice showed altered performance in the Y-maze, by the absence of preference for the novel arm. Several possible aspects of memory acquisition and consolidation may be the cause of this phenotype. The hippocampus is a region of the brain that is heavily involved in spatial memory (O'Keefe & Dostrovsky, 1971; Squire, 1993). *Brinp1* is the most highly expressed of the three *Brinps* in the hippocampal CA1, CA2, and CA3 pyramidal layers, as well as the granule cell layer of the dentate gyrus (Kawano et al., 2004). If the reported Y-maze phenotype is due to impairment in *Brinp1* KO short term memory, this may be the result of altered hippocampal function. Further testing of memory using the Morris Water Maze will elucidate whether long term memory is also impaired.

Both Y-maze and the three chamber social interaction test rely on a preference for novelty. *Brinp1* KO mice do show a preference for the novel mouse over the familiar one, but this

preference is significantly less than WT. To determine whether *Brinp1* KO mice do show a change in novelty preference, a novel object recognition experiment is required. This will determine whether the phenotypes are specific to social novelty (social interaction test), and spatial memory (Y-maze) or a general change in novelty preference.

3.11.7 Implications for the reported phenotypes of *Brinp1*, *Brinp2* and *Brinp3* knockout mice

The findings in this chapter have revealed a number of key behavioral phenotypes, especially for *Brinp1* KO mice in respect to sociability, short term memory, and both *Brinp1* and *Brinp3* KO mice relating to fear / anxiety. A summary of all behavioral testing results is shown in Table 3-3. We clearly see that the three sets of KO mice display distinct behavioral phenotypes. Unsurprisingly, the knockout mice for *Brinp1*, the most abundantly and widely expressed of the three *Brinps* in the mouse brain, displayed the most pronounced behavioral phenotype. The absence of a common set of behavioral phenotypes between all three genes demonstrates that there is unlikely to be a common process, requiring co-dependency of all three genes, similar to that of the membrane attack complex components of the complement system. The differences in phenotypes indicates that *Brinps* do not operate in a combined pathway, but instead function individually, with possible overlap in function.

It is also interesting that *Brinp2* KO mice do not show any clear impairments in behavior, despite the high level of expression in the mouse brain during development and in the adult mouse brain. *Brinp3* KO mice also do not show the same level of behavioral impairments as *Brinp1* mice, despite also being expressed in many of the same brain regions during development as *Brinp1* (Kawano et al., 2004). A possible explanation for this is compensation by another gene, possibly by one of the other two *Brinps*. Additionally, if *Brinps* function as hypothesized in neuronal migration, their absence may be compensated for by *Astn1* or *Astn2*. There is also still a need to demonstrate lack of protein in *Brinp2* or *Brinp3* KO mice to rule out alternative splicing and production of an isoform. This would be a formal but unlikely possibility as there is no evidence of *Brinp* alternative splicing.

Brinp1 KO mice were found to have the worst survival rate out of the three *Brinp* KO lines. We can therefore expect that the increased mortality would cause selective pressure within the *Brinp1* KO line. The range of any reported phenotype for the *Brinp1* KO line is limited to

those mice that survive infancy, and therefore the full effect of the absence of *Brinp1* on either histopathology or behaviour of adult mice is not observable. The continued use of WT littermate controls, generated from heterozygous breeders, insures that any artificial selection within the line, caused by neonatal death, is kept consistent between *Brinp1* KO, heterozygous and WT littermates. Limited behavioral testing data for the *Astn1* KO mouse restricts comparisons that may be drawn, however it is evident that *Brinp* KO mice do not exhibit the same cerebellum dysfunction as reported by Adams et al, 2010. This suggests that either *Brinps* do not possess the same function in cerebellum or that *Astn1* is able to compensate for the absence.

The results of this chapter provide a basis for further exploration of the function of *Brinps*. The reported *Brinp1* KO behavioral phenotypes suggest regions of the *Brinp1* KO brain that may be compromised. The absence of a motor co-ordination deficit of any of the *Brinp* KO mice changes the focus of the project away from the cerebellum and to regions of the brain associated with memory and sociability, namely the neocortex and hippocampus. A more thorough investigation of the *Brinp1* KO mouse brain is required to determine the molecular mechanism of *Brinp1* that results in such cognitive impairments, and is described in chapter 5.

Chapter 4: Characterization of *Brinp2/3* double and *Brinp1/2/3* triple knockout mice

4.1 Chapter 4 Overview

Chapter 3 reported some key behavioral perturbations for the *Brinp1* KO mice, and less apparent changes in either the *Brinp2* or *Brinp3* KO mice. *Brinp2* KO mice especially had no discernible difference in sociability, anxiety, memory. The complexity and redundancy of the mammalian system means that the function of a gene may be compensated by a homologous gene if their products are interchangeable and expressed in the same cell types (Liang & Li, 2009). Therefore, if one homologue compensates for another, the effect of deletion of a single gene can be masked (DeLuna et al., 2010). When two or more compensating genes are knocked out, this can result in an enhanced phenotype as there is no longer a gene able to replace the function of the two deleted genes, e.g. in the case of synapsin triple KO mice (Ketzer et al., 2011), and mGlu2/mGlu3 double KO mice (Lyon et al., 2011).

Brinps are paralogues that share 50% or greater homology within the gene family (Kawano et al., 2004). The absence of one of the three *Brinps* may be masked by either of the other two *Brinps*, if they have similar mechanisms of action and are expressed in a common cell type. This chapter explores the possibility that the effect of removing *Brinps* in the knockout mice is at least partially masked by gene compensation. Double and triple knockout mice were generated. In addition, the brains of single knockout mice (*Brinp1*) were examined for the up-regulation of homologous MACPF proteins.

4.1.1 Rationale for the generation of *Brinp2/3* KO mice

The high homology between *Brinp2* and *Brinp3* amino acid sequence (70%) suggests that these two genes evolved by duplication of a common ancestor (Figure 1-7). If the function of that ancestral gene has been preserved, both genes should carry out a similar role in the mammalian brain. *Brinp2* and *Brinp3* show some overlap in expression in neuron-specific areas during development, including the olfactory bulb, hippocampus, neocortex and amygdala, which indicates that they may both perform a similar function in the same cell types.

If both *Brinp2* and *Brinp3* perform similar functions in the same cell types, compensation may occur. We therefore tested whether *Brinp3* is compensating for the absence of *Brinp2* in the *Brinp2* KO mice (and vice versa), by generating and characterizing a *Brinp2/3* double KO, and

assessing the mice for an enhanced pathological or behavioral phenotype compared to that of *Brinp2* or *Brinp3* single knockout mice.

Conversely, if *Brinp2* and *Brinp3* function is not interchangeable, we would predict that the *Brinp2/3* KO phenotype would be the summation of the single KO phenotypes, with no additional or enhanced phenotype. An additional scenario is also possible, where the phenotype continues to be masked by the up-regulation of different homologues; for example by *Brinp1*, or one of the Astrotactins.

To investigate the effect of ablation of all three *Brinp* genes from a mammalian system, *Brinp1/2/3* triple KO mice were generated after the histopathological and behavioral characterization of *Brinp2/3* KO mice. Full and abbreviated names of the double and triple *Brinp* KO lines are provided in Table 4-4. The rationale for generating *Brinp1/2/3* KO mice is described following the results of *Brinp2/3* KO mice.

Table 4-4 - Nomenclature for *Brinp* double and triple KO mice

Abbreviated designation	Full name designation	Allele accession ID
<i>Brinp2/3</i> knockout (KO)	<i>Brinp2/3</i> ^{tm1.1Pib/tm1.1Pib}	MGI:5604615
		MGI:5604620
<i>Brinp1/2/3</i> knockout (KO)	<i>Brinp1/2/3</i> ^{tm1.1Pib/tm1.1Pib}	MGI:5604542
		MGI:5604615
		MGI:5604620

4.2 Generating *Brinp2/3* and *Brinp1/2/3* KO mice

4.2.1 Breeding of *Brinp2/3* triple KO mice.

Brinp2 and *Brinp3* are co-located on chromosome 1 in mice (Figure 1-9). Hence, a homologous recombination event is required to generate a *Brinp2*^{tm1.1Pib}/*Brinp3*^{tm1.1Pib} chromosome. The distance between the two genes was deemed far enough apart to allow a cross-over event during conventional breeding at a high enough frequency for generating double KO mice. *Brinp2* is found at chromosome 1 position 148.5 Mbp and *Brinp3* at 160.3 Mbp. The distance between the two genes is 11.8 Mbp, with a predicted 11.8% chance of a cross-over event occurring (1 Mbp \approx 1 cM \approx 1% probability).

Brinp3 KO and *Brinp2* het mice were first bred to generate mice heterozygous for the *Brinp2*^{tm1.1Pib} and *Brinp3*^{tm1.1Pib} alleles in the F1 generation. Genotyping of F1 generation mice is shown in Figure 4-1A. Mice heterozygous for *Brinp2*^{tm1.1Pib} and *Brinp3*^{tm1.1Pib} alleles from the F1 generation were mated. The F2 generation litters were genotyped, until cross-over events were identified that resulted in both *Brinp2*^{tm1.1Pib} and *Brinp3*^{tm1.1Pib} on the same chromosome. After genotyping of twenty-six F2 generation mice, the first cross-over event was identified. Genotyping results in Figure 4-1B show the identification of two mice where this occurred: B26 and B28. Fortunately, B28 proved to be a *Brinp2/3* double KO mouse. This would have occurred through a cross-over event of the *Brinp2* and *Brinp3* alleles in both parental gametes. B26 was found to be of genotype *Brinp2*^{+/-}/*Brinp3*^{-/-}. Mice B26 and B28 were set up as breeders, resulting in offspring that were either genotype *Brinp2*^{+/-}/*Brinp3*^{-/-} or *Brinp2/3*^{tm1.1Pib/tm1.1Pib} (*Brinp2/3* KO) mice in the F3 generation (Figure 4-1C). A *Brinp2/3* homozygous KO line was established by inter-crossing F3 generation *Brinp2/3* KO mice. Mice possessing the WT *Brinp2* and *Brinp3* alleles were also bred in parallel to generate WT mice for use as control animals.

4.2.2 Breeding of *Brinp1/2/3* triple KO mice.

Brinp1 KO mice (male) were bred with the *Brinp2*^{+/-}/*Brinp3*^{-/-} mice (female) to generate progeny heterozygous for the *Brinp1*^{tm1.1Pib} and *Brinp2*^{tm1.1Pib}/*Brinp3*^{tm1.1Pib} alleles in the F1 generation (Figure 4-2A). F1 generation heterozygous mice were then bred to generate triple KO mice. The first *Brinp1/2/3*^{tm1.1Pib/tm1.1Pib} (*Brinp1/2/3* KO) mouse was identified by genotyping in the F2 generation (Figure 4-2B).

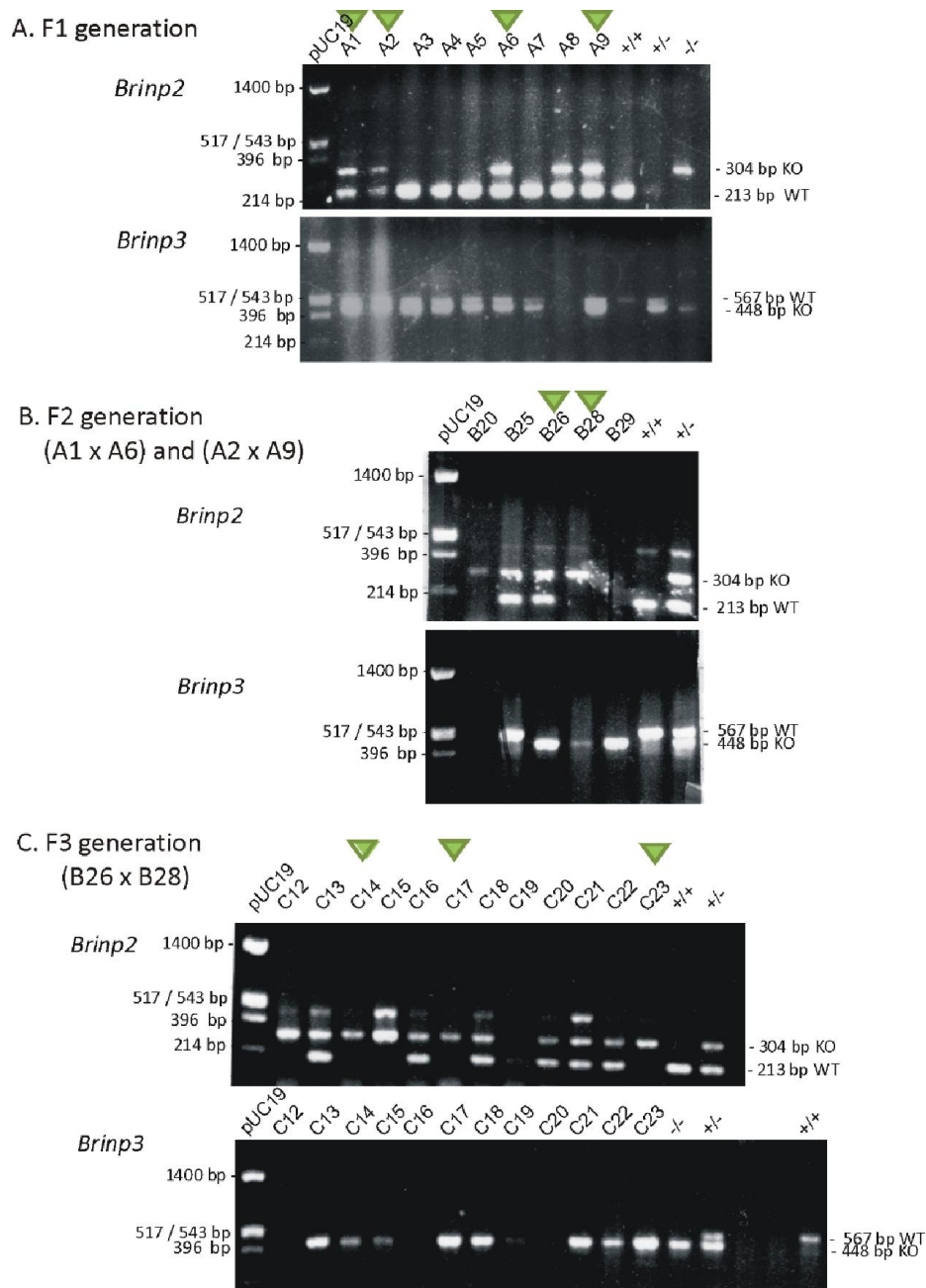


Figure 4-1 – Genotyping of mice carrying the *Brinp2*^{tm1.1Pib} and *Brinp3*^{tm1.1Pib} alleles to generate *Brinp2/3* double KO mice

- Genotyping of F1 generation mice from a cross between *Brinp2* het and *Brinp3* KO mice. Arrows identify mice heterozygous for *Brinp2*^{tm1.1Pib} and *Brinp3*^{tm1.1Pib} alleles that were selected as breeders.
- Genotyping of F2 generation mice. A1x A6 and A2x A9. Arrows identify mice with a germ line cross-over event. The first *Brinp2/3* double KO mouse (B28) was identified.
- Genotyping of F3 generation mice from breeders B26 x B28. Arrows identify *Brinp2/3* double KO mice. Controls: +/+ = WT, +/- = het, -/- = KO.

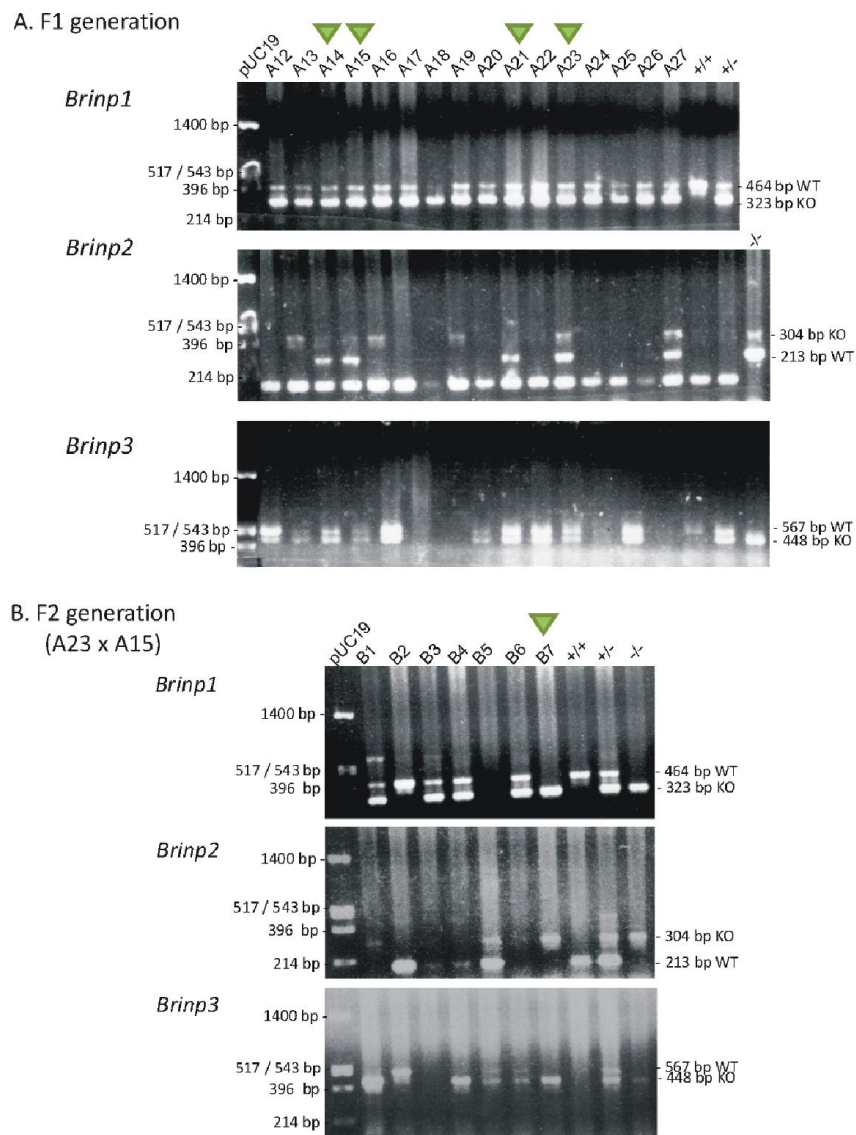


Figure 4-2 – Genotyping of mice carrying the *Brinp1*^{tm1.1Pib}, *Brinp2*^{tm1.1Pib} and *Brinp3*^{tm1.1Pib} alleles to generate *Brinp1/2/3* triple KO mice

A) Genotyping of F1 generation mice from a cross between *Brinp1* KO and *Brinp2*^{+/-}/*Brinp3*^{-/-} mice. Arrows identify mice heterozygous for *Brinp1*^{tm1.1Pib}, *Brinp2*^{tm1.1Pib} and *Brinp3*^{tm1.1Pib} alleles that were selected as breeders.

B) Genotyping of F2 generation mice from breeders A23 x A15. Arrow identifies *Brinp1/2/3* triple KO mouse, B7.

Controls: +/+ = WT, +/- = het, -/- = KO.

4.2.3 Validation of *Brinp2/3* and *Brinp1/2/3* KO mice

Validation of *Brinp2/3* and *Brinp1/2/3* KO mice was performed by RT-PCR of cDNA derived from KO mouse brain tissue of each genotype. Only PCR products of sizes corresponding with the *Brinp2*^{tm1.1Pib} and *Brinp3*^{tm1.1Pib} alleles were present for *Brinp2/3*, confirming homozygosity of both knockout alleles. For the *Brinp1/2/3* mouse cDNA, only PCR products of sizes corresponding with the *Brinp2*^{tm1.1Pib}, *Brinp2*^{tm1.1Pib} and *Brinp3*^{tm1.1Pib} alleles were present, confirming homozygosity of all three knockout exon-3 deleted alleles (Figure 4-3).

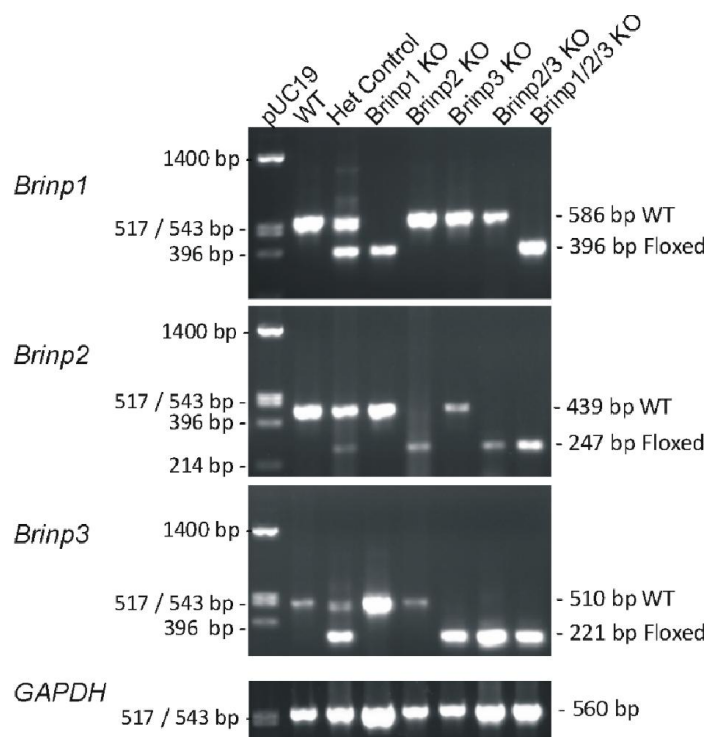


Figure 4-3 – Validation of knockout lines by RT-PCR, including *Brinp2/3* KO and *Brinp1/2/3* KO mice

Validation of *Brinp* knockout line using cDNA derived from brain tissue mRNA from WT, heterozygous and KO mice. PCR product sizes correspond to the removal of exon3 in the KO allele. Loading control: GAPDH.

4.3 Phenotyping of *Brinp2/3* KO mice

4.3.1 Postnatal weights of *Brinp2/3* KO mice.

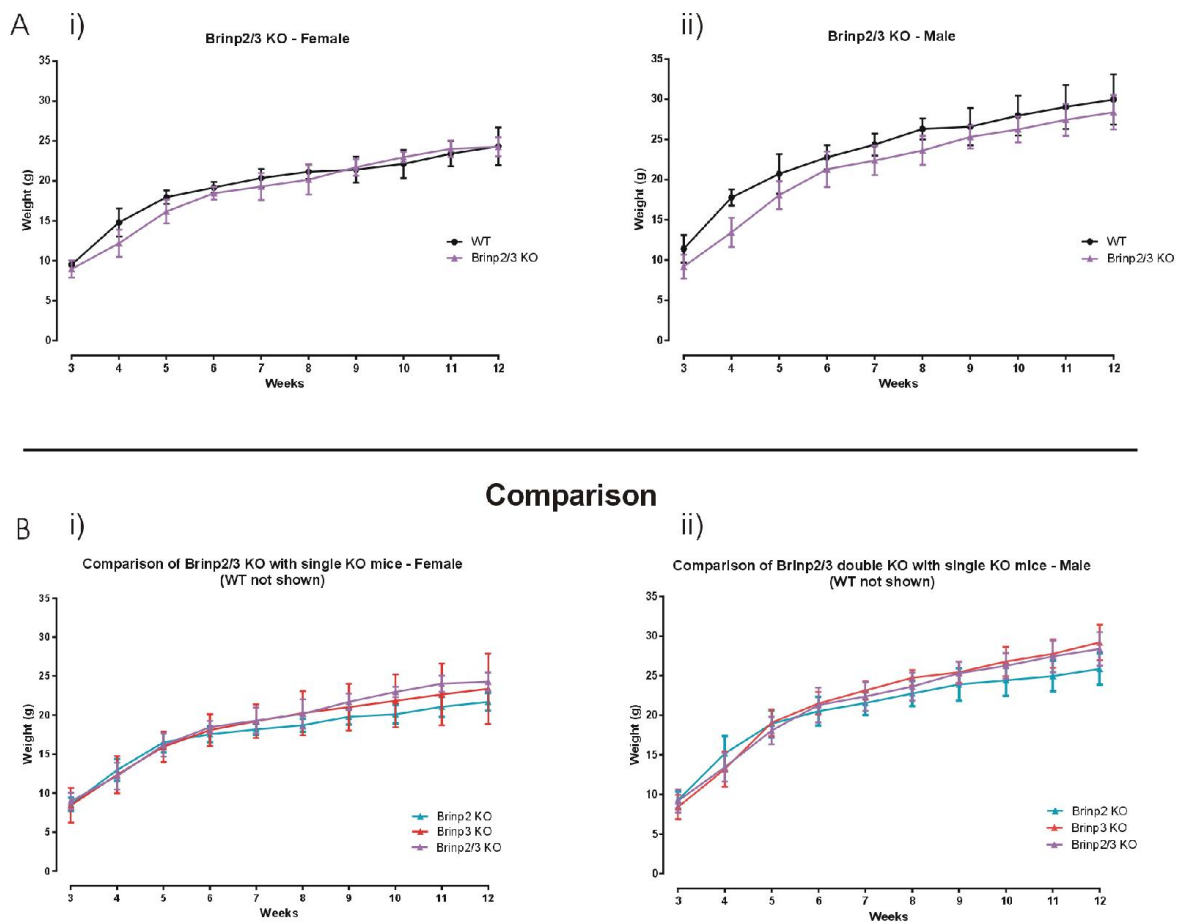
Brinp2/3 KO mice were weighed weekly from 3-12 weeks of age (Figure 4-4). *Brinp2/3* KO mice were smaller in the first few weeks, before recovering to a weight similar to that of WT. Male *Brinp2/3* KO mice weighed less than WT controls as adults. These results show a similar trend to the weights of the *Brinp3* knockouts.

4.3.2 Histopathological analysis of *Brinp2/3* KO mice

A pathological examination of *Brinp2/3* KO brains was carried out at 7 weeks of age (APN case: APN12-030). Two *Brinp2/3* KO and two WT mice were assessed. This first line phenotyping was intended to highlight any anatomical changes within the *Brinp2/3* KO mouse brain. In this instance, only the brains of *Brinp2/3* KO mice were assessed, with no analysis performed on other tissue. Whilst this limited the scope of analysis on these mice, assessment of brains was deemed of most important because of the neurobiology focus of this project. Prior to necropsy, *Brinp2/3* KO mice were assessed for general appearance and coat condition, showing no signs of ill health. Histopathology was performed under contract by the APN.

4.3.2.1 Brain pathology of *Brinp2/3* KO mice

Brinp2/3 KO mouse brains were of equivalent size to WT (Table 4-5). Brain sections showed normal structure for the forebrain, midbrain and cerebellum (Figure 4-5). The brain appeared symmetrical with no ventricular dilation. The cerebellum showed typical architecture and unremarkable Purkinje cells. There was no evidence of neuronal loss and the myelination appeared normal. In summary, *Brinp2/3* KO mouse brains showed no gross morphological changes.

Figure 4-4 – *Brinp2/3*: weights

A) Weights of male and female *Brinp2/3* KO mice, weighed from three to 12 weeks, compared to WT controls.

- i) Female *Brinp2/3* KO male did not show a significant effect of genotype on body weight: $F(1,13)=1.756$, $p=0.208$, but did show a significant week x genotype interaction effect: $F(9,117)=3.065$, $p=0.002$.
- ii) Female *Brinp2/3* KO mice showed a significant decrease in body weight, analyzed by repeat measures two-way ANOVA: $F(1,14)=6.228$, $p=0.026$, and a significant interaction effect between week x genotype: $F(9,126)=2.461$, $p=0.013$.

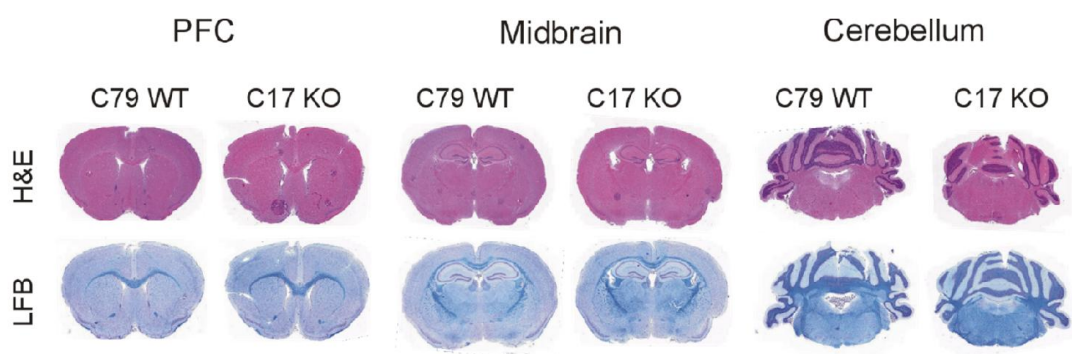
B) A comparison between *Brinp2/3* KO mice and previously reported weights for *Brinp2* and *Brinp3* KO mice, showing no significant difference between the *Brinp3* single KO and the *Brinp2/3* double KO for either i) females or ii) males.

N= 8 WT and 7 *Brinp2/3* KO mice. Results are represented as the mean \pm SD.

Table 4-5 - Macroscopic measurements of *Brinp2/3* KO mice

Compiled from data provided by the Australian Phenomics Network

Genotype	WT	WT	<i>Brinp2/3</i> KO	<i>Brinp2/3</i> KO
Mouse	C83	C79	C17	C23
Age	7 weeks	7 weeks	7 weeks	7 weeks
Sex	M	M	M	M
Weight	23.87g	23.82g	20.36g	18.83g
Brain	15x10x5mm	16x10x5mm	15x10x5mm	15x10x5mm

**Figure 4-5 Brain histopathology of *Brinp2/3* KO mice**

Coronal brain sections of *Brinp2/3* KO mice, compared to WT littermates. Representative sections are shown of the forebrain, midbrain (including medial hippocampus) and cerebellum of 7-8 week old mice. Brains were stained with Hematoxylin and Eosin (H&E, purple), and Luxol Fast Blue (LFB). Figure compiled from images provided by the Australian Phenomics Network.

4.3.3 *Brinp2/3* behavioral testing

Brinp2/3 KO mice were assessed by the same behavioral tests as previously tested for the single *Brinp* KO mice (chapter 3). Behavioral tests were carried out under contract by Travis Featherby, Neuro Research Services (The Florey Institute of Neuroscience and Mental Health): <http://www.melbournebraincentre.edu.au/content/neuro-research-services>. Data were analyzed by the candidate.

4.3.3.1 *Brinp2/3* KO mice – no detectable difference in sensory function, motor co-ordination or spatial memory

Brinp2/3 double KO mice had normal vision, as determined by the visual placing test (Figure 4-6A). The acoustic startle and pre-pulse inhibition tests demonstrated that *Brinp2/3* mice have normal hearing and sensory gating (Figure 4-6 B and C). *Brinp2/3* KO mice were also normal for motor co-ordination on the Rotarod (Figure 4-6D). The double KO mice showed no memory deficit when tested in the Y-maze (Figure 4-6E).

4.3.3.2 *Brinp2/3* KO mice – elevated plus maze

Brinp2/3 KO mice showed a similar phenotype to the *Brinp3* KO mice on the elevated plus maze, whereby the double knockouts spent an equivalent amount of time in the closed arms and the open arms (Figure 4-7).

4.3.3.3 *Brinp2/3* KO mice – locomotor cell

Brinp2/3 KO mice showed normal activity in the locomotor cell. The mice showed no change in average velocity or resting time compared to WT (Figure 4-8 A and B). *Brinp2/3* KO mice did show one notable difference – a significant decrease in vertical plane entries (Figure 4-8C).

4.3.3.4 *Brinp2/3* KO mice – three chamber social interaction test

Brinp2/3 KO mice did not show a preference for either the left or the right chamber in trial 1 of the social interaction test. There was also no significant difference of exploration of the empty cages (Figure 4-9A). *Brinp2/3* KO mice did not show a significant difference in time interacting with a novel mouse in trial 2 of the social interaction test (Figure 4-9B). *Brinp2/3* KO showed no significant difference in time interacting with the novel mouse in trial 3, but spent less time interacting with the ‘now familiar’ mouse ($p=0.033$), demonstrating reduced sociability (Figure 4-9C). The results for this test were difficult to interpret, as neither WT nor *Brinp2/3* KO mice showed a preference for the novel mouse over the familiar mouse.

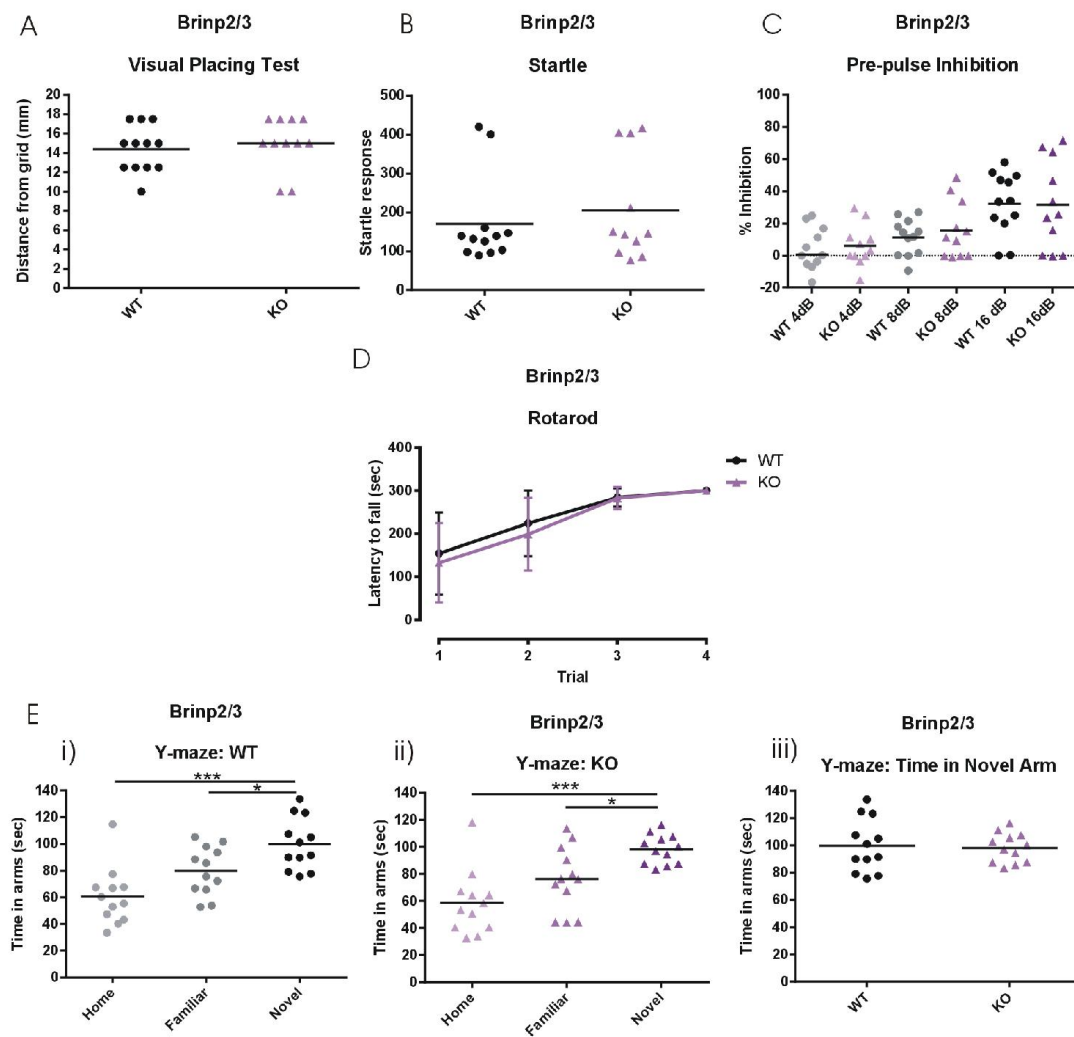


Figure 4-6 – *Brinp2/3*: Visual placing test, PPI, Rotarod and Y-maze

Figure 4-6 – *Brinp2/3*: Visual placing test, PPI, Rotarod and Y-maze

- A) Visual placing test. *Brinp2/3* displayed normal vision, measured by the distance with which mice extended their forearms when lowered towards a grid, $t(21)=0.5818$, $p=0.5669$, unpaired Student's t-test.
- B) Acoustic startle. *Brinp2/3* KO mice showed a normal startle response, $t(21)=0.6647$, $p=0.5135$, unpaired Student's t-test. Startle response is measured as displacement on a platform, and recorded in arbitrary units.
- C) Pre-pulse inhibition. *Brinp2/3* KO mice showed no significant effect of genotype on inhibition of the startle response when primed with pre-pulse tones at 4, 8 and 16 db, $F(1,33)=0.209$, $p=0.652$, two-way ANOVA. Results are represented as percentage inhibition of startle response relative to the unprimed startle response.
- D) Rotarod accelerated test (4-40 rpm x 4 trials). *Brinp2/3* KO mice showed no significant effect of genotype on Rotarod performance. $F(1,21)=0.577$, $p=0.456$, and no interaction effect of trial x genotype: $F(1,21)=0.448$, $p=0.511$, repeat measures two-way ANOVA. Results are shown as the mean \pm SD.
- E) Y-Maze:
 - i). WT litter mate control show the species-typical increase in time spent in the novel arm, $F(1,22)=11.889$, $p<0.001$, one-way ANOVA. Tukey HSD multiple comparisons: Home-Familiar: $p=0.056$, Home-Novel: $p<0.001$, Familiar-Novel: $p=0.048$.
 - ii) *Brinp2/3* KO mice also showed an increase time spent investigating the novel arm $F(1,22)=11.366$, $p<0.001$, one-way ANOVA. Tukey HSD multiple comparisons: Home-Familiar: $p=0.101$, Home-Novel: $p<0.001$, Familiar-Novel: $p=0.033$.
 - iii) Genotype comparison: *Brinp2/3* KO mice showed no significant difference to WT in time spent investigating the novel arm, $t(22)=0.2652$, $p=0.7933$, unpaired Student's t-test.

N=12 WT and 11 *Brinp2/3* KO mice. * $p<0.05$, *** $p<0.001$. Each data point indicates the response from one animal. The mean is shown as a horizontal line.

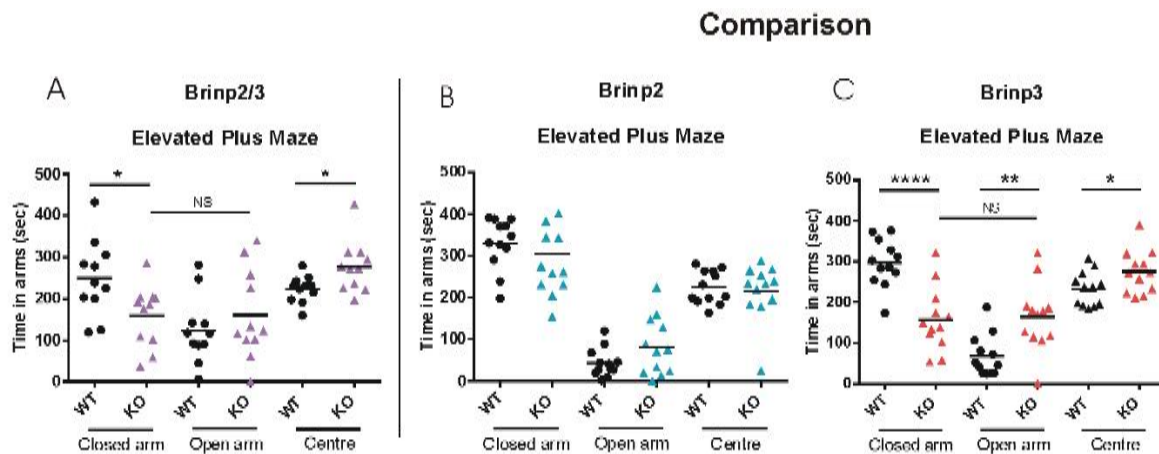
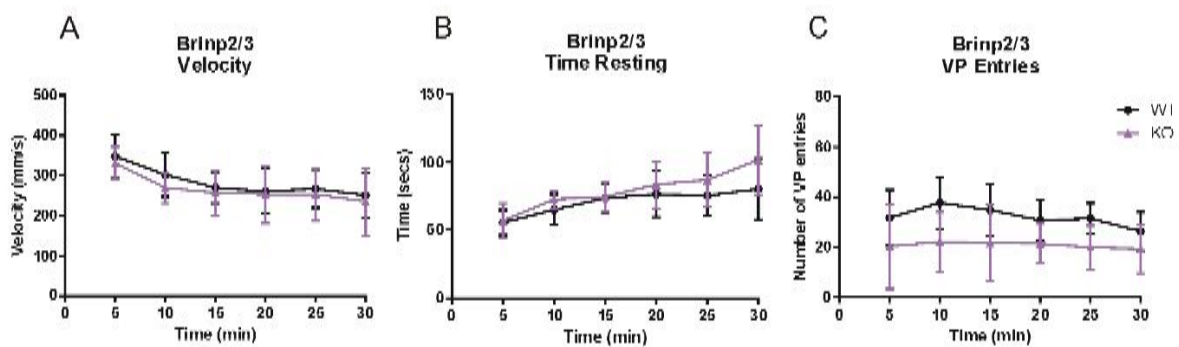


Figure 4-7 – *Brinp2/3*: Elevated plus maze

A) *Brinp2/3* KO mice also demonstrated hyper-exploratory behavior in the Elevated Plus Maze. *Brinp2/3* KO mice spent significantly and less time in the closed arms of the EPM: $t(20)=2.551$, $p=0.0190$, and significantly more time in the center of the maze: $t(20)=2.537$, $p=0.0196$. *Brinp2/3* KO mice did not show a significant difference in time spent in the open arms: $t(20)=0.9145$, $p=0.3714$. As with the *Brinp3* KO mice, *Brinp2/3* KO mice did not show a preference between time in the closed and open arms: $t(20)=0.05105$, $p=0.9598$, unpaired Student's *t*-tests.

Previous results for B) *Brinp2* KO mice and C) *Brinp3* KO mice elevated plus maze performance are provided for comparison. See Figure 3-21 for *Brinp2* KO and *Brinp3* KO mice test statistics.

$N=12$ WT and 11 *Brinp2/3* KO mice. * $p<0.05$, ** $p<0.01$, **** $p<0.0001$. NS = not significant. Each data point indicates the response from one animal. The mean is shown as a horizontal line.

Figure 4-8 – *Brinp2/3*: Locomotor cell

- A) Normal locomotor activity of *Brinp2/3* KO mice over 30 min, shown as no significant effect of genotype on average velocity in the locomotor cell: $F(1,22)=0.747$, $p=0.397$, and no interaction effect of genotype x time: $F(5,110)=0.330$, $p=0.894$, repeat measures two-way ANOVA.
- B) No main effect of genotype on time resting $F(1,22)=3.58$, $p=0.072$, and no interaction effect of genotype x time: $F(5,110)=2.118$, $p=0.069$, repeat measures two-way ANOVA.
- C) *Brinp2/3* KO mice exhibited a decrease in rearing activity in the locomotor cell, recorded as a main effect of genotype on vertical plane entries $F(1,22)=10.10$, $p=0.004$, with no interaction effect of time x genotype: $F(5,110)=1.063$, $p=0.385$, repeat measures two-way ANOVA.

Results represented as the mean \pm SD, divided into 6 x 5 min equal bins.

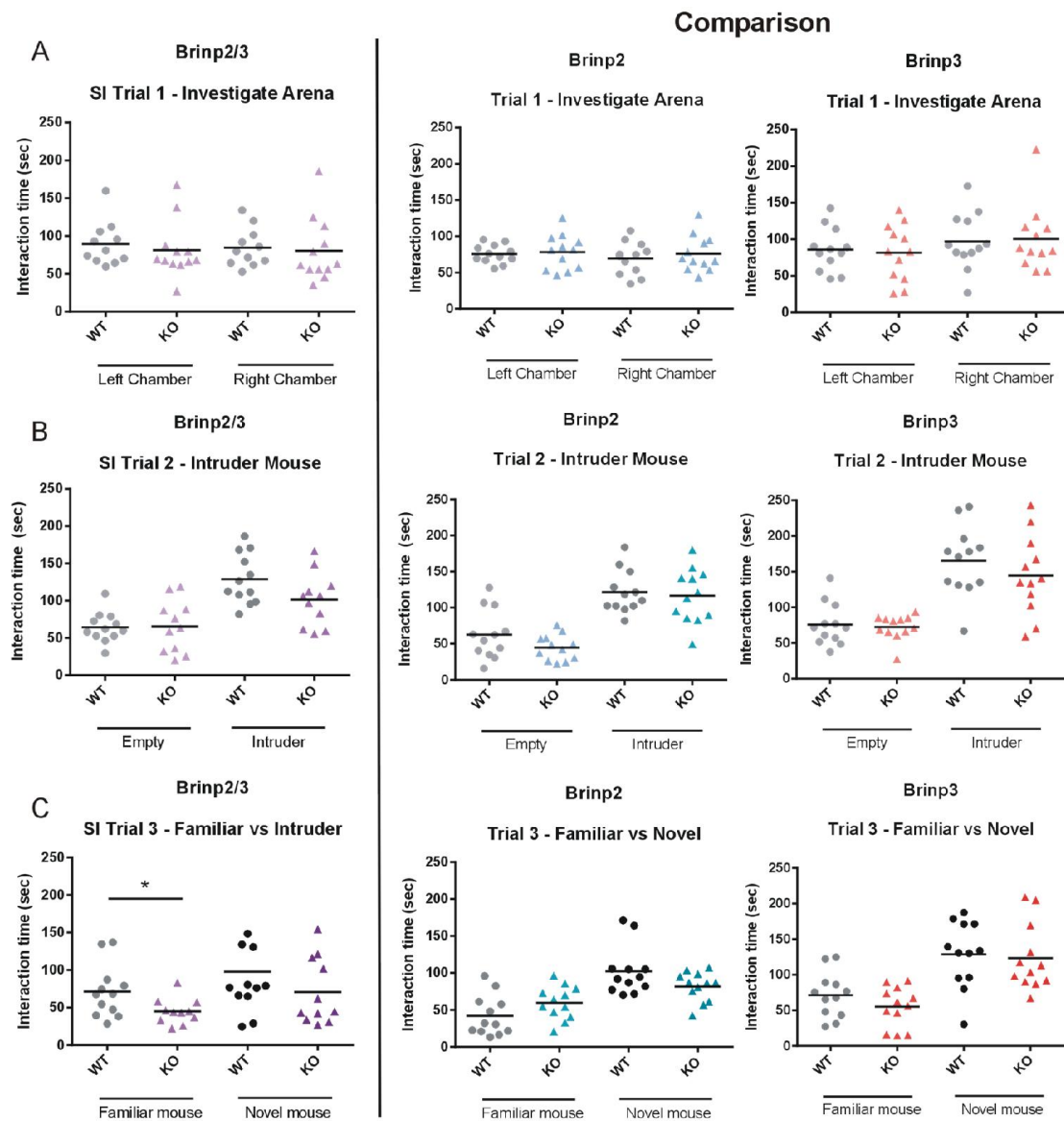


Figure 4-9 – *Brinp2/3*: Three chamber social interaction test

Figure 4-9 – *Brinp2/3*: Three chamber social interaction test

Note: Previous results for *Brinp2* and *Brinp3* KO elevated plus maze performance are provided in the second and third columns for comparison. Each data point indicates the response from one animal. The mean is shown as a horizontal line. * $p < 0.05$, unpaired Student's t-test.

- A) Trial 1 - Acclimatization of the testing arena for *Brinp2/3* mice. Results show time in the interaction zone (IZ) (defined as an area within a 1cm perimeter from the empty cage in either the left or right chamber). *Brinp2/3* KO mice showed no significant difference to WT controls. *Brinp2/3*: left chamber, $t(21)=0.5872$, $p=0.5633$, right chamber: $t(21)=0.2836$, $p=0.7795$, unpaired Student's t-tests.
- B) Trial 2 - Social interaction: Results show time in the interaction zone (IZ) of an empty cage compared with the IZ of a cage with a sex-matched stranger mouse. No significant differences were observed in time spent interacting with a sex-matched stranger mouse for *Brinp2/3* KO mice. *Brinp2/3*: empty chamber, $t(21)=0.1158$, $p=0.9089$, stranger mouse: $t(21)=1.894$, $p=0.0721$, unpaired Student's t-tests.
- C) Trial 3 - Social preference: Results show time in the IZ of the mouse used in trial 2 (familiar mouse), compared with the IZ of a cage with a novel mouse. *Brinp2/3* KO mice showed a decrease in interaction with a familiar mouse, $t(21)=2.275$, $p=0.0335$, whilst no significant differences in integration time with a novel mouse: $t(21)=1.163$, $p=0.2577$, unpaired Student's t-test.

N=12 WT, 11 *Brinp2/3* KO mice. Each data point represents a single animal. The mean is represented as a horizontal line.

4.3.4 *Brinp2/3* KO behavioral summary and conclusions

Overall, the *Brinp2/3* double KO phenotype was similar to that of the *Brinp3* KO phenotype. The double KO mice showed the same hyper-exploratory behavior on the elevated plus maze, and a subtle sociability phenotype in the three chamber social interaction test. A summary of the *Brinp2/3* KO behavioral testing is provided in Table 4-6. **Error! Reference source not found..**

The almost identical phenotype between the *Brinp2/3* KO and *Brinp3* KO points to the conclusion that there is no compensation between *Brinp2* and *Brinp3*, and therefore a) the functions of *Brinp2* and *Brinp3* are not interchangeable, or b) the loss of their function is compensated for by another gene or genes.

Table 4-6 - Behavioral analysis summary, comparing the *Brinp2/3* KO phenotype with single *Brinp* KO phenotypes.

Statistically significant behavioural phenotypes are highlighted in red.

	Behavioral Test	<i>Brinp1</i> KO	<i>Brinp2</i> KO	<i>Brinp3</i> KO	<i>Brinp2/3</i> KO
Sensory	Visual placing	No difference	No difference	No difference	No difference
	Olfaction test	No difference	No difference	No difference	No difference
Sensory processing	Acoustic startle	No difference	No difference	No difference	No difference
	Pre-pulse Inhibition	No difference	Marginal improvement	No difference	No difference
Motor co-ordination	Rotarod	No difference	Improvement	No difference	No difference
Learning / memory	Y-maze	Memory impairment	No difference	No difference	No difference
	Morris Water Maze	No difference	-	-	-
Sociability	Social interaction	Decreased sociability	No difference	No difference	No difference
	Social preference	Decreased sociability	Marginal difference	Marginal difference	Marginal difference
Anxiety / fear	Elevated plus maze	Hyper-exploratory	No difference	Hyper-exploratory	Hyper-exploratory
Hyperactivity	Locomotor cell	Hyperactivity	-	-	No difference

4.4 Phenotyping of *Brinp1/2/3* KO mice

4.4.1 Rationale for generating *Brinp1/2/3* KO mice

The results for the *Brinp2/3* KO mice indicates that *Brinp2* and *Brinp3* genes do not compensate for each other. This still leaves the possibility that it is *Brinp1* that is compensating for their absence in the *Brinp2* and *Brinp3* KO mice.

Brinp2 and *Brinp3* each share 50% homology with *Brinp1* and are expressed in overlapping regions of the mouse brain (Kawano et al., 2004). They also likely evolved from a common ancestral version of *Brinp*, which may suggest a preserved function (Figure 1-7). The relatively high homology indicates that it may be *Brinp1* that is able to compensate for the loss of either *Brinp2* or *Brinp3* by performing the same function. This was tested by removing all three *Brinps* from the mammalian system by generating and studying *Brinp1/2/3* triple KO mice.

As with the double knockout, if the function of *Brinp1* is interchangeable with *Brinp2* or *Brinp3* in the same cell types, this could result in compensation. If this is the case, it is predicted that removal of all three *Brinps* will result in a phenotype different to the *Brinp1* KO alone phenotype.

If *Brinp1*, *Brinp2* and *Brinp3* function is not interchangeable, we would predict that the *Brinp1/2/3* KO phenotype would be the sum of the single KO phenotypes, with no additional or enhanced phenotype. It is also possible that compensation by other homologous genes will mean that even when all three *Brinps* are removed, essential functions will continue.

After the establishment and characterization of single knockout lines, the *Brinp2/3* double knockouts were bred with *Brinp1* KO mice to generate *Brinp1/2/3* triple knockout mice. Triple knockouts were validated by RT-PCR for homozygosity of the *Brinp1*^{tm1.1Pib}, *Brinp2*^{tm1.1Pib} and *Brinp3*^{tm1.1Pib} alleles. These mice were assessed for viability, reproductive success and whole body organ pathology.

4.4.2 *Brinp1/2/3* KO mice exhibit low viability and poor reproductive success.

Brinp1/2/3 KO mice were generated from breeding mice heterozygous for *Brinp1* and the *Brinp2/3* allele. The triple het breeders produced litters, but resulted in poor postnatal survival. Of 21 litters born by triple het breeders, there were only 3 instances where the entire litter survived to age of weaning (P21). In the remaining cases, either a proportion of the litter

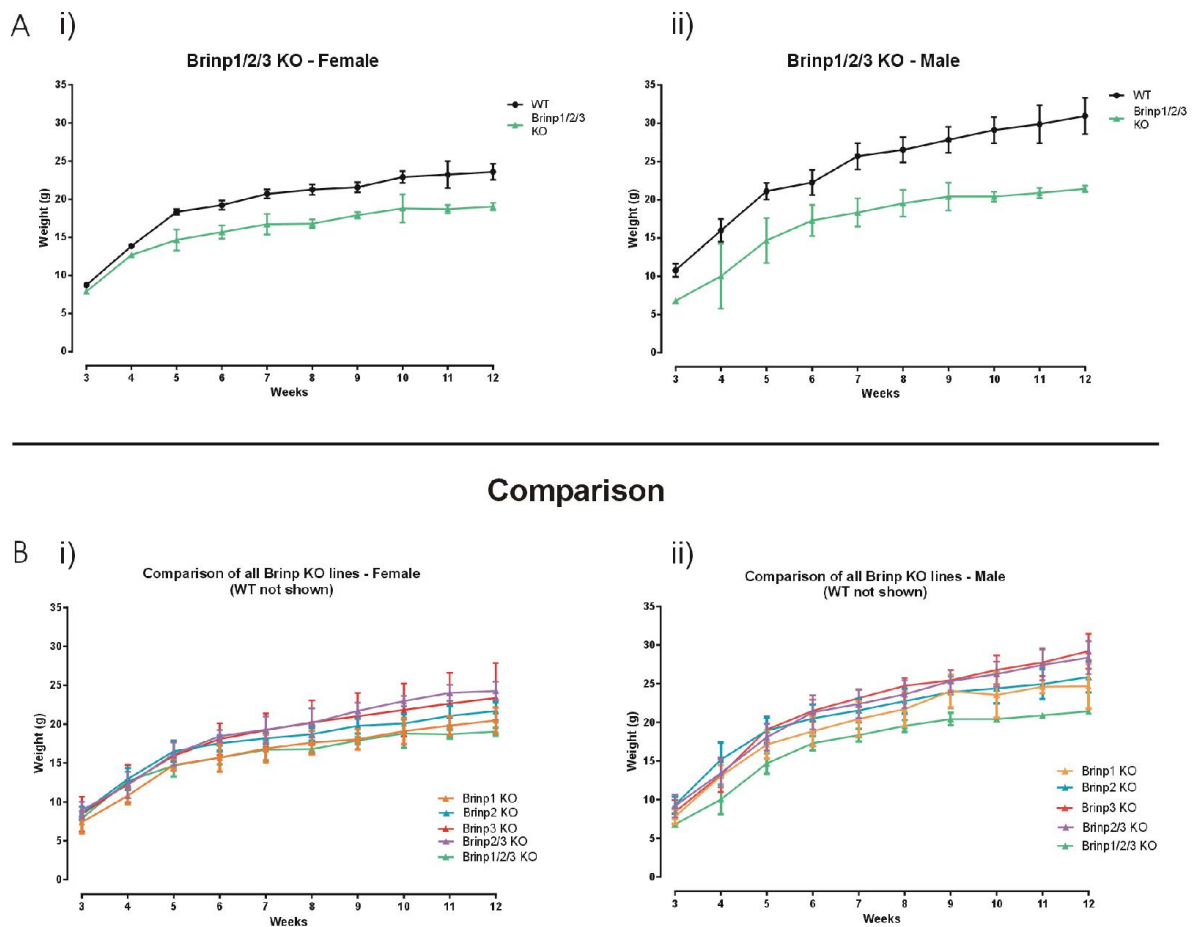
or the entire litter died as neonates. In the course of a year, a total of only nine triple KO mice survived to age of postnatal day 10 (5 males, 4 females).

An attempt at homozygous breeding of the *Brinp1/2/3* KO mice was unsuccessful. Only two males and one female knockout mice were available to be set up as breeders. A triple knockout male and female were set up as breeders for three months, but the female did not fall pregnant.

When either of the two male *Brinp1/2/3* KO mice were placed with WT females, the female breeder did not fall pregnant. The female *Brinp1/2/3* KO mouse crossed with a WT male did have one litter, which died soon after birth.

Brinp1/2/3 KO mice weighed significantly less than WT littermates (Figure 4-10A) and less than *Brinp2*, *Brinp3* or *Brinp2/3* KO mice (Figure 4-10B). Male triple KO mice also weighed and less than any of the *Brinp1* KO mice (Figure 4-10B).

Two *Brinp1/2/3* KO mice (1M, 1F) were used for histopathological analysis. One triple KO (M) was used for RT-PCR validation. Three triple KO (M) were used for cryopreservation of the line. Behavioral testing requires a cohort minimum size of 10 KO mice and 10 WT, within an age range of 8-12 weeks. Given the poor breeding and survival of the triple KO lines, construction of a behavioral testing cohort could not be achieved.

Figure 4-10 – *Brinp1/2/3*: weights

A) Five male *Brinp1/2/3* KO mice and three female *Brinp1/2/3* KO mice weighed weekly from 3-12 weeks.

i) Female *Brinp1/2/3* KO mice show a significant reduction in body weight: $F(1,3)=47.738$, $p=0.007$, with a significant interaction between week x genotype: $F(9,27)=5.736$, $p<0.001$, repeat measures two-way ANOVA, $n=3$ WT, 2 *Brinp1/2/3* KO.

ii) Male *Brinp1/2/3* KO mice also show a significant decrease in body weight: $F(1,8)=54.708$, $p<0.001$, KO, with a significant interaction between week x genotype: $F(8,64)=3.005$, $p=0.006$, repeat measures two-way ANOVA, $n=5$ WT, 5 *Brinp1/2/3* KO.

B) Comparison of weights between *Brinp1* KO, *Brinp2* KO, *Brinp3* KO, *Brinp2/3* KO and *Brinp1/2/3* KO mice.

Results represented as the mean \pm SD.

4.4.3 Histopathological analysis of *Brinp1/2/3* Triple knockout mice

A full histopathological examination was carried out on *Brinp1/2/3* triple KO mice (APN case: APN14-008). One male and one female triple knockout mouse were analyzed along with littermate WT controls. Histopathology was performed under contract by the Australian Phenomics Network (<http://www.australianphenomics.org.au/>).

4.4.3.1 Macroscopic observations for *Brinp1/2/3* KO mice

At the time of necropsy, the animals appeared well nourished, well groomed, active/curious and healthy with normal movement and gait. There were no observable dermal lesions and no nasal/ocular discharges. The gastrointestinal tract contained ample ingesta and the thoracic and abdominal viscera showed no macroscopic abnormalities. Vital organs were of comparable size to WT, except for the thymus, which was enlarged in both KO mice (Table 4-7).

Table 4-7 - Macroscopic measurements *Brinp1/2/3* KO mice
Compiled from data provided by the Australian Phenomics Network

Genotype	WT	<i>Brinp1/2/3</i> KO	WT	<i>Brinp1/2/3</i> KO
Mouse	B2	B7	J51	B73
Age	30 weeks	30 weeks	15 weeks	15 weeks
Sex	M	M	F	F
Weight	29.6g	25.8g	25.7g	20.8g
Spleen	12x2x2mm	12x4x2mm	18x5x2mm	13x8x4mm
Kidney	9x6x6mm	6x10x5mm	12x6x6mm	10x6x5mm
Lungs	Uninflated	Inflated	Inflated	Inflated
Heart	8x6x6mm	10x5x5mm	8x7x4mm	8x8x4mm
Brain	15x10x5mm	13x10x6mm	15x10x5mm	14x10x6mm
Thymus	4x4x2mm	8x6x2mm	5x3x2mm	9x9x2mm
Testes	9x5x5mm	8x6x4mm	n/a	n/a
Tail	90mm	75mm	75mm	75mm

4.4.3.2 Blood analysis for *Brinp1/2/3* KO mice

Blood results show a low platelet count for animals WT-J51, WT-B2 and KO-B73, an elevated level in the percentage of eosinophils in KO-B7 and an elevated level in the percentage of basophils in animals WT-J51 and KO-B7.

4.4.4 Brain pathology of *Brinp1/2/3* KO mice

Brains of KO mice showed no lesions of significance. Sections of brain labelled with Hematoxylin and Eosin, and Luxol Fast Blue appear symmetrical with no ventricular dilation observed, unremarkable meninges and typical lamination. The cerebellum appears symmetrical with typical architecture and Purkinje cells. There was no evidence of neuronal loss and the myelination appeared normal (Figure 4-11). Neuropathologist, Professor Catriona A McLean, Head Anatomical Pathology, Alfred Health, agreed with the findings of no significant differences in the brain or spinal cord.

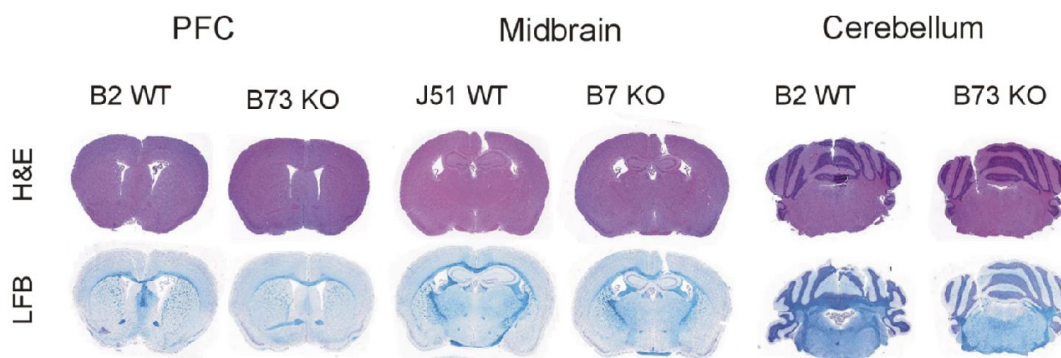


Figure 4-11 Brain histopathology of *Brinp1/2/3* KO mice

Coronal brain sections of *Brinp1/2/3* KO mice, compared to WT littermates. Representative sections are shown of the forebrain, midbrain (including medial hippocampus) and cerebellum of 7-8 week old mice. Brains were stained with Hematoxylin and Eosin (H&E, purple), and Luxol Fast Blue (LFB). Figure compiled from images provided by the APN.

4.4.5 Microscopic observations of *Brinp1/2/3* KO mice - signs of inflammation

All 25 organs investigated were of normal morphology for their developmental time points. Inflammation was detected in both triple KO mice; B73 female presented with inflammation surrounding the sebaceous gland adjacent to the tongue (Figure 4-12A). B7 male presented with inflammation to the heart in a solitary lesion, with a focal area of basophilic cells surrounded by swollen myocytes in the interventricular septum. The lesion has a central core of inflammatory cells (lymphocytes and macrophages) enclosed by brightly eosinophilic

degenerate, swollen and necrotic cardiac myocytes (Figure 4-12B). In addition, the right inner ear contains eosinophilic material, with a diffuse acute inflammation within the scala vestibuli / scala tympani. The tympanic cavity of the left middle ear contains an eosinophilic proteinaceous fluid (Figure 4-12C and D).

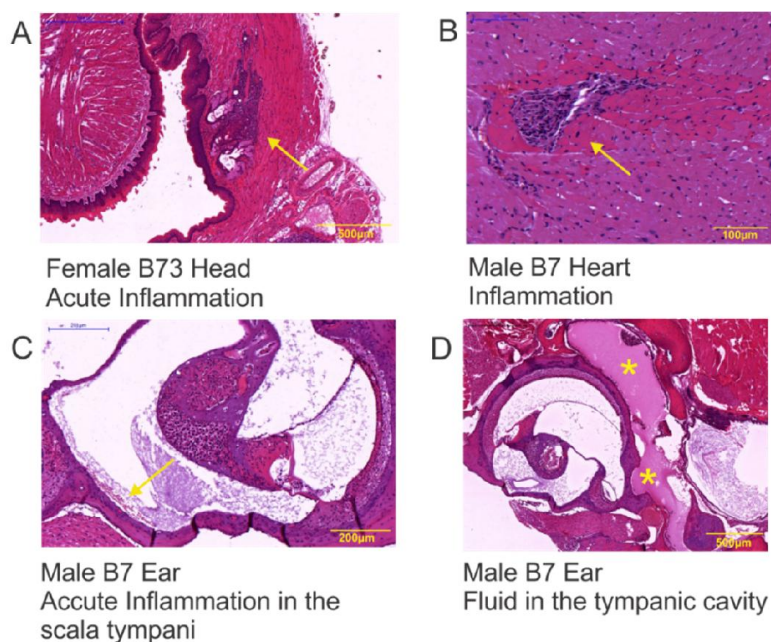


Figure 4-12 – Tissue inflammation in *Brinp1/2/3* KO mice

Brinp1/2/3 KO B73 (female): acute inflammation in the salivary gland. B) *Brinp1/2/3* KO mouse B7 (male): Solitary lesion in the interventricular septum of the heart. C) and D). Male KO B7: inflammation present in the tympani cavity of the inner ear. Arrows indicate inflammatory areas. Images provided by the Australian Phenomics Network.

4.4.6 *Brinp1/2/3* KO summary

From the few *Brinp1/2/3* KO mice that survived beyond a couple of days, it is evident that the mice are significantly smaller, whilst showing normal gross morphology except for inflammation. The confounding issues of breeding triple KO mice with a gene already known to reduce survival, made it very challenging to generate enough mice to study. A different breeding strategy would be needed to continue this line of investigation, e.g. generation of *Brinp1/2* or *Brinp1/3* KO mice.

4.5 Expression profile of *Brinps* and *Astrotactins* in the mouse brain.

The second half of this chapter explores the expression profiles of each of the five neuronal-MACPF genes. This is to determine whether similar spatial distribution could indicate an interchangeable role between any of the five neuronal MACPF genes. In addition, quantitative PCR was performed on mRNA from the brains of *Brinp1* KO mice to assess whether any of the homologous MACPF family members show changes in expression levels in response to the deletion of *Brinp1* that would indicate gene compensation. The *Astn1* and *Astn2* genes were included in this analysis because of the conserved MACPF domain. There is significant conservation between the MACPF domains of Astrotactins and *Brinps* (approximately 40%), which could indicate a common function, as outlined in the hypothesis.

4.5.1 A comparison of WT *Brinp* and *Astn* expression in the adult mouse brain.

The publications by Kawano et al (*Brinps*) and Wilson et al (Astrotactins) provided some information on the expression pattern of *Brinps* and *Astn2* in the developing and adult CNS (Kawano et al., 2004; Wilson et al., 2010). For this study, a further set of expression data was analyzed: the publically available online database from the Allen Mouse Brain Atlas (AMBA) of genome-wide atlas of gene expression in the adult C57BL/6 mouse brain: <http://mouse.brain-map.org/> (Lein et al., 2007). The standardized *in-situ* hybridization (ISH) protocol and high resolution imaging allows for a direct comparison of mRNA distribution for different brain-expressed genes, offering ideal conditions to compare expression patterns between the five neuronal-MACPF genes. The data for *Brinps* and Astrotactins expression in the CNS was compiled and analyzed, to build a picture of neuronal-MACPF expression in the adult mouse brain. Figure 4-13 shows mRNA transcript distribution of the five neuronal-MACPF genes within the adult (p56) mouse brain, displayed as sagittal and coronal sections. Higher magnification images are also provided for regions of the mouse brain where *Brinps* and Astrotactins show highest expression: 1) the olfactory bulb (Figure 4-14), 2) the hippocampus and neocortex (Figure 4-15) and 3) the cerebellum (Figure 4-16). This data provides additional information on cell type specific localization of neuronal-MACPF proteins in medial temporal coronal sections, as well as sagittal sections for *Astn1* expression in the adult mouse brain. The data highlight differences, as well as similarities between regional expression. A summary of the expression data is provided in Table 4-8.

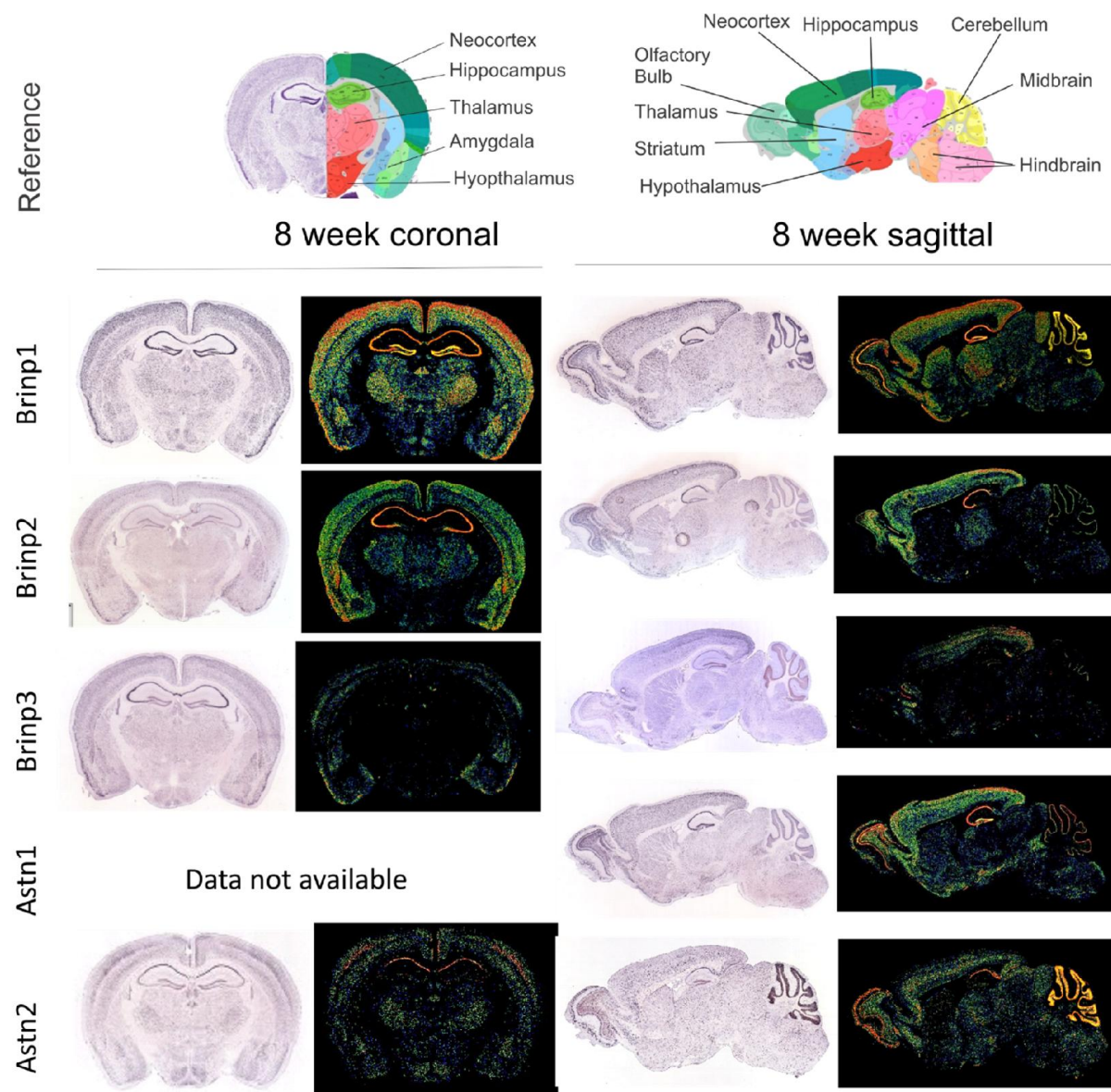


Figure 4-13 – A comparison of *Brinp1*, *Brinp2* and *Brinp3*, *Astn1* and *Astn2* mRNA distribution in the adult (P56) mouse brain in coronal and sagittal view

Columns 1 and 3 show *in-situ* hybridization showing gene expression of *Brinp1*, *Brinp2*, *Brinp3*, *Astn1* and *Astn2* as purple staining.

Columns 2 and 4 show an expression map of the same section in columns 1 and 3. Relative expression levels are represented by color. From high to low expression:

Red = +++, Yellow = ++, Green = ++, Blue = +, Black = -. Expression data compiled from resources by the Allen Mouse Brain Atlas: <http://mouse.brain-map.org/>.

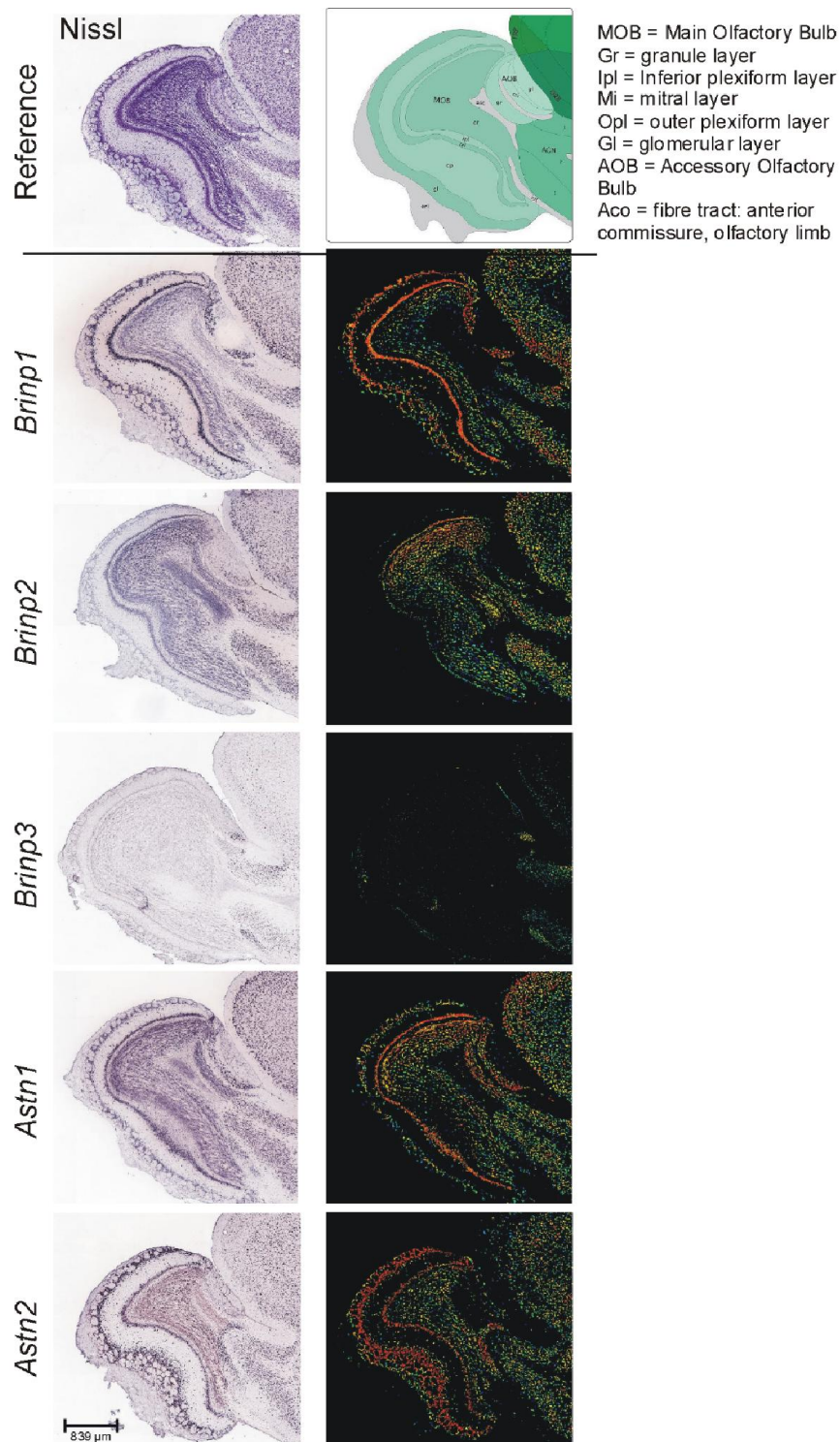


Figure 4-14 – A comparison of *Brinp1*, *Brinp2*, *Brinp3*, *Astn1* and *Astn2* mRNA distribution in the adult (P56) mouse olfactory bulb

The top panels provided a reference of olfactory bulb anatomy. The left column shows *in-situ* hybridization of the sagittal olfactory bulb. Positive gene expression is shown in purple. In the right column, relative expression levels are represented as an expression map. From high to low expression: Red = +++, Yellow = ++, Green = +, Blue = -, Black = - Expression data compiled from resources by the Allen Mouse Brain Atlas: <http://mouse.brain-map.org/>.

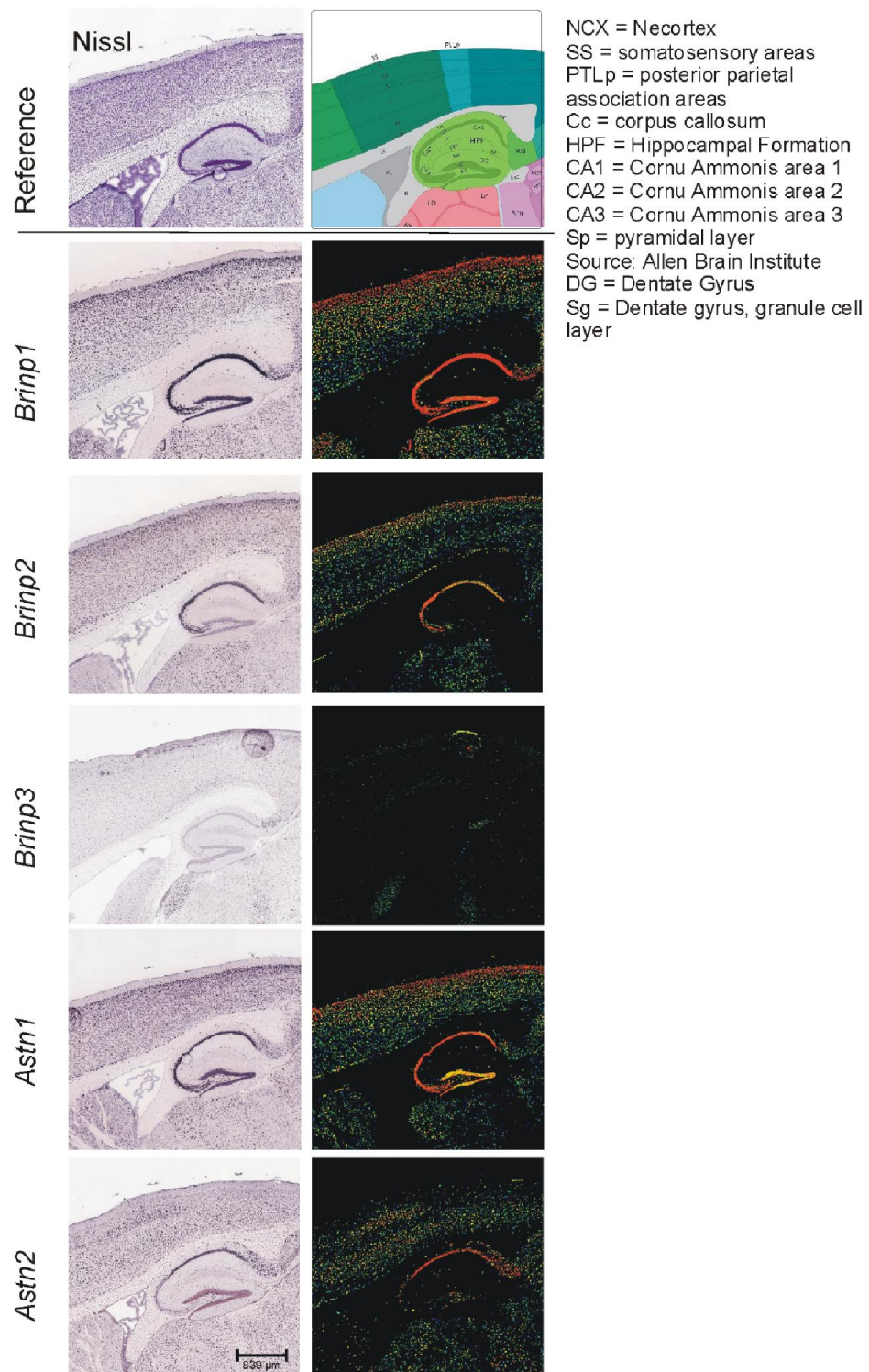


Figure 4-15 – A comparison of *Brinp1*, *Brinp2*, *Brinp3*, *Astn1* and *Astn2* mRNA distribution in the adult (P56) mouse neocortex and hippocampus

The top panels provide a reference of neocortex and hippocampus anatomy. The left column shows *in-situ* hybridization of the sagittal cortex. Positive gene expression is shown in purple. In the right column, relative expression levels are represented as an expression map. From high to low expression: Red = +++, Yellow = ++, Green = +, Blue = -, Black = -. Expression data compiled from resources by the Allen Mouse Brain Atlas: <http://mouse.brain-map.org/>.

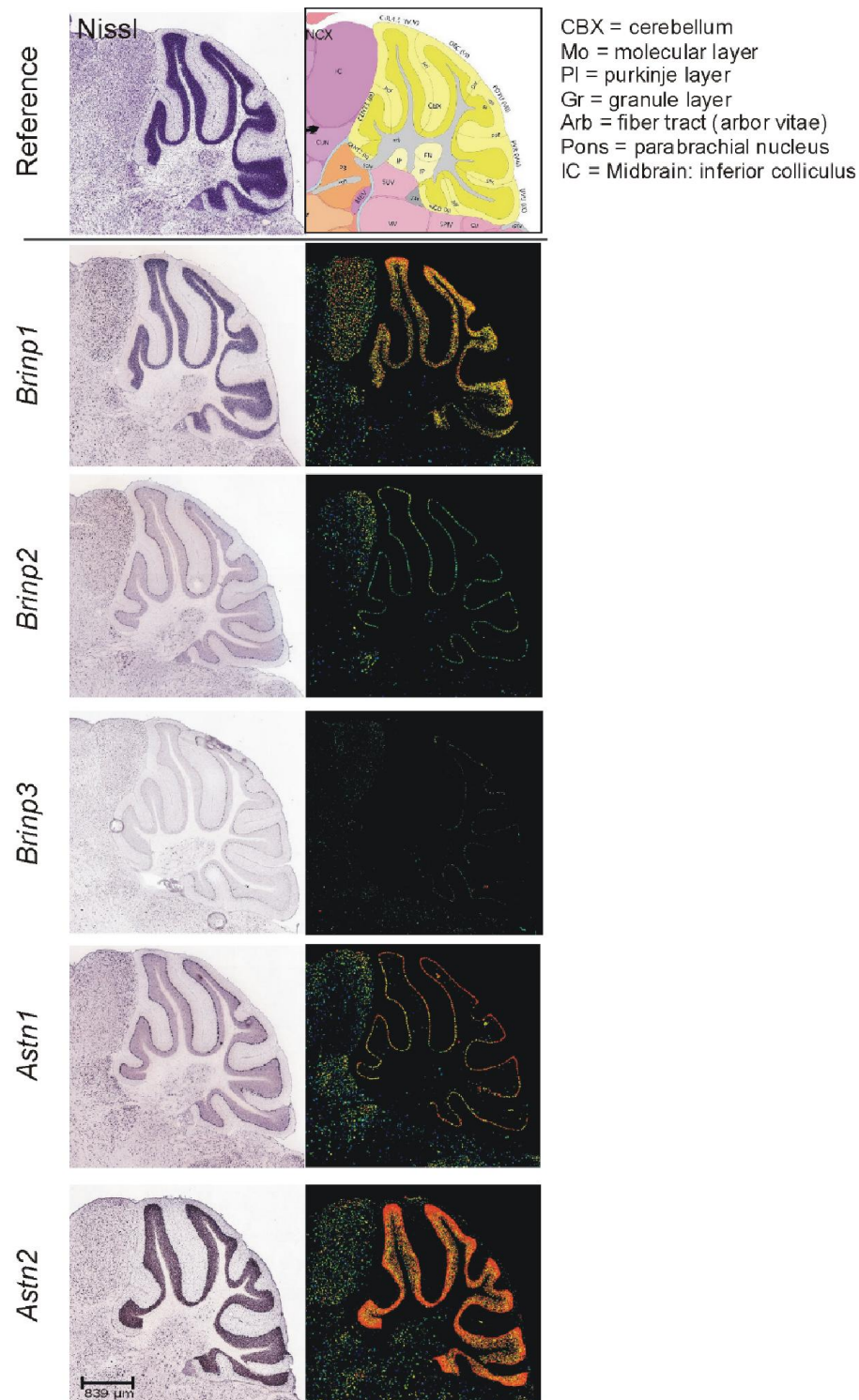


Figure 4-16 – A comparison of *Brinp1*, *Brinp2*, *Brinp3*, *Astn1* and *Astn2* mRNA distribution in the adult C57BL/6 cerebellum at 8 weeks

The top panels provide a reference of cerebellum anatomy. The left column shows *in-situ* hybridization of the sagittal cerebellum. Positive gene expression is shown in purple. In the right column, relative expression levels are represented as an expression map. From high to low expression: Red = +++, Yellow = ++, Green = ++, Blue = +, Black = -. Expression data compiled from resources by the Allen Mouse Brain Atlas: <http://mouse.brain-map.org/>.

Table 4-8 - Neuronal-MACPF expression summaryCompiled from *in-situ* hybridization data by the Allen Mouse Brain Atlas.

++++ = very high, +++ = high, ++ = medium, + = low

Tissue	<i>Astn1</i>	<i>Astn2</i>	<i>Brinp1</i>	<i>Brinp2</i>	<i>Brinp3</i>
Olfactory Bulb					
Glomerular layer	++	++++	++++	-	+
Mitral cell layer	++++	++++	++++	++	-
Granule cell layer	++	++	++	++	-
Anterior Olfactory	+++	+++	+++	+++	++
Neocortex					
Layers II / III	++++	-	++++	+++	+
Layer IV	+++	+++	+++	+	-
Layers V-VI	+++	+++	+++	++	+
Hippocampus					
CA1	++++	++++	++++	+++	-
CA2	++++	+	++++	++++	-
CA3	++++	+	++++	++++	-
Dentate gyrus	+++	+	++++	-	-
Cerebellum					
Purkinje cells	++++	++++	+++	+++	++
Granule cells	-	++++	+++	-	-
Subcortical					
Striatum	+	+	+++	-	-
Thalamus	+	++	+++	++	-
Hypothalamus	++	+	++	-	-
Amygdala					
Lateral Amygdala	++++	++	+++	++	++
Basolateral Amygdala	+++	++	++	++	+
Posterior Amygdala	+++	++	++	++	+
Midbrain					
Superior colliculus	+	++	++	-	-
Inferior colliculus	+	++	+++	+	-
Brainstem					
Pons	+	++	++	-	-
Medulla oblongata	+	++	++	+	-

All five neuronal-MACPF genes are expressed in neuron-enriched regions, as demonstrated by the overlap with neuron-specific Nissl staining. In the adult mouse olfactory bulb (Figure 4-14), *Brinp3* shows minimal expression. *Brinp1*, *Brinp2*, *Astn1* and *Astn2* are highly expressed in the mitral cell layer and the granule cell layer. *Brinp2* is notably absent from the glomerular layer, whilst *Brinp1*, *Astn1* and *Astn2* are highly expressed in this layer.

In the adult mouse hippocampus (Figure 4-15), *Brinp3* is not expressed. *Brinp1*, *Brinp2*, *Astn1* and *Astn2* are highly expressed in the pyramidal layer of the CA1 region. *Brinp1*, *Brinp2* and *Astn1* are also highly expressed in the CA2 and CA3 pyramidal layers, whilst *Astn2* levels are low in these regions. In the granule cell layer of the dentate gyrus, only *Astn1* and *Brinp1* are highly expressed, with only minimal expression of *Astn2*.

In the adult mouse neocortex (Figure 4-15), *Brinp3* shows only minimal expression. *Brinp1*, *Brinp2*, *Astn1* are highly expressed in upper layers (II/III) of the neocortex. *Astn2* is not expressed in this layer. *Brinp1*, *Astn1* and *Astn2* are expressed highly in layer V, whereas *Brinp2* shows minimal expression. *Brinp1*, *Brinp2*, *Astn1* and *Astn2* are all expressed in lower layers of the cortex (V-VI).

In the adult mouse cerebellum (Figure 4-16), *Astn2* and *Brinp1* are highly expressed in the granule cell layer and Purkinje cell layer. *Astn1*, *Brinp2* and *Brinp3* expression is restricted to the Purkinje cell layer only.

From this analysis, the following patterns of expression emerged:

- *Brinp1* is expressed in almost all neural tissue, and is the most widely expressed of the five neuronal-MACPF genes
- *Astn1* is expressed in almost all neural tissue, with the exception of the granule cell layer of the cerebellum
- *Astn2* and *Brinp2* are expressed in restricted regions of the adult mouse brain
- *Brinp2* is always expressed at the same cellular layers as *Astn1* and *Brinp1*
- *Brinp3* is always expressed in the presence of the other four neuronal MACPFs
- *Brinp1* is expressed alone in some regions lacking *Brinp2* and *Brinp3*
- *Astn1* and *Astn2* are not always expressed in the same brain regions
- *Astn2* is the most highly expressed in the cerebellum of the five neuronal MACPFs

The combinations of co-expression of neuronal MACPF genes present in the highly expressed regions of the adult mouse brain are illustrated in Figure 4-17. Overall, expression data demonstrates that whilst there is a high degree of overlap in expression in the five neuronal-MACPF genes, no two neuronal MACPF genes show identical expression profiles. Regional divergence between expression could indicate specialized functions in these brain areas.




















<i>Brinp1</i>	<i>Brinp2</i>	<i>Brinp3</i>	<i>Astn1</i>	<i>Astn2</i>	Regions with neuronal-MACPF expression in the adult mouse brain
					Granule layer: cerebellum
					Purkinje layer: cerebellum, Anterior olfactory bulb
					CA1: hippocampus Layers V / VI: Neocortex Mitral layer: olfactory bulb Granule layer: olfactory bulb
					CA2: hippocampus CA3: hippocampus Layers II/III: neocortex
					Dentate gyrus: hippocampus
					Glomerular layer: olfactory bulb Layers IV : neocortex

Figure 4-17 – Combinations of neuronal-MACPF co-expression in the adult mouse brain

Neuronal-expression patterns were analyzed from Allen Mouse Brain Atlas data. There are six different combinations of neuronal-MACPF gene expression in the adult mouse brain.

Each row represents combinations of neuronal-MACPF expression. Regions where these combinations were found are listed in the column on the right. Subcortical regions are not included in this analysis due to relatively broad and diffuse expression of neuronal-MACPFs in these areas.

4.5.2 Alterations in expression of neuronal-MACPFs in the *Brinp1* KO mouse brain

Quantitative PCR was performed on mRNA from the brains of *Brinp1* KO mice to assess whether homologous MACPF family members show changes in expression levels in response to the deletion of *Brinp1*.

Primers for each of the five neuronal MACPF genes were first validated to confirm the size and specificity (Figure 4-18A). All primer pairs amplified the correct gene, as shown by the expected PCR product size, with no additional species amplified and no species present for the minus reverse transcriptase or water control lanes.

Late embryonic brains (E18.5) showed a two-fold increase both *Astn1* and *Astn2* mRNA (Figure 4-18B). *Brinp1* mRNA (non-functional) also increased by 1.5 fold. No significant changes to the levels of *Brinp2* or *Brinp3* mRNA were evident at this developmental time point.

At 6 weeks of age, *Brinp1* KO mice showed a three-fold increase in *Astn1* mRNA and a two-fold increase in *Astn2* mRNA in the hippocampus (Figure 4-18C). *Brinp2* mRNA increased in four of the 6 mice ($p=0.08$). Down-regulation of both *Brinp1* and *Brinp2* mRNA was detected in the adult cortex, with no significant change in expression of either Astrotactin mRNA (Figure 4-18D). Normalization with both GAPDH and β -actin gave similar results.

These results demonstrate that *Astn1* and *Astn2* are upregulated in certain spatial and temporal points in the *Brinp1* KO mouse brain, which suggests that a mechanism of gene compensation between Astrotactins and *Brinp1* occurs.

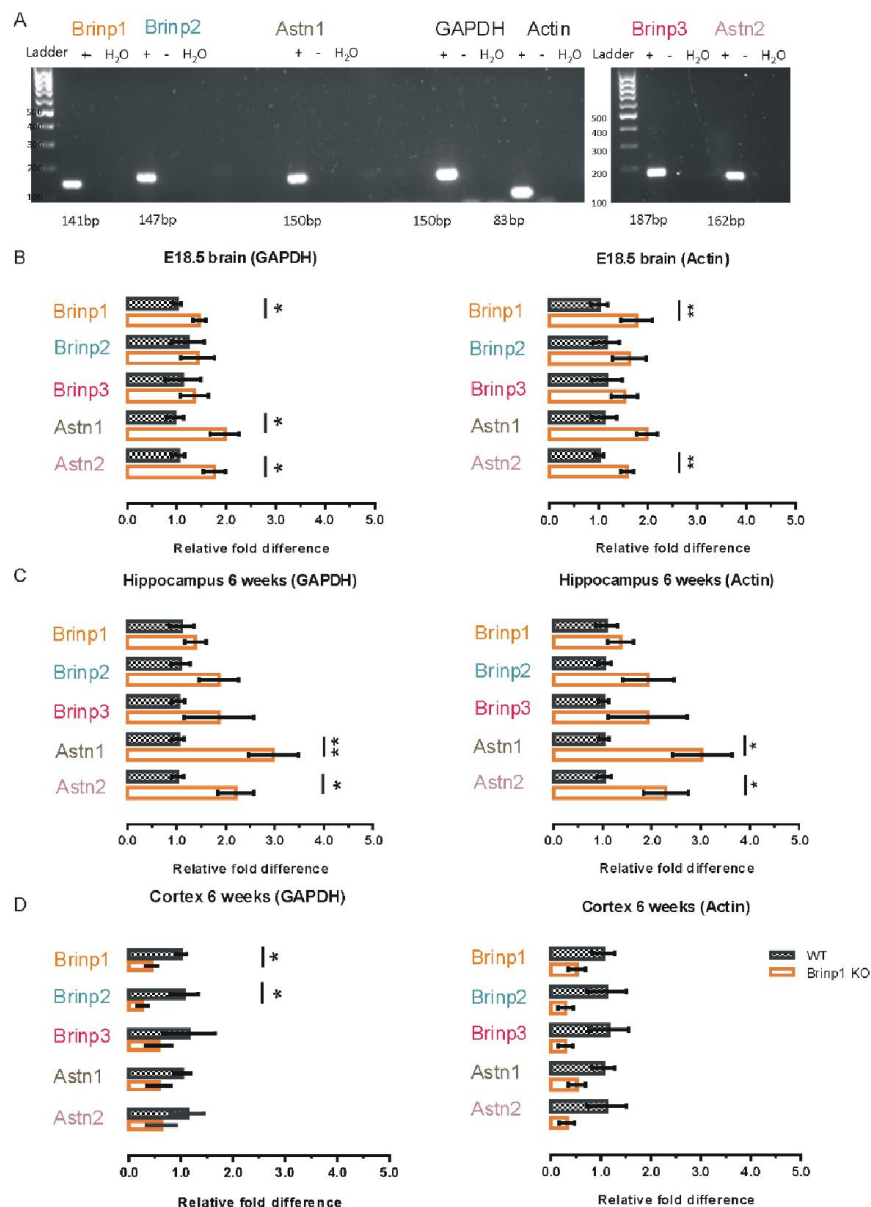


Figure 4-18 – Up-regulation of *Astn1* and *Astn2* mRNA in the embryonic brain and adult hippocampus of *Brinp1* KO mice

- A) Validation of qPCR primers on cDNA (derived WT mouse brain RNA) showing single PCR products of predicted size. No PCR products were amplified in the cDNA- or water control.
- B) An increase in *Astn1* and *Astn2* gene expression in the developing (E18.5) mouse brain.
- C) An increase in *Astn1* and *Astn2* expression was also detectable in the hippocampus at 6 weeks of the *Brinp1* KO mice.
- D) In the 6 week old *Brinp1* KO cortex, less *Brinp1* (non-functional) and *Brinp2* mRNA was detected, with no significant change in expression of either *Astn1* or *Astn2*.

N= 3 WT, 4 *Brinp1* KO, * $p < 0.05$, ** $p < 0.01$, unpaired Student's t-test. Normalization against GAPDH expression levels. All data represented as the mean \pm SD.

4.6 Chapter 4: Discussion

4.6.1 *Brinp2/3* KO mice do not exhibit an enhanced phenotype of *Brinp2* or *Brinp3* KO mice

The phenotype of *Brinp2/3* KO mice shows a high degree of similarity to that of the *Brinp3* single KO. The weight profile is almost identical, as is the hyper-exploratory phenotype detected on the elevated plus maze evident again for the *Brinp2/3* double KO mouse. The only notable difference in behavior between the *Brinp2/3* KO mice and the *Brinp3* KO mice was on the third trial of the three chamber social interaction test, where *Brinp2/3* mice show a decrease in time spent interacting with the familiar mouse. However, this result is difficult to interpret as the WT mice also did not perform as expected for this trial, with no significant between novel and familiar mouse in trial 3.

Also notable from the *Brinp2/3* KO behavioral testing was the reduced rearing behavior. This result may be due to the absence of *Brinp2* or *Brinp3* alone, as rearing behavior was not tested for the single knockout lines. A second cohort of both *Brinp2* KO and *Brinp3* KO mice would be needed to determine which of the two genes the decreased rearing phenotype can be attributed to.

The improved performance on the Rotarod reported for the *Brinp2* KO mice in chapter 3 were not evident for the *Brinp2/3* KO mice. There are two possible explanations for the non-reproducible phenotype: 1) the improved result of the *Brinp2* KO mice were due to chance or 2) the deletion of *Brinp3* reverses the effect of the absence of *Brinp2*. Given that the Rotarod performance was normal for *Brinp3* KO mice, the first explanation seems more likely.

Overall, *Brinp2/3* double mutation did not lead to an enhancement of the phenotype, but rather appears to reflect additive phenotype profiles of *Brinp2* and *Brinp3* KO mice. This implies that the relationship between *Brinp2* and *Brinp3* is either that the two genes do not compensate for each other in the *Brinp2* and *Brinp3* KO mice, or there is an additional level of redundancy with other genes. The AMBA expression data supports the conclusion that *Brinp2* and *Brinp3* are not able to compensate for each other's absence due to the very limited overlap in regional expression of the two gene in the adult mouse brain.

4.6.2 *Brinp1/2/3* KO mice have poor viability, decreased body weight, with no gross anatomical abnormalities

The viability (although compromised) of some adult *Brinp1/2/3* triple KO mice indicates that *Brinps* are not essential for survival in the mammalian system. Furthermore, the absence of all three *Brinps* results in an ostensibly normal, but significantly smaller mouse, with normal morphology of all neural and non-neural tissue, implying that *Brinps* are not essential for organogenesis or neurogenesis. The normal gross anatomy of the *Brinp1/2/3* mice is surprising given the high expression of *Brinps* in overlapping regions during murine neural development (Kawano et al., 2004). Even in the absence of all three proteins, mice were able to develop with little difference in overall gross anatomy. By H&E and Nissl staining, the brains of *Brinp1/2/3* mice did not show hippocampal fractured layers like that of the *Tuba1a* mutant mice (Keays et al., 2007). They also do not exhibit any gross malformations in cortical lamination of the cerebral or cerebellar cortices, as observed for *Reeler* mutants or *Cdk5* KO mice (Katsuyama & Terashima, 2009; Ohshima et al., 2007). In addition, *Brinp1/2/3* KO mice do not show increase in neuronal layer thickness, similar to phenotypes reported for *Cyclin-dependent kinase inhibitor 1B (p27kip)* KO mice (Geng et al., 2001), which would be predicted if *Brinps* are required to moderate G1/S phase cell cycle progression, as suggested by Terashima et. al (Terashima et al., 2010). The histopathological analysis therefore did not provide any evidence to indicate a role for *Brinps* in the developing brain.

As with the single KO mice, the absence of a histological phenotype allows for three possible explanations: 1) All three *Brinps* do not have a role in development, 2) a phenotype does exist, but it is not detectable at this level of analysis, or 3) the phenotypic effect of removing *Brinps* is masked by compensation of one or more additional genes. A greater level of histopathological analysis, using layer specific markers, is needed to determine whether *Brinp1/2/3* triple KO mice have altered neural architecture. Also, investigation of embryonic *Brinp1/2/3* triple KO mice would be required to assess for a developmental phenotype that may explain the poor viability. Furthermore, examining triple KO mice as aged mice would be required for the detection of possible tumors or neuronal degeneration.

Whilst inflammation detected in both knockout animals, this sort of inflammation is deemed relatively common by pathologists. More *Brinp1/2/3* KO mice would need to be examined to determine whether these mice are immuno-compromised. Given the canonical role of MACPF

proteins in immunity, the cause of such inflammation may be worthy of further investigation. It is possible that inflammation reported in the heart of one of the triple KO mice may be of relevance to a potential link between *Brinp2* and *Brinp3* and coronary heart disease in humans (Angelakopoulou et al., 2012; Connelly et al., 2008).

The reduction in body weight of *Brinp1/2/3* KO mice may reflect the observed phenotype of *Brinp1* KO mice. Male *Brinp1/2/3* KO mice especially are significantly smaller from even the *Brinp1* KO mice. This may be the additive effect of the reduced body weight of *Brinp1* and *Brinp2* KO mice, both of which weigh less than WT as adults. Alternatively, the loss of all three *Brinps* may be enhancing the phenotype for male mice.

By histopathological analysis, the *Brinp1/2/3* KO reproductive systems were normal for both males and females. There is also evidence that female triple KO mice are able to carry a litter to term. These observations combined suggest that the inability of knockout mice to breed is either related to impaired social behavior, or another factor not detectable by tissue analysis. The poor survival of litters from *Brinp1/2/3* heterozygous breeders may also be related to the absence of *Brinp1*, but the absence of *Brinp2* and *Brinp3* may also be contributing. These are initial observations, and a greater number of male triple KO mice would need to be generated to determine if all male knockout mice are infertile.

It was also intended to test triple KO mice for behavior, but this was not possible due to low numbers. If a triple KO mouse cohort could be generated, this would help to explain poor viability and determine whether there are enhancements of behavioral phenotypes. A suggested next step would be to generate both *Brinp1/2* double KO or *Brinp1/3* double KO mice and generate behavioral cohorts from these KO mice instead.

4.6.3 *Brinps* and Astrotactins are co-expressed in neuron-specific regions

The mRNA distribution of *Brinps* and Astrotactins in the adult mouse brain provide potential clues of function of each of the neuronal-MACPFs. *Brinps* and *Astrotactins* are each neuron-enriched genes. Cell type specific genes have been demonstrated to correspond with specific molecular functions in the mammalian brain (Lein et al., 2007). In the case of neuron enriched genes, the following functions are most commonly reported: synaptic transmission, nervous system development, neuron differentiation, regulation of synaptic plasticity, structure or

function (Lein et al., 2007). The neuronal localization of *Brinps* indicates that their role is likely to lie within one of these functions.

The Allen Mouse Brain Atlas (AMBA) expression data for Astrotactins and *Brinps*, in part agrees with the journal publications by Kawano et al (*Brinps*) and Wilson et al (Astrotactins), with some notable differences (Kawano et al., 2004; Wilson et al., 2010). The AMBA data shows broader expression of *Astn2* in multiple brain regions, including high expression in the cerebral cortex and CA1 region of the hippocampus, whilst in the publication by Wilson et al, *Astn2* it is almost exclusively expressed in the cerebellum and olfactory bulb. *Brinp2* is also shown to be more widely expressed in the AMBA data. Also, whilst *Brinp3* is highly expressed in the cerebellum in Kawano publication, *Brinp3* shows virtually no cerebellum expression in AMBA data. A possible explanation for the discrepancies is the use of probes targeting different regions of the same gene. It is possible that different isoforms may be detected due to alternative splicing.

The data sets do agree on overall expression trends. *Brinp1* and *Astn1* are the most widely expressed of the five genes in adult mouse brain. *Astn2* is highly expressed in the adult cerebellum and regions of the olfactory bulb. *Brinp2* and *Brinp3* are also expressed highly in the cerebellum and olfactory postnatally, but are not exclusive to these regions. The data also indicates that there is some regional separation between the neuronal – MACPF genes, possibly due to diversification in cell types in which they function.

An interesting finding from the analysis of neuronal-MACPF expression is the absence of *Astn1* expression from the granule layer of the adult mouse cerebellum, in contrast to the high expression of *Astn2* in this cell layer. Wilson et al, show *Astn1* to be expressed in the granule layer during cerebellar development (postnatal day 6) (Wilson et al., 2010). The AMBA data demonstrates that *Astn1* expression ceases once cerebellar granule cell migration ends, whilst *Astn2* continues to remain expressed.

The AMBA data also shows *Astn1* expression to be high in the adult mouse brain in several cortical regions, despite current understanding of *Astn1* function in facilitating neuronal migration along glial fibers at developmental stages. Since such fibers are no longer present in the adult brain, and neuronal migration virtually ceases after infancy, the high expression

of *Astn1* at p56 suggests a secondary function. This may be in forming part of an adhesion system with additional cell types, or another, yet to be determined function.

Certain questions arise from the observed differences in expression between the neuronal-MACPF genes. For example, why is *Astn2* heavily implicated in neural developmental disorders (i.e. ASD and ADHD) whilst the remaining neuronal MACPF genes show only low associations, despite *Brinp1* and *Astn1* showing broader neurological expression? The answer may reflect the specific function of *Astn2*. For example, if, as proposed by Wilson et al, 2010, *Astn2* is a mediator of neuronal migration, multiple proteins may be dependent on *Astn2* for trafficking and proper function, thus leading to a greater disease severity when disrupted. This idea is supported by a bio-informatics study of AMBA expression data, demonstrating that Autism-linked genes are significantly enriched in certain brain regions in mice, with a specific mention of *Astn2* as highly co-expressed with other ASD-linked genes (Menashe et al., 2013). This suggests that mutations in *Astn2* may have a downstream effect on multiple genes in the human brain that could lead to an ASD pathology.

4.6.3.1 Astrotactins are upregulated in the *Brinp1* KO mouse brain.

The co-expression of *Brinp1* and both *Astn1* and *Astn2* in the same cell types could indicate involvement in the same process. The increase of *Astn1* and *Astn2* in the embryonic brain (E18.5) and hippocampus of *Brinp1* KO mice suggests that Astrotactins and *Brinp1* may have a common mechanism, such that *Astn1* and *Astn2* functionally compensate for the absence of *Brinp1* during neuronal migration.

The increase in *Astn1* and *Astn2* in the *Brinp1* KO mouse brain may explain why there is no gross morphological phenotype in the triple KO mouse brain, if Astrotactins are able to compensate for function in their absence. If either Astrotactins are able to in-part or fully perform the role of *Brinps* during the development, this would again mask the effect of *Brinp* deletion.

The development of an *Astn1/Brinp1* KO mouse is suggested as a next step to test for an enhanced phenotype that would indicate that the two genes compensate for each other in the single knockout mice. An *Astn2/Brinp1* KO mouse would be difficult to generate through conventional gene targeting methods due to the very short distance between the two genes. However, the new CRISPR-Cas technology allows simultaneous mutations in the same animal

(Sander & Joung, 2014). A further step to confirm compensation between *Brinps* and Astrotactins would be to examine whether *Brinp1* is able to compensate for the absence of one or both of the other Astrotactins. Quantitative PCR analysis on *Brinp1* cDNA from *Astn1* or *Astn2* KO mouse brains would determine whether this is the case.

Lastly, whilst there is co-expression between all neuronal MACPF genes, there is also a clear distinction in regions where *Brinps* and Astrotactins are not expressed, which may allude to specialized function in particular cell types. For example, the expression distribution of *Brinp1* and *Astn2* looks identical in the granule cells of the cerebellum and glomerular layer and mitral cell layer of the olfactory bulb, whilst *Astn2*, unlike *Brinp1* shows only low expression in layers II/III of the neocortex, and CA2, CA3 and the DG of the hippocampus. This suggests that any compensation between Astrotactins and *Brinp1* would likely be region specific.

Chapter 5: In-depth characterization of *Brinp1* KO mice

5.1 Chapter 5 Overview

This final results chapter focuses on the role of *Brinp1* in neurobiology by further characterizing the *Brinp1* KO behavioral phenotype, and exploring changes in the neural architecture of the *Brinp1* KO mouse brain.

Monash University allows incorporation of published papers or manuscripts into PhD theses. Accordingly, the chapter is presented in manuscript format: 'The study of *Brinp1* KO mice reveals an ASD-like phenotype and hyperactivity, underpinned by changes in cortical lamination'. The manuscript necessarily includes some data from chapters 3 and 4, whilst the majority of the data arise from detailed characterization of the *Brinp1* KO mouse phenotype. Instances where data has been repeated from previous chapter are indicated by a hashtag (#) in the figure legend. This chapter includes further behavioral assays used for the testing of the *Brinp1* KO mice. In addition, key changes in the *Brinp1* KO mouse neocortex and hippocampus are identified that may underpin the behavioral phenotype. The paper is formatted for the journal of Molecular Autism and is currently under review.

5.2 The study of *Brinp1* KO mice reveals an ASD-like phenotype and hyperactivity, underpinned by changes in cortical lamination

5.2.1 Author names and affiliations

Susan R. Berkowicz¹, Travis J. Featherby³, Zhengdong Qu², Aminah Giousoh¹, Natalie A. Borg¹, Julian I. Heng², James C. Whisstock^{1,4}, Phillip I. Bird¹.

1. Department of Biochemistry and Molecular Biology, Monash University, Australia, 3800
2. Australian Regenerative Medicine Institute, Monash University, Australia, 3800
3. The Florey Institute of Neuroscience and Mental Health Australia, 3052
4. Australian Research Council Centre of Excellence in Advanced Molecular Imaging, Monash University, Australia, 3800

5.2.2 Corresponding authors

Professor Phillip I. Bird and Professor James C. Whisstock

5.2.3 Conflict of interest

The authors declare no competing financial interests

5.3 Acknowledgements

We thank Drs Jeanette Rientjes, Arianna Nenci and Jose Gonzalez (Monash Gene Targeting Facility) for contract production of the *Brinp1*^{tm1/Pib} mice. Behavioral testing was carried out by Travis Featherby and Brett Purcell, Neuroscience Research Services. Thank you to Dr. Emma Burrows and Professor Anthony Hannan for advice on behavioral experiments and Dr. Matilda Haas for providing feedback on the manuscript. Thank you to Luke Cossins and the Western Australia Institute of Medical Research Antibody Facility, Perth for assistance with BRINP1 antibody generation. Necroscopies were performed by the Australian Phenomics Network (APN). Monash Micro Imaging Facility provided instrumentation and training for confocal imaging. JCW and PIB groups were funded by NHMRC Program grant 490900. JCW is a National Health and Medical Research Council of Australia Senior Principal Research Fellow. JCW also acknowledges the support of an Australian Research Council Federation Fellowship.

5.4 Abstract

Background: Bone morphogenetic protein / retinoic acid inducible neural-specific protein 1 (*Brinp1*) is highly conserved and continuously expressed in the neocortex, hippocampus, olfactory bulb and cerebellum from mid-embryonic development through to adulthood. *Brinp1* is found at chromosome locus 9q33.1 in humans, at a region of DNA that has frequently been connected to neurodevelopmental disorders in genome-wide association studies.

Methods: *Brinp1* knockout (*Brinp1* KO) mice were generated by Cre-recombinase mediated removal of the 3rd exon of *Brinp1*. Knockout mice were characterized by behavioral phenotyping, and immunohistochemistry analysis of the developing and adult brain.

Results: Absence of *Brinp1* during development results in a behavioral phenotype resembling autism spectrum disorder (ASD), in which knockout mice show reduced sociability and changes in vocalization capacity. In addition, *Brinp1* KO mice are hyperactive, have impaired short-term memory, and exhibit poor reproductive success. *Brinp1* KO mice exhibit a reduced density of pyramidal neurons in layer IV of the neocortex, and increased density of parvalbumin-expressing interneurons, but show no signs of impaired neural precursor proliferation or increased apoptosis during brain development. The expression of the related neuronal migration genes *Astn1* and *Astn2* is increased in the brains of *Brinp1* KO mice, suggesting that they may ameliorate the effects of *Brinp1* loss.

Conclusions: *Brinp1* plays an important role in normal brain development and function by influencing neuronal positioning within the cortex. The perturbed cortical lamination and altered behavior of *Brinp1* KO mice resemble features of a subset of human neurological disorders namely autism spectrum disorder (ASD) and the hyperactivity aspect of attention deficit hyperactivity disorder (ADHD).

Key words: *Brinp1*; knockout; cortex; parvalbumin; autism spectrum disorder, hyperactivity.

5.5 Background

Many neurodevelopmental disorders (NDDs) result from rare genetic alterations including copy number variants (CNVs), single nucleotide polymorphisms (SNPs) and *de novo* mutations in genes affecting a variety of cellular processes (Iossifov et al., 2014; Sebat et al., 2007; Weiss, 2009). Autism is a NDD that affects an estimated 0.6% of children (Folstein & Rosen-Sheidley,

2001; Fombonne, 2005), with similar prevalence in adults (Brugha et al., 2011). Clinical diagnosis is based on atypical social behavior, impairments in verbal and non-verbal communication, and patterns of restricted interests and repetitive behaviors (First & APA, 2013). Autism patients commonly have moderate to severe impairments in expressive language (McGonigle-Chalmers et al., 2013; Tek et al., 2014). Autism also frequently occurs with at least one other NDD, for example attention deficit hyperactivity disorder (ADHD), anxiety disorder, and intellectual disability (Rybakowski et al., 2014; Tureck et al., 2014). Notably, 28% of patients diagnosed with autism also present with ADHD, diagnosed in childhood by inattention, hyperactivity and impulsivity (Simonoff et al., 2008) (First & APA, 2013).

Members of the Membrane Attack Complex/Perforin domain (MACPF) protein superfamily share a domain that facilitates oligomerisation and membrane association (Kondos et al., 2010; Rosado et al., 2008). Bone morphogenetic protein / retinoic acid inducible neural-specific protein 1 (BRINP1) is one of five MACPF members expressed in the nervous system. The 85kDa BRINP1 protein is over 50% identical to two other MACPF proteins, BRINP2 and BRINP3, and all three are expressed in an overlapping pattern in neurons in the developing and mature brain (Kawano et al., 2004). Roles for *Brinp1* have been suggested in hippocampal neurogenesis in mice (Kobayashi et al., 2014), and neural plasticity of song learning in birds (Lovell et al., 2008; Wood et al., 2008).

Brinps also share homology with Astrotactin1 (*Astn1*) and Astrotactin2 (*Astn2*), two neural proteins that facilitate glial-guided neuronal migration (Adams et al., 2002; Wilson et al., 2010). In humans, *BRINP1* and *ASTN2* are situated at a common locus on chromosome 9q33.1, while *BRINP2*, *BRINP3* and *ASTN1* are linked on chromosome 1. The *BRINP1/ASTN2* locus contains a high number of brain-specific genes (Jeffrey D. Falk, 1995), and patients with interstitial deletions of the locus show postnatal growth delay and broad neurological dysfunction (Chien et al., 2010; Gamerdinger et al., 2008; Kulharya et al., 2008). This locus has also been frequently connected to neurological disorders in genome-wide association studies (Heinzen et al., 2010; Romanos et al., 2008; Wang et al., 2010). *ASTN2* has been identified as a risk gene in both autism and ADHD (Glessner et al., 2009; Lionel et al., 2011; Lionel et al., 2014). Recently, Lionel et al. recently reported 58 mutations at the 9q33.1 loci associated with a NDD diagnosis. Whilst 46 sequenced CNVs involved *ASTN2/TRIM32* only, seven NDD

patients had CNVs that covered part or all of *BRINP1* (Lionel et al., 2014). Such findings suggest that alterations to *BRINP1* function may contribute to NDD.

To investigate the role of *BRINP1* in brain development and cognitive function, we generated *Brinp1* LoxP / Cre-recombinase conditional knockout mice. Mice lacking *Brinp1* exhibit altered lamination of the neocortex, and behavioral traits reminiscent of ASD.

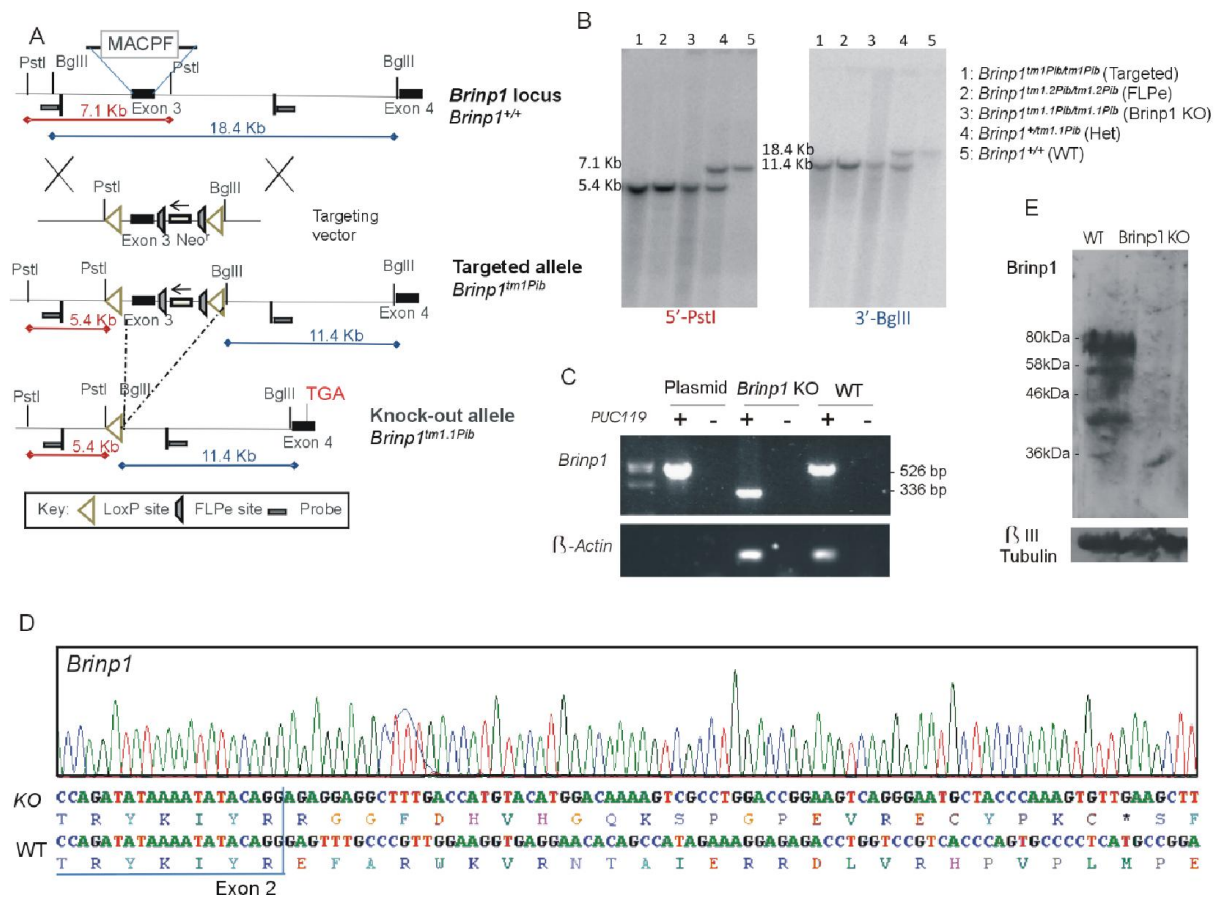
5.6 Materials and methods

See thesis Chapter 2: Materials and methods

5.7 Results

5.7.1 Generation of *Brinp1* knockout mice

A conditional *Brinp1* targeted allele (*Brinp1*^{tm1/Pib}) was designed to allow Cre-recombinase-mediated, tissue-specific deletion of *Brinp1* (Figure 5-1A). In the first instance, mice lacking *Brinp1* in all tissues were generated by breeding animals carrying the targeted allele with animals expressing Cre-recombinase from the two-cell embryonic stage onwards (global Cre-deleter). Progeny exhibiting deletion of the selection cassette and third exon of *Brinp1* (*Brinp1*^{tm1.1/Pib}) were inter-bred to generate homozygous *Brinp1*^{tm1.1Pib/tm1.1Pib} (*Brinp1* KO) animals and WT littermates. Correct targeting and deletion of exon 3 was confirmed by Southern analysis (Figure 5-1B), RT-PCR (Figure 5-1C) and DNA sequencing of RT-PCR products (Figure 5-1D). This shows that deletion of exon 3 forces splicing between the intron 2 donor and intron 4 acceptors, fusing exons 2 and 4, and changing the reading frame to introduce a truncating stop codon. Absence of BRINP1 protein was confirmed by immunoblotting (Figure 5-1E).

Figure 5-1 – *Brinp1* targeting

- A) The *Brinp1* targeting vector was designed with a Neomycin resistance cassette after exon 3, and FRT sites positioned before and after the Neo^r Cassette. The 190 bp 3rd exon of *Brinp1* contains the start of the MACPF domain. LoxP sites flank exon 3 and the Neo^r cassette. When crossed with a mouse line expressing Cre-recombinase, the recombination of LoxP sites resulted in the deletion of exon 3 and the Neo^r cassette.
- B) Genomic DNA isolated from the spleen was cleaved with PstI and Bgl II and hybridized to 500 bp genomic DNA probes from the 5' region (Pst I) and 3' region (Bgl II) of the targeting construct. In wild-type DNA, species of 7.1 kb (Pst I) and 18.4 kb (Bgl II) were detected. These products were not present in DNA from *Brinp1* KO mutants, replaced with shorter species of 5.4kb (PstI) and 11.4kb (BglII).
- C) cDNA from the brain tissue of WT or *Brinp1* KO mice was tested for exon 3 deletion by RT-PCR. Primers designed to regions of exon 2 and exon 6 resulted in a PCR product size corresponding to the removal of the 190bp exon 3 for *Brinp1* KO cDNA.
- D) Sequencing of the *Brinp1* KO allele RT-PCR product showed the expected absence of exon 3, and that splicing fuses exons 2 and 4, resulting in a frame shift that introduces a stop codon after 24 residues.
- E) By immuno-blotting, full-length 85 kDa BRINP1 was present in lysates of mouse brains at postnatal day 12, and absent in *Brinp1* KO mice.

5.7.2 *Brinp1* KO mice exhibit decreased postnatal survival and a reduced body weight.

Brinp1 KO mice born from heterozygous breeders were not observed at the expected Mendelian frequency. Only 10 out of 75 (13%) of surviving pups were *Brinp1* KO, indicating that half of the *Brinp1* KO mice died *in utero* or did not survive to weaning. Analysis of 18 full term embryos showed that *Brinp1* KO fetuses were present at expected frequencies (6 out of 18, 33%). We therefore conclude that *Brinp1* KO mice have impaired postnatal viability.

To investigate the reduced survival of *Brinp1* KO mice, the fecundity of WT x WT, het x het, *Brinp1* KO x *Brinp1* KO and WT x *Brinp1* KO breeding pairs was compared (Table 5-1). Litter numbers at birth were normal for all breeder genotypes, with no delay in first breeding or time between litters. However, post-partum survival of progeny of *Brinp1* KO x *Brinp1* KO breeders was significantly reduced, with an average of only one mouse surviving per litter after 3 days. Litter survival from het x het breeders was also reduced (average of four mice surviving per litter). Specifically, only 19 / 98 (22%) of all pups born to *Brinp1* KO x *Brinp1* KO parents, and 75% born to het x het parents, survived longer than 3 days. This was in contrast to a 91% survival rate of progeny from WT x WT breeders.

Table 5-1 - Reproductive Phenotyping #

	Male/Female			
	WT / WT	Het / Het	<i>Brinp1</i> KO / <i>Brinp1</i> KO	WT ♂/ <i>Brinp1</i> KO ♀
Days from mating to first litter	25.8	22.8	25.0	24
Days between litters	26.7	22.1	27.6	27.4
Number of litters	19	22	20	20
Number of pups born (P0)	116	100	98	96
Number of pups weaned (P21)****	105	75	19	50
% survival	91%	75%	22%	52%

Four breeders per genotype (WT/WT, Het/Het, *Brinp1* KO /*Brinp1* KO and WT ♂/*Brinp1* KO♀) were monitored over four months to investigate reproductive rates and postnatal survival. The survival of mice to age of weaning (P21) was significantly impacted by the presence of *Brinp1*-deleted allele:

**** χ^2 (3, n=249) = 63.80, $p < 0.0001$; Chi-square test.

Identical data to previously reported in chapter 3.

The offspring of *Brinp1* KO x *Brinp1* KO parents were observed post-partum. Although several pups survived birth, most were found dead 12-48 hr later. Little to no milk was present in the stomach of the animals found dead, indicating lack of adequate nutrition as a possible cause of death. Taken together, these results suggest that absence of *Brinp1* is detrimental to survival. A suggested reason for this may be that mothers lacking *Brinp1* are deficient in postnatal care of their offspring, resulting in neonatal death. The higher pup survival rate when a *Brinp1* KO female was mated with a WT male indicates that *Brinp1* in the pup also contributes to postnatal survival.

Nesting behavior of *Brinp1* KO mice was investigated to determine whether improper nest construction was a contributing factor of decreased survival of homozygous pups. Pairs of unmated adult female mice (n=5 pairs) were assessed for nest construction (Supplementary Figure 5-13). Nest construction was scored at day 1 and day 2, using the scoring criteria described by Hess et al, 2008. *Brinp1* KO mice showed no significant differences compared to WT mice in ability to construct appropriate nests from the nesting material provided. This result indicates that nest construction is not a factor affecting *Brinp1* KO pup survival.

Weekly weighing of pups from heterozygous parents revealed that *Brinp1* KO mice have impaired postnatal growth. These mice exhibited a significant delay in weight gain from age of first weighing (week 3) until adulthood in both male and females. Heterozygous females showed delayed weight gain close to that of *Brinp1* KO mice, whereas heterozygous male mice were smaller as juveniles, but their weight recovered close to WT (Figure 5-2B). Despite a 10% reduction in adult body weight, *Brinp1* KO mice had normal body length and normal brain size (Supplementary Figure 5.11).

A full pathological examination of mice at embryonic day 18.5 (E18.5) and seven week old (P49) *Brinp1* KO mice showed normal organ development (25 organs examined) including normal structures in the brain and spinal cord. Embryos were of a normal size and showed no developmental defects. Adult brains appeared symmetrical, with normal myelination and no ventricular dilation observed.

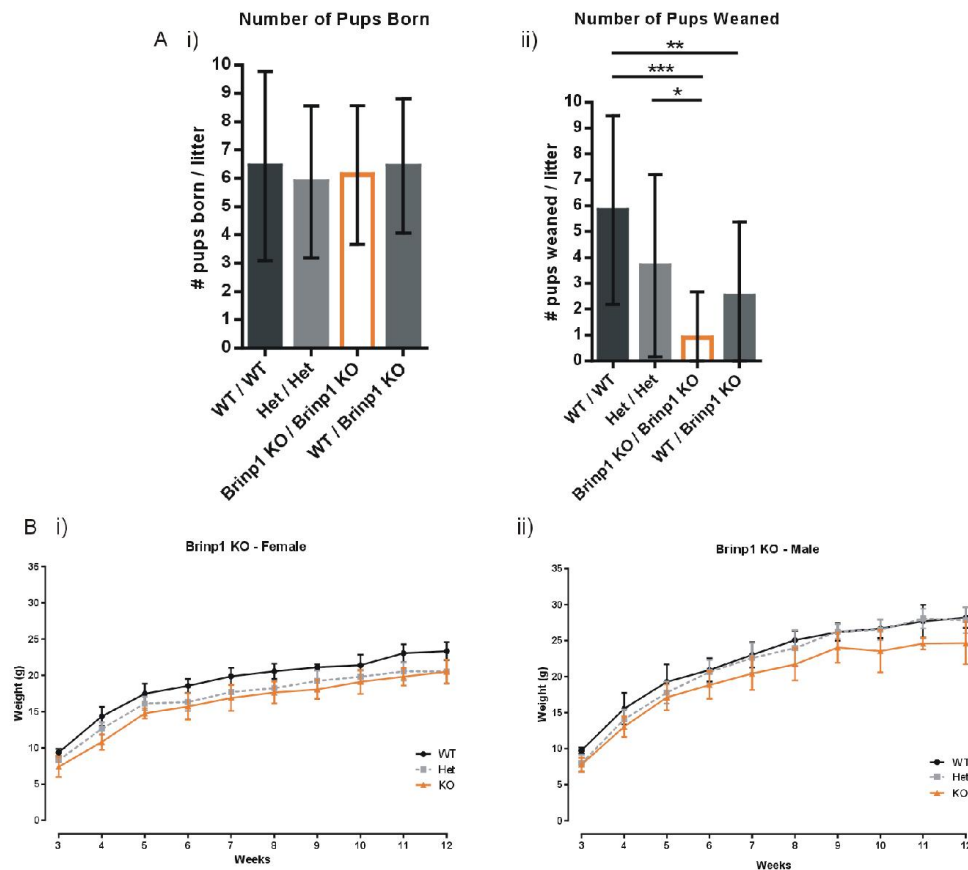


Figure 5-2 – Reduced litter survival and postnatal growth of *Brinp1* KO mice

A) i) No significant differences in number of pups per litter at postnatal day 0, from WT, heterozygous, *Brinp1* KO, and WT/ *Brinp1* KO parents. $F(3,62)=0.1624$, $p=0.9212$, one-way ANOVA.

ii) Number of pups weaned at postnatal day 21, from WT x WT, het x het, KO x KO, and WT x *Brinp1* KO parents. $F(3,62)=9.119$, $p<0.001$, one-way ANOVA. Tukey HSD multiple comparisons: WT x WT and Het x Het: $p=0.122$, WT x WT and KO x KO, $p<0.001$, WT x WT and WT x KO, $p=0.006$, Het x Het and KO x KO: $p=0.018$, Het x Het and WT x KO: $p=0.588$, KO x KO and WT x KO: $p=0.377$.

B) i) Female *Brinp1* KO mice showed a significant reduction in body weight by repeat measures two-way ANOVA: $F(2,18)=27.580$, $p<0.001$. A Tukey HSD multiple comparison test found female *Brinp1* KO mice to weigh significantly less than WT littermates of the same sex ($p<0.001$). *Brinp1* het female mice were also found to weigh significantly less than WT ($p<0.001$). No significant effect of genotype was found between female *Brinp1* het and KO mice ($p=0.362$).

ii) Male *Brinp1* KO mice also showed a significant reduction in body weight by repeat measures two-way ANOVA: $F(2,23)=8.312$, $p=0.002$. A Tukey HSD multiple comparison test found a significant difference between male WT and *Brinp1* KO mice ($p=0.002$), and male *Brinp1* het and KO mice ($p=0.013$). No significant effect of genotype was found between male WT and *Brinp1* het mice ($p=0.704$).

Results represented as the mean \pm SD * $p<0.05$, ** $p<0.01$, *** $p<0.001$, **** $p<0.0001$. # - Identical data to previously reported in chapter 3.

5.7.3 *Brinp1* KO mice have fewer layer IV neurons

Brains from adult WT or *Brinp1* KO mice were analyzed for changes in cortical anatomy and hippocampal structure using the pan-neuronal marker, NeuN, at Bregma co-ordinate -1.94, encompassing the medial hippocampus and the somatosensory cortex. The hippocampus showed a normal morphology with this antibody. On analysis of the cortex, fewer NeuN-positive and Cux1-positive pyramidal neurons were detected in layer IV of the neocortex, and proportionally more NeuN cells were evident in cortical layer V (Figure 5-3 A-E). No significant changes in total numbers of NeuN-positive cells were detected over all layers of the cortex, indicating altered neuronal distribution for *Brinp1* KO mice (Figure 5-3F). No significant changes in cellular density of layer VI of the cortex were detected using a FOXP2 antibody; a layer VI specific marker (Figure 5-3H) No significant changes in pyramidal layer thickness were detected in the medial hippocampus by NeuN labelling (Figure 5-3G).

Analysis with an antibody to Parvalbumin (PV), a marker of a subpopulation of interneurons, showed an increase in layers IV to VI, as well as an increase in PV-positive cells in the hippocampus of *Brinp1* KO mice (Figure 5-4A). No significant changes in number or distribution of other interneuron subpopulations, marked by calretinin or somatostatin were detected (Figure 5-4 E and F). Sections were also labelled for the global astrocyte marker, GFAP. No significant changes in to the cortex or hippocampus astrocyte numbers were observed (Figure 5-5).

To understand the process that results in reduced numbers of pyramidal neurons in layer IV of the neocortex, layer formation during embryonic development was examined at E12.5 (layer V and VI formation), E14.5 (layer IV formation) and E16.5 (layers II/III formation). Pregnant females, from heterozygous matings, were injected with BrdU at one of each of these time points. Due to the poor postnatal survival rates of *Brinp1* KO mice, embryos were harvested just prior to birth, at E18.5. By labelling with an anti-BrdU antibody, changes in positioning of the newly generated cells in *Brinp1* KO animals were evident, with the most prominent alterations observed in E14.5 born cells at E18.5 (Figure 5-6). At this time, a larger proportion of cells were observed in the intermediate zone (IZ), and a lower proportion of BrdU-positive cells were observed in the developing cortical plate. Fewer total numbers of E14.5 BrdU-positive cells were observed. In addition, E16.5-born cells also showed a change

in cell distribution in the *Brinp1* KO E18.5 embryos, with a lower percentage of BrdU-positive cells in the intermediate zone (bin 8). No significant changes in the overall neuronal distribution of E12.5-born cells were observed, but there was a reduction of total number of E12.5-born BrdU-positive cells. There were no significant differences in BrdU+ cell numbers detected in the sub ventricular zone any of the three injection time points. There were also no significant differences in E12.5, E14.5 or E16.5-born BrdU+ cell numbers in the dentate gyrus of the E18.5 hippocampus (Supplementary Figure 5-12).

No significant differences in Ki67-positive cells in the cortex were detected, indicating that *Brinp1* does not affect cortical cell proliferation in the E18.5 mouse brain. No significant change in the mitotic cell number was apparent at this time point in the cortex using a Phosphohistone-H3 (Phh3) antibody, a marker of mitotic activity. There was also no significant change in apoptosis in the E18.5 cortex, using a caspase 3 antibody (Figure 5-7). Together these results indicate that *Brinp1* influences neuronal positioning, and has no effect on the proliferation or survival of cells within the neocortex.

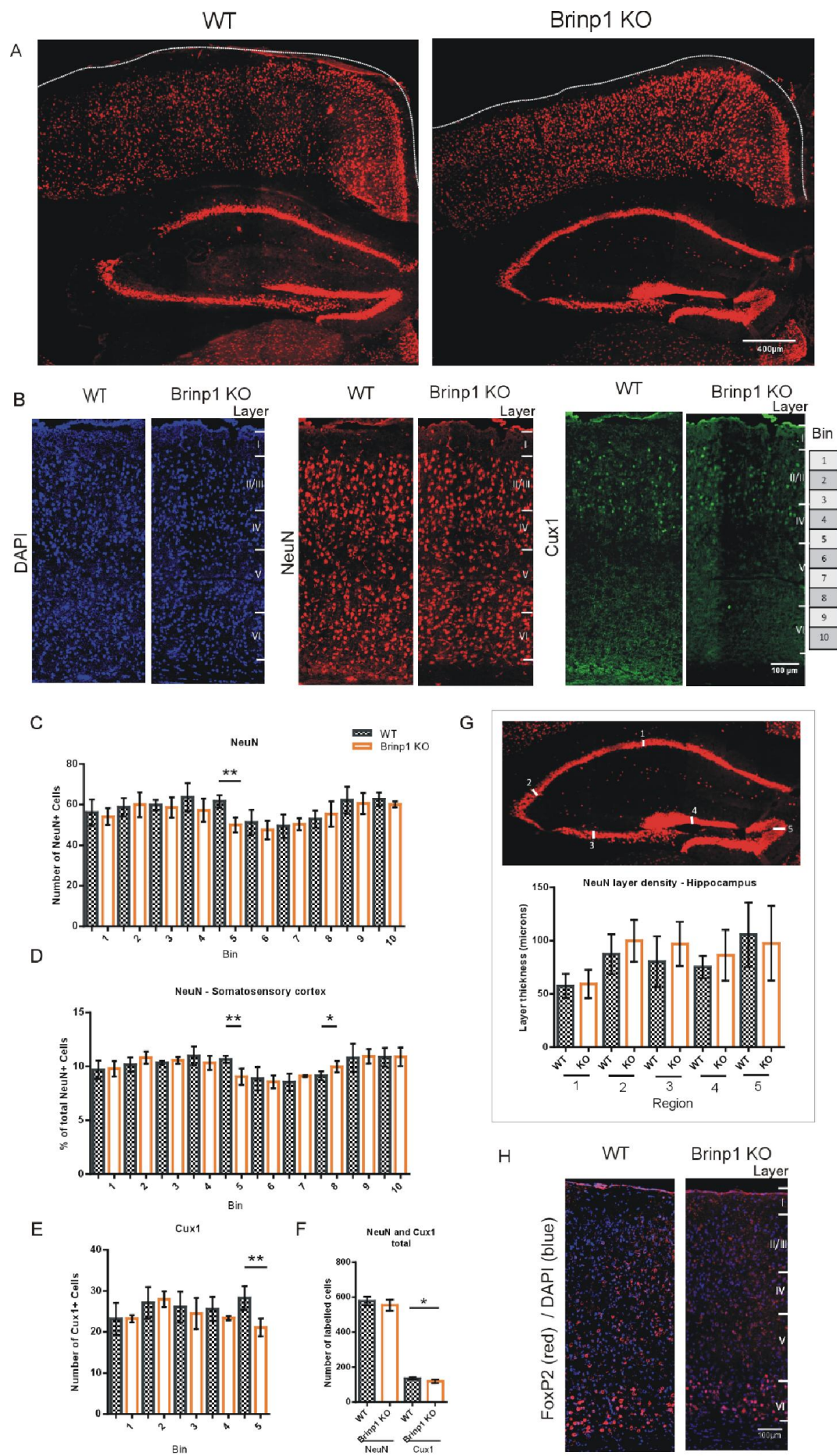


Figure 5-3 – Neuronal distribution in the adult *Brinp1* KO neocortex and hippocampus

- A) Representative coronal sections showing NeuN-positive neurons in the cortex of WT and *Brinp1* KO mice.
- B) The somatosensory *Brinp1* KO mouse neocortex, labeled with NeuN, Cux1, and counter-stained with DAPI.
- C) *Brinp1* KO mice show a decrease in number of NeuN+ cells in bin 5 of the somatosensory neocortex, corresponding to the lower half of layer IV, $t(6)=4.841$, $p=0.0029$, unpaired Student's t-test.
- D) *Brinp1* KO mice show a proportional decrease in NeuN+ cells in bin 5, $t(6)=3.978$, $p=0.0073$, and a proportional increase of NeuN+ cells in bin 8 of the somatosensory neocortex, $t(6)=2.509$, $p=0.0459$, unpaired Student's t-test.
- E) *Brinp1* KO mice show a decrease in Cux1+ cells in bin 5 of the somatosensory neocortex, corresponding to the lower half of layer IV, $t(6)=3.982$, $p=0.0073$, unpaired Student's t-test.
- F) *Brinp1* KO mice show a decrease in total number of Cux1+ cells in the somatosensory neocortex, $t(6)=2.768$, $p=0.0325$. No significant change in total number of NeuN+ cells, $t(6)=1.193$, $p=0.2779$, unpaired Student's t-test.
- G) No significant difference in NeuN layer density in the *Brinp1* KO mouse hippocampus regions CA1, CA2, CA3 or dentate gyrus.
- H) No significant difference in number of FoxP2-positive cells (layer VI) in the *Brinp1* KO mouse somatosensory cortex.

N=4 WT, 4 *Brinp1* KO. * $p < 0.05$, ** $p < 0.01$. All data represented as the mean \pm SD.

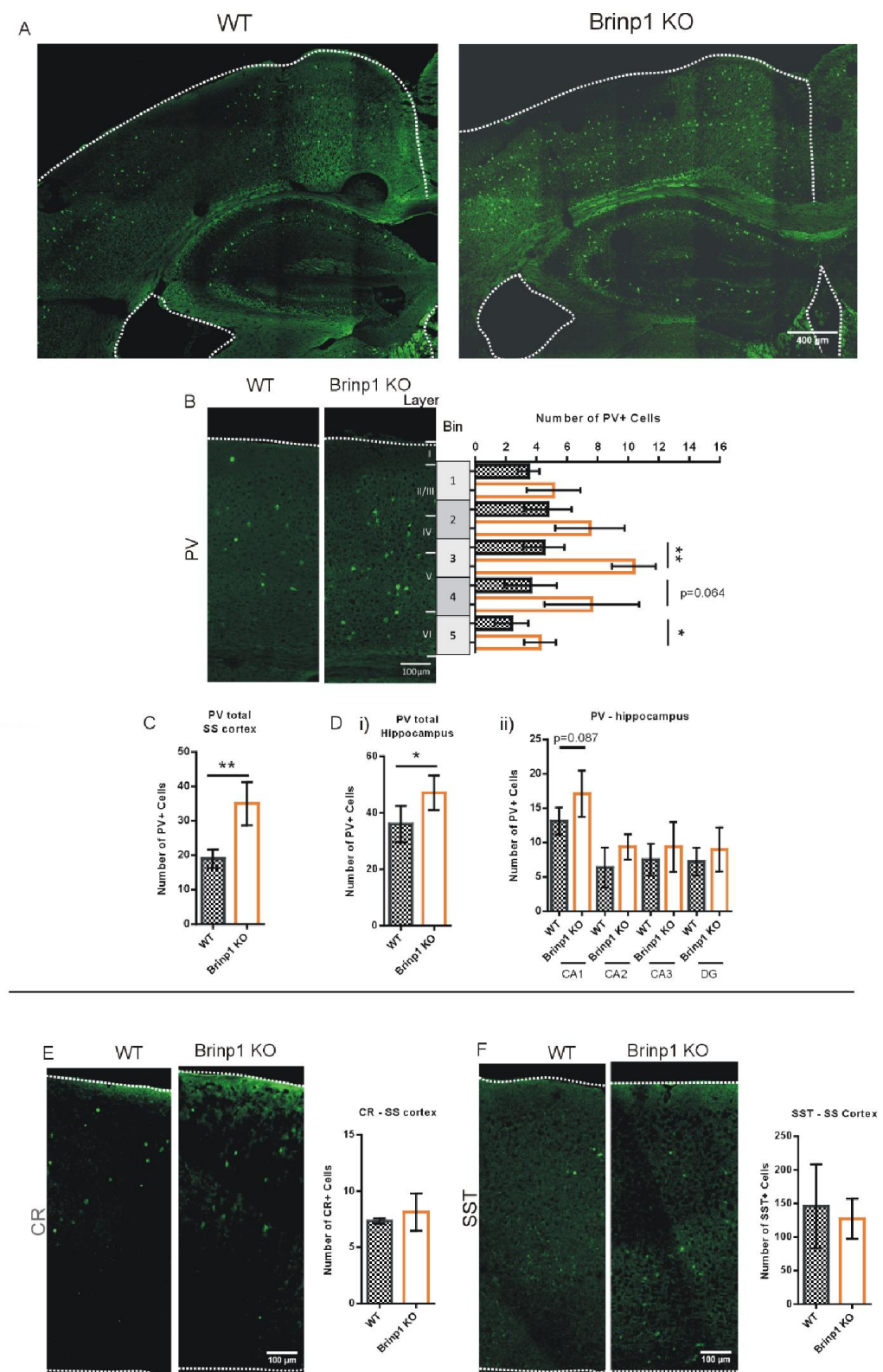
Figure 5-4 – Interneuron distribution in the adult *Brinp1* KO neocortex and hippocampus

Figure 5-4 – Interneuron distribution in the adult *Brinp1* KO neocortex and hippocampus

- A) Representative coronal section showing Parvalbumin (PV)-positive interneurons in the neocortex and medial hippocampus of WT and *Brinp1* KO mice
- B) *Brinp1* KO mice show a significant increase in number of PV-positive cells in bins 3 and 5, corresponding with layers IV/ V and VI of the somatosensory neocortex. $F(1,6)=21.602$, $p=0.004$, repeat measures ANOVA.
- C) *Brinp1* KO mice show a significant increase in total numbers of PV-positive cells in somatosensory neocortex: $t(6)=4.684$, $p=0.0034$, unpaired Student's t-test.
- D) i) *Brinp1* KO mice showed a significant increase in total numbers of PV-positive cells in the hippocampus $t(6)=2.497$, $p=0.0467$, unpaired Student's t-test.
ii) No significant differences were observed for individual regions.
- E) No significant difference in number of Calretinin (CR) positive cells in the somatosensory (SS) neocortex of *Brinp1* KO mice, $t(6)=0.9625$, $p=0.3730$, unpaired Student's t-test.
- F) No significant difference in number of Somatostatin (SST) positive cells in the somatosensory (SS) neocortex of *Brinp1* KO mice, $t(6)=0.5406$, $p=0.6082$, unpaired Student's t-test.

N=4 WT, 4 *Brinp1* KO. * $p < 0.05$, ** $p < 0.01$. All data represented as the mean \pm SD.

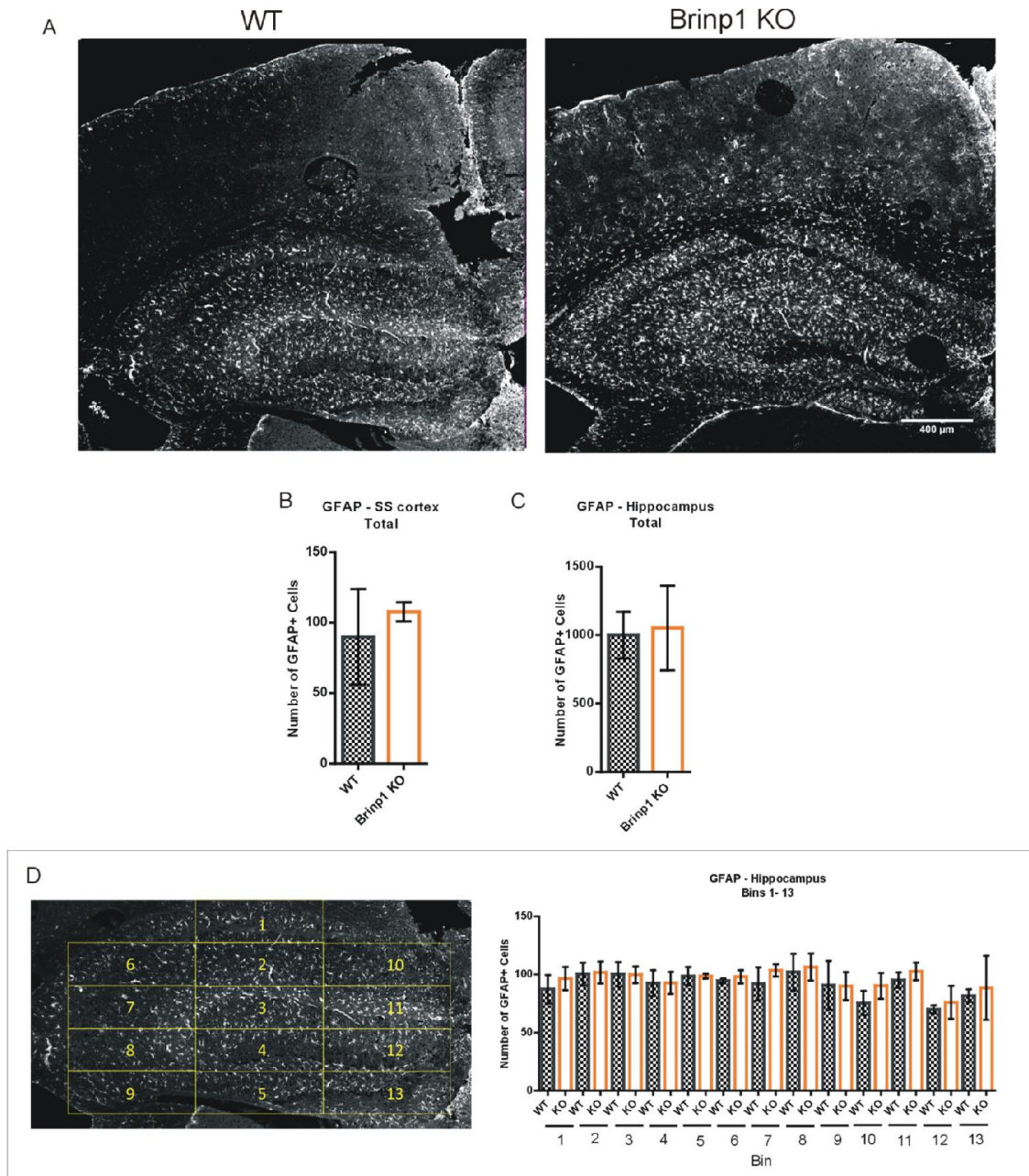


Figure 5-5 Astrocyte distribution in the adult *Brinp1* KO neocortex and hippocampus

- A) Representative coronal sections showing GFAP-positive astrocytes in the medial hippocampus and neocortex of WT and *Brinp1* KO mice.
- B) No significant change in GFAP+ cells in the somatosensory (SS) cortex of *Brinp1* KO mice, $t(6)=0.8765$, $p=0.4209$, unpaired Student's t-test.
- C) No significant change in GFAP+ cells in the hippocampus of *Brinp1* KO mice, $t(7)=0.3222$, $p=0.7567$, unpaired Student's t-test.

The hippocampus was divided into 13 equal bins and counts performed per bin. No significant change in astrocyte number were detected in any of the individual bins (1-13) or total GFAP cell count. N=4 WT, 4 *Brinp1* KO mice. All data represented as the mean \pm SD.

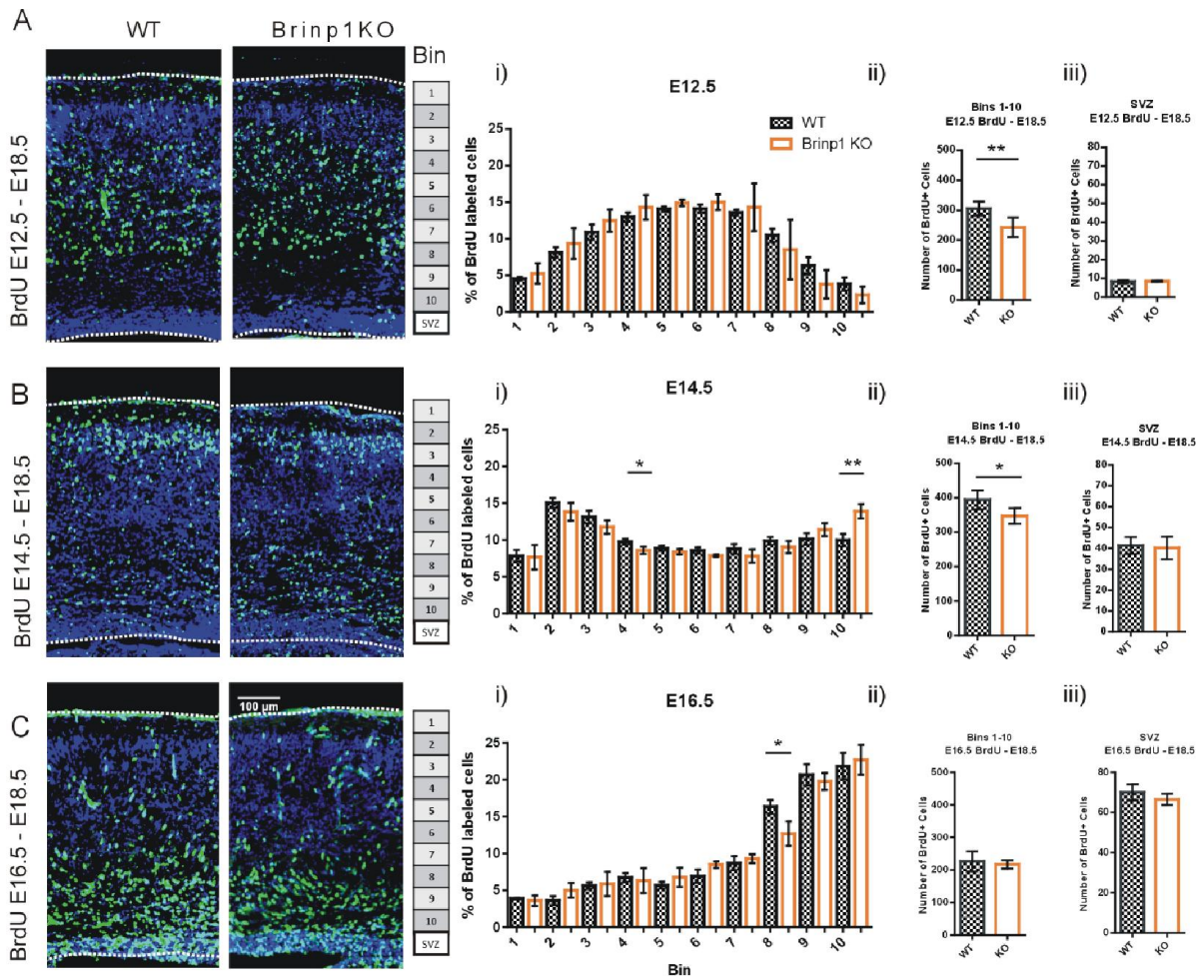


Figure 5-6 – E18.5 *Brinp1* KO mice show impaired neuronal positioning of neocortical cells generated at days E14.5 and E16.5.

Figure 5-6 – E18.5 *Brinp1* KO mice show impaired neuronal positioning of neocortical cells generated at days E14.5 and E16.5.

- A) i) No significant change in the distribution of embryonic day 12.5 (E12.5) BrdU-labelled cells (green) in the E18.5 somatosensory neocortex.
ii) *Brinp1* KO mice show a reduction in the number of E12.5-BrdU positive cells in the E18.5 somatosensory cortex: $t(8)=3.487$, $p=0.0082$, unpaired Student's t-test.
iii) No significant change in number of E12.5-BrdU positive cells observed in the E18.5 subventricular zone: $t(8)=0.2736$, $p=0.7913$, unpaired Student's t-test.
- B) i) Altered distribution of embryonic day 14.5 (E14.5) BrdU-labelled cells (green) in bin 4 and bin 10 in the E18.5 somatosensory cortex, corresponding with fewer BrdU positive cells in the cortical plate, and more in the intermediate zone.
ii) A reduction in total number of E14.5 born cells in the E18.5 neocortex was also observed: $t(6)=2.447$, $p=0.0500$, unpaired Student's t-test.
iii) No significant change in E14.5-BrdU positive cells was observed in the E18.5 subventricular zone: $t(6)=0.3246$, $p=0.7565$, unpaired Student's t-test.
- C) i) Fewer embryonic day 16.5 (E16.5) BrdU-labelled cells (green) were observed in bin 8, of the E18.5 somatosensory neocortex.
ii) No significant change in total E16.5-BrdU+ cell number were observed in the somatosensory neocortex: $t(6)=0.6164$, $p=0.5603$, unpaired Student's t-test.
iii) No significant change in E16.5-BrdU+ cell number in the subventricular zone (SVZ): $t(6)=1.548$, $p=0.1656$, unpaired Student's t-test.

* $p<0.05$, ** $p<0.01$. Data is represented as the mean \pm SD.

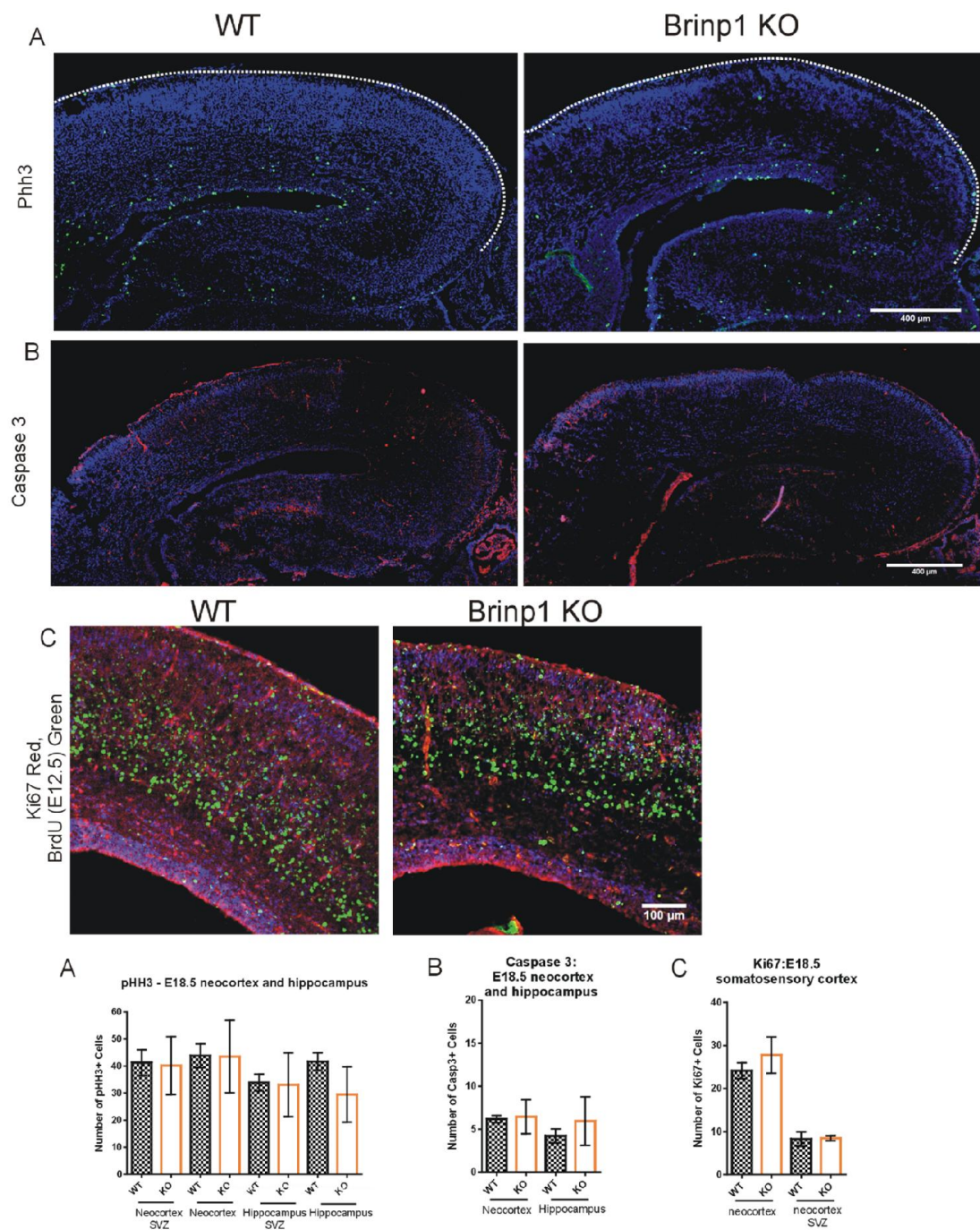


Figure 5-7 – Normal proliferation and apoptosis in the neocortex and hippocampus of *Brinp1* KO E18.5 embryos

Figure 5-7 – Normal proliferation and apoptosis in the neocortex and hippocampus of *Brinp1* KO E18.5 embryos

- A) No significant change in number of Phh3+ cells (a marker of cells undergoing mitosis) in the neocortex or hippocampus of E18.5 *Brinp1* KO brains (coronal sections). Neocortex SVZ: $t(6)=0.1509$, $p=0.8850$, neocortex: $t(6)=0.04147$, $p=0.9683$, hippocampus SVZ: $t(6)=0.1211$, $p=0.9083$, hippocampus: $t(6)=2.008$, $p=0.0914$, unpaired Student's t-tests. N=4 WT and 4 *Brinp1* KO mice.
- B) No significant change in number of activated caspase3 positive cells (a marker of cells undergoing apoptosis) in the neocortex or hippocampus of E18.5 *Brinp1* KO brain (coronal). Neocortex: $t(7)=0.2564$, $p=0.8050$, hippocampus: $t(7)=1.114$, $p=0.3020$, unpaired Student's t-tests. N=5 WT and 4 *Brinp1* KO mice.
- C) No significant change in number of Ki67+ cells (a proliferation marker) in the E18.5 somatosensory neocortex (coronal) of *Brinp1* KO mice. E12.5 administered BrdU+ cells labelled in green. Neocortex: $t(8)=1.768$, $p=0.1150$, neocortex SVZ: $t(8)=0.2736$, $p=0.7913$, unpaired Student's t-tests. N=5 WT and 5 *Brinp1* KO mice. All images counter stained with 4',6-diamidino-2-phenylindole (DAPI, blue).

5.7.4 Behavioral alterations of *Brinp1* KO mice

To evaluate the effect of *Brinp1* loss on neurological function, *Brinp1* KO mice behavior was assessed. In an initial screen, *Brinp1* KO mice showed normal auditory, visual and olfactory capabilities and normal motor co-ordination on the Rotarod.

5.7.5 *Brinp1* KO mice exhibit reduced sociability and altered vocalizations

A pronounced decrease in sociability was observed when the *Brinp1* KO mice were tested for social interaction with an unfamiliar mouse. In the first trial of the three-chamber social interaction test, *Brinp1* KO and WT mice showed no preference between the left and right empty cages. *Brinp1* KO mice did spend less time investigating the empty cages, indicating altered exploratory behavior (Figure 5-8A). In the second trial, when presented with a stranger mouse in one of the cages, *Brinp1* KO mice spent significantly less time interacting with the stranger, while showing no significant difference in interaction time with the empty cage (Figure 5-8B). *Brinp1* KO mice also exhibited increased velocity during both trials (Figure 5-8C). Results for this test were reproduced with a second cohort (n=12 mice per genotype, $P<0.05$ for reduction in time interacting with the stranger mouse).

Communication by *Brinp1* KO mice was investigated by analyzing the ultrasonic vocalization (USV) calls of male mice presented with pheromones from estrus or proestrus female mice (Wöhr, 2012). Compared to WT, *Brinp1* KO mice showed a trend towards reduced number of calls, a longer latency to call, and longer latency to investigate the cotton bud, but these parameters did not reach the 95% confidence level (Figure 5-8 D and E). No significant change in call amplitude was evident (Figure 5-8G), whilst a trend of increased peak frequency of calls was observed ($p=0.089$) (Figure 5-8H). This reduced call length reflected changes to the distribution of call types. *Brinp1* KO mice emitted a higher percentage of 'short' calls and lower percentage of 'complex' or 'composite' longer calls (Figure 5-8 I and J). This reduction in complex and composite calls indicates that *Brinp1* influences vocalization, and suggests that *Brinp1* KO mice may exhibit impairments in vocal communication.

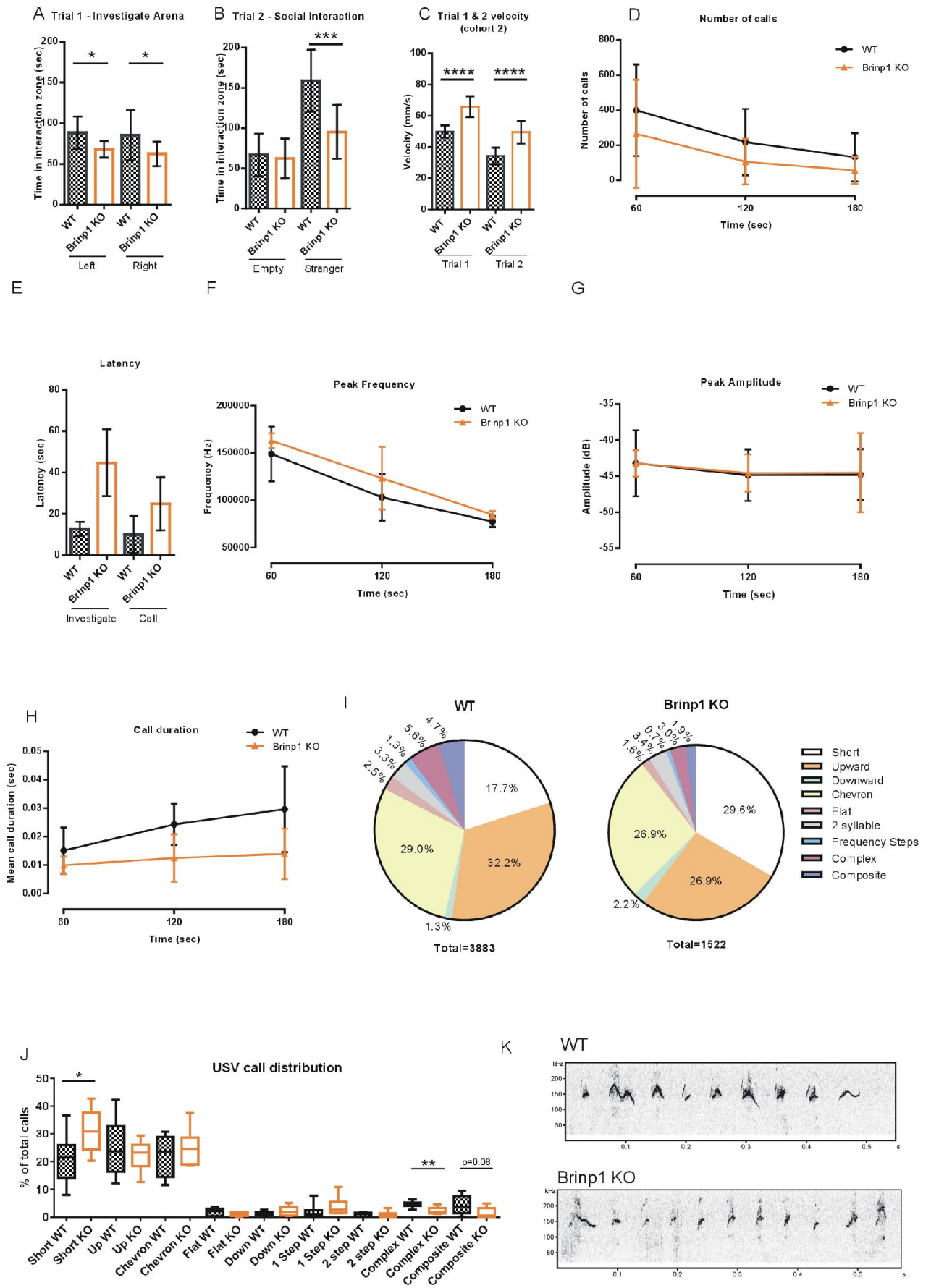


Figure 5-8 – Altered social interaction and vocalization of *Brinp1* KO mice

- A) Reduced interaction time of *Brinp1* KO mice with the empty cage during the habituation trial of the three chamber social interaction test. Left chamber: $t(18)=2.871$, $p=0.0102$, right chamber $t(18)=2.134$, $p=0.0469$, unpaired Student's t-tests, $n=10$ mice per genotype. Equivalent times were spent in left and right chamber for both WT and KO mice. #
- B) *Brinp1* KO mice show reduced interaction time with a sex-matched novel mouse. Empty chamber: $t(18)=0.3915$, $p=0.700$ Stranger mouse: $t(18)=3.951$, $p=0.0009$, unpaired Student's t-tests, $n=10$ mice per genotype. #
- C) *Brinp1* KO mice exhibited hyperactivity in both trials of three chamber social interaction test. Trial 1: $t(18)=6.529$, $p<0.0001$, trial 2: $t(17)=5.261$, $p<0.0001$, unpaired Student's t-tests. $n=10$ WT, 10 *Brinp1* KO. #
- D) Ultrasonic vocalization (USV) of adult male mice: Number of calls, divided into 1 min bins. $F(1,17)=1.693$, $p=0.21$, repeat measures two-way ANOVA. $N=10$ WT, 9 *Brinp1* KO mice.
- E) Latency of *Brinp1* KO to investigate cotton bud (nose $<1\text{cm}$ from bud), $t(17)=1.835$, $p=0.0840$, and latency to call $t(17)=0.9709$, $p=0.3452$, unpaired Student's t-tests. $N=10$ WT, 9 *Brinp1* KO.
- F) Peak call frequency of *Brinp1* KO mice, divided into 1 min bins. $F(1,17)=3.39$, $p=0.089$, repeat measures two-way ANOVA. $N=10$ WT, 9 *Brinp1* KO mice.
- G) No significant change in peak amplitude of *Brinp1* KO mice, divided into 1 min bins: $F(1,17)=0.76$, $p=0.787$, repeat measures two-way ANOVA. $N=10$ WT, 9 *Brinp1* KO mice.
- H) *Brinp1* KO mice emit shorter USV calls. Call duration data was divided into 1 min bins. $F(1,17)=8.17$, $p=0.014$, repeat measures two-way ANOVA. $N=10$ WT, 9 *Brinp1* KO mice.
- I) Pie chart showing distribution of call types of *Brinp1* KO mice. For designation of call type categories, refer to Scattoni et al. (Scattoni et al., 2008). Unidentified calls (11.7% WT, 11.3% *Brinp1* KO) were excluded.
- J) Box plot showing distribution of call types as a percentage of total calls. Boxes represent inter-quartile range. The central horizontal line shows the mean. The range is shown by error bars. * $p<0.05$, ** $p<0.01$, unpaired Student's t-test.
- K) Representative spectrogram of first calls from a WT and a *Brinp1* KO mouse.

* $p<0.05$, ** $p<0.01$, *** $p<0.001$ **** $p<0.0001$. All data represented as the mean \pm SD.

- Identical data to previously reported in chapter 3.

5.7.6 *Brinp1* KO mice are hyperactive and exhibit changes in exploratory behavior

Hyperactivity of *Brinp1* KO mice was revealed by testing animals in the locomotor cell where, over a period of 30 min, the *Brinp1* KO mice travelled 50% further, spent less time resting, and showed a consistent increase in velocity compared to WT (Figure 5-9B). *Brinp1* KO mice also spent proportionally more time in the center of the locomotor cell (Figure 5-9C). Notably, *Brinp1* KO mice showed an increase in stereotypic episodes (repeat motion within a small area) and increased rearing (vertical plane activity) (Figure 5-9D). To examine whether the absence of *Brinp1* has an effect on anxiety, mice were allowed to freely explore an elevated plus maze for 5 min. Testing of the *Brinp1* KO mice on the maze showed they spent less time spent in a closed arm, compared to wild types (Figure 5-9E). *Brinp1* KO mice showed a significant reduction in the latency to grip onto the wire cage in a wire hang test (Supplementary Figure 5-13C). Several of the knockout mice released their grip within the first couple of seconds, jumping down almost immediately to the cage below. This result indicates either an impairment in claw grip strength or a decrease in motivation to hang on to the cage.

To assess mice in an environment similar to their home cage, mice were placed in a sawdust lined, plexiglass box. Mice in this environment showed increased rearing behavior at a similar frequency to the locomotor cell. There was a decrease in the amount of time the *Brinp1* KO mice spent digging through the sawdust compared to wild type (Figure 5-9F). In addition, female *Brinp1* KO mice showed a reduced frequency of grooming (Supplementary Figure 5-13B). *Brinp1* KO mice showed a normal preference for the dark zone in a locomotor cell light/dark test, whilst again showed hyperactivity in this test (Supplementary Figure 5-14). *Brinp1* KO mice showed a normal preference for investigating an unfamiliar object in a novel object recognition test (Supplementary Figure 5.15).

5.7.7 Methylphenidate does not decrease hyperactivity of *Brinp1* KO mice

Methylphenidate (MPH) is a psycho-stimulant drug commonly used to treat hyperactivity and inattention in children diagnosed with ADHD (Kordon et al., 2011). It has previously been shown to reduce hyperactivity in established ADHD mouse models (Ellen J. Hess, 1996) (Huang & Huang, 2012). To investigate whether MPH reduces hyperactivity of *Brinp1* KO mice,

mice were treated using a published regime (Ellen J. Hess, 1996) and followed activity in the locomotor cell. Activity was determined as the distance travelled, measured at 5 min intervals. In the habituation phase prior to injection, *Brinp1* KO mice travelled significantly further than WT mice (Figure 5-9G). Saline-treated WT mice showed a gradual decrease in all facets of activity, but the saline-treated *Brinp1* KO mice did not decrease their horizontal plane activity. The effect of MPH as a stimulant at 2.5 mg/kg was indicated by an increase in activity of the WT animals peaking at 20 min post injection. This pattern of activity was comparable to that of the saline-treated *Brinp1* KO group (Figure 5-9H). The *Brinp1* KO MPH group also showed an increase in locomotor activity, above the level of both the *Brinp1* KO saline and WT MPH groups. Results at 1.25 mg/kg showed a milder effect but MPH still increased activity of both the WT and *Brinp1* KO groups (Supplementary Figure 5-16). Overall these results demonstrated that at two doses, MPH does not reduce the hyperactivity of the *Brinp1* KO mice.

5.7.8 *Brinp1* KO mice have impaired short-term memory

Brinp1 KO mice were tested for spatial learning and memory in the Y-maze test (Figure 5-9). With a two-hour interval between trials, *Brinp1* KO mice did not show the typical increase in time spent exploring a novel arm, indicating impaired short-term memory. This result was reproduced with a repeat of the test using a second cohort (n=12 mice per genotype, $p<0.05$ for reduction in percentage time spent in novel arm. To determine whether long-term memory impairment was also present, *Brinp1* KO mice were tested using the Morris Water Maze (Figure 5-9J). The *Brinp1* KO cohort showed no impairment in this test, and even showed an improvement in time ($p=0.017$), as well as a shorter swim distance ($p=0.048$), required to find the platform compared to WT on day 1 of the experiment.

5.7.9 *Brinp1* knockout mice exhibit normal sensory gating

The Pre-pulse inhibition (PPI) test is used to measure sensory gating in mice, which models deficits in human subjects diagnosed with schizophrenia. No abnormalities in sensory gating of *Brinp1* KO mice were detected by pre-pulse inhibition testing, indicating that these mice do not model this aspect of human schizophrenia (Figure 5-9K).

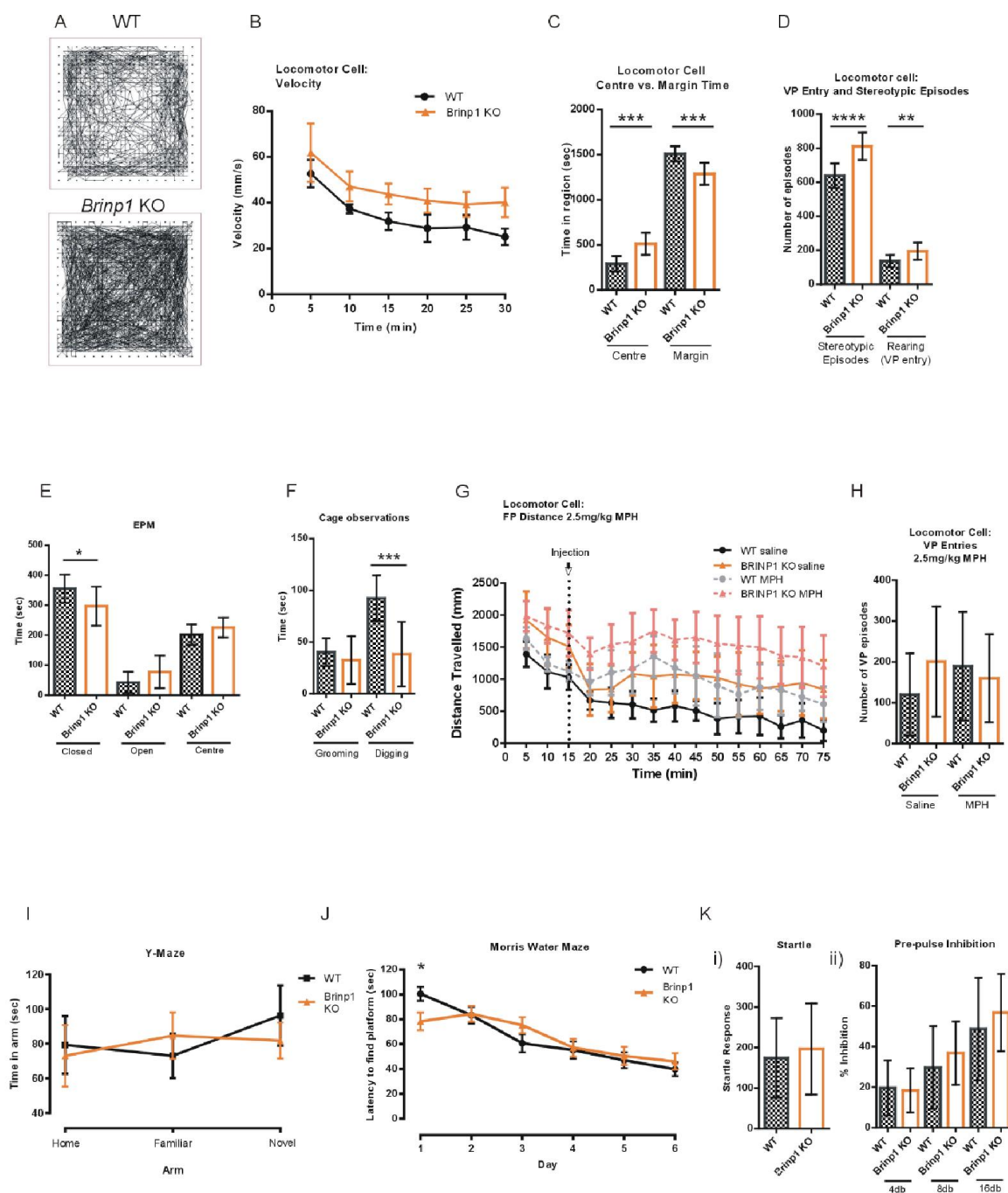


Figure 5-9 – *Brinp1* KO mice exhibit hyperactivity, altered exploratory behavior and impaired short-term memory

Figure 5-9 – *Brinp1* KO mice exhibit hyperactivity, altered exploratory behavior and impaired short-term memory

- A) Increased locomotor activity of *Brinp1* KO mice in a 30 min trial shown as a representative data trace for a WT and a *Brinp1* KO litter mate.
- B) Increased velocity of *Brinp1* KO mice in a locomotor cell $F(1,13)=26.12$, $p<0.0001$, repeat measures two-way ANOVA. $N=10$ mice per genotype.
- C) Increased exploratory behavior of *Brinp1* KO mice in the locomotor cells, shown as increased time in the center and reduced time in marginal areas, $t(18)=4.676$, $p=0.0002$, unpaired Student's t-test.
- D) *Brinp1* KO mice showed increased rearing in the locomotor cells (recorded as number of Vertical Plane entries), $t(18)=2.962$, $p=0.0084$, and increased stereotypic episodes, $t(18)=5.052$, $p<0.0001$, unpaired Student's t-tests.
- E) Elevated Plus Maze: *Brinp1* KO mice spent less time in the closed arms of the maze, indicating reduced anxiety. Closed arms: $t(22)=2.538$, $p=0.0188$, open arms: $t(22)=1.875$, $p=0.0741$. Centre: $t(22)=1.726$, $p=0.0984$, unpaired Student's t-tests. #
- F) *Brinp1* KO mice were observed for self-directed behavior in a test plexi-glass cage lined with sawdust for 20 min. No significant difference in grooming behavior was observed, $t(18)=0.9078$, $p=0.3760$. *Brinp1* KO mice showed reduced digging behavior, $t(18)=4.457$, $p=0.0003$, unpaired Student's t-test.
- G) WT and *Brinp1* KO mice locomotor activity before and after injection of MPH / saline in the locomotor cell. An acute IP injection of 2.5mg/kg of MPH increased locomotor activity for both WT and *Brinp1* KO mice, $n=10$ WT MPH, 10 *Brinp1* KO MPH, 10 WT saline, 10 *Brinp1* KO saline. Effect of drug treatment: $F(1,36)=36.079$, $p<0.0001$, repeat measures two-way ANOVA.
- H) MPH does not significantly alter the number of rearing episodes of *Brinp1* KO mice, $F(3,36)=0.9044$, $p=0.4485$, one-way ANOVA.
- I) Y-maze: Analysis by repeat measures two-way ANOVA revealed a significant main effect for arm times: $F(1,22)=3.664$, $p=0.034$, no main effect for genotype alone $F(1,22)=2.363$, $p=0.138$, whilst a significant interaction effect between genotype x arm: $F(3,44)=3.505$, $p=0.039$. $N=12$ mice per genotype. Results indicate that *Brinp1* KO mice did not display an increase in time spent exploring the novel arm, in comparison to WT controls. #
- J) *Brinp1* KO mice showed no impairment in learning the location of the hidden platform in the Morris Water Maze, and improvement in locating the platform on day 1. No significant main effect of genotype on time locating the platform: $F(1,18)=0.007$, $p=0.933$, and no interaction effect of trial x genotype: $F(5,90)=1.317$, $p=0.264$, repeat measures two-way ANOVA. $N=10$ mice per genotype. Data presented as the mean \pm SE.
- K) *Brinp1* KO mice showed i) normal startle response, $t(22)=0.5077$, $p=0.6167$, unpaired Student's t-test and ii) normal pre-pulse inhibition (PPI), $F(1,22)=0.512$, $p=0.482$, repeat measures two-way ANOVA. $N=12$ mice per genotype. #

Data presented as the mean \pm SD except where otherwise stated. * $p<0.05$, ** $p<0.01$, *** $p<0.001$, **** $p<0.0001$.

Identical data to previously reported in chapter 3.

5.7.10 Increased expression of *Astn1* and *Astn2* in the developing brain of *Brinp1* KO mice.

Quantitative PCR was performed on mRNA from the brains of *Brinp1* KO mice to assess whether homologous MACPF family members are up-regulated. The late embryonic brain (E18.5) showed a two-fold increase both *Astn1* and *Astn2* mRNA (Figure 5-10A). *Brinp1* mRNA also increased by 1.5 fold. No significant changes to the levels of *Brinp2* or *Brinp3* mRNA were evident at this developmental time point. At 6 weeks of age, *Brinp1* KO mice showed a three-fold increase in *Astn1* mRNA and a two- fold increase in *Astn2* mRNA in the hippocampus (Figure 5-10B). *Brinp2* mRNA increased in four of the 6 mice ($p=0.08$). Down-regulation of both *Brinp1* and *Brinp2* mRNA was detected in the adult cortex, with no significant change in expression of either Astrotactin mRNA. Normalization with *GAPDH* and β -*actin* gave similar results.

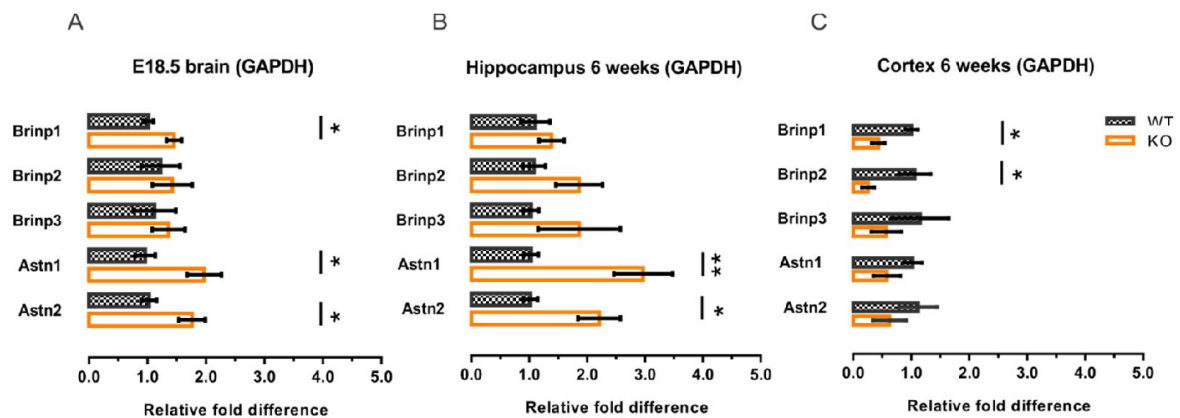


Figure 5-10 – Up-regulation of *Astn1* and *Astn2* mRNA in the embryonic brain and adult hippocampus of *Brinp1* KO mice

- A) qPCR showing a significant increase in *Astn1* mRNA ($t(9)=2.800$, $p=0.0207$) and *Astn2* mRNA ($t(9)=2.829$, $p=0.0222$, unpaired Student's t-test), in the developing (E18.5) mouse brain. Levels of exon-3 deleted *Brinp1* mRNA also increase ($t(9)=2.733$, $p=0.0231$). No significant changes overserved for *Brinp2* mRNA levels ($t(9)=0.4109$, $p=0.6908$), or *Brinp3* mRNA levels: ($t(9)=0.5277$, $p=0.6105$, unpaired Student's t-test). #
- B) An increase in *Astn1* and *Astn2* expression was also detectable in the hippocampus at 6 weeks of the *Brinp1* KO mice: *Astn1*: $t(9)=3.384$, $p=0.0081$, *Astn2*: $t(9)=2.821$, $p=0.0200$, unpaired Student's t-tests. No significant changes were detected in levels of *Brinp1* mRNA ($t(9)=0.8505$, $p=0.4171$) *Brinp2* mRNA ($t(9)=1.616$, $p=0.1405$), or *Brinp3* mRNA ($t(9)=1.047$, $p=0.3222$, unpaired Student's t-tests). #
- C) In the 6 week old *Brinp1* KO cortex, less exon-3 deleted *Brinp1* mRNA ($t(5)=3.611$, $p=0.0154$), and *Brinp2* mRNA ($t(5)=3.113$, $p=0.0265$) were detected, with no significant change in expression of either *Astn1*, *Astn2* or *Brinp3* *Astn1*: $t(5)=1.572$, $p=0.1909$, *Astn2*: $t(5)=1.139$, $p=0.3182$, *Brinp3*: $t(5)=1.133$, $p=0.3087$, unpaired Student's t-tests. #

N= 3 WT, 4 *Brinp1*KO, * $p<0.05$, ** $p<0.01$. Normalization against GAPDH expression levels. All data represented as the mean \pm SE. # - Identical data to previously reported in chapter 4.

5.8 Chapter 5: Discussion

5.8.1 *Brinp1* KO mice model core social communication symptoms ASD

Our study of *Brinp1* KO mice has revealed behavioral phenotypes that resemble social and communication impairments found within the human autism spectrum. The three-chamber social interaction test is an accepted behavioral test to investigate social deficits relevant to autism (Silverman et al., 2010). Using this test, *Brinp1* KO mice spent significantly less time interacting with a stranger sex-matched mouse: a sign of social withdrawal. Furthermore, testing of ultrasonic vocalizations of adult male mice is a key method for behavioral phenotyping of NDDs (Scattoni et al., 2009; Wöhr, 2012). Male *Brinp1* KO mice exhibited an altered vocalization phenotype when presented with pheromones from estrus females. The shorter call duration of *Brinp1* KO mice, with fewer complex calls, indicates altered communication ability.

Brinp1 KO mice showed poor postnatal survival. The marked reduction in sociability and communication observed in *Brinp1* KO adults may manifest in reduced attentiveness towards litters, thereby hindering neonate survival if mothers fail to provide adequate thermal insulation, nourishment and post-parturition care towards their pups. The reduction in grooming behavior of female *Brinp1* KO mice may affect litter survival, as maternal licking of newborn pups has been shown to impact brain development (Champagne et al., 2007; Pedersen et al., 2011). Reduced survival may also be a result of flawed two-way communication between dam and pup. Future investigation of the social communication deficits of *Brinp1* KO mice should determine whether *Brinp1* KO pups emit altered vocalizations. It would also be interesting to investigate ultrasonic vocalization between two interacting *Brinp1* KO mice.

Repetitive movements such as increased grooming are reported in some but not all mouse models of autism (Jamain et al., 2008; Yang et al., 2012). Changes in grooming behavior were not observed for the *Brinp1* KO mice. Increased stereotypic episodes and increased rearing were observed in the locomotor cell, although this alone does not model the repetitive movements of autism as such movements may be the result of hyperactivity.

Taken together, the above observations suggest that *Brinp1* KO mice model key aspects of human autism spectrum disorder, since poor sociability, delayed language, and impaired communication skills are fundamental facets of the pathology.

5.8.2 *Brinp1* KO mice are hyperactive, with short-term memory impairment.

Brinp1 KO mice are hyperactive, evidenced by a 50% increase in horizontal plane activity in the locomotor cell. They also display changes in exploratory behavior, showing increased rearing and reduced anxiety-like behavior. *Brinp1* KO mice have a 10% reduction in body mass. This may be due to increased energy expenditure due to hyperactivity, and is consistent with variants in the *BRINP1* locus at 9q33.1 in patients with growth delay (Chien et al., 2010).

Methylphenidate (Ritalin) is a psychostimulant commonly used in the treatment of ADHD symptoms (Kordon et al., 2011; van der Meere et al., 1995), although a considerable proportion of patients do not respond (Contini et al., 2013). We examined the predictive validity of *Brinp1* KO mice as a model for ADHD by investigating their response to methylphenidate. Methylphenidate did not reduce the hyperactivity of *Brinp1* KO mice, indicating that *Brinp1* deletion is unlikely to directly affect the dopaminergic pathways of the prefrontal cortex, as hypothesized for ADHD etiology (Giros et al., 1996). A future direction would be to examine the effect of other drugs, such as atomoxetine (a norepinephrine reuptake inhibitor) (Bymaster et al., 2002) or clonidine (and α_2 -adrenergic receptor agonist) (Hunt et al., 1995), on hyperactivity as well as sociability of *Brinp1* KO mice.

Brinp1 KO mice did not spend more time exploring the novel arm of the Y-maze compared to the familiar arm, when testing with a two-hour interval between trials, indicating impaired short-term memory. The *Brinp1* KO mice performed normally in the Morris Water Maze, demonstrating that long-term memory is unaffected. The spatial memory impairment may model cognitive impairment evident in a subset of autistic patients. *Brinp1* KO mice showed no impairment in sensory gating (a common symptom of patients with schizophrenia).

5.8.3 *Brinp1* KO mice exhibit changes in cortical lamination.

Disorganization of layer IV and V of the cortex has been reported in children with autism (Stoner et al., 2014). Thinning of cortical lamina has also been reported in ASD and ADHD patients (Casanova et al., 2013; Hoekzema et al., 2012; Shaw et al., 2007). Changes in

neuronal migration result in abnormal lamination of the neocortex and associated behavioral deficits in mouse models of NDDs (Valiente & Marin, 2010). For example, CNTNAP2 knockout mice - an established model of autism - show impaired neuronal migration in the neocortex, and present with social deficits, hyperactivity and memory impairment (Penagarikano et al., 2011). JNA/+ mice that have a mutation in the TUBA1 gene exhibit hyperactivity, memory impairment, and show changes in cortical lamination as a result of impaired neuronal migration (Keays et al., 2007). Other examples of NDD mouse models with altered cortical lamination as a result of changes in neuronal migration include the Reeler mouse (Reelin) (Folsom & Fatemi, 2013) and Lis1 mutants (Paylor et al., 1999).

Brinp1 KO mice exhibit reduced pyramidal neuronal density in layer IV of the cortex, detected with the pan-neuronal marker NeuN, and Cux1, a layer II-IV pyramidal neuron marker. BrdU injection at E14.5 showed altered positioning of cells that form the perturbed layer (layer IV), which may explain the reduced density of pyramidal neurons in the adult mouse brain. Given no changes in cell proliferation or turnover were detected, the mis-localization of neurons destined for layer IV in *Brinp1* KO mice suggests that *Brinp1* influences neuronal migration. A change in distribution of BrdU-positive cells was also detected in mice injected at E16.5, possibly indicating impaired migration of cells forming the upper layers of the cortex (layers II-III). Interestingly, mRNA of the MACPF family members *Astn1* and *Astn2* increased in the embryonic brain (E18.5) and hippocampus of *Brinp1* KO mice. Both *Astn1* and *Astn2* are reported to facilitate neuronal migration (Adams et al., 2002; Wilson et al., 2010). This suggests that Astrotactins and *Brinp1* have similar functions, and perhaps work in a common pathway, such that *Astn1* and *Astn2* functionally compensate for the absence of *Brinp1* during neuronal migration.

More parvalbumin-positive (PV) neurons were detected in the adult *Brinp1* KO mouse neocortex and hippocampus. PV neurons are a subset of GABA-ergic interneurons that play an inhibitory role in the cortex. Cortical interneurons are known to alter their migratory trajectory as they arrive within the cortex (Kriegstein & Noctor, 2004; Metin et al., 2006). We postulate that the absence of *Brinp1* also results in disrupted migration of PV-positive interneuron populations, resulting in a greater density of this subpopulation in defined regions of the neocortex. Further investigation is needed to determine whether the increase in PV-positive interneurons in the somatosensory cortex results in the hypothesized loss of

such interneurons in other cortical regions. As cortical interneurons have a critical role in regulating network excitability generated by pyramidal interneurons (Lovett-Barron et al., 2012) the loss of pyramidal neurons and gain of PV-positive interneurons may therefore shift the balance between cortical excitation and inhibition, resulting in the reported behavioral changes. An imbalance between excitation and inhibition has been observed in the brains of humans with ASD (Enticott et al., 2013; Rubenstein & Merzenich, 2003; Thatcher et al., 2009).

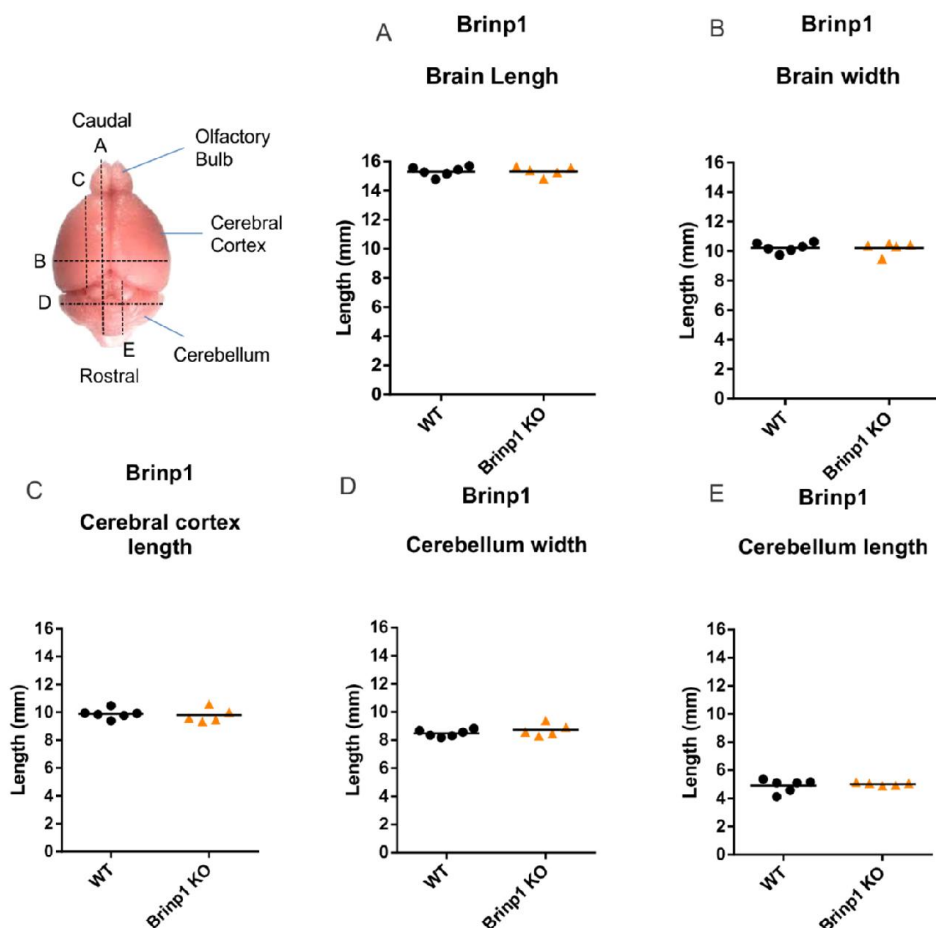
During the final stages of our study Kobayashi et al., reported a different line of *Brinp1* KO mice (*Brinp1*-exon8)(Kobayashi et al., 2014). Our observations are consistent with some, but not all of their findings. Both *Brinp1* knockout lines exhibit increased activity; reduced sociability, reduced anxiety, and impaired working memory. Importantly, however, Kobayashi et al. did not investigate communication (or report potentially associated breeding difficulties), whereas our findings reveal a communication deficit suggesting an ASD-like endophenotype which is consistent with reports of autism and language delay reported in patients with de novo human mutations at the 9q33.1 locus.

Kobayashi et al. also reported that adult *Brinp1*-exon8 knockout animals exhibit increased hippocampal neurogenesis and more PV interneurons in the hippocampus, and concluded that the altered behaviors reflect a hippocampal-specific defect. No cortical or other perturbations were reported in the *Brinp1*-exon 8 knockout mice. By contrast, our *Brinp1* knockout animals display cortical mis-lamination during embryonic development, and there is no evidence of increased cell proliferation in the embryonic cortex. We also found no evidence for an increased embryonic hippocampal cell proliferation. Like Kobayashi et al., we observed an increase in PV⁺ neurons in the adult hippocampus, but this is not hippocampus-specific, as we also detected additional PV⁺ neurons in the neocortex. Given these observations, we therefore disagree with the Kobayashi et al. conclusion that *Brinp1* is a negative regulator of cell proliferation and that the behavioral alterations in mice lacking BRINP1 arise due to disruption of the hippocampus. Our findings demonstrate that distributions of pyramidal neurons within the *Brinp1* KO neocortex, which combined with changes in PV-positive interneurons in the neocortex and hippocampus, likely underpin the reported behavioral phenotypes.

An explanation for the differences between the two studies may lie in differences between the two *Brinp1* mutant alleles. The Kobayashi study involved a conventionally targeted *Brinp1* KO line carrying a deletion of exon 8, which removes the terminal 418 residues of the 760 residue protein but retains the promoter and the potential to express a smaller protein containing the MACPF domain (No protein analysis was carried out on the *Brinp1*-exon8 mice). By contrast, our knockout allele removes exon 3 and truncates the protein after the first 74 amino acids (preceding the MACPF domain), and immunoblotting established that BRINP1 production was abolished. Our targeting strategy also included removal of the neomycin selection cassette, which is known to have effects on survival and physiology if retained in the targeted locus (Pham et al., 1996; Scacheri et al., 2001). The *Brinp1*-exon 8 allele does not have the selection cassette removed, which may influence the phenotype.

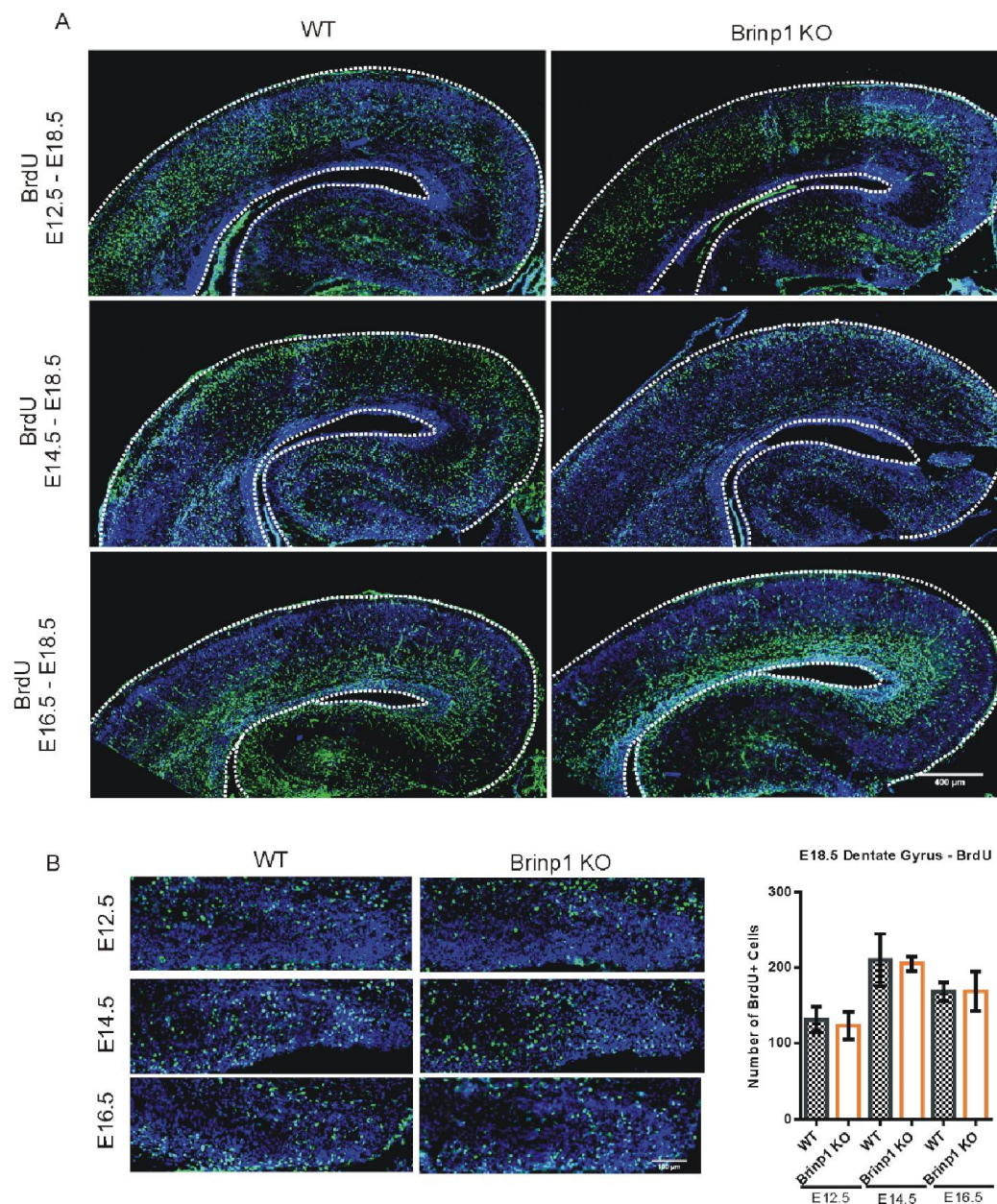
5.9 Conclusions

Brinp1 KO mice exhibit reduced sociability, vocalization impairments, hyperactivity, and alterations in short term memory. These behavioral phenotypes appear to show face validity for the core social communication deficits of autism spectrum disorder, along with the hyperactivity aspect of attention deficit hyperactivity disorder. The reported changes in cortical lamination of pyramidal neurons in layer IV of the neocortex, and the increase in PV-positive interneurons in the *Brinp1* KO mouse neocortex and hippocampus, likely underpin such behavioral changes. These findings demonstrate the important role in normal brain development and suggest *Brinp1* as a candidate gene for neurodevelopmental disorders, with closest relevance to ASD.



Supplementary Figure 5.11 – Brain dimensions of adult *Brinp1* knockout mice

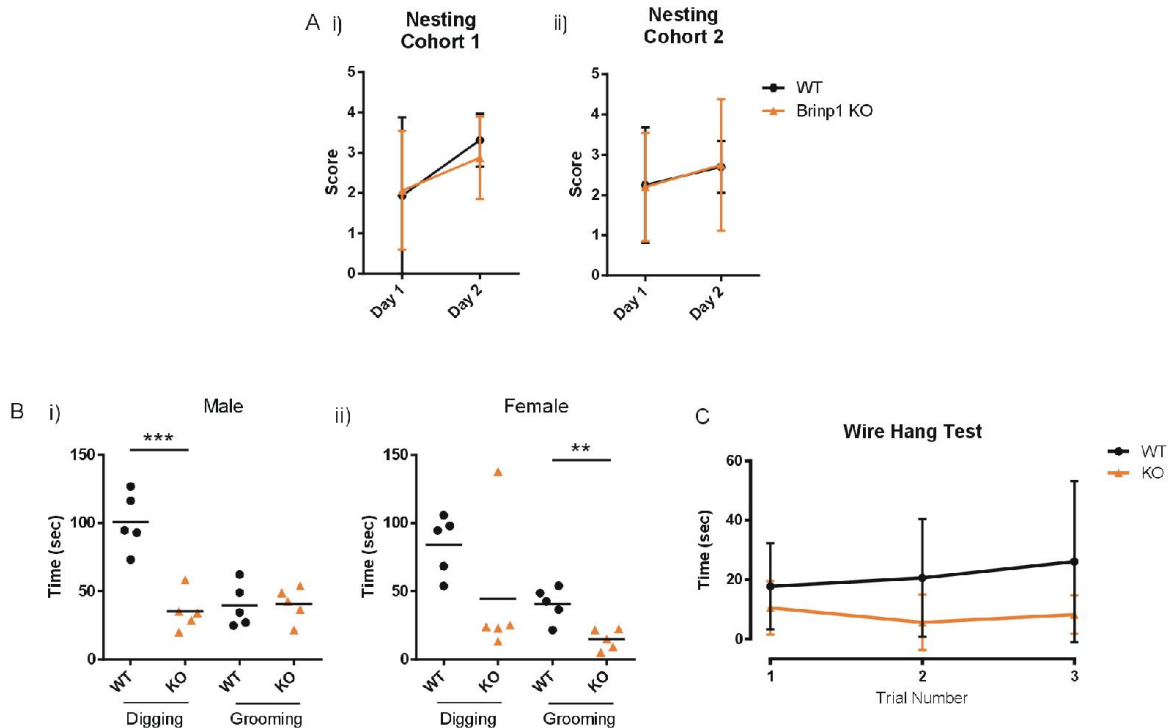
Brain measurements of mice that had previously been used for behavioral testing (from *Brinp1* Cohort 2) at 16 - 19 weeks of age were measured for A) Brain length, $t(9)=0.04992$, $p=0.9613$. B) Brain width, $t(9)=0.1069$, $p=0.9172$. C) Cerebral cortex length $t(9)=0.3568$, $p=0.7295$. D) Cerebellum width $t(9)=1.178$, $p=0.2688$. E) Cerebellum length, $t(9)=0.5267$, $p=0.6111$, unpaired Student's t-tests. Each data point indicates the response from one animal. The mean is shown as a horizontal line.



Supplementary Figure 5-12 – Distribution of BrdU positive cells in the cortex of E18.5 *Brinp1* KO embryos

- A) Coronal sections from E18.5 WT and *Brinp1* KO embryos, showing BrdU+ cell distribution following administration of BrdU to *Brinp1* heterozygous dams at the following time points: embryonic day 12.5 (E12.5), day 14.5 (E14.5) or day 16.5 (E16.5).
- B) No significant change in cell number of E12.5, E14.5 or E16.5 born cells (BrdU-labelled) in the E18.5 dentate gyrus. E12.5: $t(8)=0.7758$, $p=0.4602$, E14.5: $t(8)=0.2668$, $p=0.7973$, E16.5: $t(8)=0.01437$, $p=0.9890$, unpaired Student's t-test.

N=5 WT and 5 *Brinp1* KO mice. All images counter stained with 4',6-diamidino-2-phenylindole (DAPI, blue).



Supplementary Figure 5-13 – *Brinp1* KO mice: nesting observations, cage observations, and wire hang test

A) *Brinp1* KO nesting experiment. Five pairs of *Brinp1* KO females aged 2-3 month were tested for nest construction using the scoring system developed by Hess et al, 2008. *Brinp1* KO mice showed no impairment in nest construction at day 1 or day 2 after nest material was provided. Similar results were shown when the experiment was repeated with a second cohort. Results are shown as the mean \pm SD.

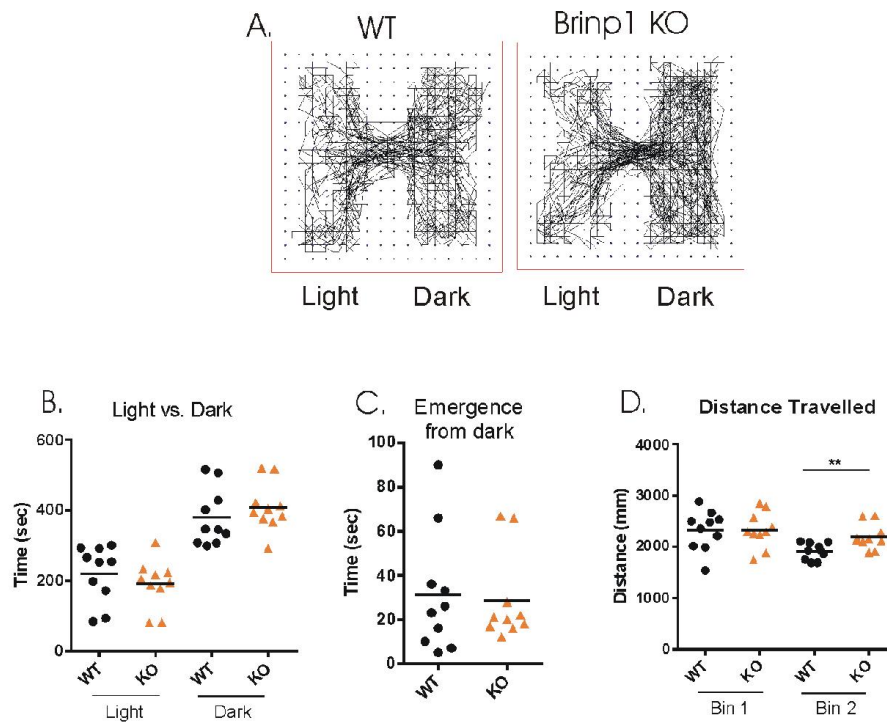
B) *Brinp1* KO self-directed behavior. *Brinp1* KO mice were observed for self-directed behavior in a test plexiglass cage lined with sawdust for 20 min. *Brinp1* KO mice showed a decrease in time digging, and a decrease in grooming duration (females only).

i) Male *Brinp1* KO mice showed a significant increase in digging duration: $t(8)=5.765$, $p=0.0004$, whilst no significant change in grooming duration: $t(8)=0.1366$, $p=0.8947$, unpaired Student's t -tests.

ii) Female *Brinp1* KO mice did not show a significant change in digging duration: $t(8)=1.555$, $p=0.1585$, but did exhibit a decrease in time grooming: $t(8)=3.977$, $p=0.0041$, unpaired Student's t -tests.

$N=5$ mice of each sex per genotype. $**p<0.01$, $***p<0.001$. Each data point represents the response from a single animal. The mean is shown as a horizontal line.

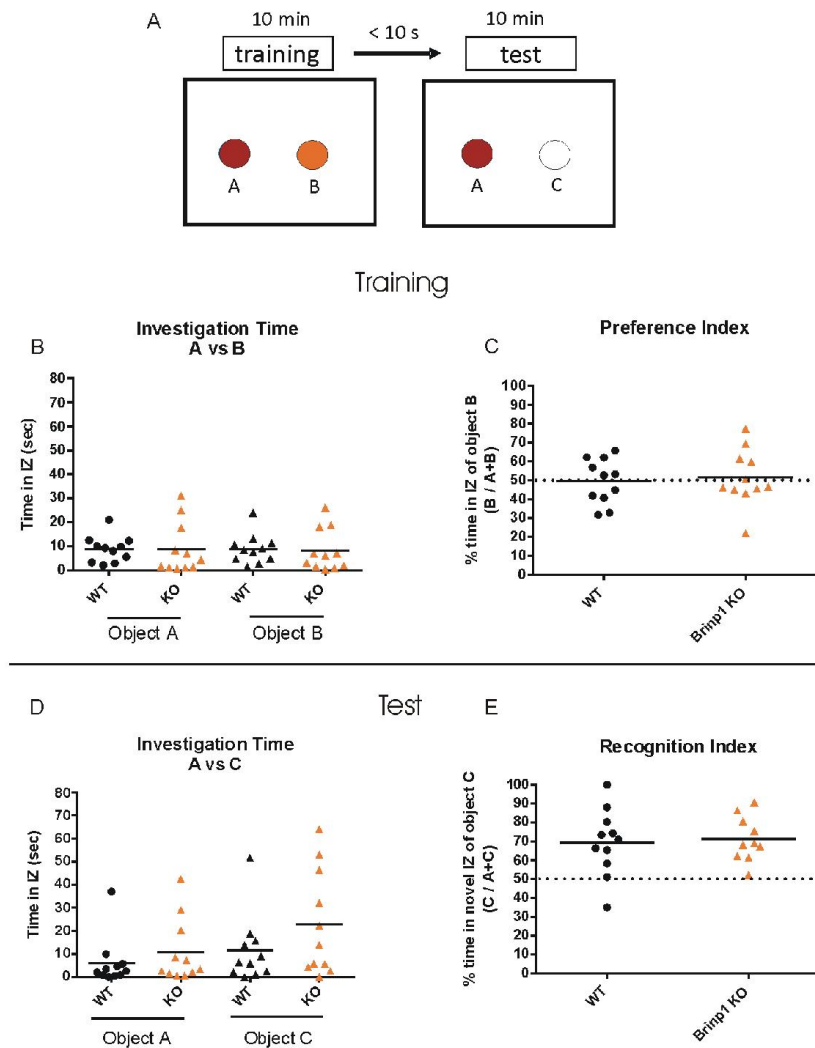
C) Wire hang test: *Brinp1* KO mice showed a significant reduction in time gripping onto a wire grid before releasing their grip, $F(1,22)=8.957$, $p=0.007$, repeat measures two-way ANOVA. There was no interaction effect between trial and genotype: $F(2,44)=0.865$, $p=0.428$. Each mouse was tested three times (trials 1, 2 and 3), with a 10 min interval between trials. Results shown as the mean \pm SD.



Supplementary Figure 5-14 – *Brinp1* KO mice: locomotor cell - light / dark

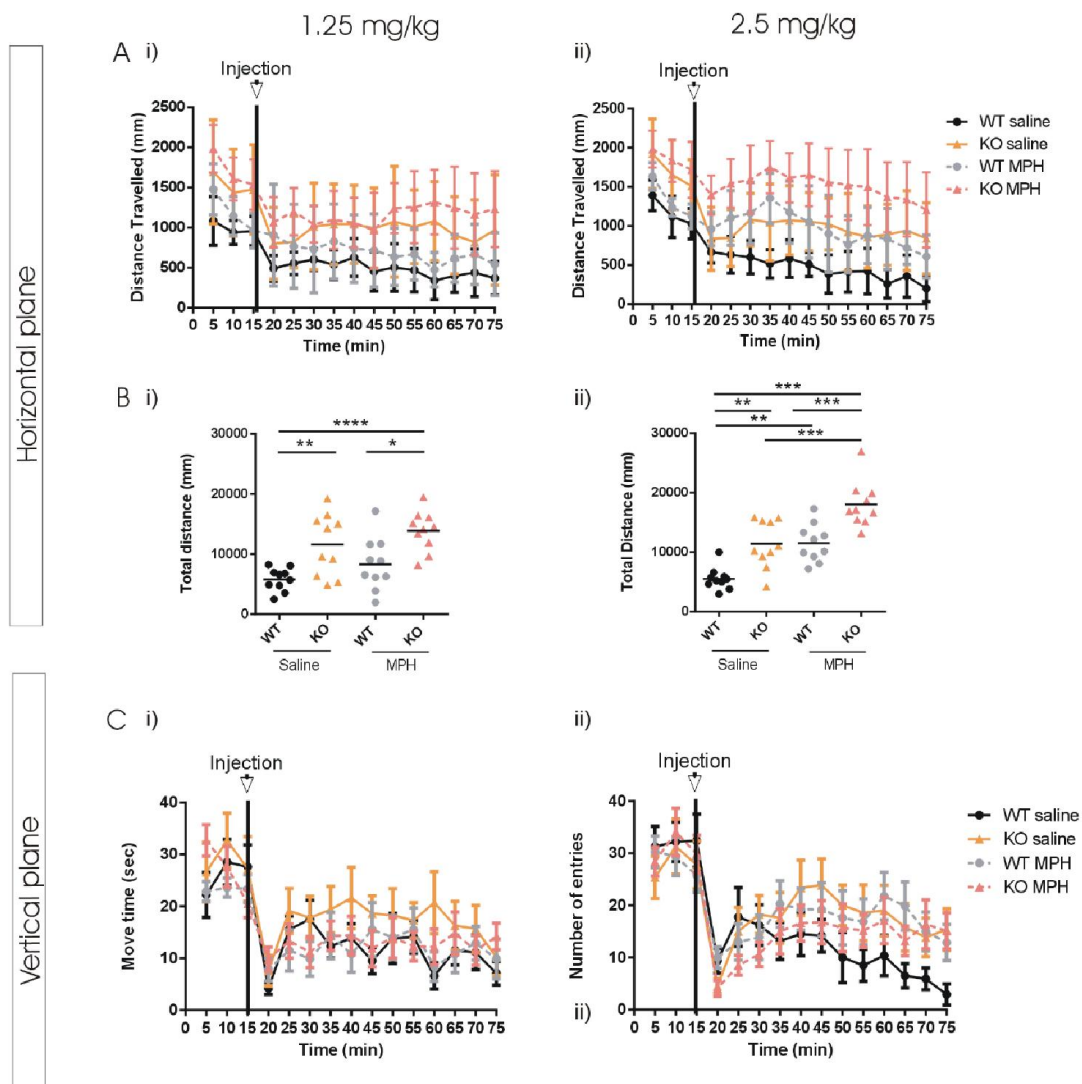
- A) Data traces illustrate movement of WT and *Brinp1* KO mice in the locomotor cell dark and light zones, for a 10 min duration.
- B) *Brinp1* KO mice showed no significant difference to WT in duration in light or dark zones. Light: $t(18)=0.8853$, $p=0.3877$. Dark: $t(18)=0.8853$, $p=0.3877$, unpaired Student's t-tests.
- C) *Brinp1* KO mice showed no significant difference to WT in initial time taken to emerge from the dark zone, $t(18)=0.2318$, $p=0.8193$, unpaired Student's t-test.
- D) *Brinp1* KO mice exhibited hyperactivity during the second 5 min interval of testing (bin 2), measured as horizontal plane distance in both light and dark zones. Bin 1: $t(18)=0.07573$, $p=0.9405$, Bin 2: $t(18)=3.012$, $p=0.0075$, unpaired Student's t-tests.

N=10 mice per genotype. ** $p<0.01$. Each data point indicates the response from one animal. The mean is shown as a horizontal line.



Supplementary Figure 5.15 – *Brinp1* KO mice: Novel object recognition test

- A) Arena layout for objects in the training and test trials. The same arena (35cm x 35cm x 35cm) was used for the training and test trials, with object B was replaced with object C between trials. A = familiar object, C = novel object. Trial durations are listed above.
- B) WT and *Brinp1* KO mice spend equivalent time investigating object A and object B in the training trial. Object A: $t(20)=0.04995$, $p=0.9607$. Object B: $t(20)=0.1954$, $p=0.8470$, unpaired Student's t-tests.
- C) Preference index (%) = $B / (A + B)$, where A and B are defined as time investigating object A and object B respectively. WT and *Brinp1* KO mice show a preference index of 50% in the training trial. This result demonstrates no bias for either object.
- D) No significant difference in time investigating object A and object C in the test trial for WT and *Brinp1* KO mice. Object A: $t(20)=0.8710$, $p=0.3941$, Object C: $t(20)=1.367$, $p=0.1869$, unpaired Student's t-test.
- E) Recognition index (%) = $C / (A + C)$, where A and C are defined as time investigating object A and C respectively. WT and *Brinp1* KO mice show a recognition index of 70% in the test trial. This result demonstrates that both WT and *Brinp1* KO mice showed a preference for a novel object over a familiar object. Each data point indicates the response from one animal. The mean is shown as a horizontal line.

Supplementary Figure 5-16 – The effect of MPH on *Brinp1* KO mice locomotor activity

Supplementary Figure 5-16 – The effect of MPH on *Brinp1* KO mice locomotor activity

- A) Horizontal plane distance travelled for WT and *Brinp1* KO mice, divided into 5 min bins, after doses of 1.25 mg/ml or 2.5 mg/ml of MPH or saline. Results are represented as the mean \pm SD.
- i) 1.25 mg/kg MPH / saline:
Analysis by repeat measures ANOVA performed on the distance travelled post injection (20 min+) showed an effect of genotype $F(1,36)=21.443$, $p<0.001$, and a close to significant effect of 1.25 mg/kg drug treatment $F(1,36)=3.852$, $p=0.057$.
 - ii) 2.5 mg/kg MPH / saline:
Analysis by repeat measures ANOVA performed on number of distance travelled post injection (20 min+) revealed an effect of genotype $F(1,36)=34.862$, $p<0.001$, and an effect of 2.5 mg/kg drug treatment $F(1,36)=36.079$, $p<0.001$, whereby administration of MPH resulted in a significant increase in distance travelled for both WT and KO mice.
- B) MPH increased the total horizontal plane distance travelled post injection (20 min+) for WT and *Brinp1* KO mice. Each data point represents the response from a single animal. The mean is shown as a horizontal line.
- i) A dose of 1.25 mg/kg of either saline or MPH resulted in a significant effect of treatment on total distance travelled: $F(3,36)=8.434$, $p<0.001$, one-way ANOVA. Multiple comparisons: WT saline and KO saline: $p=0.010$. WT saline and WT MPH: $p=0.481$. WT saline and KO MPH: $p<0.001$. KO saline and WT MPH: $p=0.252$. KO saline and KO MPH: $p=0.549$. WT MPH and KO MPH: $p=0.014$.
 - ii) A dose of 2.5 mg/kg of either saline or MPH resulted in a significant effect of treatment on total distance travelled: $F(3,36)=23.679$, $p<0.001$, one-way ANOVA. Multiple comparisons: WT saline and KO saline: $p=0.002$. WT saline and WT MPH: $p=0.002$. WT saline and KO MPH: $p<0.001$. KO saline and WT MPH: $p=1$. KO saline and KO MPH: $p<0.001$. WT MPH and KO MPH: $p=0.001$.
- C) Number of vertical plane entries for *Brinp1* KO and WT mice, divided into 5 min bins, after doses of 1.25 mg/ml or 2.5 mg/ml of MPH compared to saline. Results are represented as the mean \pm SD.
- i) 1.25 mg/kg MPH / saline:
No effect of genotype ($F(1,36)=1.202$, $p=0.208$) or drug: $F(1,36)=0.389$, $p=0.537$ on number of vertical plane entries, repeat measures two-way ANOVA performed on number of VP entries post injection (20 min +).
 - ii) 2.5 mg/kg MPH / saline:
No effect of genotype ($F(1,36)=0.263$, $p=0.611$), or drug: ($F(1,36)=0.137$, $p=0.713$) on number of vertical plane entries; repeat measures two-way ANOVA performed on number of VP entries post injection (20 min +).

Chapter 6: General Discussion

6.1 Discussion Overview

This thesis sheds light on the role of *Brinps* in neurobiology and neural development, and provides possible avenues for future investigation. To address the key aims, the discussion is divided into sections relating to the questions listed under the thesis aims (section 1.9), ending with an evaluation on whether the study findings align with the hypothesized model for *Brinps* (section 1.8), and suggested future directions.

6.1.1 Given that *Brinps* are almost exclusively expressed in the nervous system of mammals, does their absence result in changes to behavior?

A wide range of behavioral tests carried out in this study demonstrate the significant effect that the absence of *Brinp1* has on behavior. These behavioral phenotypes are comparable with other KO mouse models of NDDs. In Table 6-2, a comparison is provided for the *Brinp1* KO mouse phenotypes with two highly cited examples of established ASD mouse models: CNTNAP2 KO mice (Penagarikano et al., 2011) and ProSAP1/Shank2 KO mice (Schmeisser 2012). These examples are two of approximately twenty well-established ASD mouse models (Crawley, 2012), and were selected as examples because of similarities to *Brinp1* KO phenotype. Hyperactivity is a commonly reported secondary phenotype for ASD mouse models, with many other ASD KO models exhibiting increased activity, including examples provided, as well as FMR1 and NLGN3 KO mice (Bakker et al., 1994; Radyushkin et al., 2009). The *Brinp1* KO behavioral phenotype appears to show closest resemblance to CNTNAP2 KO mice. CNTNAP2 encodes a neuronal transmembrane protein member of the neurexin superfamily involved in neuron-glia interactions and clustering of K⁺ channels in myelinated axons (Poliak et al., 1999; 2003). The similarities in behavioral phenotype may be coincidental, considering some discrepancies in phenotype, however the resemblance in behavioral and pathological perturbations could indicate similar functions of the two genes.

As mentioned in section 5.8.3, a *Brinp1*-exon 8 KO mouse has been characterized by a competing group. Their results were published towards the end of our investigation into the *Brinp1*-exon3 KO phenotype (Kobayashi et al., 2014). Table 6-2 also provides a comparison of our reported phenotypes of the exon-3 deleted *Brinp1* KO mouse to the *Brinp1* exon-8 deleted mouse. The similar results from the characterization of two independent *Brinp1* knockout lines by different targeting strategies strengthens the conclusions of both studies.

Table 6-2 – Phenotype of *Brinp1* KO mice compared to examples of established ASD mouse models

		<i>Brinp1</i> KO mice		Comparison ASD mouse models	
Phenotype		<i>Brinp1</i> -exon3 KO (Berkowicz et al, 2015)	<i>Brinp1</i> -exon8 KO (Kobayashi et al., 2014)	CNTNAP2 KO (Penagarikano et al., 2011)	Shank2 KO (Schmeisser 2012)
Behavioural phenotype: Face Validity for ASD	Sociability interaction	↓ Social interaction	↓ Social interaction	↓ Social interaction	↓ Social interaction
	Altered USVs	↓ Call duration	-	↓ Number of calls	↓ Number of calls
	Repetitive grooming	↓ Grooming (♀ only)	-	↑ Grooming	↑ Grooming
Additional behavioral phenotype	Hyperactivity	↑ Activity	↑ Activity	↑ Activity	↑ Activity
	Hyper-exploration	↑ Exploration	↑ Exploration	-	↓ Exploration
	Memory impairment	↓ Altered memory	↓ Altered memory	↓ Spatial memory	↔
	Nest construction	↔	-	↓ nest construction	-
	Digging	↓ Digging	-	↓ Digging	↓ Digging
	Motor co-ordination	↔	↓ Co-ordination	↑ Co-ordination	↔
	Other phenotypes	-	-	Epilepsy	-
Neuropathology phenotype	Cortical Lamination	Altered projection neuron distribution	-	Altered projection neuron distribution	-
	Interneuron numbers	↑ PV+ cells	↑ PV+ cells	↓ PV+, CLB2+, NPY+ cells	-
	Neurogenesis	↔	↑ DG neurogenesis	-	-
	Dendrite morphology	-	-	-	↓ Dendritic spines.
	Synaptic transmission	-	-	↓ Neuronal synchronicity	↓ Neuronal synchronicity
	Changes in gene expression	↑ <i>Astn1</i> and <i>Astn2</i>	-	-	↓ Glutamate receptor
Predictive validity	Rescue of behavioural phenotype	↔ to methylphenidate (MPH increases activity)	-	Risperidone ↓ hyperactivity and repetitive grooming	mGluR5 antagonist ↑ sociability (Won et al., 2012)

Key: ↑ = increase, ↓ = decrease, ↔ = unchanged, - = untested, ♀ = female, CLB2 = calbindin2, NPY = neuropeptide Y, PV = parvalbumin

Both lines display the same core behavioral phenotypes of increased hyperactivity, decreased sociability, reduced anxiety and slight impairment in working memory. Our results add further insight into the *Brinp1* KO phenotype by exploring other aspects of behavior such as changes in ultrasonic vocalization, neonatal survival, and changes in self-directed behavior (digging and grooming).

6.1.2 *Brinp1*, *Brinp2* and *Brinp3* KO mice in context of neurodevelopmental disorders

In order for a knockout mouse genotype to be a good model for NDDs, three features should ideally be similar to the human disease. The behavioral and pathological phenotypes should match symptoms of the disease (face validity), the gene locus should associate with the disease in humans (construct validity) and the same treatments should be effective for both humans and the animal model (predictive validity) (Chadman et al., 2009; Nestler & Hyman, 2010). In reality, no mouse model matches all these criteria, due to differences in brain complexity between mice and humans, and the multigenic nature of NDDs. Listed below is a summary of potential implications of the *Brinp1* KO phenotype for neurodevelopmental disorders ASD, ADHD, ID and schizophrenia.

Autism Spectrum Disorder

The neuro-anatomical findings for the *Brinp1* KO mice are of particular interest due to studies reporting post-mortem anatomical changes in the autistic brain. For example, an increase in PV interneurons has been reported in the CA1 and CA3 hippocampal regions of post mortem autistic individuals (Lawrence et al., 2010). Disruptions in layer IV cortical lamination has also been reported in patients with autism (Stoner et al., 2014).

As described in chapter 5, *Brinp1* KO mice show aspects of face validity for ASD. It is satisfying that the behavioral phenotypes of the *Brinp1* KO mice appear to model the neurodevelopmental disorders connected at the *BRINP1/ASTN2* 9q33.1 loci (Lesch et al., 2008; Lionel et al., 2014; Romanos et al., 2008), and thereby showing a degree of construct validity. There is already some evidence that alterations to the *BRINP1* locus is associated with NDDs (Lionel et al., 2014). So far it is mutations to the *ASTN2* gene that have been found to show significant correlation with NDDs including ASD and ADHD (Lionel et al., 2014). The results from the *Brinp1* KO behavioral testing indicate that mutations in *BRINP1* may also

contribute to NDDs in humans, with a strong likelihood of ASD presentation based on the *Brinp1* KO phenotype. With the continual identification of additional risk genes from GWAS and CNV studies, *BRINP1* may also emerge as a risk gene for ASD.

The *Brinp1* KO mice have yet to be tested with drugs which have been shown to improve symptoms of ASD mouse models, and is a suggested area for future investigation. Predictive validity of *Brinp1* KO mice to ASD could be tested with Risperidone, which reduced the hyperactivity of CNTNAP2 KO mice (Penagarikano et al., 2011). An alternative approach would be testing *Brinp1* KO mice with a mGluR5 antagonist, which reverse the ASD-like phenotypes of Shank2 KO and FMR1 KO mice (Vinueza Veloz et al., 2012; Won et al., 2012).

Attention Deficit Hyperactivity Disorder

The hyperactivity phenotype of *Brinp1* KO mice shows face validity for one aspect of ADHD. There is still a need to test the knockout mice for face validity to aspects of inattention and impulsivity. The 5-choice serial reaction time test would be an ideal approach, as this paradigm has been established for assessing both attention and impulse control in rodents (Asinof & Paine, 2014; Higgins & Breysse, 2008).

Whilst the hyper-exploratory behavior of the *Brinp1* and *Brinp3* KO mice was not investigated further in this thesis, this behaviour may be interconnected with the reported hyperactivity, as hyper-exploratory behaviour has been reported for ADHD mouse models, such as the DAT1 KO mouse (Yamashita et al., 2013).

In this study, predictive validity of *Brinp1* KO mice for ADHD was tested by the administration of methylphenidate. By responding to the drug in a similar manner to WT (increased activity), the results indicated that *Brinp1* KO mice pathology is different to ADHD patients that respond positively to MPH. This does not necessarily preclude a link between *BRINP1* and ADHD, as many ADHD patients do not respond to MPH (Contini et al., 2013). Other drugs that could be used to test for *Brinp1* KO mice predictive validity to ADHD include amphetamine (a dopamine reuptake inhibitor) or Atomoxetine (a nor-epinephrine re-uptake inhibitor).

Intellectual Disability

The increase of PV-positive interneurons in the hippocampus and neocortex may contribute to the reported memory impairment of *Brinp1* KO mice, since interneuron dysfunction has been reported in several mouse models of intellectual disability, which also display memory deficits (Marin, 2012). The results from this study indicate alterations to the *BRINP1* locus may result in changes in neuronal connectivity that contribute to learning impairments associated with ID and ASD co-morbidity.

Schizophrenia

Whilst the *BRINP1* locus has been associated with schizophrenia (Vawter et al., 2011), there is limited face validity for *Brinp1* KO mice for the disorder. *Brinp1* KO mice showed no deficit in sensory gating, which is compromised in many patients with schizophrenia (Boutros et al., 2009; Sanchez-Morla et al., 2008). However, altered sensory gating is just one aspect of this complex disorder, and the only endophenotype that can be reliably modelled in mice. Therefore the result does not preclude a potential association between *BRINP1* and schizophrenia.

Other neurological disorder

As a final point in relation to neurological disorders, the mice in this study were tested at an age equivalent to early human adulthood. This leaves open the possibility of an age related phenotype for *Brinp* KO mice. Investigation of aging in *Brinp1* KO mice would allow assessment of a phenotype relevant to *BRINP1* association to age onset disorders such as Parkinson's disease and Alzheimer's disease (Do et al., 2011; Edwards et al., 2010; Heinzen et al., 2010). Now that the *Brinp1* KO line has been established, a suggested future area of investigation is the behavioral study of aged *Brinp1* KO mice to determine whether *BRINP1* disruption influence cognitive decline or age-related motor function.

The findings of this study are summarized in Figure 6-1; linking behavioral phenotypes of neuronal-MACPFs with genetic studies of human NDD and knowledge of underlying cellular processes.



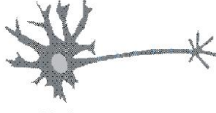
Chromosome	Gene	 Human	 Mouse	 Cellular Process
Chromosome 9 – Humans 4 – Mice	<i>BRINP1</i>	<ul style="list-style-type: none"> Undisclosed Neurodevelopmental Disorder 	<ul style="list-style-type: none"> Decreased sociability Shorter USV calls Hyperactivity Hyper-exploration Reduced neonate survival Altered memory 	<ul style="list-style-type: none"> Altered lamination of projection neurons Increased in PV-positive Interneurons
	<i>ASTN2</i>	<ul style="list-style-type: none"> ASD ADHD Intellectual disability Tourette's syndrome 	<ul style="list-style-type: none"> Unknown 	<ul style="list-style-type: none"> Neuronal migration Trafficking of Astn1
Chromosome 1 – Humans 1 – Mice	<i>ASTN1</i>	<ul style="list-style-type: none"> Undisclosed Neurodevelopmental disorder Alcohol dependence 	<ul style="list-style-type: none"> Impaired motor co-ordination 	<ul style="list-style-type: none"> Glial guided neuronal migration
	<i>BRINP2</i>	<ul style="list-style-type: none"> Addiction 	<ul style="list-style-type: none"> Enhanced Rotarod Performance 	<ul style="list-style-type: none"> Unknown
	<i>BRINP3</i>	<ul style="list-style-type: none"> Unknown 	<ul style="list-style-type: none"> Hyper-exploration 	<ul style="list-style-type: none"> Unknown

Figure 6-1 – Summary of neuronal-MACPF gene association with neurodevelopmental disorders, knockout mouse phenotypes, and cellular processes

Findings from this study are emphasized in bold text.

6.1.3 Evaluating the hypothesis: *Brinps* facilitate migration of post-mitotic neurons

If all three *Brinps* are required for the same cellular process, in the same cell type, we would expect to see identical phenotypes when any single gene is absent in a knockout animal. This is not the case, with each of the three *Brinp* KO lines having a distinct behavioral phenotype, and the *Brinp1* KO showing the most pronounced phenotype. The *Brinp2/3* KO mouse showed no clear phenotypic enhancement or additional phenotypes compared to the single gene knockouts of *Brinp2* and *Brinp3*, indicating that these two genes have separate molecular roles in the mammalian brain. This is supported by *in-situ* hybridization data, where *Brinp2* and *Brinp3* are expressed at different developmental time points and often in different brain regions (Kawano et al, 2004, Allen Mouse Brain Atlas). The up-regulation of Astrotactins in the *Brinp1* KO mouse brain suggests that *Brinp1* may function in a similar developmental process to *Astn1* and *Astn2*, possibly in neuronal migration.

The perturbations in the *Brinp1* KO neocortex are suggestive of a neuronal migration defect. These experimental data hint at a role of *Brinp1* in neuronal migration similar to that of either Astrotactin. There is however no obvious overlap between the *Brinp1* and *Astn1* KO behavioral phenotypes, but it should be noted that the *Astn1* KO mice have not been fully characterized by standard behavioral tests. The lack of a motor co-ordination deficit of the *Brinp1* KO mice implies normal cerebellar development and no impairment in granule cell migration in the cerebellar cortex, as observed for the *Astn1* KO mice. It is difficult to explain the absence of a motor co-ordination phenotype, given that *Brinp1* is highly expressed in the same cerebellum layers as *Astn1*. If the lack of *Brinp1* is compensated for by *Astn1*, a *Brinp1/Astn1* double KO should show a greater impairment in motor co-ordination than *Astn1* KO alone.

The generation and characterization of an *Astn2* KO mouse is a key next step to understanding the molecular role of neuronal-MACPFs in the developing cortex. *Brinp1* and *Astn2* are expressed in overlapping brain regions in the mouse brain. If the *Astn2* behavioral phenotype is akin to the autism-like deficits of the *Brinp1* KO mouse, this would strengthen the hypothesis that *Astn2* and *Brinp1* have a common function *in vivo*. The *Astn2* KO mouse is predicted to show neuronal migration deficits, based on vitro experiments describing a role of *Astn2* in facilitating neuronal migration (Wilson et al., 2010). The mice may show a similar

neuronal layering deficit of the *Brinp1* KO neocortex, as well as changes in PV-positive interneuron numbers. Also, if *Brinp1* and Astrotactins do have a common function, the *Brinp1/Astn1* double KO or *Brinp1/Astn2* double KO are predicted to have an increased severity of the neuroanatomical and behavioral phenotypes, which would result in more dramatic neuroanatomical defects.

6.1.4 Future directions

6.1.4.1 Determine a link between the *Brinp1* KO behavioural phenotypes and reported anatomical changes.

The increase in PV+ interneurons in both the neocortex and hippocampus of *Brinp1* KO mice, along with the decrease in pyramidal layer IV neurons in the somatosensory cortex provide an insight into the effect of *Brinp1* on neuronal distribution within the mammalian brain. The cortical perturbations in these regions strongly correlate with the high expression of *Brinp1* in the developing and adult mouse brain mouse for regions described in chapter 4 (Allen Mouse Brain Atlas)(Kawano et al., 2004).

The next step in this investigation would be to connect the observed cortical perturbations for *Brinp1* KO mice with the reported behavioral phenotypes, by investigating changes in brain activity. We hypothesize that the perturbations in neuronal distribution will impact local neuro-circuitry activity within the cortex, resulting in changes in cortical excitability. This is particularly likely, as GABAergic interneurons are recognized as playing a crucial role in the precise timing of neuronal activity (Sohal et al., 2009). A suggested approach to investigate neuronal excitability would be to investigate neuronal firing in the brains of *Brinp1* KO mice, in a similar manner to the two-photon calcium imaging performed on CNTNAP2 KO mice (Penagarikano et al., 2011). This experiment measured network activity *in vivo* using calcium-sensitive dyes, where changes in fluorescence reflect changes in spontaneous firing of individual neurons within cortex (Golshani & Portera-Cailliau, 2008). Similar techniques can also be performed *in vitro* by measuring neuronal network activity in cortical brain slices (Dawitz et al., 2011). CNTNAP2 KO show asynchronous firing of neurons within networks within the somatosensory neocortex (Penagarikano et al., 2011). This is of particular relevance due to the reported changes in PV+ interneuron and projection neuron populations in both CNTNAP2 and *Brinp1* KO mice, and increasing evidence of abnormal

neural synchrony as a pathophysiological mechanism in ASD (Belmonte et al., 2004; Uhlhaas & Singer, 2006) *Brinp1* KO mice are predicted to also exhibit asynchronous neuronal firing in the somatosensory neocortex.

Experimental evidence is still needed to explain the mechanism that leads to an increase in PV-positive cells in the *Brinp1* KO mouse brain. To test our hypothesis of impaired neuronal migration being the underlying cause, we would need to determine whether the increase in interneuron populations is offset by a loss of interneurons in other regions of the neocortex. Investigation of other brain regions outside the somatosensory cortex, such as the prefrontal cortex, would determine whether the cortical perturbations are a global or represent a localized change in the mouse brain. One possible experimental approach is to track interneuron populations by crossing the *Brinp1* KO mice with an interneuron-GFP line, e.g. PV-EGFP line to monitor the positioning of PV-positive interneurons during embryonic development (Meyer et al., 2002). This would allow for the tracking of interneurons from their origin in the ganglionic eminence, as they migrate into the developing neocortex and hippocampus.

This thesis focuses on the neuro-anatomical changes in the *Brinp1* KO mouse. Questions remain as to whether neuroanatomical changes are also present in the *Brinp2* or *Brinp3* KO mouse. A suggested future focus for the *Brinp3* KO mouse is the investigation of neuroanatomical changes in the amygdala, in order to explore the cellular basis of the apparent reduced anxiety of these mice. Additionally, the investigation of the *Brinp1/2/3* KO brain may reveal more severe changes in cortical lamination. Viability issues concerning the *Brinp1/2/3* KO mice could be overcome by altering breeding strategies. For example generating and breeding *Brinp1/2/3^{FLPe}* mice, before crossing with a global Cre-recombinase line may improve survival. Alternatively, neuron-specific *Brinp1/2/3* KO mice could be generated by breeding *Brinp1/2/3^{FLPe}* mice with a Nestin-Cre line.

6.1.4.2 Determine the molecular role for *Brinps*.

There is still a need to determine where in neurons *Brinps* are expressed. Determining whether the subcellular localization is at the cell body, along axons / dendrites, or at the synapse, would greatly help to determine the role for *Brinps* in the adult mouse brain.

Demonstration of *Brinps* in endosomes or at the cell membrane of migrating neurons would be needed to verify a role in cell adhesion and/or neuronal migration.

Attempts were made during the course of this study to identify endogenous BRINP1 with a custom made monoclonal and polyclonal antibody on neuronal cultures and brain tissue to investigate localization. Whilst the polyclonal antibody detected endogenous BRINP1 by immunoblotting, no consistent detection of endogenous protein could be observed by immunofluorescence of WT primary neurons or immunohistochemistry of WT cortical sections. The development of an antibody that detects endogenous BRINP1 on fixed tissue or cells would provide key information on the subcellular localization of BRINP1, which would in turn help decipher the molecular mechanism of BRINP1. The development of antibodies to BRINP2 and BRINP3 would also provide information on BRINP2 and BRINP3 subcellular localization and molecular role.

Key molecular experiments are still required to determine whether a combined role *in vivo* would occur via protein-protein interaction of neuronal-MACPF proteins. Interaction would be confirmed by immuno-precipitation experiment using either an Astrotactin2 and BRINP1 antibody, or tagging of both proteins and pull down using an antibody to the tagged protein. Alternatively, performing the *in vitro* migration blocking assays as described by Fishell and Hatten, using a BRINP1 antibody could determine a role for BRINP1 in glial guided neuronal migration (Fishell & Hatten, 1991). Whilst these results from this thesis indicate a possible role for BRINP1 in neuronal migration, further experiments are needed to verify the result, e.g. demonstration of *in vivo* neuron glia binding in the presence / absence of a BRINP1 antibody.

Chapter 7: Appendix

7.1 Anti-BRINP1 antibody generation

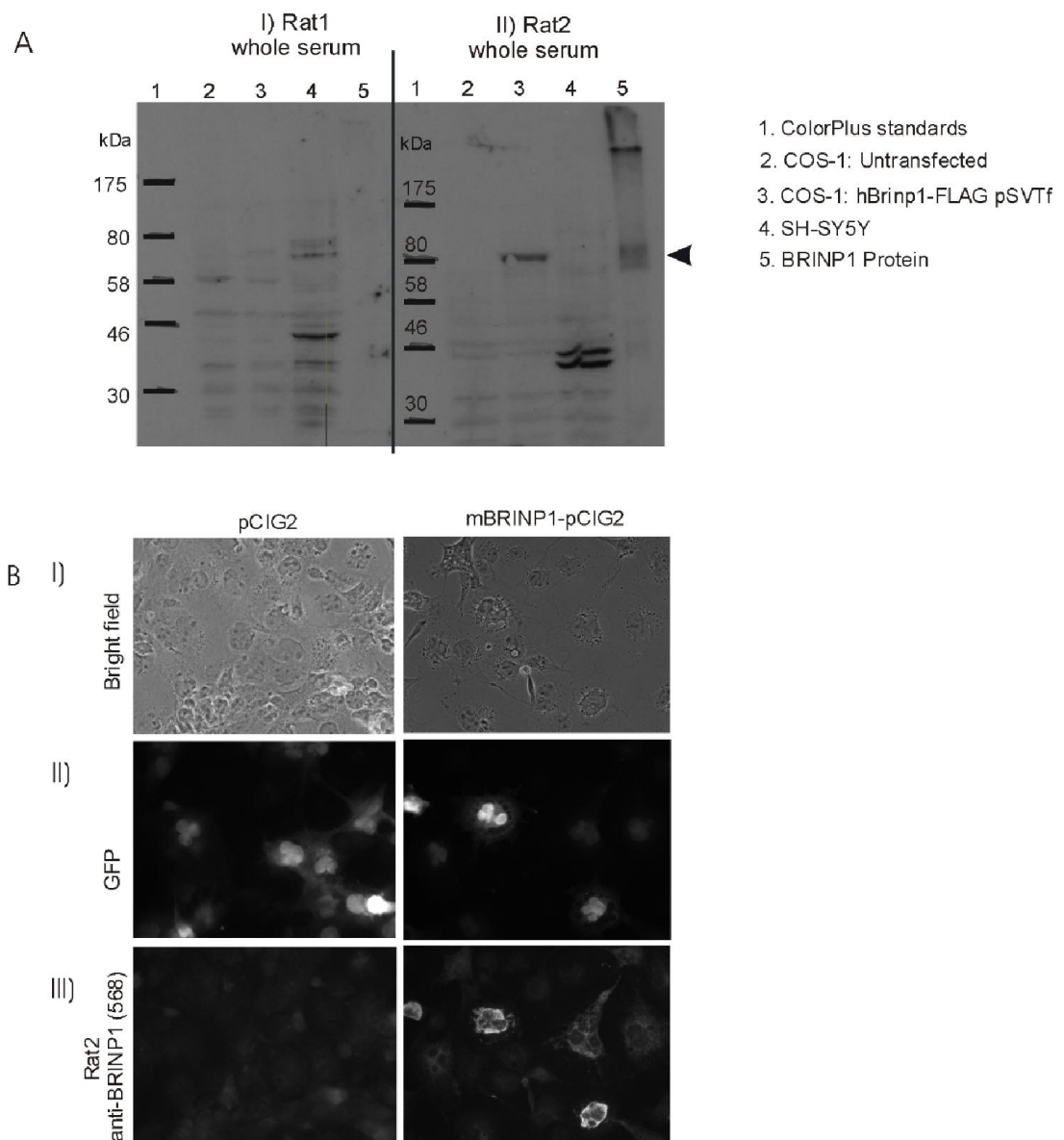
Full length recombinant BRINP1 protein (85kDa) was made by the laboratory of Dr. Natalie Borg using a Baculovirus expression system. Denatured protein in gel pieces was sent to the Western Australia Institute of Medical Research Antibody Facility, where the protein was injected into two rats (rat 1 and rat 2). The rats received additional boosts (2nd, 3rd and 4th boosts), from a mixture of soluble and insoluble BRINP1 protein fragments. Following the 4th boost, rats were sacrificed and serum from rat 1 and rat 2 were provided to the candidate.

The 4th bleed serum from rat 1 and rat 2 were validated by immunoblotting of COS-1 cell lysates that had been transiently transfected with a human-BRINP1-FLAG *pSVTf* expression vector. A negative control of untransfected COS-1 lysates, and a positive control of recombinant full length protein were tested alongside. In addition, the neuroblastoma cell line SH-SY5Y was also tested. Rat 2 sera showed the best recognition to hBRINP1 for both the transfected COS1 cells and recombinant BRINP1 protein, evident as a prominent 85 kDa protein species. A protein species of this size was absent from the untransfected COS-1 cell lysates (Appendix Figure 6-2A).

The rat 2 4th bleed serum was tested by indirect immunofluorescence on COS-1 cells that had been transiently transfected with a mouse-BRINP1 *pCig2-ires-GFP* expression vector. COS-1 cells transfected with the *pCig2-ires-GFP* expression vector were tested alongside as a negative control. Transient transfection of the COS-1 cells was observed as GFP fluorescence in the nuclei for both transfections. Indirect immunofluorescence was performed using the rat2 sera, followed by an anti-rat AF568 secondary antibody. This resulted in mBRINP1 *pCig2-ires-GFP* transfected cells showing positive staining. No fluorescence at the 568 nm wavelength was observed for the *pCig2-ires-GFP* negative control cells (Appendix Figure 6-2B). This result, together with the immunoblotting result, demonstrates specificity of the rat 2 sera to human and mouse BRINP1 antigen.

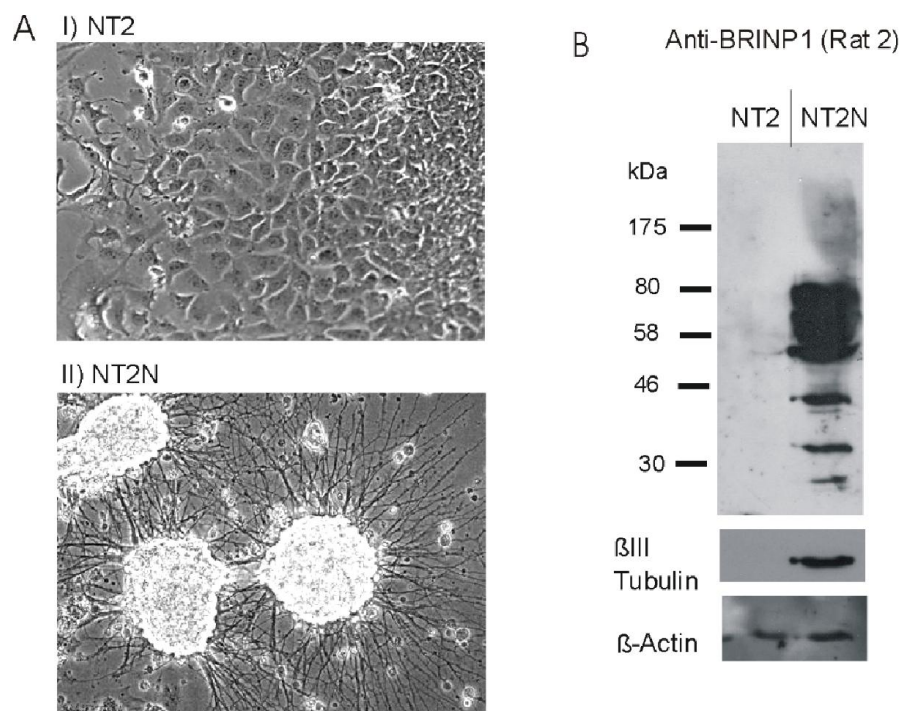
The rat2 sera was tested for recognition of endogenous BRINP1 using NT2N cells; a differentiated form of the human teratocarcinoma-derived Ntera2/D1 (NT2) cell line. NT2 cells were differentiated using 5 μ M all-trans retinoic acid into NT2N, following a protocol developed by Cheung et al (Cheung et al., 1999). NT2 and NT2N cell lysates were probed by immunoblotting with the rat 2 anti-BRINP1 sera. BRINP1 was shown to be induced upon

differentiation, by the presence of an 85 kDa species in the NT2N differentiated cells, which was not present for the NT2 cells (Appendix Figure 6-3). The rat2 anti-BRINP1 sera was therefore used as the polyclonal antibody for validation of *Brinp1* KO mice in Figure 3-10.



Appendix Figure 6-2 – BRINP1 antibody validation

- A) Testing of 4th bleed sera from two rats immunized with full length BRINP1 (Rat 1 and Rat 2). Results show immunoblotting of COS-1 cell lysates (mock), COS-1 cell lysates transfected with human-BRINP1-FLAG *pSVTf*, SH-SY5Y cell lysates and full-length recombinant BRINP1 protein. A prominent 85 kDa protein species was present for the hBRINP1 transfected COS-1 lysates when probed with the Rat 2 sera.
- B) COS-1 lysates were transfected with pCIG2-GFP (mock) and BRINP1 pCIG2-GFP.
- I) Bright field images of pCIG2 and mBRINP1-pCIG2 transfected COS-1 cells.
- II) pCIG2 and mBRINP1-pCIG2 transfected cells show nuclear GFP fluorescence.
- III) The anti-BRINP1 Rat2 sera detects recombinant BRINP1 in mBRINP1-pCIG2 transfected cells. No fluorescence observed for pCIG2 transfected (mock) COS-1 cells.



Appendix Figure 6-3 – BRINP1 is induced upon differentiation with retinoic acid

- A) A monolayer of undifferentiated teratocarcinoma-derived Ntera2/D1 cell line, NT2 (figure I) was differentiated with 5 μ M all-trans retinoic acid, following a protocol developed by Cheung et. al (Cheung et al., 1999), into neuron-like NT2N neural spheres, with neurite outgrowth (figure II).
- B) Immuno-blotting of NT2 and NT2N cell lysates, probed with the rat 2 anti-BRINP1 sera (1:200). Loading controls are β III tubulin (a marker of differentiated neurons) and β -Actin (present in both differentiated and undifferentiated cells). BRINP1 was detected in the differentiated NT2N lysate as a 85 kDa species. Smaller species were also detected by the antibody, indicating BRINP1 processing or breakdown products.

7.2 Supplementation of *Brinp1* het breeder diet with sunflower seeds.

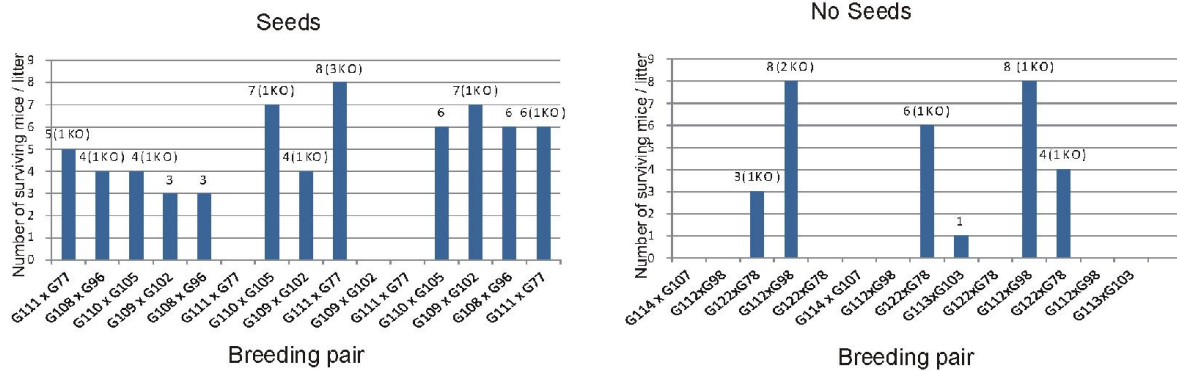
Dietary supplementation of sunflower seeds has been reported to improve survival of rodents with poor reproductive rates (Hess et al., 1981). As reported in chapter 3 of this thesis, *Brinp1* heterozygous and knockout mice exhibited reduced neonate survival (Figure 3-12). An experiment was conducted to investigate dietary supplementation for the *Brinp1* line in an attempt to improve litter survival.

Eight breeding pairs of *Brinp1* heterozygous mice were set up. Breeders were of the same generation, and heterozygous littermate breeders were divided between the two groups of four breeding pairs (group 1 and group 2). Group one was fed a standard diet of Barastoc animal feed. The second group were fed the same Barastoc animal feed and an addition to their diet of sunflower seeds (approximately 3 g). Sunflower seeds were given to breeders weekly from when initially set up, and to pups in the first week of being weaned. Litters were monitored for four months.

Whilst there was no significant difference in the total number of litters between WT and knockout mice, the survival rate of pups from breeders fed a seed diet dramatically improved; doubling from 30 pups to 63 pups. 57% of the 'No seeds' litters resulted in death of the entire litter (8 out of 14 litters). In contrast, only 3 out of 15 litters (20%) did not survive when breeders were fed seeds. For those litters that did survive, there was no significant change in the average number of pups per litter, or ratio of *Brinp1* KO mice. These results indicate that sunflower seeds improve overall litter survival, with no specific effect on *Brinp1* KO survival (Appendix Figure 6-4).

Following this experiment, the diet of breeders and weaned infants from all mouse lines (*Brinp1*, *Brinp2*, *Brinp3*, *Brinp2/3* and *Brinp1/2/3*) was supplemented with sunflower seeds. For the reported reproductive rates of *Brinp1* KO mice in chapter 5 (Table 5-1) all breeders were fed on a diet supplemented with sunflower seeds.

A.



B.

	Seeds	No seeds
Number of litters born	15	14
Number of full litters found dead	3	8
Number of pups born (recorded)*	66	39
Number of pups weaned (P21)	63	30
Number of <i>Brinp1</i> KO mice	10 (17%)	6 (20%)

Appendix Figure 6-4 – The effect of dietary supplementation with sunflower seeds on the reproductive success of *Brinp1* heterozygous breeders.

Four pairs of *Brinp1* heterozygous breeders were fed a weekly dietary supplement of sunflower seeds. A control group of four pairs of heterozygous breeders were fed only a standard diet, without sunflower seed supplementation.

- A) Graphs show the number of mice per litter surviving to age of weaning for every litter born over the four month experiment. The number of *Brinp1* KO mice born is shown in brackets above.
- B) Litter sizes and postnatal survival of offspring from *Brinp1* heterozygous mice supplemented with sunflower seeds. *In some instances, litters were cannibalized before litter sizes could be recorded.

7.3 Bibliography

- Adams, N. C., Tomoda, T., Cooper, M., Dietz, G., & Hatten, a. M. E. (2002). Mice that lack astrotactin have slowed neuronal migration. *Development*.
- Ahmed, A. O., & Bhat, I. A. (2014). Psychopharmacological treatment of neurocognitive deficits in people with schizophrenia: a review of old and new targets. *CNS Drugs*, 28(4), 301-318. doi: 10.1007/s40263-014-0146-6
- Alarcon, M., Abrahams, B. S., Stone, J. L., Duvall, J. A., Perederiy, J. V., Bomar, J. M., et al. (2008). Linkage, association, and gene-expression analyses identify CNTNAP2 as an autism-susceptibility gene. *Am J Hum Genet*, 82(1), 150-159. doi: 10.1016/j.ajhg.2007.09.005
- Alkam, T., Hiramatsu, M., Mamiya, T., Aoyama, Y., Nitta, A., Yamada, K., et al. (2011). Evaluation of object-based attention in mice. *Behav Brain Res*, 220(1), 185-193. doi: 10.1016/j.bbr.2011.01.039
- Altman, J. (1969). Autoradiographic and histological studies of postnatal neurogenesis. 3. Dating the time of production and onset of differentiation of cerebellar microneurons in rats. *J Comp Neurol*, 136(3), 269-293. doi: 10.1002/cne.901360303
- Altman, J., & Bayer, S. A. (1990). Prolonged sojourn of developing pyramidal cells in the intermediate zone of the hippocampus and their settling in the stratum pyramidale. *J Comp Neurol*, 301(3), 343-364. doi: 10.1002/cne.903010303
- Alvarez-Buylla, A. (1997). Mechanism of migration of olfactory bulb interneurons. *Semin Cell Dev Biol*, 8(2), 207-213. doi: 10.1006/scdb.1996.0134
- Amaral, D. G., Schumann, C. M., Nordahl, C. W., Amaral, D. G., Schumann, C. M., & Nordahl, C. W. (2008). Neuroanatomy of autism. *Trends Neurosci*, 31(3), 137-145. doi: 10.1016/j.tins.2007.12.005
- Anderson, S. A., Kaznowski, C. E., Horn, C., Rubenstein, J. L., & McConnell, S. K. (2002). Distinct origins of neocortical projection neurons and interneurons in vivo. *Cereb Cortex*, 12(7), 702-709.
- Anderson, S. A., Marin, O., Horn, C., Jennings, K., & Rubenstein, J. L. (2001). Distinct cortical migrations from the medial and lateral ganglionic eminences. *Development*, 128(3), 353-363.
- Andrews, W., Liapi, A., Plachez, C., Camurri, L., Zhang, J., Mori, S., et al. (2006). Robo1 regulates the development of major axon tracts and interneuron migration in the forebrain. *Development*, 133(11), 2243-2252. doi: 10.1242/dev.02379
- Ang, E. S., Jr., Haydar, T. F., Gluncic, V., & Rakic, P. (2003). Four-dimensional migratory coordinates of GABAergic interneurons in the developing mouse cortex. *J Neurosci*, 23(13), 5805-5815.
- Angelakopoulou, A., Shah, T., Sofat, R., Shah, S., Berry, D., Cooper, J., et al. (2012). Comparative analysis of genome-wide association studies signals for lipids, diabetes, and coronary heart disease: Cardiovascular Biomarker Genetics Collaboration. *European Heart Journal*. doi: 10.1093/eurheartj/ehr225
- Armstrong, C., Krook-Magnuson, E., & Soltesz, I. (2012). Neurogliaform and Ivy Cells: A Major Family of nNOS Expressing GABAergic Neurons. *Front Neural Circuits*, 6, 23. doi: 10.3389/fncir.2012.00023
- Arnold, L. E., Hodgkins, P., Kahle, J., Madhoo, M., Arnold, L. E., & Kewley, G. (2015). Long-Term Outcomes of ADHD: Academic Achievement and Performance. *J Atten Disord*. doi: 10.1177/1087054714566076
- Asinof, S. K., & Paine, T. A. (2014). The 5-choice serial reaction time task: a task of attention and impulse control for rodents. *J Vis Exp*(90), e51574. doi: 10.3791/51574
- Bakker, C. E., Verheij, C., Willemsen, R., van der Helm, R., Oerlemans, F., Vermey, M., et al. (1994). Fmr1 knockout mice: a model to study fragile X mental retardation. The Dutch-Belgian Fragile X Consortium. *Cell*, 78(1), 23-33.
- Bayer, S. A. (1980). Development of the hippocampal region in the rat. II. Morphogenesis during embryonic and early postnatal life. *J Comp Neurol*, 190(1), 115-134. doi: 10.1002/cne.901900108

- Bayer, S. A. (1983). 3H-thymidine-radiographic studies of neurogenesis in the rat olfactory bulb. *Exp Brain Res*, 50(2-3), 329-340.
- Beetz, C., Brodoehl, S., Patt, S., Kalff, R., & Deufel, T. (2005). Low expression but infrequent genomic loss of the putative tumour suppressor DBCCR1 in astrocytoma. *Oncol Rep*, 13(2), 335-340.
- Bellani, M., Nobile, M., Bianchi, V., van Os, J., & Brambilla, P. (2013). Genotype by environment interaction and neurodevelopment III. Focus on the child's broader social ecology. *Epidemiol Psychiatr Sci*, 22(2), 125-129. doi: 10.1017/S2045796013000061
- Belmonte, M. K., Allen, G., Beckel-Mitchener, A., Boulanger, L. M., Carper, R. A., & Webb, S. J. (2004). Autism and abnormal development of brain connectivity. *J Neurosci*, 24(42), 9228-9231. doi: 10.1523/JNEUROSCI.3340-04.2004
- Berke, G. (1995). The CTL's kiss of death. *Cell*, 81(1), 9-12.
- Bernardini, L., Alesi, V., Loddo, S., Novelli, A., Bottillo, I., Battaglia, A., et al. (2010). High-resolution SNP arrays in mental retardation diagnostics: how much do we gain? *Eur J Hum Genet*, 18(2), 178-185. doi: 10.1038/ejhg.2009.154
- Bhakdi, S., & Trnnum-Jensen, J. (1978). Molecular nature of the complement lesion. *Proc Natl Acad Sci U S A*, 75(11), 5655-5659.
- Bhakdi, S., & Trnnum-Jensen, J. (1986). C5b-9 assembly: average binding of one C9 molecule to C5b-8 without poly-C9 formation generates a stable transmembrane pore. *J Immunol*, 136(8), 2999-3005.
- Bis, J. C., DeCarli, C., Smith, A. V., van der Lijn, F., Crivello, F., Fornage, M., et al. (2012). Common variants at 12q14 and 12q24 are associated with hippocampal volume. *Nat Genet*, 44(5), 545-551. doi: 10.1038/ng.2237
- Boutros, N. N., Brockhaus-Dumke, A., Gjini, K., Vedeniapin, A., Elfakhani, M., Burroughs, S., et al. (2009). Sensory-gating deficit of the N100 mid-latency auditory evoked potential in medicated schizophrenia patients. *Schizophr Res*, 113(2-3), 339-346. doi: 10.1016/j.schres.2009.05.019
- Brazel, C. Y., Romanko, M. J., Rothstein, R. P., & Levison, S. W. (2003). Roles of the mammalian subventricular zone in brain development. *Prog Neurobiol*, 69(1), 49-69.
- Brown, W. T., Jenkins, E. C., Cohen, I. L., Fisch, G. S., Wolf-Schein, E. G., Gross, A., et al. (1986). Fragile X and autism: a multicenter survey. *Am J Med Genet*, 23(1-2), 341-352.
- Brugha, T. S., McManus, S., Bankart, J., Scott, F., Purdon, S., Smith, J., et al. (2011). Epidemiology of autism spectrum disorders in adults in the community in England. *Arch Gen Psychiatry*, 68(5), 459-465. doi: 10.1001/archgenpsychiatry.2011.38
- Butt, S. J., Fuccillo, M., Nery, S., Noctor, S., Kriegstein, A., Corbin, J. G., et al. (2005). The temporal and spatial origins of cortical interneurons predict their physiological subtype. *Neuron*, 48(4), 591-604. doi: 10.1016/j.neuron.2005.09.034
- Bymaster, F. P., Katner, J. S., Nelson, D. L., Hemrick-Luecke, S. K., Threlkeld, P. G., Heiligenstein, J. H., et al. (2002). Atomoxetine increases extracellular levels of norepinephrine and dopamine in prefrontal cortex of rat: a potential mechanism for efficacy in attention deficit/hyperactivity disorder. *Neuropsychopharmacology*, 27(5), 699-711. doi: 10.1016/S0893-133X(02)00346-9
- Cannon, T. D., Chung, Y., He, G., Sun, D., Jacobson, A., van Erp, T. G., et al. (2015). Progressive reduction in cortical thickness as psychosis develops: a multisite longitudinal neuroimaging study of youth at elevated clinical risk. *Biol Psychiatry*, 77(2), 147-157. doi: 10.1016/j.biopsych.2014.05.023
- Carper, R. A., & Courchesne, E. (2005). Localized enlargement of the frontal cortex in early autism. *Biol Psychiatry*, 57(2), 126-133. doi: 10.1016/j.biopsych.2004.11.005
- Carvalho, E., Tinoco, E., Deeley, K., Duarte, P., Faveri, M., Marques, M., et al. (2010). FAM5C Contributes to Aggressive Periodontitis. *PLoS One*. doi: 10.1371/journal.pone.0010053.t001
- Casanova, M. F., El-Baz, A. S., Kamat, S. S., Dombroski, B. A., Khalifa, F., Elnakib, A., et al. (2013). Focal cortical dysplasias in autism spectrum disorders. *Acta Neuropathol Commun*, 1, 67. doi: 10.1186/2051-5960-1-67

- Caviness, V. S., Jr. (1982). Neocortical histogenesis in normal and reeler mice: a developmental study based upon [3H]thymidine autoradiography. *Brain Res*, 256(3), 293-302.
- Cha, J. D., Kim, H. J., & Cha, I. H. (2011). Genetic alterations in oral squamous cell carcinoma progression detected by combining array-based comparative genomic hybridization and multiplex ligation-dependent probe amplification. *Oral Surg Oral Med Oral Pathol Oral Radiol Endod*, 111(5), 594-607. doi: 10.1016/j.tripleo.2010.11.020
- Chadman, K. K., Yang, M., & Crawley, J. N. (2009). Criteria for validating mouse models of psychiatric diseases. *Am J Med Genet B Neuropsychiatr Genet*, 150B(1), 1-11. doi: 10.1002/ajmg.b.30777
- Champagne, F. A., Curley, J. P., Keverne, E. B., & Bateson, P. P. (2007). Natural variations in postpartum maternal care in inbred and outbred mice. *Physiol Behav*, 91(2-3), 325-334. doi: 10.1016/j.physbeh.2007.03.014
- Cheung, W. M., Fu, W. Y., Hui, W. S., & Ip, N. Y. (1999). Production of human CNS neurons from embryonal carcinoma cells using a cell aggregation method. *Biotechniques*, 26(5), 946-948, 950-942, 954.
- Chien, S. C., Li, Y. C., Li, L. H., Wu, J. Y., Hsu, P. C., Shi, S. L., et al. (2010). A new familial insertion, ins(18;9)(q12.2;q33.1q31.1) with a 9q31.1-9q33.1 deletion in a girl with a cleft lip and palate. *Am J Med Genet A*, 152A(7), 1862-1867. doi: 10.1002/ajmg.a.33452
- Chiquet-Ehrismann, R., & Tucker, R. P. (2011). Tenascins and the importance of adhesion modulation. *Cold Spring Harb Perspect Biol*, 3(5). doi: 10.1101/cshperspect.a004960
- Chun, J. J., & Shatz, C. J. (1989). Interstitial cells of the adult neocortical white matter are the remnant of the early generated subplate neuron population. *J Comp Neurol*, 282(4), 555-569. doi: 10.1002/cne.902820407
- Clarke, P. G. (1992). Neuron death in the developing avian isthmo-optic nucleus, and its relation to the establishment of functional circuitry. *J Neurobiol*, 23(9), 1140-1158. doi: 10.1002/neu.480230907
- Connelly, J. J., Shah, S. H., Doss, J. F., Gadson, S., Nelson, S., Crosslin, D. R., et al. (2008). Genetic and functional association of FAM5C with myocardial infarction. *BMC Med Genet*, 9, 33. doi: 10.1186/1471-2350-9-33
- Contini, V., Rovaris, D. L., Victor, M. M., Grevet, E. H., Rohde, L. A., & Bau, C. H. (2013). Pharmacogenetics of response to methylphenidate in adult patients with Attention-Deficit/Hyperactivity Disorder (ADHD): a systematic review. *Eur Neuropsychopharmacol*, 23(6), 555-560. doi: 10.1016/j.euroneuro.2012.05.006
- Cooper, J. A. (2014). Molecules and mechanisms that regulate multipolar migration in the intermediate zone. *Front Cell Neurosci*, 8, 386. doi: 10.3389/fncel.2014.00386
- Corbin, J. G., Nery, S., & Fishell, G. (2001). Telencephalic cells take a tangent: non-radial migration in the mammalian forebrain. *Nat Neurosci*, 4 Suppl, 1177-1182. doi: 10.1038/nn749
- Cortese, S., & Castellanos, F. X. (2012). Neuroimaging of attention-deficit/hyperactivity disorder: current neuroscience-informed perspectives for clinicians. *Curr Psychiatry Rep*, 14(5), 568-578. doi: 10.1007/s11920-012-0310-y
- Crawley, J. N. (2012). Translational animal models of autism and neurodevelopmental disorders. *Dialogues Clin Neurosci*, 14(3), 293-305.
- Creese, I., Burt, D. R., & Snyder, S. H. (1976). Dopamine receptor binding predicts clinical and pharmacological potencies of antischizophrenic drugs. *Science*, 192(4238), 481-483.
- Curtis, M. A., Monzo, H. J., & Faull, R. L. (2009). The rostral migratory stream and olfactory system: smell, disease and slippery cells. *Prog Brain Res*, 175, 33-42. doi: 10.1016/S0079-6123(09)17503-9
- D'Angelo, M. E., Dunstone, M. A., Whisstock, J. C., Trapani, J. A., & Bird, P. I. (2012). Perforin evolved from a gene duplication of MPEG1, followed by a complex pattern of gene gain and loss within Euteleostomi. *BMC Evol Biol*, 12, 59. doi: 10.1186/1471-2148-12-59
- D'angelo, M. (2014). The evolution of the immune pore forming protein, Perforin. *PhD Thesis*.

- Dahlhaus, M., Li, K. W., van der Schors, R., Saiepour, M. H., van Nierop, P., Heimel, J. A., et al. (2011). <The Synaptic Proteome during Development and Plasticity of the Mouse Visual Cortex.pdf>. doi: 10.1074/
- Danglot, L., Triller, A., & Marty, S. (2006). The development of hippocampal interneurons in rodents. *Hippocampus*, 16(12), 1032-1060. doi: 10.1002/hipo.20225
- Dawitz, J., Kroon, T., Hjorth, J. J., & Meredith, R. M. (2011). Functional calcium imaging in developing cortical networks. *J Vis Exp*(56). doi: 10.3791/3550
- Del Rio, J. A., Martinez, A., Auladell, C., & Soriano, E. (2000). Developmental history of the subplate and developing white matter in the murine neocortex. Neuronal organization and relationship with the main afferent systems at embryonic and perinatal stages. *Cereb Cortex*, 10(8), 784-801.
- DeLuna, A., Springer, M., Kirschner, M. W., & Kishony, R. (2010). Need-based up-regulation of protein levels in response to deletion of their duplicate genes. *PLoS Biol*, 8(3), e1000347. doi: 10.1371/journal.pbio.1000347
- Deutsch, E., Weigel, A. V., Akin, E. J., Fox, P., Hansen, G., Haberkorn, C. J., et al. (2012). Kv2.1 cell surface clusters are insertion platforms for ion channel delivery to the plasma membrane. *Mol Biol Cell*, 23(15), 2917-2929. doi: 10.1091/mbc.E12-01-0047
- Devlin, B., & Scherer, S. W. (2012). Genetic architecture in autism spectrum disorder. *Curr Opin Genet Dev*, 22(3), 229-237. doi: 10.1016/j.gde.2012.03.002
- Dinnissen, M., Dietrich, A., van den Hoofdakker, B. J., & Hoekstra, P. J. (2015). Clinical and pharmacokinetic evaluation of risperidone for the management of autism spectrum disorder. *Expert Opin Drug Metab Toxicol*, 11(1), 111-124. doi: 10.1517/17425255.2015.981151
- Do, C., Tung, J., Dorfman, E., Kiefer, A., Drabant, E., Francke, U., et al. (2011). Web-Based Genome-Wide Association Study Identifies Two Novel Loci and a Substantial Genetic Component for Parkinson's Disease. doi: 10.1371/journal.pgen.1002141.t001
- Drgon, T., Johnson, C. A., Nino, M., Drgonova, J., Walther, D. M., & Uhl, G. R. (2011). "Replicated" genome wide association for dependence on illegal substances: genomic regions identified by overlapping clusters of nominally positive SNPs. *Am J Med Genet B Neuropsychiatr Genet*, 156(2), 125-138. doi: 10.1002/ajmg.b.31143
- Edmondson, J. C., Liem, R. K., Kuster, J. E., & Hatten, M. E. (1988). Astrotactin: a novel neuronal cell surface antigen that mediates neuron-astroglial interactions in cerebellar microcultures. *J Cell Biol*, 106(2), 505-517.
- Edwards, T. L., Scott, W. K., Almonte, C., Burt, A., Powell, E. H., Beecham, G. W., et al. (2010). Genome-wide association study confirms SNPs in SNCA and the MAPT region as common risk factors for Parkinson disease. *Ann Hum Genet*, 74(2), 97-109. doi: 10.1111/j.1469-1809.2009.00560.x
- Egashira, N., Tanoue, A., Matsuda, T., Koushi, E., Harada, S., Takano, Y., et al. (2007). Impaired social interaction and reduced anxiety-related behavior in vasopressin V1a receptor knockout mice. *Behav Brain Res*, 178(1), 123-127. doi: 10.1016/j.bbr.2006.12.009
- Elias, L. A., Turmaine, M., Parnavelas, J. G., & Kriegstein, A. R. (2010). Connexin 43 mediates the tangential to radial migratory switch in ventrally derived cortical interneurons. *J Neurosci*, 30(20), 7072-7077. doi: 10.1523/JNEUROSCI.5728-09.2010
- Ellen J. Hess, K. A. C., Michael C. Wilson. (1996). Mouse Model of Hyperkinesia Implicates SNAP-25 in Behavioral Regulation. *The Journal of Neuroscience*.
- Enticott, P. G., Kennedy, H. A., Rinehart, N. J., Tonge, B. J., Bradshaw, J. L., & Fitzgerald, P. B. (2013). GABAergic activity in autism spectrum disorders: an investigation of cortical inhibition via transcranial magnetic stimulation. *Neuropharmacology*, 68, 202-209. doi: 10.1016/j.neuropharm.2012.06.017
- Fatemi, S. H. (2001). Reelin mutations in mouse and man: from reeler mouse to schizophrenia, mood disorders, autism and lissencephaly. *Mol Psychiatry*, 6(2), 129-133. doi: 10.1038/sj.mp.4000129

- Faux, C., Rakic, S., Andrews, W., & Britto, J. M. (2012). Neurons on the move: migration and lamination of cortical interneurons. *Neurosignals*, 20(3), 168-189. doi: 10.1159/000334489
- Feierstein, C. E. (2012). Linking adult olfactory neurogenesis to social behavior. *Front Neurosci*, 6, 173. doi: 10.3389/fnins.2012.00173
- Fernandez, T. V., Sanders, S. J., Yurkiewicz, I. R., Ercan-Sencicek, A. G., Kim, Y. S., Fishman, D. O., et al. (2012). Rare copy number variants in tourette syndrome disrupt genes in histaminergic pathways and overlap with autism. *Biol Psychiatry*, 71(5), 392-402. doi: 10.1016/j.biopsych.2011.09.034
- Fine, E. J., Ionita, C. C., & Lohr, L. (2002). The history of the development of the cerebellar examination. *Semin Neurol*, 22(4), 375-384. doi: 10.1055/s-2002-36759
- Fink, J. M., Hirsch, B. A., Zheng, C., Dietz, G., Hatten, M. E., & Ross, M. E. (1997). Astrotactin (ASTN), a gene for glial-guided neuronal migration, maps to human chromosome 1q25.2. *Genomics*, 40(1), 202-205. doi: 10.1006/geno.1996.4538
- First, M. B., & APA. (2013). *DSM-5 handbook of differential diagnosis* (First edition. ed.).
- Fishell, G., & Hatten, M. E. (1991). Astrotactin provides a receptor system for CNS neuronal migration. *Development*, 113(3), 755-765.
- Folsom, T. D., & Fatemi, S. H. (2013). The involvement of Reelin in neurodevelopmental disorders. *Neuropharmacology*, 68, 122-135. doi: 10.1016/j.neuropharm.2012.08.015
- Folstein, S. E., & Rosen-Sheidley, B. (2001). Genetics of autism: complex aetiology for a heterogeneous disorder. *Nat Rev Genet*, 2(12), 943-955. doi: 10.1038/35103559
- Fombonne, E. (2005). Epidemiology of autistic disorder and other pervasive developmental disorders. *J Clin Psychiatry*, 66 Suppl 10, 3-8.
- Gaertner, H. J., Fischer, E., & Hoss, J. (1989). Side effects of clozapine. *Psychopharmacology (Berl)*, 99 Suppl, S97-100.
- Gamerding, U., Eggermann, T., Schubert, R., Schwanitz, G., & Kreiss-Nachtsheim, M. (2008). Rare interstitial deletion 9q31.2 to q33.1 de novo: longitudinal study in a patient over a period of more than 20 years. *Am J Med Genet A*, 146A(9), 1180-1184. doi: 10.1002/ajmg.a.32122
- Gandal, M. J., Nesbitt, A. M., McCurdy, R. M., & Alter, M. D. (2012). Measuring the maturity of the fast-spiking interneuron transcriptional program in autism, schizophrenia, and bipolar disorder. *PLoS One*, 7(8), e41215. doi: 10.1371/journal.pone.0041215
- Gao, S., Worm, J., Guldberg, P., Eiberg, H., Krogh, A., Sorensen, J. A., et al. (2004). Loss of heterozygosity at 9q33 and hypermethylation of the DBCCR1 gene in oral squamous cell carcinoma. *Br J Cancer*, 91(4), 760-764. doi: 10.1038/sj.bjc.6601980
- Garber, K. (2007). Neuroscience. Autism's cause may reside in abnormalities at the synapse. *Science*, 317(5835), 190-191. doi: 10.1126/science.317.5835.190
- Gecz, J. (2004). The molecular basis of intellectual disability: novel genes with naturally occurring mutations causing altered gene expression in the brain. *Front Biosci*, 9, 1-7.
- Geng, Y., Yu, Q., Sicinska, E., Das, M., Bronson, R. T., & Sicinski, P. (2001). Deletion of the p27Kip1 gene restores normal development in cyclin D1-deficient mice. *Proc Natl Acad Sci U S A*, 98(1), 194-199. doi: 10.1073/pnas.011522998
- Gilman, S. R., Iossifov, I., Levy, D., Ronemus, M., Wigler, M., & Vitkup, D. (2011). Rare de novo variants associated with autism implicate a large functional network of genes involved in formation and function of synapses. *Neuron*, 70(5), 898-907. doi: 10.1016/j.neuron.2011.05.021
- Giros, B., Jaber, M., Jones, S. R., Wightman, R. M., & Caron, M. G. (1996). Hyperlocomotion and indifference to cocaine and amphetamine in mice lacking the dopamine transporter. *Nature*, 379(6566), 606-612. doi: 10.1038/379606a0
- Glessner, J. T., Wang, K., Cai, G., Korvatska, O., Kim, C. E., Wood, S., et al. (2009). Autism genome-wide copy number variation reveals ubiquitin and neuronal genes. *Nature*, 459(7246), 569-573. doi: 10.1038/nature07953
- Gluzman, Y. (1981). SV40-transformed simian cells support the replication of early SV40 mutants. *Cell*, 23(1), 175-182.

- Golshani, P., & Portera-Cailliau, C. (2008). In vivo 2-photon calcium imaging in layer 2/3 of mice. *J Vis Exp*(13). doi: 10.3791/681
- Govek, E. E., Hatten, M. E., & Van Aelst, L. (2011). The role of Rho GTPase proteins in CNS neuronal migration. *Dev Neurobiol*, 71(6), 528-553. doi: 10.1002/dneu.20850
- Guo, J., & Anton, E. S. (2014). Decision making during interneuron migration in the developing cerebral cortex. *Trends Cell Biol*, 24(6), 342-351. doi: 10.1016/j.tcb.2013.12.001
- Gurkan, C. K., & Hagerman, R. J. (2012). Targeted Treatments in Autism and Fragile X Syndrome. *Res Autism Spectr Disord*, 6(4), 1311-1320. doi: 10.1016/j.rasd.2012.05.007
- Gustafsson, P., Hansson, K., Eidevall, L., Thernlund, G., & Svedin, C. G. (2008). Treatment of ADHD with amphetamine: short-term effects on family interaction. *J Atten Disord*, 12(1), 83-91. doi: 10.1177/1087054707308482
- Haag, E. S., Sly, B. J., Andrews, M. E., & Raff, R. A. (1999). Apexrin, a novel extracellular protein associated with larval ectoderm evolution in *Heliocidaris erythrogramma*. *Dev Biol*, 211(1), 77-87. doi: 10.1006/dbio.1999.9283
- Habuchi, T., Luscombe, M., Elder, P. A., & Knowles, M. A. (1998). Structure and methylation-based silencing of a gene (DBCCR1) within a candidate bladder cancer tumor suppressor region at 9q32-q33. *Genomics*, 48(3), 277-288. doi: 10.1006/geno.1997.5165
- Hack, I., Hellwig, S., Junghans, D., Brunne, B., Bock, H. H., Zhao, S., et al. (2007). Divergent roles of ApoER2 and Vldlr in the migration of cortical neurons. *Development*, 134(21), 3883-3891. doi: 10.1242/dev.005447
- Hager, G., Dodt, H. U., Zieglgansberger, W., & Liesi, P. (1995). Novel forms of neuronal migration in the rat cerebellum. *J Neurosci Res*, 40(2), 207-219. doi: 10.1002/jnr.490400209
- Hampson, D. R., Gholizadeh, S., & Pacey, L. K. (2012). Pathways to drug development for autism spectrum disorders. *Clin Pharmacol Ther*, 91(2), 189-200. doi: 10.1038/clpt.2011.245
- Hatten, M. E. (2002). New directions in neuronal migration. *Science*, 297(5587), 1660-1663. doi: 10.1126/science.1074572
- Hatten, R. B. F. a. M. E. (1993). Multiple Receptor Systems Promote CNS Neural Migration. *The Journal of Neuroscience*.
- Heinzen, E. L., Need, A. C., Hayden, K. M., Chiba-Falek, O., Roses, A. D., Strittmatter, W. J., et al. (2010). Genome-wide scan of copy number variation in late-onset Alzheimer's disease. *J Alzheimers Dis*, 19(1), 69-77. doi: 10.3233/JAD-2010-1212
- Hemberger, M., Himmelbauer, H., Ruschmann, J., Zeitze, C., & Fundele, R. (2000). cDNA subtraction cloning reveals novel genes whose temporal and spatial expression indicates association with trophoblast invasion. *Dev Biol*, 222(1), 158-169. doi: 10.1006/dbio.2000.9705
- Hess, H. H., Newsome, D. A., Knapka, J. J., & Bieri, J. G. (1981). Effects of sunflower seed supplements on reproduction and growth of RCS rats with hereditary retinal dystrophy. *Lab Anim Sci*, 31(5 Pt 1), 482-488.
- Hess, S., Rohr, S., Dufour, B., Gaskill, B., Pajor, E., & Garner, J. (2008). Home Improvement: C57BL/6J Mice Given More Naturalistic Nesting Materials Build Better Nests. *Journal of the American Association for Laboratory Animal Science*, 47(6), 25-31.
- Higgins, G. A., & Breyse, N. (2008). Rodent model of attention: the 5-choice serial reaction time task. *Curr Protoc Pharmacol*, Chapter 5, Unit5 49. doi: 10.1002/0471141755.ph0549s41
- Hill, S. Y., Weeks, D. E., Jones, B. L., Zezza, N., & Stiffler, S. (2012). ASTN1 and alcohol dependence: family-based association analysis in multiplex alcohol dependence families. *Am J Med Genet B Neuropsychiatr Genet*, 159B(4), 445-455. doi: 10.1002/ajmg.b.32048
- Hoekstra, R. A., Happe, F., Baron-Cohen, S., Hoekstra, R. A., Happe, F., & Ronald, A. (2009). Association between extreme autistic traits and intellectual disability: insights from a general population twin study. *Br J Psychiatry*, 195(6), 531-536. doi: 10.1192/bjp.bp.108.060889
- Hoekzema, E., Carmona, S., Ramos-Quiroga, J. A., Richarte Fernandez, V., Picado, M., Bosch, R., et al. (2012). Laminar thickness alterations in the fronto-parietal cortical mantle of patients with

- attention-deficit/hyperactivity disorder. *PLoS One*, 7(12), e48286. doi: 10.1371/journal.pone.0048286
- Hu, P., Wang, Y., Meng, L. L., Qin, L., Ma, D. Y., Yi, L., et al. (2013). 1q25.2-q31.3 Deletion in a female with mental retardation, clinodactyly, minor facial anomalies but no growth retardation. *Mol Cytogenet*, 6(1), 30. doi: 10.1186/1755-8166-6-30
- Hu, W. F., Chahrour, M. H., & Walsh, C. A. (2014). The diverse genetic landscape of neurodevelopmental disorders. *Annu Rev Genomics Hum Genet*, 15, 195-213. doi: 10.1146/annurev-genom-090413-025600
- Huang, F. L., & Huang, K. P. (2012). Methylphenidate improves the behavioral and cognitive deficits of neurogranin knockout mice. *Genes Brain Behav*, 11(7), 794-805. doi: 10.1111/j.1601-183X.2012.00825.x
- Huang, G., Liu, H., Han, Y., Fan, L., Zhang, Q., Liu, J., et al. (2007). Profile of acute immune response in Chinese amphioxus upon *Staphylococcus aureus* and *Vibrio parahaemolyticus* infection. *Dev Comp Immunol*, 31(10), 1013-1023. doi: 10.1016/j.dci.2007.01.003
- Hunt, R. D., Arnsten, A. F., & Asbell, M. D. (1995). An open trial of guanfacine in the treatment of attention-deficit hyperactivity disorder. *J Am Acad Child Adolesc Psychiatry*, 34(1), 50-54. doi: 10.1097/00004583-199501000-00013
- Husmann, K., Faissner, A., & Schachner, M. (1992). Tenascin promotes cerebellar granule cell migration and neurite outgrowth by different domains in the fibronectin type III repeats. *J Cell Biol*, 116(6), 1475-1486.
- International Multiple Sclerosis Genetics, C., Hafler, D. A., Compston, A., Sawcer, S., Lander, E. S., Daly, M. J., et al. (2007). Risk alleles for multiple sclerosis identified by a genomewide study. *N Engl J Med*, 357(9), 851-862. doi: 10.1056/NEJMoa073493
- Iossifov, I., O'Roak, B. J., Sanders, S. J., Ronemus, M., Krumm, N., Levy, D., et al. (2014). The contribution of de novo coding mutations to autism spectrum disorder. *Nature*. doi: 10.1038/nature13908
- Ishino, T., Yano, K., Chinzei, Y., & Yuda, M. (2004). Cell-passage activity is required for the malarial parasite to cross the liver sinusoidal cell layer. *PLoS Biol*, 2(1), E4. doi: 10.1371/journal.pbio.0020004
- Jamain, S., Radyushkin, K., Hammerschmidt, K., Granon, S., Boretius, S., Varoqueaux, F., et al. (2008). Reduced social interaction and ultrasonic communication in a mouse model of monogenic heritable autism. *Proc Natl Acad Sci U S A*, 105(5), 1710-1715. doi: 10.1073/pnas.0711555105
- Jeffrey D. Falk, i. H. U., and J. Gregor Sutcliffe. (1995). Identification and Characterization of Transcribed Sequences on Human Chromosome 9q32-34. *Journal of Molecular Neuroscience*.
- Johnstone, E. C., Crow, T. J., Frith, C. D., Husband, J., & Kreel, L. (1976). Cerebral ventricular size and cognitive impairment in chronic schizophrenia. *Lancet*, 2(7992), 924-926.
- Kadota, K., Ishino, T., Matsuyama, T., Chinzei, Y., & Yuda, M. (2004). Essential role of membrane-attack protein in malarial transmission to mosquito host. *Proc Natl Acad Sci U S A*, 101(46), 16310-16315. doi: 10.1073/pnas.0406187101
- Kalin, N. H., Shelton, S. E., & Davidson, R. J. (2004). The role of the central nucleus of the amygdala in mediating fear and anxiety in the primate. *J Neurosci*, 24(24), 5506-5515. doi: 10.1523/JNEUROSCI.0292-04.2004
- Kapur, S. (2004). How antipsychotics become anti-"psychotic"--from dopamine to salience to psychosis. *Trends Pharmacol Sci*, 25(8), 402-406. doi: 10.1016/j.tips.2004.06.005
- Kapur, S., Mizrahi, R., & Li, M. (2005). From dopamine to salience to psychosis--linking biology, pharmacology and phenomenology of psychosis. *Schizophr Res*, 79(1), 59-68. doi: 10.1016/j.schres.2005.01.003
- Karoly, H. C., Stevens, C. J., Magnan, R. E., Harlaar, N., Hutchison, K. E., & Bryan, A. D. (2012). Genetic Influences on Physiological and Subjective Responses to an Aerobic Exercise Session among Sedentary Adults. *J Cancer Epidemiol*, 2012, 540563. doi: 10.1155/2012/540563

- Kashevarova, A. A., Nazarenko, L. P., Skryabin, N. A., Salyukova, O. A., Chechetkina, N. N., Tolmacheva, E. N., et al. (2014). Array CGH analysis of a cohort of Russian patients with intellectual disability. *Gene*, 536(1), 145-150. doi: 10.1016/j.gene.2013.11.029
- Kasper, S., & Resinger, E. (2003). Cognitive effects and antipsychotic treatment. *Psychoneuroendocrinology*, 28 Suppl 1, 27-38.
- Katsuyama, Y., & Terashima, T. (2009). Developmental anatomy of reeler mutant mouse. *Dev Growth Differ*, 51(3), 271-286. doi: 10.1111/j.1440-169X.2009.01102.x
- Kawano, H., Nakatani, T., Mori, T., Ueno, S., Fukaya, M., Abe, A., et al. (2004). Identification and characterization of novel developmentally regulated neural-specific proteins, BRINP family. *Brain Res Mol Brain Res*, 125(1-2), 60-75. doi: 10.1016/j.molbrainres.2004.04.001
- Keays, D. A., Tian, G., Poirier, K., Huang, G. J., Siebold, C., Cleak, J., et al. (2007). Mutations in alpha-tubulin cause abnormal neuronal migration in mice and lissencephaly in humans. *Cell*, 128(1), 45-57. doi: 10.1016/j.cell.2006.12.017
- Keshavan, M. S., Tandon, R., Boutros, N. N., & Nasrallah, H. A. (2008). Schizophrenia, "just the facts": what we know in 2008 Part 3: neurobiology. *Schizophr Res*, 106(2-3), 89-107. doi: 10.1016/j.schres.2008.07.020
- Ketzef, M., Kahn, J., Weissberg, I., Becker, A. J., Friedman, A., & Gitler, D. (2011). Compensatory network alterations upon onset of epilepsy in synapsin triple knock-out mice. *Neuroscience*, 189, 108-122. doi: 10.1016/j.neuroscience.2011.05.030
- Keverne, E. B. (2002). Mammalian pheromones: from genes to behaviour. *Curr Biol*, 12(23), R807-809.
- Khalaf-Nazzal, R., & Francis, F. (2013). Hippocampal development - Old and new findings. *Neuroscience*, 248C, 225-242. doi: 10.1016/j.neuroscience.2013.05.061
- Kinoshita, T., Hong, K., & Inoue, K. (1981). Soluble C5b-9 complex of guinea pig complement: demonstration of its heterogeneity and the mechanism of its C9 hemolytic activity as transfer of reversibly bound C9 molecules from the complex. *Mol Immunol*, 18(5), 423-431.
- Kobayashi, M., Nakatani, T., Koda, T., Matsumoto, K., Ozaki, R., Mochida, N., et al. (2014). Absence of BRINP1 in mice causes increase of hippocampal neurogenesis and behavioral alterations relevant to human psychiatric disorders. *Mol Brain*, 7, 12. doi: 10.1186/1756-6606-7-12
- Koch, C., & Reid, R. C. (2012). Neuroscience: Observatories of the mind. *Nature*, 483(7390), 397-398. doi: 10.1038/483397a
- Kondos, S. C., Hatfaludi, T., Voskoboinik, I., Trapani, J. A., Law, R. H., Whisstock, J. C., et al. (2010). The structure and function of mammalian membrane-attack complex/perforin-like proteins. *Tissue Antigens*, 76(5), 341-351. doi: 10.1111/j.1399-0039.2010.01566.x
- Konrad, K., & Eickhoff, S. B. (2010). Is the ADHD brain wired differently? A review on structural and functional connectivity in attention deficit hyperactivity disorder. *Hum Brain Mapp*, 31(6), 904-916. doi: 10.1002/hbm.21058
- Kordon, A., Stollhoff, K., Niederkirchner, K., Mattejat, F., Rettig, K., & Schauble, B. (2011). Exploring the impact of once-daily OROS(R) methylphenidate (MPH) on symptoms and quality of life in children and adolescents with ADHD transitioning from immediate-release MPH. *Postgrad Med*, 123(5), 27-38. doi: 10.3810/pgm.2011.09.2457
- Krause, J., la Fougere, C., Krause, K. H., Ackenheil, M., & Dresel, S. H. (2005). Influence of striatal dopamine transporter availability on the response to methylphenidate in adult patients with ADHD. *Eur Arch Psychiatry Clin Neurosci*, 255(6), 428-431. doi: 10.1007/s00406-005-0602-x
- Kriegstein, A. R., & Gotz, M. (2003). Radial glia diversity: a matter of cell fate. *Glia*, 43(1), 37-43. doi: 10.1002/glia.10250
- Kriegstein, A. R., & Noctor, S. C. (2004). Patterns of neuronal migration in the embryonic cortex. *Trends Neurosci*, 27(7), 392-399. doi: 10.1016/j.tins.2004.05.001
- Kulharya, A. S., Flannery, D. B., Norris, K., Lovell, C., Levy, B., & Velagaleti, G. V. (2008). Fine mapping of breakpoints in two unrelated patients with rare overlapping interstitial deletions of 9q with mild dysmorphic features. *Am J Med Genet A*, 146A(17), 2234-2241. doi: 10.1002/ajmg.a.32397

- Kwon, C. H., Luikart, B. W., Powell, C. M., Zhou, J., Matheny, S. A., Zhang, W., et al. (2006). Pten regulates neuronal arborization and social interaction in mice. *Neuron*, 50(3), 377-388. doi: 10.1016/j.neuron.2006.03.023
- Laumonnier, F., Cuthbert, P. C., & Grant, S. (2007). <BRINP1 at the PSD - The role of neuronal complexes in human x-linked brain diseases.pdf>.
- Lawrence, Y. A., Kemper, T. L., Bauman, M. L., & Blatt, G. J. (2010). Parvalbumin-, calbindin-, and calretinin-immunoreactive hippocampal interneuron density in autism. *Acta Neurol Scand*, 121(2), 99-108. doi: 10.1111/j.1600-0404.2009.01234.x
- Lawrie, S. M., & Abukmeil, S. S. (1998). Brain abnormality in schizophrenia. A systematic and quantitative review of volumetric magnetic resonance imaging studies. *Br J Psychiatry*, 172, 110-120.
- Lee, S., Hjerling-Leffler, J., Zagha, E., Fishell, G., & Rudy, B. (2010). The largest group of superficial neocortical GABAergic interneurons expresses ionotropic serotonin receptors. *J Neurosci*, 30(50), 16796-16808. doi: 10.1523/JNEUROSCI.1869-10.2010
- Lein, E. S., Hawrylycz, M. J., Ao, N., Ayres, M., Bensinger, A., Bernard, A., et al. (2007). Genome-wide atlas of gene expression in the adult mouse brain. *Nature*, 445(7124), 168-176. doi: 10.1038/nature05453
- Leo, D., & Gainetdinov, R. R. (2013). Transgenic mouse models for ADHD. *Cell Tissue Res*, 354(1), 259-271. doi: 10.1007/s00441-013-1639-1
- Lesch, K. P., Timmesfeld, N., Renner, T. J., Halperin, R., Roser, C., Nguyen, T. T., et al. (2008). Molecular genetics of adult ADHD: converging evidence from genome-wide association and extended pedigree linkage studies. *J Neural Transm*, 115(11), 1573-1585. doi: 10.1007/s00702-008-0119-3
- Liang, H., & Li, W. H. (2009). Functional compensation by duplicated genes in mouse. *Trends Genet*, 25(10), 441-442. doi: 10.1016/j.tig.2009.08.001
- Lieberman, J. A., Kane, J. M., & Alvir, J. (1987). Provocative tests with psychostimulant drugs in schizophrenia. *Psychopharmacology (Berl)*, 91(4), 415-433.
- Lieberman, J. A., Stroup, T. S., McEvoy, J. P., Swartz, M. S., Rosenheck, R. A., Perkins, D. O., et al. (2005). Effectiveness of antipsychotic drugs in patients with chronic schizophrenia. *N Engl J Med*, 353(12), 1209-1223. doi: 10.1056/NEJMoa051688
- Lionel, A. C., Crosbie, J., Barbosa, N., Goodale, T., Thiruvahindrapuram, B., Rickaby, J., et al. (2011). Rare copy number variation discovery and cross-disorder comparisons identify risk genes for ADHD. *Sci Transl Med*, 3(95), 95ra75. doi: 10.1126/scitranslmed.3002464
- Lionel, A. C., Tammimies, K., Vaags, A. K., Rosenfeld, J. A., Ahn, J. W., Merico, D., et al. (2014). Disruption of the ASTN2/TRIM32 locus at 9q33.1 is a risk factor in males for autism spectrum disorders, ADHD and other neurodevelopmental phenotypes. *Hum Mol Genet*. doi: 10.1093/hmg/ddt669
- Lionel, A. C., Tammimies, K., Vaags, A. K., Rosenfeld, J. A., Ahn, J. W., Merico, D., et al. (2014). Disruption of the ASTN2/TRIM32 locus at 9q33.1 is a risk factor in males for autism spectrum disorders, ADHD and other neurodevelopmental phenotypes. *Hum Mol Genet*, 23(10), 2752-2768. doi: 10.1093/hmg/ddt669
- Lockhart, D. J., & Barlow, C. (2001). Expressing what's on your mind: DNA arrays and the brain. *Nat Rev Neurosci*, 2(1), 63-68. doi: 10.1038/35049070
- Lodato, S., Rouaux, C., Quast, K. B., Jantrachotechatchawan, C., Studer, M., Hensch, T. K., et al. (2011). Excitatory projection neuron subtypes control the distribution of local inhibitory interneurons in the cerebral cortex. *Neuron*, 69(4), 763-779. doi: 10.1016/j.neuron.2011.01.015
- Lopez, J. A., Susanto, O., Jenkins, M. R., Lukyanova, N., Sutton, V. R., Law, R. H., et al. (2013). Perforin forms transient pores on the target cell plasma membrane to facilitate rapid access of granzymes during killer cell attack. *Blood*, 121(14), 2659-2668. doi: 10.1182/blood-2012-07-446146

- Lovell, P. V., Clayton, D. F., Replogle, K. L., & Mello, C. V. (2008). Birdsong “Transcriptomics”: Neurochemical Specializations of the Oscine Song System. doi: 10.1371/journal.pone.0003440.g001
- Lovett-Barron, M., Turi, G. F., Kaifosh, P., Lee, P. H., Bolze, F., Sun, X. H., et al. (2012). Regulation of neuronal input transformations by tunable dendritic inhibition. *Nat Neurosci*, 15(3), 423-430, S421-423. doi: 10.1038/nn.3024
- Luskin, M. B. (1993). Restricted proliferation and migration of postnatally generated neurons derived from the forebrain subventricular zone. *Neuron*, 11(1), 173-189.
- Luskin, M. B., & Shatz, C. J. (1985). Neurogenesis of the cat's primary visual cortex. *J Comp Neurol*, 242(4), 611-631. doi: 10.1002/cne.902420409
- Luth, H. J., Blumcke, I., Winkelmann, E., & Celio, M. R. (1993). The calcium-binding protein calretinin is localized in a subset of interneurons in the rat cerebral cortex: a light and electron immunohistochemical study. *J Hirnforsch*, 34(1), 93-103.
- Lyon, L., Burnet, P. W., Kew, J. N., Corti, C., Rawlins, J. N., Lane, T., et al. (2011). Fractionation of spatial memory in GRM2/3 (mGlu2/mGlu3) double knockout mice reveals a role for group II metabotropic glutamate receptors at the interface between arousal and cognition. *Neuropsychopharmacology*, 36(13), 2616-2628. doi: 10.1038/npp.2011.145
- Ma, Y., Hu, H., Berrebi, A. S., Mathers, P. H., & Agmon, A. (2006). Distinct subtypes of somatostatin-containing neocortical interneurons revealed in transgenic mice. *J Neurosci*, 26(19), 5069-5082. doi: 10.1523/JNEUROSCI.0661-06.2006
- Maggio, J. C., Maggio, J. H., & Whitney, G. (1983). Experience-based vocalization of male mice to female chemosignals. *Physiol Behav*, 31(3), 269-272.
- Makris, N., Biederman, J., Valera, E. M., Bush, G., Kaiser, J., Kennedy, D. N., et al. (2007). Cortical thinning of the attention and executive function networks in adults with attention-deficit/hyperactivity disorder. *Cereb Cortex*, 17(6), 1364-1375. doi: 10.1093/cercor/bhl047
- Marin, O. (2012). Interneuron dysfunction in psychiatric disorders. *Nat Rev Neurosci*, 13(2), 107-120. doi: 10.1038/nrn3155
- Marin, O., & Rubenstein, J. L. (2001). A long, remarkable journey: tangential migration in the telencephalon. *Nat Rev Neurosci*, 2(11), 780-790. doi: 10.1038/35097509
- Marin, O., Valiente, M., Ge, X., & Tsai, L. H. (2010). Guiding neuronal cell migrations. *Cold Spring Harb Perspect Biol*, 2(2), a001834. doi: 10.1101/cshperspect.a001834
- Markram, H., Toledo-Rodriguez, M., Wang, Y., Gupta, A., Silberberg, G., & Wu, C. (2004). Interneurons of the neocortical inhibitory system. *Nat Rev Neurosci*, 5(10), 793-807. doi: 10.1038/nrn1519
- Martin, J. R., Raibaud, A., & Ollo, R. (1994). Terminal pattern elements in Drosophila embryo induced by the torso-like protein. *Nature*, 367(6465), 741-745. doi: 10.1038/367741a0
- Martin, L. J. (2001). Neuronal cell death in nervous system development, disease, and injury (Review). *Int J Mol Med*, 7(5), 455-478.
- McConnell, S. K., Ghosh, A., & Shatz, C. J. (1989). Subplate neurons pioneer the first axon pathway from the cerebral cortex. *Science*, 245(4921), 978-982.
- McConnell, S. K., Ghosh, A., & Shatz, C. J. (1994). Subplate pioneers and the formation of descending connections from cerebral cortex. *J Neurosci*, 14(4), 1892-1907.
- McGarry, L. M., Packer, A. M., Fino, E., Nikolenko, V., Sipky, T., & Yuste, R. (2010). Quantitative classification of somatostatin-positive neocortical interneurons identifies three interneuron subtypes. *Front Neural Circuits*, 4, 12. doi: 10.3389/fncir.2010.00012
- McGonigle-Chalmers, M., Alderson-Day, B., Fleming, J., Alderson-Day, B., Fleming, J., & Monsen, K. (2013). Profound expressive language impairment in low functioning children with autism: an investigation of syntactic awareness using a computerised learning task. *J Autism Dev Disord*, 43(9), 2062-2081. doi: 10.1007/s10803-012-1753-z
- McManus, M. F., Nasrallah, I. M., Gopal, P. P., Baek, W. S., & Golden, J. A. (2004). Axon mediated interneuron migration. *J Neuropathol Exp Neurol*, 63(9), 932-941.

- Menashe, I., Grange, P., Larsen, E. C., Banerjee-Basu, S., & Mitra, P. P. (2013). Co-expression profiling of autism genes in the mouse brain. *PLoS Comput Biol*, 9(7), e1003128. doi: 10.1371/journal.pcbi.1003128
- Metin, C., Baudoin, J. P., Rakic, S., & Parnavelas, J. G. (2006). Cell and molecular mechanisms involved in the migration of cortical interneurons. *Eur J Neurosci*, 23(4), 894-900. doi: 10.1111/j.1460-9568.2006.04630.x
- Meyer, A. H., Katona, I., Blatow, M., Rozov, A., & Monyer, H. (2002). In vivo labeling of parvalbumin-positive interneurons and analysis of electrical coupling in identified neurons. *J Neurosci*, 22(16), 7055-7064. doi: 20026742
- Mikaelian, D. O., Warfield, D., & Norris, O. (1974). Genetic progressive hearing loss in the C57-b16 mouse. Relation of behavioral responses to cochlear anatomy. *Acta Otolaryngol*, 77(5), 327-334.
- Ming, G. L., & Song, H. (2011). Adult neurogenesis in the mammalian brain: significant answers and significant questions. *Neuron*, 70(4), 687-702. doi: 10.1016/j.neuron.2011.05.001
- Mitchell, K. J. (2011). The genetics of neurodevelopmental disease. *Curr Opin Neurobiol*, 21(1), 197-203. doi: 10.1016/j.conb.2010.08.009
- Miyoshi, G., Butt, S. J., Takebayashi, H., & Fishell, G. (2007). Physiologically distinct temporal cohorts of cortical interneurons arise from telencephalic Olig2-expressing precursors. *J Neurosci*, 27(29), 7786-7798. doi: 10.1523/JNEUROSCI.1807-07.2007
- Miyoshi, G., Hjerling-Leffler, J., Karayannis, T., Sousa, V. H., Butt, S. J., Battiste, J., et al. (2010). Genetic fate mapping reveals that the caudal ganglionic eminence produces a large and diverse population of superficial cortical interneurons. *J Neurosci*, 30(5), 1582-1594. doi: 10.1523/JNEUROSCI.4515-09.2010
- Molyneaux, B. J., Arlotta, P., Menezes, J. R., & Macklis, J. D. (2007). Neuronal subtype specification in the cerebral cortex. *Nat Rev Neurosci*, 8(6), 427-437. doi: 10.1038/nrn2151
- Moretti, P., Bouwknecht, J. A., Teague, R., Paylor, R., & Zoghbi, H. Y. (2005). Abnormalities of social interactions and home-cage behavior in a mouse model of Rett syndrome. *Hum Mol Genet*, 14(2), 205-220. doi: 10.1093/hmg/ddi016
- Mori, K., Takahashi, Y. K., Igarashi, K. M., & Yamaguchi, M. (2006). Maps of odorant molecular features in the Mammalian olfactory bulb. *Physiol Rev*, 86(2), 409-433. doi: 10.1152/physrev.00021.2005
- Morita-Yamamuro, C., Tsutsui, T., Sato, M., Yoshioka, H., Tamaoki, M., Ogawa, D., et al. (2005). The Arabidopsis gene CAD1 controls programmed cell death in the plant immune system and encodes a protein containing a MACPF domain. *Plant Cell Physiol*, 46(6), 902-912. doi: 10.1093/pcp/pci095
- Moy, S. S., Nadler, J. J., Magnuson, T. R., & Crawley, J. N. (2006). Mouse models of autism spectrum disorders: the challenge for behavioral genetics. *Am J Med Genet C Semin Med Genet*, 142C(1), 40-51. doi: 10.1002/ajmg.c.30081
- Mueser, K. T., & McGurk, S. R. (2004). Schizophrenia. *Lancet*, 363(9426), 2063-2072. doi: 10.1016/S0140-6736(04)16458-1
- Muller-Eberhard, H. J. (1986). The membrane attack complex of complement. *Annu Rev Immunol*, 4, 503-528. doi: 10.1146/annurev.iy.04.040186.002443
- Muller, E. E., Sawano, S., & Schally, A. V. (1967). Growth hormone-releasing activity in the hypothalamus of animals of different species. *Gen Comp Endocrinol*, 9(3), 349-352.
- Nakahira, E., & Yuasa, S. (2005). Neuronal generation, migration, and differentiation in the mouse hippocampal primordium as revealed by enhanced green fluorescent protein gene transfer by means of in utero electroporation. *J Comp Neurol*, 483(3), 329-340. doi: 10.1002/cne.20441
- Nakatani, J., Tamada, K., Hatanaka, F., Ise, S., Ohta, H., Inoue, K., et al. (2009). Abnormal behavior in a chromosome-engineered mouse model for human 15q11-13 duplication seen in autism. *Cell*, 137(7), 1235-1246. doi: 10.1016/j.cell.2009.04.024

- Nery, S., Fishell, G., & Corbin, J. G. (2002). The caudal ganglionic eminence is a source of distinct cortical and subcortical cell populations. *Nat Neurosci*, 5(12), 1279-1287. doi: 10.1038/nn971
- Nestler, E. J., & Hyman, S. E. (2010). Animal models of neuropsychiatric disorders. *Nat Neurosci*, 13(10), 1161-1169. doi: 10.1038/nn.2647
- Noctor, S. C., Flint, A. C., Weissman, T. A., Dammerman, R. S., & Kriegstein, A. R. (2001). Neurons derived from radial glial cells establish radial units in neocortex. *Nature*, 409(6821), 714-720. doi: 10.1038/35055553
- Noctor, S. C., Flint, A. C., Weissman, T. A., Wong, W. S., Clinton, B. K., & Kriegstein, A. R. (2002). Dividing precursor cells of the embryonic cortical ventricular zone have morphological and molecular characteristics of radial glia. *J Neurosci*, 22(8), 3161-3173. doi: 10.1523/JNEUROSCI.0026-02.2002
- O'Keefe, J., & Dostrovsky, J. (1971). The hippocampus as a spatial map. Preliminary evidence from unit activity in the freely-moving rat. *Brain Res*, 34(1), 171-175.
- O'Rourke, N. A., Dailey, M. E., Smith, S. J., & McConnell, S. K. (1992). Diverse migratory pathways in the developing cerebral cortex. *Science*, 258(5080), 299-302.
- Ohshima, T., Hirasawa, M., Tabata, H., Mutoh, T., Adachi, T., Suzuki, H., et al. (2007). Cdk5 is required for multipolar-to-bipolar transition during radial neuronal migration and proper dendrite development of pyramidal neurons in the cerebral cortex. *Development*, 134(12), 2273-2282. doi: 10.1242/dev.02854
- Olsson, B., & Rett, A. (1985). Behavioral observations concerning differential diagnosis between the Rett syndrome and autism. *Brain Dev*, 7(3), 281-289.
- Oshiro, N., Kobayashi, C., Iwanaga, S., Nozaki, M., Namikoshi, M., Spring, J., et al. (2004). A new membrane-attack complex/perforin (MACPF) domain lethal toxin from the nematocyst venom of the Okinawan sea anemone *Actinaria villosa*. *Toxicon*, 43(2), 225-228. doi: 10.1016/j.toxicon.2003.11.017
- Pantelis, C., Velakoulis, D., McGorry, P. D., Wood, S. J., Suckling, J., Phillips, L. J., et al. (2003). Neuroanatomical abnormalities before and after onset of psychosis: a cross-sectional and longitudinal MRI comparison. *Lancet*, 361(9354), 281-288. doi: 10.1016/S0140-6736(03)12323-9
- Parnavelas, J. G. (2000). The origin and migration of cortical neurones: new vistas. *Trends Neurosci*, 23(3), 126-131.
- Paylor, R., Hirotune, S., Gambello, M. J., Yuva-Paylor, L., Crawley, J. N., & Wynshaw-Boris, A. (1999). Impaired learning and motor behavior in heterozygous *Pafah1b1* (*Lis1*) mutant mice. *Learn Mem*, 6(5), 521-537.
- Pedersen, C. A., Vadlamudi, S., Boccia, M. L., & Moy, S. S. (2011). Variations in Maternal Behavior in C57BL/6J Mice: Behavioral Comparisons between Adult Offspring of High and Low Pup-Licking Mothers. *Front Psychiatry*, 2, 42. doi: 10.3389/fpsy.2011.00042
- Penagarikano, O., Abrahams, B. S., Herman, E. I., Winden, K. D., Gdalyahu, A., Dong, H., et al. (2011). Absence of *CNTNAP2* leads to epilepsy, neuronal migration abnormalities, and core autism-related deficits. *Cell*, 147(1), 235-246. doi: 10.1016/j.cell.2011.08.040
- Petilla Interneuron Nomenclature, G., Ascoli, G. A., Alonso-Nanclares, L., Anderson, S. A., Barrionuevo, G., Benavides-Piccione, R., et al. (2008). Petilla terminology: nomenclature of features of GABAergic interneurons of the cerebral cortex. *Nat Rev Neurosci*, 9(7), 557-568. doi: 10.1038/nrn2402
- Pham, C. T., MacIvor, D. M., Hug, B. A., Heusel, J. W., & Ley, T. J. (1996). Long-range disruption of gene expression by a selectable marker cassette. *Proc Natl Acad Sci U S A*, 93(23), 13090-13095.
- Phang, D., Rehage, M., Bonafede, B., Hou, D., Xing, W., Mohan, S., et al. (2010). Inactivation of insulin-like-growth factors diminished the anabolic effects of pregnancy-associated plasma protein-A (PAPP-A) on bone in mice. *Growth Horm IGF Res*, 20(3), 192-200. doi: 10.1016/j.gth.2010.01.001
- Picciotto, M. R., & Wickman, K. (1998). Using knockout and transgenic mice to study neurophysiology and behavior. *Physiol Rev*, 78(4), 1131-1163.

- Pilz, D. T., Matsumoto, N., Minnerath, S., Mills, P., Gleeson, J. G., Allen, K. M., et al. (1998). LIS1 and XLIS (DCX) mutations cause most classical lissencephaly, but different patterns of malformation. *Hum Mol Genet*, 7(13), 2029-2037.
- Pleasure, S. J., Anderson, S., Hevner, R., Bagri, A., Marin, O., Lowenstein, D. H., et al. (2000). Cell migration from the ganglionic eminences is required for the development of hippocampal GABAergic interneurons. *Neuron*, 28(3), 727-740.
- Ponting, C. P. (1999). Chlamydial homologues of the MACPF (MAC/perforin) domain. *Curr Biol*, 9(24), R911-913.
- Porcionatto, M. A. (2006). The extracellular matrix provides directional cues for neuronal migration during cerebellar development. *Braz J Med Biol Res*, 39(3), 313-320. doi: /S0100-879X2006000300001
- Powell, E. M. (2013). Interneuron development and epilepsy: early genetic defects cause long-term consequences in seizures and susceptibility. *Epilepsy Curr*, 13(4), 172-176. doi: 10.5698/1535-7597-13.4.172
- Prather, M. D., Lavenex, P., Mauldin-Jourdain, M. L., Mason, W. A., Capitanio, J. P., Mendoza, S. P., et al. (2001). Increased social fear and decreased fear of objects in monkeys with neonatal amygdala lesions. *Neuroscience*, 106(4), 653-658.
- Purper-Ouakil, D., Ramoz, N., Lepagnol-Bestel, A. M., Gorwood, P., & Simonneau, M. (2011). Neurobiology of attention deficit/hyperactivity disorder. *Pediatr Res*, 69(5 Pt 2), 69R-76R. doi: 10.1203/PDR.0b013e318212b40f
- Radyushkin, K., Hammerschmidt, K., Boretius, S., Varoqueaux, F., El-Kordi, A., Ronnenberg, A., et al. (2009). Neuroligin-3-deficient mice: model of a monogenic heritable form of autism with an olfactory deficit. *Genes Brain Behav*, 8(4), 416-425. doi: 10.1111/j.1601-183X.2009.00487.x
- Rakic, P. (1971). Neuron-glia relationship during granule cell migration in developing cerebellar cortex. A Golgi and electronmicroscopic study in Macacus Rhesus. *J Comp Neurol*, 141(3), 283-312. doi: 10.1002/cne.901410303
- Rakic, P. (1972). Mode of cell migration to the superficial layers of fetal monkey neocortex. *J Comp Neurol*, 145(1), 61-83. doi: 10.1002/cne.901450105
- Rakic, P. (1974). Neurons in rhesus monkey visual cortex: systematic relation between time of origin and eventual disposition. *Science*, 183(4123), 425-427.
- Rakic, P. (1978). Neuronal migration and contact guidance in the primate telencephalon. *Postgrad Med J*, 54 Suppl 1, 25-40.
- Reszka, S. S., Boyd, B. A., McBee, M., Hume, K. A., & Odom, S. L. (2014). Brief report: concurrent validity of autism symptom severity measures. *J Autism Dev Disord*, 44(2), 466-470. doi: 10.1007/s10803-013-1879-7
- Robertson, H. R., & Feng, G. (2011). Annual Research Review: Transgenic mouse models of childhood-onset psychiatric disorders. *J Child Psychol Psychiatry*, 52(4), 442-475. doi: 10.1111/j.1469-7610.2011.02380.x
- Romanos, M., Freitag, C., Jacob, C., Craig, D. W., Dempfle, A., Nguyen, T. T., et al. (2008). Genome-wide linkage analysis of ADHD using high-density SNP arrays: novel loci at 5q13.1 and 14q12. *Mol Psychiatry*, 13(5), 522-530. doi: 10.1038/mp.2008.12
- Rommelse, N. N., Franke, B., Geurts, H. M., Hartman, C. A., & Buitelaar, J. K. (2010). Review: Shared heritability of attention-deficit/hyperactivity disorder and autism spectrum disorder. *Eur Child Adolesc Psychiatry*, 19(3), 281-295. doi: 10.1007/s00787-010-0092-x
- Rosado, C. J., Buckle, A. M., Law, R. H., Butcher, R. E., Kan, W. T., Bird, C. H., et al. (2007). A common fold mediates vertebrate defense and bacterial attack. *Science*, 317(5844), 1548-1551. doi: 10.1126/science.1144706
- Rosado, C. J., Kondos, S., Bull, T. E., Kuiper, M. J., Law, R. H., Buckle, A. M., et al. (2008). The MACPF/CDC family of pore-forming toxins. *Cell Microbiol*, 10(9), 1765-1774. doi: 10.1111/j.1462-5822.2008.01191.x

- Rubenstein, J. L., & Merzenich, M. M. (2003). Model of autism: increased ratio of excitation/inhibition in key neural systems. *Genes Brain Behav*, 2(5), 255-267.
- Rubia, K., Halari, R., Cubillo, A., Mohammad, A. M., Scott, S., & Brammer, M. (2010). Disorder-specific inferior prefrontal hypofunction in boys with pure attention-deficit/hyperactivity disorder compared to boys with pure conduct disorder during cognitive flexibility. *Hum Brain Mapp*, 31(12), 1823-1833. doi: 10.1002/hbm.20975
- Russell, V. A., Sagvolden, T., & Johansen, E. B. (2005). Animal models of attention-deficit hyperactivity disorder. *Behav Brain Funct*, 1, 9. doi: 10.1186/1744-9081-1-9
- Rybakowski, F., Bialek, A., Chojnicka, I., Dziechciarz, P., Horvath, A., Janas-Kozik, M., et al. (2014). [Autism spectrum disorders - epidemiology, symptoms, comorbidity and diagnosis]. *Psychiatr Pol*, 48(4), 653-665.
- Saha, S., Chant, D., Welham, J., & McGrath, J. (2005). A systematic review of the prevalence of schizophrenia. *PLoS Med*, 2(5), e141. doi: 10.1371/journal.pmed.0020141
- Sanchez-Morla, E. M., Garcia-Jimenez, M. A., Barabash, A., Martinez-Vizcaino, V., Mena, J., Cabranes-Diaz, J. A., et al. (2008). P50 sensory gating deficit is a common marker of vulnerability to bipolar disorder and schizophrenia. *Acta Psychiatr Scand*, 117(4), 313-318. doi: 10.1111/j.1600-0447.2007.01141.x
- Sander, J. D., & Joung, J. K. (2014). CRISPR-Cas systems for editing, regulating and targeting genomes. *Nat Biotechnol*, 32(4), 347-355. doi: 10.1038/nbt.2842
- Scacheri, P. C., Crabtree, J. S., Novotny, E. A., Garrett-Beal, L., Chen, A., Edgemon, K. A., et al. (2001). Bidirectional transcriptional activity of PGK-neomycin and unexpected embryonic lethality in heterozygote chimeric knockout mice. *Genesis*, 30(4), 259-263.
- Scanlon, M. F. (1992). Endocrine functions of the hypothalamus and alterations in neuroendocrine function--focus on thyrotropin and growth hormone. *Prog Brain Res*, 93, 19-29; discussion 29-30.
- Scattoni, M. L., Crawley, J., & Ricceri, L. (2009). Ultrasonic vocalizations: a tool for behavioural phenotyping of mouse models of neurodevelopmental disorders. *Neurosci Biobehav Rev*, 33(4), 508-515. doi: 10.1016/j.neubiorev.2008.08.003
- Scattoni, M. L., Gandhi, S. U., Ricceri, L., & Crawley, J. N. (2008). Unusual repertoire of vocalizations in the BTBR T+tf/J mouse model of autism. *PLoS One*, 3(8), e3067. doi: 10.1371/journal.pone.0003067
- Schmeisser, M. J., Ey, E., Wegener, S., Bockmann, J., Stempel, A. V., Kuebler, A., et al. (2012). Autistic-like behaviours and hyperactivity in mice lacking ProSAP1/Shank2.
- Schmidt, M. J., & Mirnics, K. (2012). Modeling interneuron dysfunction in schizophrenia. *Dev Neurosci*, 34(2-3), 152-158. doi: 10.1159/000336731
- Schwarzer, S., Mashanov, G. I., Molloy, J. E., & Tinker, A. (2013). Using total internal reflection fluorescence microscopy to observe ion channel trafficking and assembly. *Methods Mol Biol*, 998, 201-208. doi: 10.1007/978-1-62703-351-0_15
- Scoville, W. B., & Milner, B. (1957). Loss of recent memory after bilateral hippocampal lesions. *J Neurol Neurosurg Psychiatry*, 20(1), 11-21.
- Sebat, J., Lakshmi, B., Malhotra, D., Troge, J., Lese-Martin, C., Walsh, T., et al. (2007). Strong association of de novo copy number mutations with autism. *Science*, 316(5823), 445-449. doi: 10.1126/science.1138659
- Sharma, A., & Couture, J. (2014). A review of the pathophysiology, etiology, and treatment of attention-deficit hyperactivity disorder (ADHD). *Ann Pharmacother*, 48(2), 209-225. doi: 10.1177/1060028013510699
- Shaw, P., Eckstrand, K., Sharp, W., Blumenthal, J., Lerch, J. P., Greenstein, D., et al. (2007). Attention-deficit/hyperactivity disorder is characterized by a delay in cortical maturation. *Proc Natl Acad Sci U S A*, 104(49), 19649-19654. doi: 10.1073/pnas.0707741104

- Shim, U. J., Lee, I. S., Kang, H. W., Kim, J., Kim, W. T., Kim, I. Y., et al. (2013). Decreased DBC1 Expression Is Associated With Poor Prognosis in Patients With Non-Muscle-Invasive Bladder Cancer. *Korean J Urol*, 54(9), 631-637. doi: 10.4111/kju.2013.54.9.631
- Shorts-Cary, L., Xu, M., Ertel, J., Kleinschmidt-Demasters, B. K., Lillehei, K., Matsuoka, I., et al. (2007). Bone morphogenetic protein and retinoic acid-inducible neural specific protein-3 is expressed in gonadotrope cell pituitary adenomas and induces proliferation, migration, and invasion. *Endocrinology*, 148(3), 967-975. doi: 10.1210/en.2006-0905
- Sild, M., & Ruthazer, E. S. (2011). Radial glia: progenitor, pathway, and partner. *Neuroscientist*, 17(3), 288-302. doi: 10.1177/1073858410385870
- Silverman, J. L., Yang, M., Lord, C., & Crawley, J. N. (2010). Behavioural phenotyping assays for mouse models of autism. *Nat Rev Neurosci*, 11(7), 490-502. doi: 10.1038/nrn2851
- Simonoff, E., Pickles, A., Charman, T., Chandler, S., Loucas, T., & Baird, G. (2008). Psychiatric disorders in children with autism spectrum disorders: prevalence, comorbidity, and associated factors in a population-derived sample. *J Am Acad Child Adolesc Psychiatry*, 47(8), 921-929. doi: 10.1097/CHI.0b013e318179964f
- Slotnick, B. M. (1973). Fear behavior and passive avoidance deficits in mice with amygdala lesions. *Physiol Behav*, 11(5), 717-720.
- Sohal, V. S., Zhang, F., Yizhar, O., & Deisseroth, K. (2009). Parvalbumin neurons and gamma rhythms enhance cortical circuit performance. *Nature*, 459(7247), 698-702. doi: 10.1038/nature07991
- Soriano, E., Cobas, A., & Fairen, A. (1986). Asynchronism in the neurogenesis of GABAergic and non-GABAergic neurons in the mouse hippocampus. *Brain Res*, 395(1), 88-92.
- Soriano, E., Cobas, A., & Fairen, A. (1989). Neurogenesis of glutamic acid decarboxylase immunoreactive cells in the hippocampus of the mouse. I: Regio superior and regio inferior. *J Comp Neurol*, 281(4), 586-602. doi: 10.1002/cne.902810408
- Spilsbury, K., O'Mara, M. A., Wu, W. M., Rowe, P. B., Symonds, G., & Takayama, Y. (1995). Isolation of a novel macrophage-specific gene by differential cDNA analysis. *Blood*, 85(6), 1620-1629.
- Squire, L. R. (1993). The hippocampus and spatial memory. *Trends Neurosci*, 16(2), 56-57.
- Steckel, E. W., Welbaum, B. E., & Sodetz, J. M. (1983). Evidence of direct insertion of terminal complement proteins into cell membrane bilayers during cytolysis. Labeling by a photosensitive membrane probe reveals a major role for the eighth and ninth components. *J Biol Chem*, 258(7), 4318-4324.
- Stephens, K. E., Miller, K. Y., & Miller, B. L. (1999). Functional analysis of DNA sequences required for conidium-specific expression of the SpoC1-C1C gene of *Aspergillus nidulans*. *Fungal Genet Biol*, 27(2-3), 231-242. doi: 10.1006/fgbi.1999.1145
- Stevens, L. M., Frohnhofer, H. G., Klingler, M., & Nusslein-Volhard, C. (1990). Localized requirement for torso-like expression in follicle cells for development of terminal anlagen of the *Drosophila* embryo. *Nature*, 346(6285), 660-663. doi: 10.1038/346660a0
- Stitt, T. N., Gasser, U. E., & Hatten, M. E. (1991). Molecular mechanisms of glial-guided neuronal migration. *Ann N Y Acad Sci*, 633, 113-121.
- Stoner, R., Chow, M. L., Boyle, M. P., Sunkin, S. M., Mouton, P. R., Roy, S., et al. (2014). Patches of disorganization in the neocortex of children with autism. *N Engl J Med*, 370(13), 1209-1219. doi: 10.1056/NEJMoa1307491
- Strand, A. D., Aragaki, A. K., Baquet, Z. C., Hodges, A., Cunningham, P., Holmans, P., et al. (2007). Conservation of regional gene expression in mouse and human brain. *PLoS Genet*, 3(4), e59. doi: 10.1371/journal.pgen.0030059
- Su, A. I., Wiltshire, T., Batalov, S., Lapp, H., Ching, K. A., Block, D., et al. (2004). A gene atlas of the mouse and human protein-encoding transcriptomes. *Proc Natl Acad Sci U S A*, 101(16), 6062-6067. doi: 10.1073/pnas.0400782101
- Sultan, K. T., Brown, K. N., & Shi, S. H. (2013). Production and organization of neocortical interneurons. *Front Cell Neurosci*, 7, 221. doi: 10.3389/fncel.2013.00221

- Swartzwelder, H. S. (1981). Deficits in passive avoidance and fear behavior following bilateral and unilateral amygdala lesions in mice. *Physiol Behav*, 26(2), 323-326.
- Tamamaki, N., Fujimori, K. E., & Takauji, R. (1997). Origin and route of tangentially migrating neurons in the developing neocortical intermediate zone. *J Neurosci*, 17(21), 8313-8323.
- Tamamaki, N., Nakamura, K., Okamoto, K., & Kaneko, T. (2001). Radial glia is a progenitor of neocortical neurons in the developing cerebral cortex. *Neurosci Res*, 41(1), 51-60.
- Tan, S. S., Kalloniatis, M., Sturm, K., Tam, P. P., Reese, B. E., & Faulkner-Jones, B. (1998). Separate progenitors for radial and tangential cell dispersion during development of the cerebral neocortex. *Neuron*, 21(2), 295-304.
- Tandon, R., Keshavan, M. S., & Nasrallah, H. A. (2008). Schizophrenia, "just the facts" what we know in 2008. 2. Epidemiology and etiology. *Schizophr Res*, 102(1-3), 1-18. doi: 10.1016/j.schres.2008.04.011
- Tandon, R., Keshavan, M. S., & Nasrallah, H. A. (2008). Schizophrenia, "Just the Facts": what we know in 2008 part 1: overview. *Schizophr Res*, 100(1-3), 4-19. doi: 10.1016/j.schres.2008.01.022
- Taniguchi, H., Lu, J., & Huang, Z. J. (2013). The spatial and temporal origin of chandelier cells in mouse neocortex. *Science*, 339(6115), 70-74. doi: 10.1126/science.1227622
- Tarantino, L. M., & Bucan, M. (2000). Dissection of behavior and psychiatric disorders using the mouse as a model. *Hum Mol Genet*, 9(6), 953-965.
- Taylor, S. F., & Tso, I. F. (2014). GABA abnormalities in schizophrenia: A methodological review of in vivo studies. *Schizophr Res*. doi: 10.1016/j.schres.2014.10.011
- Tek, S., Mesite, L., Fein, D., & Naigles, L. (2014). Longitudinal analyses of expressive language development reveal two distinct language profiles among young children with autism spectrum disorders. *J Autism Dev Disord*, 44(1), 75-89. doi: 10.1007/s10803-013-1853-4
- Terashima, M., Kobayashi, M., Motomiya, M., Inoue, N., Yoshida, T., Okano, H., et al. (2010). Analysis of the expression and function of BRINP family genes during neuronal differentiation in mouse embryonic stem cell-derived neural stem cells. *J Neurosci Res*, 88(7), 1387-1393. doi: 10.1002/jnr.22315
- Thatcher, R. W., North, D. M., Neubrandner, J., Biver, C. J., Cutler, S., & Defina, P. (2009). Autism and EEG phase reset: deficient GABA mediated inhibition in thalamo-cortical circuits. *Dev Neuropsychol*, 34(6), 780-800. doi: 10.1080/87565640903265178
- Tole, S., & Grove, E. A. (2001). Detailed field pattern is intrinsic to the embryonic mouse hippocampus early in neurogenesis. *J Neurosci*, 21(5), 1580-1589.
- Toshiyuki, N., & Ichiro, M. (2004). Molecular mechanisms regulating cell type specific expression of BMP/RA Inducible Neural-specific Protein-1 that suppresses cell cycle progression: roles of NRSF/REST and DNA methylation. *Brain Res Mol Brain Res*, 125(1-2), 47-59. doi: 10.1016/j.molbrainres.2004.03.017
- Tschopp, J., Masson, D., & Stanley, K. K. (1986). Structural/functional similarity between proteins involved in complement- and cytotoxic T-lymphocyte-mediated cytolysis. *Nature*, 322(6082), 831-834. doi: 10.1038/322831a0
- Tureck, K., Matson, J. L., Cervantes, P., & Konst, M. J. (2014). An examination of the relationship between autism spectrum disorder, intellectual functioning, and comorbid symptoms in children. *Res Dev Disabil*, 35(7), 1766-1772. doi: 10.1016/j.ridd.2014.02.013
- Turgeon, B., & Meloche, S. (2009). Interpreting Neonatal Lethal Phenotypes in Mouse Mutants: Insights Into Gene Function and Human Diseases. *Physiol Rev*. doi: 10.1152/physrev.00040.2007.-The
- Uhlhaas, P. J., & Singer, W. (2006). Neural synchrony in brain disorders: relevance for cognitive dysfunctions and pathophysiology. *Neuron*, 52(1), 155-168. doi: 10.1016/j.neuron.2006.09.020
- Valcanis, H., & Tan, S. S. (2003). Layer specification of transplanted interneurons in developing mouse neocortex. *J Neurosci*, 23(12), 5113-5122.

- Valera, E. M., Faraone, S. V., Murray, K. E., & Seidman, L. J. (2007). Meta-analysis of structural imaging findings in attention-deficit/hyperactivity disorder. *Biol Psychiatry*, 61(12), 1361-1369. doi: 10.1016/j.biopsych.2006.06.011
- Valiente, M., & Marin, O. (2010). Neuronal migration mechanisms in development and disease. *Curr Opin Neurobiol*, 20(1), 68-78. doi: 10.1016/j.conb.2009.12.003
- Valverde, F., De Carlos, J. A., & Lopez-Mascaraque, L. (1995). Time of origin and early fate of preplate cells in the cerebral cortex of the rat. *Cereb Cortex*, 5(6), 483-493.
- van der Meere, J., Shalev, R., Borger, N., & Gross-Tsur, V. (1995). Sustained attention, activation and MPH in ADHD: a research note. *J Child Psychol Psychiatry*, 36(4), 697-703.
- van Heijst, B. F., & Geurts, H. M. (2015). Quality of life in autism across the lifespan: a meta-analysis. *Autism*, 19(2), 158-167. doi: 10.1177/1362361313517053
- van Strien, A. M., Keijsers, C. J., Derijks, H. J., & van Marum, R. J. (2015). Rating scales to measure side effects of antipsychotic medication: A systematic review. *J Psychopharmacol*, 29(8), 857-866. doi: 10.1177/0269881115593893
- Vawter, M. P., Mamdani, F., & Macciardi, F. (2011). An integrative functional genomics approach for discovering biomarkers in schizophrenia. *Brief Funct Genomics*, 10(6), 387-399. doi: 10.1093/bfgp/elr036
- Verloes, A., Elmaleh, M., Gonzales, M., Laquerriere, A., & Gressens, P. (2007). [Genetic and clinical aspects of lissencephaly]. *Rev Neurol (Paris)*, 163(5), 533-547.
- Verweij, K. J., Zietsch, B. P., Medland, S. E., Gordon, S. D., Benyamin, B., Nyholt, D. R., et al. (2010). A genome-wide association study of Cloninger's temperament scales: implications for the evolutionary genetics of personality. *Biol Psychol*, 85(2), 306-317. doi: 10.1016/j.biopsycho.2010.07.018
- Vinueza Veloz, M. F., Buijsen, R. A., Willemsen, R., Cupido, A., Bosman, L. W., Koekkoek, S. K., et al. (2012). The effect of an mGluR5 inhibitor on procedural memory and avoidance discrimination impairments in Fmr1 KO mice. *Genes Brain Behav*, 11(3), 325-331. doi: 10.1111/j.1601-183X.2011.00763.x
- Voineagu, I., Wang, X., Johnston, P., Lowe, J. K., Tian, Y., Horvath, S., et al. (2011). Transcriptomic analysis of autistic brain reveals convergent molecular pathology. *Nature*, 474(7351), 380-384. doi: 10.1038/nature10110
- Voskoboinik, I., Dunstone, M. A., Baran, K., Whisstock, J. C., & Trapani, J. A. (2010). Perforin: structure, function, and role in human immunopathology. *Immunol Rev*, 235(1), 35-54. doi: 10.1111/j.0105-2896.2010.00896.x
- Voskoboinik, I., Smyth, M. J., & Trapani, J. A. (2006). Perforin-mediated target-cell death and immune homeostasis. *Nat Rev Immunol*, 6(12), 940-952. doi: 10.1038/nri1983
- Vrijenhoek, T., Buizer-Voskamp, J. E., van der Stelt, I., Strengman, E., Sabatti, C., Geurts van Kessel, A., et al. (2008). Recurrent CNVs disrupt three candidate genes in schizophrenia patients. *Am J Hum Genet*, 83(4), 504-510. doi: 10.1016/j.ajhg.2008.09.011
- Wang, K. S., Liu, X. F., & Aragam, N. (2010). A genome-wide meta-analysis identifies novel loci associated with schizophrenia and bipolar disorder. *Schizophr Res*, 124(1-3), 192-199. doi: 10.1016/j.schres.2010.09.002
- Wang, K. S., Tonarelli, S., Luo, X., Wang, L., Su, B., Zuo, L., et al. (2014). Polymorphisms within ASTN2 gene are associated with age at onset of Alzheimer's disease. *J Neural Transm*. doi: 10.1007/s00702-014-1306-z
- Wegiel, J., Kuchna, I., Nowicki, K., Imaki, H., Wegiel, J., Marchi, E., et al. (2010). The neuropathology of autism: defects of neurogenesis and neuronal migration, and dysplastic changes. *Acta Neuropathol*, 119(6), 755-770. doi: 10.1007/s00401-010-0655-4
- Wehmeier, P. M., Schacht, A., Barkley, R. A., Wehmeier, P. M., Schacht, A., & Barkley, R. A. (2010). Social and emotional impairment in children and adolescents with ADHD and the impact on quality of life. *J Adolesc Health*, 46(3), 209-217. doi: 10.1016/j.jadohealth.2009.09.009

- Weiss, L. A. (2009). Autism genetics: emerging data from genome-wide copy-number and single nucleotide polymorphism scans. *Expert Rev Mol Diagn*, 9(8), 795-803. doi: 10.1586/erm.09.59
- Wichterle, H., Garcia-Verdugo, J. M., Herrera, D. G., & Alvarez-Buylla, A. (1999). Young neurons from medial ganglionic eminence disperse in adult and embryonic brain. *Nat Neurosci*, 2(5), 461-466. doi: 10.1038/8131
- Wichterle, H., Turnbull, D. H., Nery, S., Fishell, G., & Alvarez-Buylla, A. (2001). In utero fate mapping reveals distinct migratory pathways and fates of neurons born in the mammalian basal forebrain. *Development*, 128(19), 3759-3771.
- Wilson, P. M., Fryer, R. H., Fang, Y., & Hatten, M. E. (2010). Astn2, a novel member of the astrotactin gene family, regulates the trafficking of ASTN1 during glial-guided neuronal migration. *J Neurosci*, 30(25), 8529-8540. doi: 10.1523/JNEUROSCI.0032-10.2010
- Wöhr, M. (2012). Ultrasonic Communication in Mouse Models of Autism. *Proceedings of Measuring Behavior*.
- Won, H., Lee, H. R., Gee, H. Y., Mah, W., Kim, J. I., Lee, J., et al. (2012). Autistic-like social behaviour in Shank2-mutant mice improved by restoring NMDA receptor function. *Nature*, 486(7402), 261-265. doi: 10.1038/nature11208
- Wonders, C. P., & Anderson, S. A. (2006). The origin and specification of cortical interneurons. *Nat Rev Neurosci*, 7(9), 687-696. doi: 10.1038/nrn1954
- Wong, R., Vasilyev, V. V., Ting, Y. T., Kutler, D. I., Willingham, M. C., Weintraub, B. D., et al. (1997). Transgenic mice bearing a human mutant thyroid hormone beta 1 receptor manifest thyroid function anomalies, weight reduction, and hyperactivity. *Mol Med*, 3(5), 303-314.
- Wood, J. G., Martin, S., & Price, D. (1992). Evidence that the earliest generated cells of the murine cerebral cortex form a transient population in the subplate and marginal zone. *Brain Res Dev Brain Res*, 66(1), 137-140.
- Wood, W. E., Olson, C. R., Lovell, P. V., & Mello, C. V. (2008). Dietary retinoic acid affects song maturation and gene expression in the song system of the zebra finch. *Dev Neurobiol*, 68(10), 1213-1224. doi: 10.1002/dneu.20642
- Xing, Y., Ouyang, Z., Kapur, K., Scott, M. P., & Wong, W. H. (2007). Assessing the conservation of mammalian gene expression using high-density exon arrays. *Mol Biol Evol*, 24(6), 1283-1285. doi: 10.1093/molbev/msm061
- XU Jun-Yu1, X. Q.-Q., XIA Jun. (2012). A review on the current neuroligin mouse models. *Acta Physiologica Sinica*.
- Xu, Q., Cobos, I., De La Cruz, E., Rubenstein, J. L., & Anderson, S. A. (2004). Origins of cortical interneuron subtypes. *J Neurosci*, 24(11), 2612-2622. doi: 10.1523/JNEUROSCI.5667-03.2004
- Yamashita, M., Sakakibara, Y., Hall, F. S., Numachi, Y., Yoshida, S., Kobayashi, H., et al. (2013). Impaired cliff avoidance reaction in dopamine transporter knockout mice. *Psychopharmacology (Berl)*, 227(4), 741-749. doi: 10.1007/s00213-013-3009-9
- Yang, M., Bozdagi, O., Scattoni, M. L., Wöhr, M., Roulet, F. I., Katz, A. M., et al. (2012). Reduced excitatory neurotransmission and mild autism-relevant phenotypes in adolescent Shank3 null mutant mice. *J Neurosci*, 32(19), 6525-6541. doi: 10.1523/JNEUROSCI.6107-11.2012
- Zheng, C., Heintz, N., & Hatten, M. E. (1996). CNS gene encoding astrotactin, which supports neuronal migration along glial fibers. *Science*, 272(5260), 417-419.
- Zugman, A., Gadelha, A., Assuncao, I., Sato, J., Ota, V. K., Rocha, D. L., et al. (2013). Reduced dorso-lateral prefrontal cortex in treatment resistant schizophrenia. *Schizophr Res*, 148(1-3), 81-86. doi: 10.1016/j.schres.2013.05.002